



**Development and Evaluation of Lipid-Based Oral Delivery Systems for  
Oxyresveratrol**

**Yaowaporn Sangsen**

**A Thesis Submitted in Partial Fulfillment of the Requirements for the  
Degree of Doctor of Philosophy in Pharmaceutical Sciences  
Prince of Songkla University**

**2016**

**Copyright of Prince of Songkla University**



**Development and Evaluation of Lipid-Based Oral Delivery Systems for  
Oxyresveratrol**

**Yaowaporn Sangsen**

**A Thesis Submitted in Partial Fulfillment of the Requirements for the  
Degree of Doctor of Philosophy in Pharmaceutical Sciences  
Prince of Songkla University**

**2016**

**Copyright of Prince of Songkla University**

**Thesis Title**                      Development and Evaluation of Lipid-Based Oral Delivery  
Systems for Oxyresveratrol

**Author**                                Miss Yaowaporn Sangsen

**Major Program**                    Pharmaceutical Sciences

---

**Major Advisor****Examining Committee:**

.....Chairperson  
(Assoc. Prof. Dr. Ruedeekorn Wiwattanapatapee)(Assoc. Prof. Dr. Satit Puttipatkhachorn)

**Co-Advisor**

.....Committee  
(Assoc. Prof. Dr. Ruedeekorn Wiwattanapatapee)

.....Committee  
(Assist. Prof. Dr. Kamonthip Wiwattanawongsa) (Assoc. Prof. Dr. PrapapornBoonme)

.....Committee  
(Assist. Prof. Dr. Kamonthip Wiwattanawongsa)

The Graduate School, Prince of Songkla University, has approved this  
thesis as partial fulfillment of the requirements for the Degree of Doctor of Philosophy in  
Pharmaceutical Sciences.

.....  
(Assoc. Prof. Dr. Teerapol Srichana)  
Dean of Graduate School

This is to certify that the work here submitted is the result of the candidate's own investigations. Due acknowledgement has been made of any assistance received.

.....  
(Assoc. Prof. Dr. Ruedeekorn Wiwattanapatpee)  
Major Advisor

.....  
(Miss Yaowaporn Sangsen)  
Candidate



I hereby certify that this work has not already been accepted in substance for any degree, and is not being concurrently submitted in candidature for any degree.

.....

(Miss Yaowaporn Sangsen)

Candidate

ชื่อวิทยานิพนธ์	การพัฒนาและประเมินระบบนำส่งยาแบบไขมันสำหรับรับประทานของออกซีเรสเวราทรอล
ผู้เขียน	นางสาวเยาวพร แสงเสน
สาขาวิชา	เภสัชศาสตร์
ปีการศึกษา	2558

## บทคัดย่อ

วัตถุประสงค์ของงานวิจัยนี้คือการพัฒนาและประเมินระบบนำส่งยาแบบไขมันสองระบบที่แตกต่างกันได้แก่ ระบบนาโนพาร์ทิเคิลไขมัน และระบบเซฟไมโครอิมัลชันฟายด์สำหรับรับประทานของออกซีเรสเวราทรอล ออกซีเรสเวราทรอลเป็นสารประกอบโพลีฟีนอลซึ่งสกัดจากแก่นของต้นมะหาด มีฤทธิ์ทางเภสัชวิทยามากมาย เช่น ฤทธิ์ป้องกันระบบประสาท และฤทธิ์ต้านไวรัสหลายชนิดทั้งไวรัสเริมและไวรัสฮิสตา เป็นต้น อย่างไรก็ตามเมื่อให้โดยการรับประทานออกซีเรสเวราทรอลมีค่าชีวประสิทธิผลที่ต่ำ เนื่องจากถูกเปลี่ยนแปลงสภาพของยาที่ตับและลำไส้เล็กอย่างมาก ทั้งนี้ยังเกี่ยวข้องกับกลไกภูมิคุ้มกันกลับ ซึ่งเป็นข้อจำกัดที่สำคัญในการใช้ประโยชน์ทางคลินิกของออกซีเรสเวราทรอล

ระบบนาโนพาร์ทิเคิลไขมันสองชนิด ซึ่งประกอบด้วยโซลิดลิพิดนาโนพาร์ทิเคิลและนาโนสตรักเจอร์ลิพิดแคร์ริเออร์ ถูกพัฒนาขึ้นและเปรียบเทียบคุณสมบัติทางกายภาพและการเพิ่มชีวประสิทธิผลของออกซีเรสเวราทรอลเมื่อให้โดยการรับประทาน โซลิดลิพิดนาโนพาร์ทิเคิลถูกเตรียมโดยเทคนิคการปั่นด้วยความเร็วสูงที่ความเร็ว 24,000 รอบต่อนาที เป็นเวลา 15 นาที สูตรตำรับที่เหมาะสมซึ่งประกอบด้วยออกซีเรสเวราทรอล 0.3%, Compritol® 888 ATO 5%, Tween80® 3.75% และ soy lecithin 1.875 % สามารถชะลอการปลดปล่อยยาในของเหลวเลียนแบบในทางเดินอาหารเมื่อเทียบกับสารแขวนตะกอนของออกซีเรสเวราทรอล การเตรียมนาโนสตรักเจอร์ลิพิดแคร์ริเออร์ใช้วิธีเดียวกัน แตกต่างกันที่การแทนที่ไขมันแข็งบางส่วนด้วยน้ำมัน Labrafac CC® โดยสูตรที่เหมาะสมซึ่งมีน้ำมัน 50% ของวัฏภาคไขมัน มีขนาดอนุภาค  $96.0 \pm 0.9$  นาโนเมตร ซึ่งเล็กกว่าโซลิดลิพิดนาโนพาร์ทิเคิลที่มีขนาดอนุภาค  $107.5 \pm 0.3$  นาโนเมตร พร้อมทั้งมีการกระจายขนาดเป็นเนื้อเดียวกันและศักย์ซีต้าที่สูง อนุภาคทรงกลมของนาโนสตรักเจอร์ลิพิดแคร์ริเออร์มีประสิทธิภาพกักเก็บออกซีเรสเวราทรอลสูงถึง  $88.5 \pm 0.1\%$  และมีความคงตัวมากกว่าโซลิดลิพิดนาโนพาร์ทิเคิลอย่างมีนัยสำคัญ หลังจากเก็บรักษาที่  $4 \pm 2$  องศาเซลเซียส เป็นเวลา 12 เดือน โครงสร้างผลึกของอนุภาคนาโนสตรักเจอร์ลิพิดแคร์ริเออร์มีระเบียบน้อยกว่าอนุภาคโซลิดลิพิดนาโนพาร์ทิเคิล และยาที่สะสมอยู่ในรูปแบบออสถฐานในอนุภาคไขมันได้รับการยืนยันด้วยวิธีการวัดแยกปริมาณความร้อนแบบส่องกราด

และวิธีการการเลี้ยงเบนรังสีเอ็กซ์ นอกจากนี้นาโนสตรักเจอร์ลิพิดแคร์รีเออร์สามารถชะลอการปลดปล่อยยาได้ดีกว่าโซลิดลิพิดนาโนพาร์ทิเคิลและยาที่ไม่ได้พัฒนาเป็นสูตรตำรับ การศึกษาความเป็นพิษต่อเซลล์ Caco-2 โดยวิธี MTT พบว่านาโนพาร์ทิเคิลไขมันที่บรรจุยาไม่มีความเป็นพิษที่ความเข้มข้นของออกซีเรสเวราทรอลสูงสุด 400 ไมโครโมลาร์ การศึกษาการซึมผ่านของยาในเซลล์ Caco-2 พบว่าอัตราส่วนฟลักซ์ย้อนกลับของออกซีเรสเวราทรอลเดี่ยวเป็น 2.55 แสดงถึงการเป็นสารตั้งต้นของการขนส่งแบบย้อนกลับ นอกจากนี้โซลิดลิพิดนาโนพาร์ทิเคิลและ นาโนสตรักเจอร์ลิพิดแคร์รีเออร์ยังลดการซึมผ่านแบบคัตหลังลง 2.8 เท่าและ 3.3 เท่าตามลำดับเมื่อเปรียบเทียบกับยาที่ไม่ได้พัฒนาเป็นสูตรตำรับ ดังนั้นระบบนาโนพาร์ทิเคิลไขมันสามารถลดการขนส่งแบบย้อนกลับได้อย่างมีนัยสำคัญ พร้อมกับอัตราส่วนฟลักซ์ย้อนกลับเป็น 0.59 และ 1.01 สำหรับนาโนสตรักเจอร์ลิพิดแคร์รีเออร์และโซลิดลิพิดนาโนพาร์ทิเคิลตามลำดับ เกสซ์จลนศาสตร์ในหนู Wistar แสดงถึงโพรไฟล์ของการไหลเวียนระหว่างลำไส้และตับของออกซีเรสเวราทรอล โซลิดลิพิดนาโนพาร์ทิเคิลและนาโนสตรักเจอร์ลิพิดแคร์รีเออร์เพิ่มการดูดซึมของออกซีเรสเวราทรอลเมื่อเปรียบเทียบกับยาที่ไม่ได้พัฒนาเป็นสูตรตำรับถึง 125% และ 177% ตามลำดับ ซึ่งสอดคล้องกับผลการศึกษาในเซลล์

การศึกษาผลของภูมิภาคสารลดแรงตึงผิวต่อการดูดซึมยาของระบบเซลล์-ไมโครอิมัลชันฟายด์จำนวน 4 สูตรตำรับ ซึ่งแตกต่างกันที่สารลดแรงตึงผิวรวมสองชนิด (Tween80<sup>®</sup> และ Labrasol<sup>®</sup>) และสองระดับ (ต่ำ 5% และ สูง 15%) โดยสูตรทั้งหมดแสดงการปลดปล่อยออกซีเรสเวราทรอลอย่างรวดเร็วในของเหลวเลียนแบบในกระเพาะอาหารพีเอช 1.2 หลังจากเจือจางกับสารตัวกลางต่างๆ ขนาดหยดไมโครอิมัลชันของระบบที่ใช้ Tween80<sup>®</sup> ซึ่งมีค่า 26-36 นาโนเมตร มีขนาดเล็กกว่าระบบที่ใช้ Labrasol<sup>®</sup> ซึ่งมีค่า 34-45 นาโนเมตร ความเข้มข้นสูงสุดที่ไม่เป็นพิษต่อเซลล์ Caco-2 ของสูตรตำรับเซลล์ไมโครอิมัลชันฟายด์อยู่ที่ 100 ไมโครโมลาร์ของออกซีเรสเวราทรอล และที่ความเข้มข้นนี้สองระบบที่มีระดับของสารลดแรงตึงผิวสูง เพิ่มการดูดซึมของออกซีเรสเวราทรอลผ่านเซลล์ Caco-2 เมื่อเทียบกับระบบที่มีระดับของสารลดแรงตึงผิวต่ำและยาที่ไม่ได้พัฒนาเป็นสูตรตำรับได้ 1.4-1.7 เท่า และ 1.9-2.0 เท่าตามลำดับ นอกจากนี้ระบบเซลล์ไมโครอิมัลชันฟายด์ทั้งสองลดการขนส่งแบบย้อนกลับได้ถึง 4.4-5.3 เท่า เปรียบเทียบกับยาที่ไม่ได้พัฒนาเป็นสูตรตำรับ ซึ่งผลเพิ่มการดูดซึมในเซลล์เพาะเลี้ยงสอดคล้องกับผลการศึกษาในสัตว์ทดลอง โดยสูตรตำรับที่มีสารลดแรงตึงผิวสูงในระบบของ Tween80<sup>®</sup> ( $F_{r,0-10h}$  786%) ให้ค่าการดูดซึมที่สูงกว่ากลุ่มเดียวกันของระบบ Labrasol<sup>®</sup> ( $F_{r,0-10h}$  218%) อย่างมีนัยสำคัญ ผลการศึกษานี้บ่งชี้ถึงความสำคัญของตัวแปรต่างๆ ในระบบเซลล์ไมโครอิมัลชันฟายด์ เช่น ชนิดและปริมาณของสารลดแรงตึงผิวในการเพิ่มชีวประสิทธิผลของยาเมื่อให้โดยการรับประทาน

การพัฒนาแบบนำส่งแบบไขมันทั้งสามชนิด ได้แก่ โซลิดลิพิดนาโนพาร์ทิเคิล นาโนสตรักเจอร์ลิพิดแคร์รีเออร์ และเซลล์ไมโครอิมัลชันฟายด์ โดยใช้ส่วนประกอบและวิธีการที่

แตกต่างกัน ทำให้ได้สูตรตำรับที่เหมาะสมมีลักษณะเป็นของเหลว ซึ่งระบบเซลฟ์ไมโครอิมัลชันไฟยัดเป็นน้ำมันสีเหลือง ส่วนนาโนพาร์ทิเคิลไขมันเป็นสารแขวนลอยที่มีความหนืดต่ำ ระบบเซลฟ์ไมโครอิมัลชันไฟยัดสามารถบรรจุยาได้มากกว่าระบบนาโนพาร์ทิเคิลไขมันประมาณ 13 เท่า นอกจากนี้ยังมีขนาดอนุภาคและการกระจายขนาดที่น้อยกว่าระบบนาโนพาร์ทิเคิลไขมันอย่างมีนัยสำคัญอีกด้วย แต่หลังจากเก็บรักษาเป็นเวลาสามเดือนระบบเซลฟ์ไมโครอิมัลชันไฟยัดมีความคงตัวน้อยกว่าระบบนาโนพาร์ทิเคิลไขมัน เนื่องจากการลดลงของออกซีเรสเวราทรอลในสูตรตำรับ จากการทดสอบด้วยวิธี MTT ระบบเซลฟ์ไมโครอิมัลชันไฟยัดแสดงให้เห็นถึงความเป็นพิษต่อเซลล์ Caco-2 มากกว่าระบบนาโนพาร์ทิเคิลไขมันของออกซีเรสเวราทรอลถึง 4 เท่า และที่ความเข้มข้น 100 ไมโครโมลาร์ซึ่งไม่เป็นพิษต่อเซลล์ดังกล่าว สูตรเซลฟ์ไมโครอิมัลชันไฟยัดและสูตรตำรับของนาโนพาร์ทิเคิลไขมันทั้งสองแสดงความเท่าเทียมกันในการเพิ่มการดูดซึมของออกซีเรสเวราทรอลได้ 2.5-3 เท่า และลดการขนส่งแบบย้อนกลับลง 1.3-1.8 เท่าเมื่อเทียบกับยาที่ไม่ได้พัฒนาเป็นสูตรตำรับ

โดยสรุป ระบบเซลฟ์ไมโครอิมัลชันไฟยัดที่พัฒนาขึ้น เป็นระบบนำส่งที่เหมาะสมของออกซีเรสเวราทรอล ซึ่งมีศักยภาพในการเพิ่มการดูดซึม ลดการขนส่งแบบย้อนกลับ และเพิ่มชีวประสิทธิผลของยาเมื่อให้โดยรับประทาน

<b>Thesis Title</b>	Development and Evaluation of Lipid-Based Oral Delivery Systems for Oxyresveratrol
<b>Author</b>	Miss Yaowaporn Sangsen
<b>Major Program</b>	Pharmaceutical Sciences
<b>Academic Year</b>	2015

## ABSTRACT

The aims of this study were to develop two different lipid-based systems including lipid nanoparticles system and self-microemulsifying drug delivery system (SMEDDS) for oral delivery of oxyresveratrol (OXY). OXY is an active polyphenol compound extracted from the heartwood of the *Artocarpus lakoocha* Roxburgh. This compound possesses many pharmacological activities, for example neuroprotective activity and anti-viral activities against several types of herpes simplex virus (HSV-1 and HSV-2) and varicella zoster viruses (VZV). However, its low oral bioavailability due to extensive hepatic and intestinal metabolism along with involved efflux pump mechanisms, are the important limitations for its clinical usefulness.

Two types of OXY-loaded lipid nanoparticle systems, solid lipid nanoparticles (SLN) and nanostructured lipid carriers (NLC) were developed and compared in terms of their physical properties and enhancement of the oral bioavailability of OXY. The starting SLN formulation was prepared by a hot/high speed homogenization technique at 24,000 rpm and 15 min, respectively. The most appropriate compositions of the OXY-loaded SLN (OXY-SLN) consisted of OXY (0.3%), Compritol<sup>®</sup> 888 ATO (5%), Tween80<sup>®</sup> (3.75%) and soy lecithin (1.875%). Moreover, the optimized formulation exhibited a retarded release profile of OXY with no initial burst release compared to the OXY suspension in the simulated gastrointestinal fluids. The OXY-loaded NLC (OXY-NLC) were formulated by the same procedure as for SLN production, but the replacing some proportion of solid lipid with Labrafac CC<sup>®</sup> oil. The optimized OXY-NLC (50% oil of lipid phase) produced smaller nanoparticle sizes ( $96.0 \pm 0.9$  nm) than that of the OXY-SLN ( $107.5 \pm 0.3$  nm) with homogeneous size distribution and high zeta potential. The spherical NLC offered significantly higher entrapment

efficiency for OXY ( $88.5 \pm 0.1\%$ ) and a better stability than the SLN, after 12 months storage at 4 °C. However, the NLC yielded less ordered crystalline structure than that of the SLN and an amorphous state of the drug accumulated in the NLC was confirmed by differential scanning calorimetry (DSC) and powder X-ray diffraction (PXRD). The *in vitro* release profiles of the OXY-NLC showed a more sustained release compared to the SLN and unformulated OXY. The MTT toxicity assay showed that the lipid nanoparticles containing OXY were compatible to the Caco-2 cells at up to 400  $\mu\text{M}$  of OXY. For the permeability study on the Caco-2 cells, the efflux ratio (ER) of the unformulated OXY was 2.55 and this indicated that it was a substrate for the efflux transporters of OXY. Moreover, the SLN and NLC were reduced by 2.8 fold and 3.3 fold, respectively, in the secretory permeability of OXY compared to that of an unformulated OXY. Thus, the lipid nanoparticles system had a significantly meliorated efflux transport of OXY with ER ( $\leq 1$ ) of 0.59 and 1.01 for NLC and SLN, respectively. The pharmacokinetic profile in the Wistar rats implied an enterohepatic recycling of OXY. In a similar way to the *in vitro* study, the SLN and NLC increased the relative bioavailability of OXY to 125% and 177%, respectively, compared with the unformulated OXY.

Four formulations of SMEDDS containing two types (Tween80<sup>®</sup> and Labrasol<sup>®</sup>) and two levels (low; 5% and high; 15%) of co-surfactants were evaluated for the impact of the surfactant phase on the oral absorption of OXY. All formulations showed a rapid release of OXY in the simulated gastric fluid (SGF) pH 1.2. After dilution with different media, the microemulsion droplet sizes of the Tween80<sup>®</sup>-based (~26 to 36 nm) were smaller than those of the Labrasol<sup>®</sup>-based systems (~34 to 45 nm). The non-toxic concentrations of all SMEDDS on the Caco-2 monolayers were maximum at 100  $\mu\text{M}$  of OXY. At this concentration, both systems with high levels of surfactant increased the Caco-2 cells permeability of OXY compared to those with low levels of surfactant (1.4-1.7 folds) and the unformulated OXY (1.9-2.0 folds). Furthermore, there was a reduction (4.4-5.3 folds) in the efflux transport of OXY from both systems compared to the unformulated OXY. The *in vitro* results were in good agreement with the *in vivo* absorption studies of such OXY-SMEDDS. Significantly greater values of  $C_{\text{max}}$  and  $\text{AUC}_{0-10\text{h}}$  ( $p < 0.05$ ) were obtained from the high levels of Tween80<sup>®</sup>-based ( $F_{\text{r},0-10\text{h}}$  786%) compared to those from the Labrasol<sup>®</sup>-based system ( $F_{\text{r},0-10\text{h}}$  218%). These findings indicated the importance of formulation variables such as type and quantity of surfactant in the SMEDDS that enhanced oral drug bioavailability.

The three lipid-based formulations (SLN, NLC and SMEDDS) were successfully formulated using different optimized compositions and methods. The developed liquid formulations of OXY had a very different appearance of the yellowish oily SMEDDS and a low viscous suspension of the lipid nanoparticles. The non-aqueous SMEDDS had about a 13-fold higher drug loading than the lipid nanoparticles. The smaller particle sizes and the size distribution (PDI,  $0.073 \pm 0.010$ ) was significantly different ( $p < 0.05$ ) from the OXY-SMEDDS compared to those of the OXY-NLC and OXY-SLN (PDI, 0.2-0.3). However, the SMEDDS was less stable than the SLN and NLC under normal storage conditions according to the decrease of the total content of OXY. Using the MTT assay, the OXY-SMEDDS showed a 4-fold greater toxicity on the Caco-2 cells than the lipid nanoparticles containing OXY. At the non-toxic concentration of 100  $\mu\text{M}$ , both the SMEDDS and the lipid nanoparticles provided a similar 2.5-3 fold enhanced permeability and a 1.3-1.8 fold reduced efflux transport compared to the unformulated OXY ( $p < 0.05$ ).

In conclusion, the developed SMEDDS could potentially be used as a suitable delivery system with enhanced absorption, a reduced efflux transport and an improved oral bioavailability for OXY.

## ACKNOWLEDGEMENT

I am deeply grateful to my thesis advisor, Assoc. Prof. Dr. Ruedeekorn Wiwattanapatapee for the continuous support and encouragement throughout the course of this research. I also sincerely thank my research co-advisor, Assist. Prof. Dr. Kamonthip Wiwattanawongsa, for her teaching and advice, not only the research methodologies but also many other concepts in life. Furthermore, I would like to thank examining committees, Assoc. Prof. Dr. Satit Puttipipatkachorn and Assoc. Prof. Dr. Prapaporn Boonme for their invaluable comments and helpful suggestions.

I would also like to extend my sincere thanks to Prof. Dr. Kittisak Likhitwitayawuid and Assoc. Prof. Dr. Boonchoo Sritularak for offering the opportunity and usefulness guidance to work with the beneficial compound. Special thanks go to Assist. Prof. Dr. Potchanapond Graidist for her allowing to perform the cell culture experiments in the Excellent Research Laboratory of Cancer Molecular Biology, Department of Biomedical Sciences, Faculty of Medicine, Prince of Songkla University. I would not have achieved this far and this thesis would not have been completed without all the support that I have always received from them.

Additionally, I would like to thank Dr. Brian Hodgson for his kindness in writing format proofing. I gratefully acknowledge the Thailand Research Fund (Research Contract Number: BRG 5580004) for financial support. I also would like to thank Faculty of Pharmaceutical Sciences, Prince of Songkla University for supporting the research facilities.

Finally, I would like to express my most appreciation to my parents, my friends and also those whose names are not mentioned here but have greatly inspired and encouraged me until this study comes to a perfect end.

Yaowaporn Sangsen



## CONTENTS

<b>Contents</b>	<b>Page</b>
บทคัดย่อ.....	v
Abstract.....	viii
Acknowledgement .....	xi
List of Tables .....	xiii
List of Figures.....	xiv
List of Abbreviations and Symbols .....	xvii
List of papers.....	xxi
Reprints were made with permission from the publishers .....	xxii
Introduction .....	1
Objectives .....	53
Results and discussion .....	54
Concluding remarks.....	77
References .....	79
Appendices .....	99
Reprint of papers and manuscripts.....	100
Paper 1 .....	101
Paper 2 .....	110
Paper 3 .....	120
Paper 4 .....	131
Vitae.....	160

## LIST OF TABLES

<b>Table</b>		<b>Page</b>
1	Summary of liquid lipids (oils) used in the preparation of the NLC for oral delivery	25
2	Example of poorly water-soluble drugs and substances incorporated into lipid nanoparticles for oral delivery	33
3	Examples of hydrophilic substances, proteins and peptides incorporated into lipid nanoparticles for oral delivery	36
4	Marketed products of lipid nanoparticles for oral drug delivery	38
5	Example of oils, surfactants, co-surfactants or co-solvents used in SMEDDS formulations	41
6	The commercial products of SMEDDS for oral delivery (Shukla <i>et al.</i> , 2012; Anand, 2015)	45
7	Summary of homogenization conditions compositions and properties of the optimum S2 formulation	56
8	Physicochemical characteristics and stability data at $4 \pm 2^\circ\text{C}$ of the blank formulations, OXY-SLN and OXY-NLC	58
9	Pharmacokinetics data of OXY after oral administration of OXY-loaded SLN and NLC, compared with the unformulated OXY (equivalent to 180 mg/kg of OXY). *p < 0.05, comparison with aqueous suspension; # p < 0.05, comparison with SLN.	66
10	Pharmacokinetics data of OXY after the oral administration of different SMEDDS formulations and unformulated OXY (equivalent to 180 mg/kg of OXY). The values are presented as mean values $\pm$ SD (n = 7). P < 0.05, in comparison with the unformulated OXY (*); LT (**); LL (***); HL (#).	72

## LIST OF FIGURES

Figure		Page
1	The Lakoocha plant with heartwoods (Likhitwitayawuid, 2008)	5
2	Chemical structure of oxyresveratrol (Xu <i>et al.</i> , 2014)	15
3	The metabolic pathways of OXY proposed from <i>in vitro</i> hepatic microsomes of both rat and human (adapted from Mei <i>et al.</i> , 2012).	17
4	The metabolic pathways of OXY proposed from <i>in vivo</i> studies after oral administration of 100 mg/kg OXY (Huang <i>et al.</i> , 2010).	18
5	Three different drug incorporation model of the SLN (Modified from Muchow <i>et al.</i> , 2008)	23
6	Three different types of the NLC (Modified from Müller <i>et al.</i> , 2002)	24
7	The appearance of OXY-loaded lipid nanoparticles (SLN and NLC3)	57
8	TEM images at $\times 100$ K of SLN (A) at 0 month; SLN (B), NLC1 (C), and NLC3 (D) after 3-months storage	59
9	DSC thermograms of OXY (A); freeze dried powders of NLC3 (B); NLC1 (C); SLN (D); physical mixtures of C888 and OXY (E); and C888 (F)	60
10	Powder X-ray images of C888 (A); OXY (B); physical mixtures of C888 and OXY (C), and freeze dried powders of SLN (D); NLC1 (E) and NLC3 (F)	62
11	<i>In vitro</i> OXY release profiles of SLN and NLC formulations with different lipid to oil ratios (NLC1, NLC2, NLC3) compared with the unformulated OXY in SGF (pH 1.2) and SIF (pH 6.8). Data represents the mean $\pm$ SD (n = 3).	62
12	The percentage of Caco-2 cell viability to different concentrations of OXY (A), OXY-loaded SLN (B) and OXY-loaded NLC (C) (n = 8), duplications.	63

## LIST OF FIGURES (continued)

Figure		Page
13	Bidirectional transport across the Caco-2 monolayers of OXY and developed OXY-formulations. The data are presented as the apparent permeability coefficient ( $P_{app}$ ) in the absorptive (AP-BL) and the secretory directions (BL-AP). <sup>#</sup> $p < 0.05$ , comparison with OXY400; <sup>##</sup> $p < 0.05$ , comparison with SLN400.	64
14	Plasma concentrations of OXY vs. time profiles after oral administration of OXY-loaded SLN and NLC, compared with the unformulated OXY (180 mg/kg of OXY). Data represents the mean $\pm$ SD (n = 7).	65
15	Ternary phase diagram of Cremophor RH40 <sup>®</sup> -based SMEDDS (system D) containing different co-surfactants including Lauroglycol FCC <sup>®</sup> (D1), Tween80 <sup>®</sup> (D2), Labrasol <sup>®</sup> (D3), PG <sup>®</sup> (D4) and PEG400 (D5). Gray areas represent the region of efficient self-microemulsification (Grade I), and the dots represent the compositions that were evaluated.	67
16	Example of capsule filled with OXY-SMEDDS formulation which produced transparent microemulsion and its morphology observed by TEM	68
17	The dissolution profiles of OXY from the capsule (dark lines) and the dialysis bag (dot line) filled with the SMEDDS formulations in simulated gastric fluid (SGF, pH 1.2) without pepsin. Data are represented by a mean $\pm$ SD (n = 3).	68
18	The percentage of Caco-2 cell viability to different concentrations of OXY, blank SMEDDS and OXY-SMEDDS; A) LT, B) HT, C) LL, D) HL, (n = 8), duplications.	69

## LIST OF FIGURES (continued)

Figure		Page
19	Bidirectional transport across the Caco-2 monolayers of OXY and different OXY-SMEDDS. The data are presented as the apparent permeability coefficients ( $P_{app}$ ) in the absorptive (AP-BL) and the secretory directions (BL-AP). $p < 0.05$ , comparison with OXY (*); LT (#); LL (##) at the equivalent dose of OXY (100 $\mu$ M).	70
20	Plasma concentrations vs. time profiles after the oral administration of OXY-SMEDDS and unformulated OXY (equivalent to 180 mg/kg of OXY). Comparison of different surfactant concentrations of SMEDDS; low LT and high HT (A), and low LL and high HL (B), for Tween80 <sup>®</sup> -based (T) and Labrasol <sup>®</sup> -based (L) systems, respectively. Comparison of different surfactant types of SMEDDS; LT and LL (C), and HT and HL (D), for low (L) and high (H) concentrations, respectively. All values reported are mean values $\pm$ SD (n = 7).	72
21	Diagram of production process of lipid nanoparticles compared to preparation of SMEDDS	73
22	Physical characteristics and stability data (0, 1, 3 months) of the OXY formulated as SLN, NLC and SMEDDS; (A) Mean size, (B) PDI and (C) %Total drug content (TDC). Data represents the mean $\pm$ S.D. (n = 3).	74
23	Bidirectional transport across the Caco-2 monolayers of OXY and developed OXY-formulations. The data are presented as the apparent permeability coefficient ( $P_{app}$ ) in the absorptive (AP-BL) and the secretory directions (BL-AP). * $p < 0.05$ , comparison with OXY100; ** $p < 0.05$ , comparison with SLN100.	76

**LIST OF ABBREVIATIONS AND SYMBOLS**

$\alpha$	alpha
$\beta$	beta
$^{\circ}\text{C}$	degree celcius
$\Omega$	ohms
$\mu\text{g}$	micrograms
$\mu\text{L}$	microliters
$\mu\text{M}$	micromolars
$\text{A}\beta_{25-35}$	amyloid beta 25-35 protein
ACV	acyclovir
AFM	atomic force microscopy
AP	apical side
AUC	area under the curve
BBB	blood brain barrier
BL	basolateral side
BSC	biopharmaceutical classification system
cm	centrimeters
$\text{cm}^{-1}$	per centrimeters
$\text{cm}^2$	square centrimeters
C18	carbon-18
C888	Compritol 888 ATO <sup>®</sup>
$C_{\text{max}}$	maximum concentration
CYP	cytochrome P-450
DMSO	dimethyl sulfoxide
DNA	deoxyribonucleic acid
DSC	differential scanning calorimetry
e.g.	for example
$\text{EC}_{50}$	effective concentration at 50%
EE	entrapment efficiency
EHC	enterohepatic recycling
ER	efflux ratio

**LIST OF ABBREVIATIONS AND SYMBOLS (continued)**

$F_r$	relative bioavailability
g	grams
GI	gastrointestinal tract
GMS	glyceryl monostearate
GRAS	generally recognized as safe
h	hours
$h^{-1}$	per hours
HIV	human immunodeficiency virus
HLB	hydrophilic-lipophilic balance
HPLC	high performance liquid chromatography
HSV	herpes simplex virus
i.e.	that is
iNOS	inducible nitric oxide synthase
IC <sub>50</sub>	inhibition concentration at 50%
K	kilo
kg	kilograms
L	liters
Lab CC	Labrafac <sup>®</sup> CC
LC	loading capacity
LD <sub>50</sub>	lethal dose at 50%
LBDDS	lipid-based drug delivery systems
m	meters
mg	milligrams
min	minutes
mL	milliliters
mol	mole
mV	millivolts
M	molars
MIC	minimum inhibition concentration
MRPs	multidrug resistance proteins

**LIST OF ABBREVIATIONS AND SYMBOLS (continued)**

MS	mass spectroscopy
MTT	3-[4,5-dimethylthiazol-2-yl]-2,5-diphenyl-tetrazolium bromide
MW	molecular weight
n	number of sample or release exponent
ng	nanograms
nm	nanometers
NLC	nanostructured lipid carriers
NO	nitric oxide
o/w	oil-in-water
OXY	oxyresveratrol
P188	Poloxamer <sup>®</sup> 188
<i>P</i> <sub>app</sub>	apparent permeability coefficient
PCS	photon correlation spectroscopy
PDI	polydispersity index
PEG	polyethylene glycol
P-gp	p-glycoprotein
PG	propylene glycol
PS	particle size
$r^2$	correlation coefficient
rpm	revolution per minute
RNS	reactive nitrogen species
ROS	reactive oxygen species
RSD	relative standard deviation
RT	room temperature
s	second
SD	standard deviation
SEM	scanning electron microscopy
SGF	simulated gastric fluid
SIF	simulated intestinal fluid
SLN	solid lipid nanoparticles



**LIST OF ABBREVIATIONS AND SYMBOLS (continued)**

SMEDDS	self-microemulsifying drug delivery systems
SOD	superoxide dismutase
$t_{1/2}$	half-life time
TDC	total drug content
TEER	trans-epithelial electrical resistance
TEM	transmission electron microscopy
TLC	thin layer liquid chromatography
$T_{max}$	time to reach maximum concentration
UGT	glucuronosyl transferase
USP	U.S. pharmacopeia
UV-vis	Ultraviolet-visible
VZV	varicella zoster virus
w/w	weight by weight
XRD	X-Ray diffractometry
ZP	zeta potential

## LIST OF PAPERS

This thesis is based on the following papers which mentioned to the respectively experimental design in the text. The papers are attached in appendices at the end of the thesis (Page 101 to 159). Reprints are published with permission of the journals.

- Paper 1 Sangsen, Y., Likhitwitayawuid, K., Sritularak, B., Wiwattanawongsa, K. and Wiwattanapataptee, R. 2013. Novel solid lipid nanoparticles for oral delivery of oxyresveratrol: Effect of the formulation parameters on the physicochemical properties and *in vitro* release. *Int. J. Med. Sci. Eng.* 7: 873-897.
- Paper 2 Sangsen, Y., Wiwattanawongsa, K., Likhitwitayawuid, K., Sritularak, B. and Wiwattanapataptee, R. 2015. Modification of oral absorption of oxyresveratrol using lipid based nanoparticles. *Colloids Surf., B.* 131: 182-190.
- Paper 3 Sangsen, Y., Wiwattanawongsa, K., Likhitwitayawuid, K., Sritularak, B., Graidist, P. and Wiwattanapataptee, R. 2016. Influence of surfactants in self-microemulsifying formulations on enhancing oral bioavailability of oxyresveratrol: Studies in Caco-2 cells and *in vivo*. *Int. J. Pharm.* 498(1-2): 294-303.
- Paper 4 Sangsen, Y., Wiwattanawongsa, K., Likhitwitayawuid, K., Sritularak, B. and Wiwattanapataptee, R. Comparisons between a self-microemulsifying system and lipid nanoparticles of oxyresveratrol on the physicochemical properties and Caco-2 cells permeability (Submitted for publication).

## REPRINTS WERE MADE WITH PERMISSIONS FROM THE PUBLISHERS

10/29/2015

Rightslink® by Copyright Clearance Center



# RightsLink®

[Home](#)
[Account Info](#)
[Help](#)


**Title:** Modification of oral absorption of oxyresveratrol using lipid based nanoparticles

Logged in as:  
Yaowaporn Sangsen

**Author:** Yaowaporn Sangsen, Kamonthip Wiwattanawongsa, Kittisak Likhitwitayawuid, Boonchoo Sritularak, Ruedeekorn Wiwattanapatapee

[LOGOUT](#)

**Publication:** Colloids and Surfaces B: Biointerfaces

**Publisher:** Elsevier

**Date:** 1 July 2015

Copyright © 2015 Elsevier B.V. All rights reserved.

### Order Completed

Thank you very much for your order.

This is a License Agreement between Yaowaporn Sangsen ("You") and Elsevier ("Elsevier"). The license consists of your order details, the terms and conditions provided by Elsevier, and the [payment terms and conditions](#).

[Get the printable license.](#)

License Number	3737770304239
License date	Oct 28, 2015
Licensed content publisher	Elsevier
Licensed content publication	Colloids and Surfaces B: Biointerfaces
Licensed content title	Modification of oral absorption of oxyresveratrol using lipid based nanoparticles
Licensed content author	Yaowaporn Sangsen, Kamonthip Wiwattanawongsa, Kittisak Likhitwitayawuid, Boonchoo Sritularak, Ruedeekorn Wiwattanapatapee
Licensed content date	1 July 2015
Licensed content volume number	131
Licensed content issue number	n/a
Number of pages	9
Type of Use	reuse in a thesis/dissertation
Portion	full article
Format	both print and electronic
Are you the author of this Elsevier article?	Yes
Will you be translating?	Yes
Number of languages	1
Languages	English and Thai
Title of your thesis/dissertation	Development and Evaluation of Lipid-Based Oral Delivery Systems for Oxyresveratrol
Expected completion date	Dec 2015
Estimated size (number of pages)	200
Elsevier VAT number	GB 494 6272 12
Permissions price	0.00 USD
VAT/Local Sales Tax	0.00 USD / 0.00 GBP
Total	0.00 USD

12/28/2015

Rightslink® by Copyright Clearance Center



RightsLink®

Home

Account  
Info

Help



**Title:** Influence of surfactants in self-microemulsifying formulations on enhancing oral bioavailability of oxyresveratrol: studies in Caco-2 cells and in vivo

**Author:** Yaowaporn Sangsen, Kamonthip Wiwattanawongsa, Kittisak Likhitwitayawuid, Boonchoo Sritularak, Potchanapond Graidist, Ruedeeekorn Wiwattanapatpee

**Publication:** International Journal of Pharmaceutics

**Publisher:** Elsevier

**Date:** 10 February 2016

Copyright © 2015 Elsevier B.V. All rights reserved.

Logged in as:  
Yaowaporn Sangsen  
Account #:  
3000969881

LOGOUT

### Order Completed

Thank you very much for your order.

This is a License Agreement between Yaowaporn Sangsen ("You") and Elsevier ("Elsevier"). The license consists of your order details, the terms and conditions provided by Elsevier, and the [payment terms and conditions](#).

[Get the printable license.](#)

License Number	3777200088417
License date	Dec 27, 2015
Licensed content publisher	Elsevier
Licensed content publication	International Journal of Pharmaceutics
Licensed content title	Influence of surfactants in self-microemulsifying formulations on enhancing oral bioavailability of oxyresveratrol: studies in Caco-2 cells and in vivo
Licensed content author	Yaowaporn Sangsen, Kamonthip Wiwattanawongsa, Kittisak Likhitwitayawuid, Boonchoo Sritularak, Potchanapond Graidist, Ruedeeekom Wiwattanapatpee
Licensed content date	10 February 2016
Licensed content volume number	498
Licensed content issue number	1-2
Number of pages	10
Type of Use	reuse in a thesis/dissertation
Portion	full article
Format	both print and electronic
Are you the author of this Elsevier article?	Yes
Will you be translating?	Yes
Number of languages	1
Languages	English and Thai
Title of your thesis/dissertation	Development and Evaluation of Lipid-Based Oral Delivery Systems for Oxyresveratrol
Expected completion date	Dec 2015
Estimated size (number of pages)	200
Elsevier VAT number	GB 494 6272 12
Permissions price	0.00 USD
VAT/Local Sales Tax	0.00 USD / 0.00 GBP
Total	0.00 USD

## INTRODUCTION

### 1.1 General introduction

Oxyresveratrol (*Trans*-2,4,3',5'-tetrahydroxystilbene; OXY) is a polyphenolic compound extracted from heartwood of Thai traditional herb, *Artocarpus lakoocha* Roxburgh (Moraceae) (Likhitwitayawuid *et al.*, 2005). It has been reported to possess many pharmacological activities. For example, it has anti-tyrosinase activity (Kim *et al.*, 2002b), strong antioxidant with anti-inflammatory activity (Oh *et al.*, 2002; Lee *et al.*, 2014) and potent neuroprotective activity (Weber *et al.*, 2012). Recently, its anti-viral activities have been established with activities against several types of herpes simplex virus (HSV-1 and HSV-2) (Lipipun *et al.*, 2011; Sasivimolphan *et al.*, 2012), various varicella zoster viruses (VZV) (Sasivimolphan *et al.*, 2009), influenza virus (Liu *et al.*, 2010) as well as human immunodeficiency virus type 1 (HIV-1) (Likhitwitayawuid *et al.*, 2005). These pharmacological activities have triggered efforts to transform OXY into therapeutic agent. However, there are some important limitations for the oral administration of OXY such as first pass metabolism by metabolic enzyme in both intestine and liver (Hu *et al.*, 2014). Moreover, its poor oral absorption due to intermediate permeability with involved efflux mechanism of both p-glycoprotein (P-gp) and multidrug resistance proteins (MRPs) family at gut membrane (Mei *et al.*, 2012). Once into the blood stream it is cleared by extensive hepatic metabolism and its rapid elimination results in a short half-life time in the body leading to a low oral bioavailability and largely restricts its clinical use (Charoenlarp *et al.*, 1991; Huang *et al.*, 2008b; Huang *et al.*, 2010). To overcome the challenges in oral administration of OXY, the effective formulations and delivery strategies are needed.

Lipid-based drug delivery systems (LBDDS) have been emerged interestingly to use as drug carriers in oral route. Lipid-based formulations may include oil solutions or suspensions, liposomes and emulsions (Pouton and Porter, 2008; Mu *et al.*, 2013). Besides conventional lipid-based systems, solid lipid nanoparticles (SLN) have proved to be efficient and attractive alternatives as colloidal drug carriers. The SLN is designed by replacing the liquid lipid (oil) component of an oil-in-water (o/w) emulsion with solid lipids that are solid at body and room temperature (RT). The SLN

has many advantages such as good biocompatibility and biodegradability when prepared with physiologically accepted excipients that are generally recognized as safe (GRAS) status, protection the drug from chemical or enzyme degradation in the gastrointestinal (GI) tract and controlled drug release (Müller *et al.*, 2000). Moreover, many particle synthetic methods can be easily scaled up to commercial products (Mehnert and Mäder, 2001). Either hydrophobic or hydrophilic drug could be trapped by lipid matrix of the nanoparticles which structurally similar to the fat in daily food (Chakraborty *et al.*, 2009; Souto and Müller, 2010). The lipid nanoparticles enhanced drug absorption by many of ways such as increased the permeability of drug entrapped across lipid bilayers of the epithelium and facilitates draining the drug into lymphatic absorption leading to avoidance the hepatic metabolism (Tiwari and Pathak, 2011).

In addition, its nano-sized particles and high dispersibility confer high surface area to adhere at the absorptive site leads to promote direct uptake through the intestinal cells (Tiwari and Pathak, 2011). Moreover, the lipid matrix reduced exposure of the entrapped drug to intestinal efflux system. Also, the presence of surfactant in the SLN promotes the oral absorption of the drug due to its inhibiting activity to the efflux transporters and deforming the cell membrane (Shono *et al.*, 2004; Souto and Müller, 2010). In the second generation of lipid nanoparticles, nanostructured lipid carriers (NLC) have been produced by replacing the solid lipids of SLN with liquid lipid (oil) to generate special structures within a lipid matrix that remains benefits same as in the SLN. Remarkably, the NLC system have been produced for improving of the potential limitations of SLN such as drug loading capacity, early drug expulsion and long term stability (Üner, 2006). Both SLN and NLC have been enhanced successfully oral bioavailability for several drugs (Almeida and Souto, 2007; Souto and Müller, 2010; Tiwari and Pathak, 2011; Neves *et al.*, 2013). Therefore, the preparation processes and compositions of the lipid nanoparticle systems that affect their physicochemical properties and absorption behaviors should be considered to obtain effective formulations for oral OXY.

According to the manifest advantages of LBDDS, the development of another lipid formulation of OXY especially liquid self-microemulsifying drug delivery systems (SMEDDS) was provoked. The system successfully improved oral bioavailability of various compounds and launched as marketed SMEDDS products such as Sandimmune<sup>®</sup> and Neoral<sup>®</sup> (Cyclosporine A) (Gursoy and Benita, 2004; Kohli *et*

*al.*, 2010; Setthacheewakul *et al.*, 2010; Sermkaew *et al.*, 2013). The SMEDDS which is the isotropic mixture of oils, surfactants, and co-surfactants/co-solvents, that form transparent o/w microemulsions after dilution with a GI fluid under the mild agitation of the gastric movements (Gursoy and Benita, 2004). The thermodynamically stable microemulsions with droplet sizes of less than 50 nm provide many advantages. For example, they are easy to prepare and scale up to commercial products, fast dispersion, increased drug solubility and rapid dissolution rate of the drug. In addition, the SMEDDS can avoid damage of the drugs by acid and enzymatic degradation in the GI tract (Kohli *et al.*, 2010). The oral absorption by the SMEDDS may occur mainly via generating mixed micelles of an emulsified lipid exposed to bile salts and then uptake by enterocytes. Moreover, the benefits of surfactants commonly used, e.g. polyoxyethylene castor oil derivatives and polyethylene glycol esters, also have been implicated (Ujhelyi *et al.*, 2012; Seljak *et al.*, 2014). In addition to good miscibility with many oil types and well stabilizing the oil droplets, these surfactants could enhance drug permeability in many ways (Zhang *et al.*, 2003; Sha *et al.*, 2005; Lin *et al.*, 2007b). Some surfactants could modify pharmacokinetics of the drugs after oral administration (Ellis *et al.*, 1996; Lind *et al.*, 2008; Prokop and Davidson, 2008). Because of these beneficial activities of surfactant, hence the investigation of the effects of the surfactant phase on drug absorption will be useful for the design of effective SMEDDS formulations for OXY. Although, both lipid nanoparticles and oily SMEDDS could be potential carriers for oral delivery of OXY, however, the distinguishing features of different lipid formulations such as composition used, particle size, release properties and degradation of the formulations could affect to distinct absorption behaviors (Porter *et al.*, 2008; Pouton and Porter, 2008).

The *in vitro* cell culture studies, thus, have been used to evaluate the permeability and predict absorption phenomena of compounds or formulations across barriers of intestinal epithelia. The Caco-2 monolayers-based screening model is one of the *in vitro* rapid and effective methods to estimate *in vivo* drug performance according to the good correlation of the model to the human intestinal epithelium (Artursson and Karlsson, 1991). The Caco-2 cells, which originate from a colorectal adenocarcinoma patient, spontaneously differentiates become to monolayers of enterocyte-like cells resemble to human intestinal epithelium on porous membrane. Moreover, this system allows determining the transport mechanisms including passive and active transports as

well as efflux mediated mechanism of P-gp and MRPs. Furthermore, the Caco-2 monolayers also provide the information of cytotoxicity and pharmacological activities of the compounds and/or the formulations.

The purposes of this study were to develop lipid-based formulations as the potential oral delivery of OXY. The different lipid formulations of OXY including solid lipid systems of SLN and NLC were formulated and compared with the oily SMEDDS. For the lipid nanoparticles systems, the effects of the preparation conditions and formulated ingredients on their appearance, physical characteristics including particle size, size distribution, total drug content, entrapment efficiency, drug loading capacity, and *in vitro* drug release properties were firstly determined to obtain suitable conditions for further development of SLN and NLC formulations (Paper 1). Then, the NLC formulations containing different solid lipid to liquid lipid ratios were evaluated additionally in term of zeta potential, morphology by TEM, crystallization and polymorphism by DSC and XRD analysis, and storage stability to select the optimized NLC formulation. Lastly, the improved oral bioavailability of the NLC was investigated further by *in vitro* absorption and *in vivo* studies in the Wistar rats compared to the SLN formulation and the unformulated OXY (Paper 2).

To compare with lipid nanoparticles, the various formulations of liquid OXY-SMEDDS were formulated using different types and concentrations of surfactants/co-surfactants. The influence of the surfactants used on the physical properties including self-microemulsifying performance, microemulsion droplet size, size distribution, morphology observed by TEM, total drug content, and the *in vitro* release of the distinct formulations were evaluated. Moreover, the effects of the surfactant-based SMEDDS on the *in vitro* toxicity and drug permeability were compared using the Caco-2 cells model. Next, the pharmacokinetic studies of each of formulations were examined and compared with the unformulated OXY (Paper 3).

Finally, the distinct behaviors, stability, and absorption fate of OXY from the three lipid-based systems, including SLN, NLC and SMEDDS, were considering compared. In order to optimize absorption capability of this important molecule by such formulations, the toxicity, the enhanced drug transport and the efflux protein inhibition of each developed formulations by the Caco-2 cells absorption model were compared to the unformulated OXY (Paper 4).



## 1.2 Related literature

### 1.2.1 Oxyresveratrol

#### 1.2.1.1 Introduction

Lakoocha or Monkey fruit (*Artocarpus lakoocha* Roxburgh) is belonging to the Moraceae family which cultivated widely in South and Southeast Asia (Kochummen, 1978). It is a large perennial which grows up to 15-20 m in height. The outer bark is gray-brown flaky, while the inner shell is brown-red often with white rubber. The hard wood and yellow-dark brown heartwood are identified. Its leaves are oblong, elliptical or ovate. It has soft-multiple fruit with agee sphere shape (Figure 1).



**Figure 1** The Lakoocha plant with heartwoods (Likhitwitayawuid, 2008)

In Thailand, this plant is called “Ma-Haad” which has been used for many aspects such as animal foods and construction materials. For decades, some parts of the plant have been reported to ease some illness symptoms in Thai traditional remedies, for example root, bark and leaves used for fever reliever and toxic reducer. In Thai Pharmacopoeia, the dried powder of water-extracted heartwood of this herbal “Puag-Haad” has been used as anthelmintics for treatment of roundworm and flatworm (Farnsworth and Bunyapraphatsara, 1992).

As known of the benefits of the Ma-Haad used in Thai traditional medicines, deep investigations have been known that main active compound in the heartwood as “Oxyresveratrol (OXY)”. Whereupon, there have been reports on various biological activities of OXY other than anthelmintic activities, such as tyrosinase

inhibitory activity, antioxidant, anti-inflammatory activity, anti-microbial activities, anti-hypertensive activity, anti-cancer activities, anti-atherosclerotic activity, anti-diabetic activity, anti-malarial activity, anti-viral activities and neuroprotective activity (Gautam and Patel, 2014).

### 1.2.1.2 Pharmacological activities of OXY

#### I) Anthelmintic activity

In Thai traditional Pharmacopoeia, the “Puag-Haad” containing the major active OXY in powder or tablet forms have been introduced to treat many types of worm. Charoenlarp and colleagues (1981), for example, selected the 39 volunteers diagnosed with intestinal parasites to investigate the effective of the herbal on anthelmintic activity. The volunteers were dosed the “Puag-Haad” powder 5 g in water during fasted state, then were taken 45 mL of saturated magnesium sulfate solution in 2 h later, and parasites in the feces of the volunteers were observed during 8 h. The clinical trial presented that the 7 volunteers were discontinued trials due to immediate nausea and vomiting. However, either articulate or head of tapeworms (*Taenia saginata* and *Taenia solium*) was excreted in feces of 30 treated volunteers. Following investigation process described above, this group tried to reduce the adverse effect by decreasing oral dose of the “Puag-Haad”. The 49 patients diagnosed with intestinal parasites were divided into two groups including 25 and 24 patients for intake of 2 g and 3 g of the “Puag-Haad”, respectively. The results showed that the cure rate after intake 2 g and 3g of the herbal was 42% and 80%, respectively, while insignificant nausea was observed in both doses (Charoenlarp *et al.*, 1989). Furthermore, the patients oral dosing 3 g of the “Puag-Haad” were compared with other groups of the antihelminthic drugs including prasiquantel 300 mg and niclosamide 2 g for treatment of *Taenia saginata*. The cure rate percentage was 93.3, 100, 60 for the patient intake of the “Puag-Haad”, prasiquantel, niclosamide, respectively. Therefore, the single dose of “Puag-Haad” 3 g achieves the equal to 300 mg prasiquantel and better effective than 2 g niclosamide (Charoenlarp, 1993).

The mechanism of the crude extract of *A. lakoocha* containing 70% of OXY on treatment of parasitic flatworm (*Fasciola gigantica*) was studied by relative

motility (RM) assay and scanning electron microscope (SEM) (Saowakon *et al.*, 2009). The crude extract of *A. lakoocha* at concentrations of 750 and 1000 µg/mL rapidly reduced the parasite's motility up to 12 h and killed the worms between 12 to 24 h exposures. At this concentration, the crude extract also inhibited 100% of the larval migration. This was similar to 175 µg/mL of triclabendazole (TCZ) which used as the positive control. The crude extract initially affected the tegumental damage of adult *F. gigantica* and then promoted the severity of the damages by increasing concentration of the crude extract inside the parasites.

The safety of "Puag-Haad" has been reported by many researchers (Tanunkat, 1990; Charoenlarp *et al.*, 1991; Farnsworth and Bunyapraphatsara, 1992). The toxicity after oral administration of 40 and 400 mg/kg Puag-Haad extract and 720 mg/kg OXY in rats and rabbits, for example, was evaluated. During 7 days of observation, no sign of toxicity and some blood parameter values such as cholesterol, blood urea nitrogen, and platelet was insignificantly changed in the tested animals. In addition, the unchanged OXY was found in urine of the rabbits after 2-4 h of oral administration. The researchers recommended the lethal dose 50% (LD<sub>50</sub>) of Puag-Haad extract in ether and OXY was 5.30 and 7.48 g/kg, respectively (Ngamwat *et al.*, 1987).

## II) Tyrosinase inhibitory activity

Tyrosinase is an enzyme found in many organisms including humans. In human, it plays a role on production of the black or brown pigments called melanins of skin or hair. Thus, compounds that inhibit tyrosinase activity can be used as whitening agent. The heartwood extract of Ma-Haad contains a high amount of active compound "OXY". *In vitro* study, OXY with inhibition concentration (IC<sub>50</sub>) 12.7 µM presented about 10 fold potential than kojic acid, which usually as skin whitening agent in cosmeceutical formulations (IC<sub>50</sub> 133.4 µM). The inhibition activity of OXY to tyrosinase enzyme was dose-dependent. However, source of enzyme and tested substrate also affected to mechanism on the enzyme inhibition of the OXY (Likhitwitayawuid *et al.*, 2006; Likhitwitayawuid, 2008).

*In vivo* studies, the 70% OXY contained in heartwood extract of Ma-Haad was determined the effective of skin whitening activity in UV-B induced black skin Guinea pigs model (n=6). At 4th week, the results presented the significant higher %

whitening obtained from the extract ( $7.59 \pm 1.40\%$ ) than kojic acid ( $5.38 \pm 1.55\%$ ) and propylene glycol (PG) ( $3.26 \pm 1.15\%$ ) (Tengamnuay *et al.*, 2003; 2006). Furthermore, the whitening activity of the 0.25% Ma-Haad extract (containing 80% OXY) in PG comparing with 0.25% licorice extract and 3% kojic acid, was investigated in female volunteers (Pheansri, 2001; Tengamnuay *et al.*, 2006). Three groups (n=20) of the volunteers were applied the tested sample at one of the upper arm twice daily with self-control (only PG). Based on melanin value, difference % whitening was calculated compared to the control (PG). During 12 weeks, the whitening activities of the Ma-Haad extract was remarkably rapid and higher than licorice extract and kojic acid. Also, the whitening activities of lotion of 0.1% Ma-Haad extract had superior than that of 0.1% licorice lotion from initial to 4th week of experiment. All data revealed the potential of the Ma-Haad extract containing active OXY as the whitening agent.

### III) Anti-oxidative activity

OXY, is one of natural hydroxystilbenes, has a polyphenol structure related to protective effects against reactive oxygen (ROS) and nitrogen species (RNS). Oh *et al.* (2002) has reported this activity of OXY extracted from mulberry twigs. The results showed OXY scavenged superoxide ion ( $IC_{50}$  3.81  $\mu$ M) by superoxide dismutase (SOD) assay kit. In general free radical model, OXY ( $IC_{50}$  28.9  $\mu$ M) indicated more effective scavenger for 2,2-diphenyl-1-picryl-hydrazyl (DPPH) when compared to resveratrol ( $IC_{50}$  38.5  $\mu$ M) and trans-4-hydroxystilbene ( $IC_{50}$  39.6  $\mu$ M). For primary glial cell cultures, the cells pretreated with OXY showed the lowest damage after  $H_2O_2$  exposure. Among the hydroxystilbenes tested, the 5  $\mu$ M of OXY was a more effective scavenger for nitric oxide (NO; 7.7  $\mu$ M) determined by spectrofluorimetric cell-free assay (Lorenz *et al.*, 2003). In agree with the results of Povichit and coworkers (2010a), OXY isolated from the heartwood of *A. lakoocha* showed almost 2 times potent antioxidant activity than resveratrol with the  $IC_{50}$  values  $0.43 \pm 0.03$  mg/mL by thiobarbituric acid-reactive substance (TBARS) method. Yoon and colleagues (2014) also reported the antioxidant capacity of fermented *Smilax china* root due to OXY that was determined by the 2,2'-azino-bis (3-ethylbenzthiazoline-6-sulfonic acid) (ABTS) assay.

### IV) Anti-inflammatory activity

The anti-inflammatory activities of OXY extracted from Mori cortex were evaluated using the carrageenin-induced inflammation model in rats. The results

showed OXY significantly reduced paw edema. The mechanism of action of the compound was examined on lipopolysaccharide (LPS)-induced responses in murine macrophage cell line RAW 264.7. Moreover, the researchers suggested that OXY inhibited nitrite accumulation in the culture medium via the dose-dependent inhibition of iNOS expression through down-regulation of NF-kappaB binding activity and significant inhibition of cyclooxygenase-2 (COX-2) activity (Chung *et al.*, 2003). Another mechanism in anti-inflammatory effects of OXY from *Morus alba*, was investigated by Chen and coworkers (2013). The results on leukocyte migration showed OXY suppressed CXCR4-mediated T cell migration via mechanistic activities of the inhibition of the MEK/ERK signaling pathway. The anti-inflammatory benefits of OXY may involve other immune cells. Furthermore, these findings confirmed by Lee *et al.* (2014) that OXY suppressed inflammatory mediated productions of NO, PGE<sub>2</sub>, IL-6, GM-CSF and also restrained mRNA and protein expressions of iNOS, COX-2, IL-6, and GM-CSF in LPS-stimulated macrophages cells. Moreover, OXY suppressed the phosphorylation of Akt and JNK and p38 MAPKs, and the NF-kappaB p65 subunit translocation into the nucleus. Therefore, OXY inhibited inflammatory responses by the blocking of MAPK or MEK/ERK and NF-kappaB signaling pathway in macrophages.

## **V) Anti-viral activities**

### **a) Anti-human immunodeficiency virus (HIV) activity**

In 1998, the first paper of anti-HIV effects of natural stilbenes “oligostilbenes” from leaves of *Hopea malibato* (Dai *et al.*, 1998) was published. Therewith, OXY extracted from *A. gomezianus* exhibited potent inhibition effect against a wild-type HIV-1/LAI and a moderate inhibitor of HIV (EC<sub>50</sub> 28.2 mM) *in vitro* (Likhitwitayawuid *et al.*, 2005). Wang *et al.* (2014) showed more potential anti-HIV-1 activities of OXY in butanol extract than other solvent extract in HIV-infected TZMB-L cells. Among tested stilbenes, OXY showed highest inhibition rate (93.18 ± 1.74%) at a concentration 100 µg/mL. Moreover, no cytotoxicity was found at a concentration ranged from 0.8-100 µg/mL.

### **b) Anti-herpes simplex virus (HSV) activity**

The active compound OXY from *A. lakoocha* Roxburgh has a potent inhibitory activities against HSV. The infection of two types of the DNA virus, HSV-1 and HSV-2 are transfer easily by direct contact to infected patients and becomes more

complicated diseases. HSV-1 is responsible to upper part of body infections such as encephalitis, corneal infection and facial infection, while HSV-2 is mostly related to the genital tract infection and neonatal herpes (Jagtap and Bapat, 2010). Since discover of binding of stilbenedisulfonic acid at the animal cells after cell membrane modification by HSV itself in 1978, the anti-HSV effects of the stilbenes become more interesting (Thompson *et al.*, 1978). Then, many reports on the effectiveness of OXY as anti-HSV compound were published by Likhitwitayawuid and his colleague. For example, they showed firstly the moderate inhibitory effect of OXY on viral growth with  $EC_{50}$  63.5 and 55.3  $\mu$ M for HSV-1 and HSV-2, respectively compared to efficient activity of acyclovir *in vitro* (Likhitwitayawuid *et al.*, 2005). Additionary, mechanism of action of OXY on cutaneous HSV infection *in vitro* Vero cells was determined (Chuanasa *et al.*, 2008). The results showed that the  $IC_{50}$  for plaque formation of OXY for clinical viral isolates, thymidine kinase (TK)-deficient and phosphonoacetic acid (PAA)-resistant HSV-1 were 19.8, 23.3, 23.5, 24.8, 25.5 and 21.7  $\mu$ g/mL, respectively. Moreover, OXY could inhibit viral replication at both early and late phase. The pretreatment of OXY also inhibited the viral replication of both HSV-1 and HSV-2. The anti-HSV-1 effect of OXY could be synergist when combination with acyclovir (ACV). Also, the effect of OXY against each ten clinical isolates of HSV-1 and HSV-2 were confirmed with  $IC_{50}$  20.9-29.5 and 22.2-27.5  $\mu$ g/mL for HSV-1 and HSV-2, respectively (Lipipun *et al.*, 2011). For *in vitro* skin permeation studies, the microemulsion incorporated OXY showed 93.04 times enhanced permeation through shed snake skin after 6 h compared to that of 20% OXY in Vaseline<sup>®</sup>.

The therapeutic efficacy of OXY was studied in mice cutaneous infected HSV. The data indicated topical administration at three times daily of 10% OXY cream was significantly more effective than that of 30% OXY ointment ( $p < 0.01$ ). Furthermore, the 10% OXY cream applied three times daily was as effective as that of 5% ACV cream applied five times daily in delaying the development of skin lesions and protection from death ( $p > 0.05$ ) (Lipipun *et al.*, 2011). In addition, the topical application of 20-30% OXY-microemulsion applied five times daily for 7 days after infection was suitable for keep the mice life from the HSV-1 infection as well (Sasivimolphan *et al.*, 2012). From these data, it demonstrated the success of the topical delivery of the OXY against cutaneous HSV infection. For oral OXY administration, the HSV infected mice was treated with 500 mg/kg/dose of OXY at 8 h before and three times daily. After 7

days treatment, the results showed the significant delay in herpetic skin lesion development ( $p < 0.05$ ). However, the death of the mice was not significantly reduced at this oral OXY dose when comparing to the control mice (2% DMSO solution). Furthermore, no toxicity after oral administration (3 times a day for 7 days) at this OXY dose (500 mg/kg/dose) was observed (Chuanasa *et al.*, 2008).

### **c) Other anti-viral activities**

Other than described above, OXY has anti-viral activities against other virus species. For example, OXY exhibited anti-varicella-zoster virus (VZV) activity with *in vitro*  $IC_{50}$  values between 12.80-12.99  $\mu\text{g/mL}$  for wild type, TK-deficient and two types of DNA polymerase mutants with ACV-resistance. A mechanism of OXY for this effect was different from ACV (Sasivimolphan *et al.*, 2009). Moreover, its anti-viral activity against African swine fever virus, which affected seriously to porcine production, has been reported (Galindo *et al.*, 2011). *In vitro* studies, the results displayed a potent and dose-dependent effect of OXY which extracted from mulberry twigs. Its anti-viral activity achieved a 98–100% reduction in viral titers at non-toxic concentration of OXY. The OXY inhibited viral DNA replication, late viral protein synthesis and viral factory formation.

## **VI) Neuroprotective activity**

Neuroprotective effects of OXY have been associated to its antioxidant and anti-inflammatory activity as described above. As in the paper published by Jin *et al.* (2002), OXY purified from mulberry twigs inhibited lipid oxidation in rat brain homogenate with  $IC_{50}$  value as 0.29  $\mu\text{M}$ . Oxidative stress was one of the major pathological factors affected to neuron cell death in brain injury. Thus, the inhibitory capacity of OXY on neuron apoptosis in transient rat middle cerebral artery occlusion (MCAO) model of brain ischemia was studied (Andrabi *et al.*, 2004). After twice intraperitoneal (i.p.) injection of OXY, OXY at 10 and 20 mg/kg reduced the neurological loss by significantly reduced the brain infarct volume about 54% and 63%, respectively, comparing to vehicle-treated MCAO rats. The decreasing of neuron apoptosis of OXY indicated by diminished loss of neuron proteins including MAP-2 and NeuN, decreased cytochrome c release from mitochondria leading to reduced caspase-3 activation in MCAO rats and also reduced DNA fragmentation. These results demonstrated that the neuroprotective effect of OXY in *in vivo* cerebral ischemia model may beneficial for

development as a therapeutic neuroprotectant to heal brain injury. Next, this research groups deeply investigated the ability of OXY across the blood–brain barrier (BBB) in healthy rats. The data of tissue extraction and *in vivomicrodialysis* method showed a low content OXY to penetrate the BBB in healthy animals. However, a 6.6-fold increased OXY levels in the infarct region of MCAO rat compared to control rats. The researchers suggested that OXY had direct protective effect in the brain by crossing the BBB and suitable use as synergistic agent for the treatment of neurodegenerative disorders that causally from oxidative or nitrosative stress (Breuer *et al.*, 2006). Weber and colleagues (2012) demonstrated the neuroprotective ability of OXY, which found in mulberry wood (*Morus alba* L.), on stretch-induced trauma in co-cultures of neurons and glia cells, or by exposing cultures to high levels of glutamate. The results showed OXY at 25-100  $\mu\text{M}$  significantly inhibited neuronal death after 24 h post-injury, however, it could not inhibit the neuronal loss after exposing to high glutamate concentrations (100  $\mu\text{M}$ ) *in vitro*. Other mechanism of neuroprotective effect of OXY related to Alzheimer's disease (AD) was assessed by Ban *et al.* (2006). OXY isolated from *Smilacischinaerhizome* (1-10 mM) significantly inhibited 10 mM Amyloid  $\beta$  protein ( $\text{A}\beta_{25-35}$ )-induced neurotoxicity on cultured rat cortical neurons which was measured a 3-[4,5-dimethylthiazol-2-yl]-2,5-diphenyl-tetrazolium bromide (MTT) assay and Hoechst 33342 staining. Moreover, the study implied that OXY prevents  $\text{A}\beta_{25-35}$ -induced neuronal cell damage by interfering with the increase of calcium ion, and then by inhibiting glutamate release and ROS generation. Besides its neuroprotectant against AD, stroke and trauma, OXY also occupied neuroprotective effects against Parkinson disease (PD). The finding of pre- and post-treated Neuroblastoma SH-SY5Y cells with OXY decreased release of lactate dehydrogenase, the activity of caspase-3, and the generation of intracellular ROS triggered by 6-hydroxydopamine (6-OHDA). This effect caused by penetrating cell membrane and then acting as an intracellular antioxidant of OXY. In addition, OXY evidently meliorate phosphorylation level of JNK and c-Jun and Akt signaling, and increased the SIRT1 levels, which may offer new pathways for the neuroprotective effects of OXY (Chao *et al.*, 2008).

## VII) Anti-cancer activities

Some studies reported the cytotoxicity to cancer cells of OXY. For example, OXY showed inhibition effects on protein kinase C (PKC) (Hu *et al.*, 1995) and



cytochrom P450 (CYP) 1A1,1A2, and 1B1, which probably associated to the tumor promoters (Kim *et al.*, 2002a). Even no cytotoxicity of OXY on human KB nasopharyngeal cells, BC breast cancer cells and NCI-H187 lung cancer cells, but the *cis*-isomer methoxy derivatives of OXY showed potent toxic effects to the three cancer cells with  $IC_{50} \leq 1 \mu\text{M}$  (Likhitwitayawuid *et al.*, 2006). However, the *in vitro* anti-breast tumor cell activity of OXY, extracted from *Smilax china* L., was firstly demonstrated (Wu *et al.*, 2010). The MTT assay, the  $IC_{50}$  values of OXY were 4.5 and 5.6  $\mu\text{g/mL}$  against MCF-7 and MDA-MB-231 cells, respectively. Moreover, it induced cell apoptosis with apoptosis rate of 32.8% and 30.9% for MCF-7 and MDA-MB-231, respectively. Likewise, Bertram and Davies (2009) presented the potential toxicity of OXY on PC-3 Prostrate cancer cells ( $IC_{50} \sim 7 \mu\text{g/mL}$ ) observed by Alamar Blue Assay. In addition, a 2-time more potent toxicity than resveratrol in HT-29 human colon cancer cells was evaluated by MTT test (Li *et al.*, 2010).

### VIII) Other activities

Other than the activities described above, OXY exhibited a 5-fold stronger anti-glycation activities than aminoguanidine with  $IC_{50}$  was 2.0  $\mu\text{g/mL}$  (Povichit *et al.*, 2010b). In addition, OXY showed a potent inhibitory effect ( $IC_{50} 32.80 \pm 0.96 \mu\text{M}$ ) of  $\alpha$ -glucosidase, which plays a role in glycemic control leading to achieve normal glycemia in diabetic patients. Moreover, the noncompetitive inhibitor of OXY was stronger than acarbose, anti-diabetic drug ( $IC_{50} 229.80 \pm 1.19 \mu\text{M}$ ) (He and Lu, 2013). Lastly, OXY decreased the blood sugar level in mice therefore it could be promoted as a novel hypoglycemic drug for relief diabetes mellitus (Xu *et al.*, 2014).

Another one is anti-microbial activities of OXY including anti-bacterial and anti-fungal activity. For instance, Mazimba *et al.* (2011) found that OXY had the activities against many bacteria types such as *S. aureus*, *B. subtilis*, *M. flavus*, *S. faecalis*, *S. abony* and *P. aeruginosa* with the minimum inhibition concentration (MIC) of 125-250  $\mu\text{g/mL}$ . Also, the MIC of OXY for three strains of methicillin-resistant *S. aureus* (MRSA) was at 125  $\mu\text{g/mL}$ . Moreover, the finding indicated that OXY combined with ciprofloxacin or gentamicin could decrease bacterial numbers to less than the detectable limit after 24h by time-kill assay (Joung *et al.*, 2015). For anti-fungal activity, OXY also showed activity against many human pathogenic fungi including filamentous dermatophytes such as *T. mentagrophytes* LMGO 09, *T. rubrum* LMGO 08, *T. rubrum*

LMGO 06, and Yeast species such as *C. Krusei* LMGO 174 strains with the MIC 8-16 µg/mL (Basset *et al.*, 2012).

### 1.2.1.3 Physicochemical properties and stability of OXY

The report on the isolation of OXY from heartwood of *A. lakoocha* Roxburgh (Ma-Haad) was first introduced in 1957 (Mongolsuk *et al.*, 1957). The organic solvents such as ether (Mongolsuk *et al.*, 1957), acetone (Djapic *et al.*, 2003) and ethanol (Maneechai *et al.*, 2009), had been used for decades as solvents for OXY extraction from the plants. However, these solvents are considerable toxic to human and environment. Instead of these, other eco-friendly procedures are interesting for production of OXY such as bioconversion using  $\beta$ -glucosidase (Kim *et al.*, 2010). There are many methods for identification of OXY in the extract such as determinations of crystal color and melting point, fluorescence under UV light, thin layer chromatography (TLC) and high performance liquid chromatography (HPLC) (Hu *et al.*, 1995; Huang *et al.*, 2008a; Maneechai *et al.*, 2009).

The off-white powder of OXY with >99% purity yielded using efficient aqueous extraction and purification had been reported by Likhitwitayawuid group (Sritularak *et al.*, 1998; Likhitwitayawuid *et al.*, 2005). OXY is one member of stilbene group, contains four hydroxyl (-OH) groups in the chemical structure namely 2,4,3',5'-tetrahydroxystilbene (Figure 2). Its structure has a *trans*-conformation of C=C double bond between benzene rings which occupies 9.39 degrees of angle (Xu *et al.*, 2014). The needle-shaped crystals of OXY are connected with water molecules through hydrogen bonds between OH groups of OXY into a three-dimensional structure (Deng *et al.*, 2012). The natural polyphenolic OXY has a molecular formula of C<sub>14</sub>H<sub>12</sub>O<sub>4</sub> with molecular weight 244.24 g/mol. The compound has melting point of 196-204°C and shows blue fluorescence under UV light in a TLC system. The ability of UV light absorption due to aromaticity of its structure has been reported (Hu *et al.*, 1995; Xiong *et al.*, 2008; Zhao *et al.*, 1998). Moreover, the infrared absorption with maximum absorption at 3290 cm<sup>-1</sup> and other absorption at 1400-1600 cm<sup>-1</sup> represented OH-stretching and aromatic structure, respectively (Sritularak *et al.*, 1998).

OXY is freely soluble in methanol, ethanol, acetone, soluble in acetonitrile, dimethyl sulfoxide (DMSO), dimethyl formamide, ether and also water which

presented as  $\log P = 1.1$ . But it is insoluble in chloroform (Takemoto *et al.*, 2010). According to its structure, OXY is chemically unstable and pH-sensitive. When the pH of the buffer was lowered to 6.0, it can keep >95% of intact OXY amount during 2 h. It means that the compound is not stable in basic conditions (Mei *et al.*, 2012). Furthermore, OXY is easily oxidized by prooxidant agents (Rodríguez-Bonilla *et al.*, 2010). Xu *et al.* (2014) recommended the suitable storage conditions was in aqueous solvent at pH 5.38 and dark environment at  $-40^{\circ}\text{C}$  to keep its good stability.

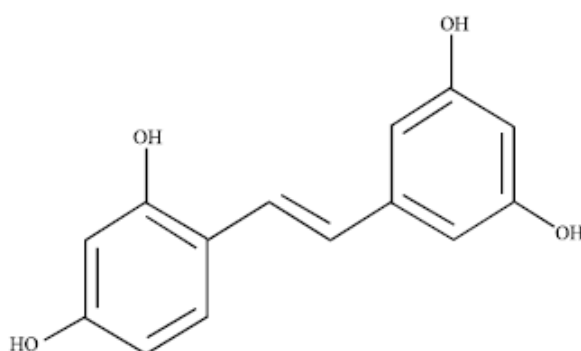


**Figure 2** Chemical structure of oxyresveratrol (Xu *et al.*, 2014)

#### 1.2.1.4 Pharmacokinetic properties of OXY

##### I) Absorption

The low plasma level of OXY after oral administration has been documented. Charoenlarp *et al.* (1991) have demonstrated the oral absorption of OXY after 3 g OXY administered OXY to 9 male healthy volunteers. The plasma concentrations-time profile of OXY, determined by HPLC method, showed slow absorption with maximum concentration ( $C_{\max}$ ), time to reach maximum concentration ( $T_{\max}$ ), and absorption rate constant of OXY were  $0.70 \pm 0.35 \mu\text{g/mL}$ ,  $1.38 \pm 0.16 \text{ h}$  and  $0.74 \pm 0.09 \text{ h}^{-1}$ , respectively. As reported by Qiu *et al.* (1996), OXY converted from mulberroside A, a main compound in Mori cortex extract, showed the absorption ratio of 50% in blood circulation in rats. Tian *et al.* (2014) developed highly sensitive HPLC-MS/MS method to determine pharmacokinetic of OXY in Sprague-Dawley rat. By this system,  $C_{\max}$  of OXY ( $0.42 \pm 0.44 \mu\text{g/mL}$ ) was attained at  $0.50 \pm 0.19 \text{ h}$  detected.

However the absorption rate obtained from different species could be diverted. Mei *et al.* (2012) explained the absorption behavior of OXY using Caco-2 cells permeability model. The study showed passive diffusion of OXY across Caco-2 cells with intermediate permeability ( $P_{app} \times 10^{-6}$  cm/s) which predominantly involved efflux-mediated mechanisms including P-gp and MRPs family. The higher secretory transport than absorptive transport consequences to efflux ratio (ER) of OXY was more than 1 and increased inversely with dose tested suggesting OXY was substrate of the efflux transporters. Limitation of the oral absorption of OXY was due to its high polar affecting to its intestinal permeability and involving efflux pump transport.

## II) Distribution

In 2006, Breuer and colleagues investigated the extent of OXY across the BBB in rats by tissue extraction method. The results revealed that low amount of OXY in brain tissue ( $0.038 \pm 0.010$   $\mu\text{g/g}$  tissue) after i.p. injection of 40 mg/kg OXY. While, greater amount of OXY was obtained in liver ( $0.139 \pm 0.007$   $\mu\text{g/g}$ ) and plasma ( $0.626 \pm 0.059$   $\mu\text{g/mL}$ ) than in brain. After oral administration of Smilacaceae extract of *Smilax china* L., the results showed high tissue distribution of OXY in heart, liver, spleen, lung and kidney. Moreover, the large volume of distribution ( $V_d$ ) of OXY ( $77.73 \pm 21.90$  L/kg) was reported (Bertram and Davies, 2009).

## III) Metabolism

The low oral bioavailability of OXY (~14%) was mainly due to the extensive hepatic metabolism of this compound (Bertram and Davies, 2009). *In vitro* metabolic stability in humans and rat liver microsomes (LMs) suggested that OXY underwent extreme phase II metabolism (major glucuronidation and minor sulfation), that could predict significant hepatic first-pass metabolism in human and rats (Figure 3). Based on these finding, four monoglucuronides and one monosulfate OXY formed in both human and rat LMs. However, rat LMs presented higher activities of both conjugation reaction for OXY than those of human. Main metabolite of OXY in human was detected as 2-O- $\beta$ -D-glucuronosyl OXY (~93% of total OXY glucuronides), while the exact structure of major metabolite in rat (~85% of total glucuronidated OXY) is under identification. Moreover, the glucuronidated metabolism of OXY in human LMs was compared to human intestinal microsomes (IMs). The glucuronidation by UDP-glucuronosyl transferase (UGT) isoforms preferred at C-2 position resulted in the G4

was predominant metabolite in both liver and intestinal microsomes. The finding indicated that first-pass metabolism of OXY in human occur in both liver and intestine. The main UGT responsible for OXY glucuronidations in LMs was UGT1A9, while multiple UGT isoforms as UGT1A1, 1A3, 1A6, 1A7, 1A8, 1A10 and 2B7, catalyzed the glucuronidation in IMs (Hu *et al.*, 2014).

In agreement with the *in vitro* finding, Huang *et al.* (2010) has identified the metabolic pathway of OXY in rats after oral dosing of 100 mg/kg OXY. Based on LC-MS/MS analysis, seven conjugated metabolites of OXY were detected in either urine or bile including glucuronide, methyl and sulfate. These conjugates offered increased hydrophilicity of OXY and ready for excretion. The proposed pathway of OXY metabolism is shown in Figure 4.

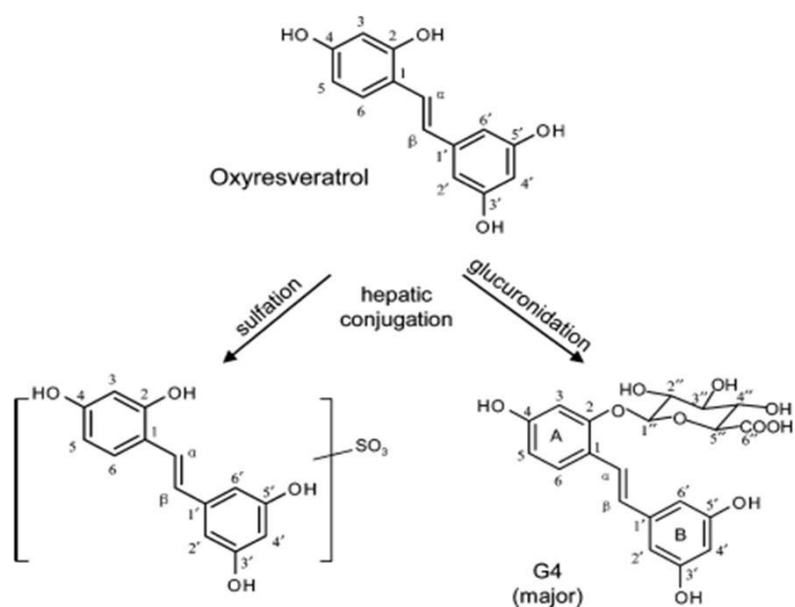


**Figure 3** The metabolic pathways of OXY proposed from *in vitro* hepatic microsomes of both rat and human (adapted from Mei *et al.*, 2012).

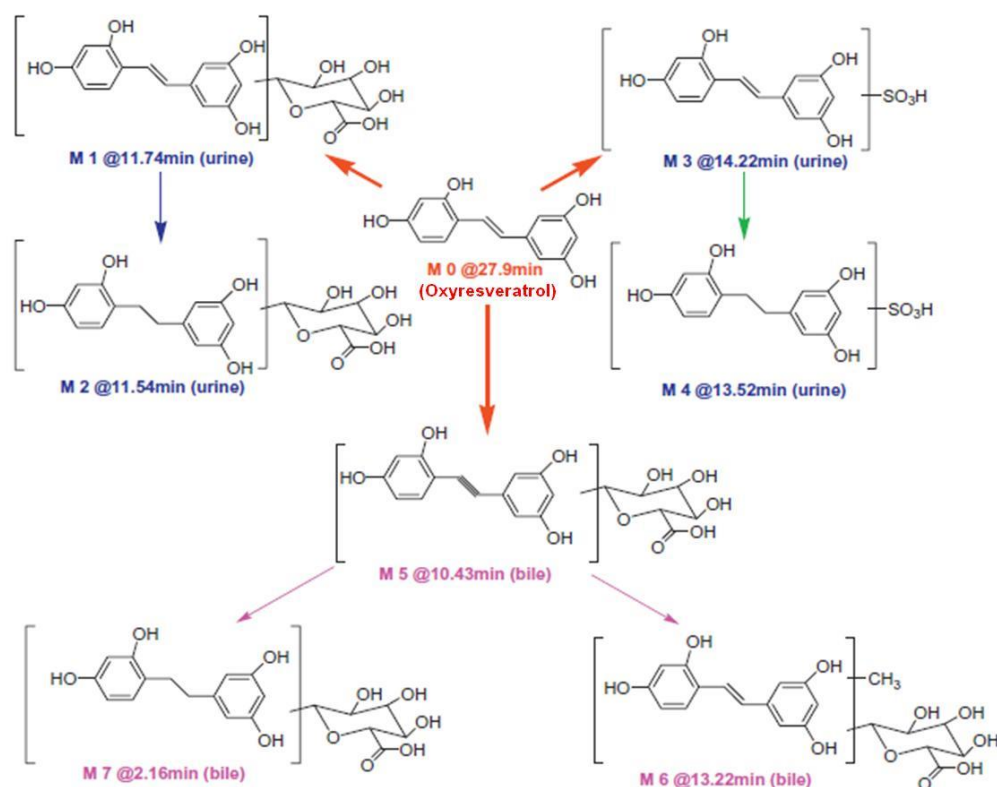


**Figure 4** The metabolic pathways of OXY proposed from *in vivo* studies after oral administration of 100 mg/kg OXY (Huang *et al.*, 2010).

#### IV) Excretion

As known in the blood stream, OXY was cleared by phase II hepatic conversion and predominantly excreted in metabolite forms in both urinary and biliary excretion. Moreover, low extent of unchanged form of OXY was also rapidly eliminated with elimination rate constant of  $0.73 \pm 0.09 \text{ h}^{-1}$  which was same as absorption rate constant. This resulted in a short half-life time in plasma ( $t_{1/2}$ ;  $0.96 \pm 0.11 \text{ h}$ ) in the human body of the male healthy volunteers after intake 3 g of OXY (Charoenlarp *et al.*, 1991). Bertram *et al.* (2010) quantified urinary disposition of OXY after oral dosing OXY suspension in 2% methylcellulose (230 mg/kg) in rat. The pharmacokinetic data indicated that high elimination rate of  $\sim 0.59 \text{ h}^{-1}$  and low unchanged fraction excreted in urine ( $F_e$ ) of 0.027% with mean  $t_{1/2}$  in urine of 5.30 h. In addition, the glucuronide conjugate was found as the major form of OXY excreted in urine. Furthermore, Huang *et al.* (2009b) published the cumulative excretion of OXY, which from the traditional Chinese plant, in bile and urine samples was 0.29% and 0.84%, respectively. Last, Tian

and coworkers (2014) presented the pharmacokinetics of OXY in rat plasma after orally received low dose of 10 mg/kg. The data showed high clearance of OXY following  $CL_z/F$  of  $15.20 \pm 1.68$  L/h/kg.

#### 1.2.1.5 Strategies for improving oral bioavailability of OXY

OXY possesses many pharmacological and biological activities that are tremendous advantages to be medical benefits. However, its low oral bioavailability after oral administration caused by the low permeation across intestinal epithelium associated to efflux mediated mechanism, extensive first-pass metabolism by liver and intestine, and rapid excretion restrict its clinical application. Based on effective strategies, an oral OXY bioavailability could be improved by overcome its drawbacks using potential delivery systems. However, only topical delivery systems of OXY were successful developed such as ointment, cream, microemulsion and liposome. Also, beta-cyclodextrin complexes with OXY is another promising system. Nevertheless, until present, there is still no report on effective delivery systems of OXY for oral administration.

Recently, the delivery system of OXY by complexation with natural cyclodextrin has been introduced to improve its solubilization and protect from prooxidant agents. The system was claimed to enhance bioavailability of many compounds (Rodríguez-Bonilla *et al.*, 2010). *In vitro* physicochemical studies indicated that the efficient interaction of OXY with beta-cyclodextrin was more than with alpha- and gamma-cyclodextrin. In all the conditions tested, OXY could form complexes with beta-cyclodextrin at a 1:1 stoichiometry. Moreover, the formation constants ( $K_f$ ) values suggested that a strong of the complexes depended on various factors like proportion of organic solvents, temperature, pH, type of cyclodextrin and structure of drug compound.

Topical formulations of OXY such as ointment, cream, microemulsion and liposome have been developed in recent years for treating viral infections. For example, microemulsion formulations of OXY were prepared and its efficacy in treatment of cutaneous HSV-1 infection in mice was evaluated (Sasivilomphan *et al.*, 2012). The optimized o/w microemulsion which consisted of 10%, 35%, 35%, 20% w/w of isopropyl myristate oil, Tween80<sup>®</sup>, isopropyl alcohol and water, respectively, was successful produced with high solubility of OXY as  $196.34 \pm 0.80$  mg/mL. After 20% w/w

OXY incorporation, the obtained droplet size and polydispersity index (PDI) was  $179.90 \pm 84.17$  nm and  $0.34 \pm 0.01$ , respectively. The OXY-microemulsion was stable after accelerated and long-term stability study. The microemulsion loaded 20% OXY about 93-folds improved *in vitro* skin permeation comparing to OXY in Vaseline<sup>®</sup>. In addition, the developed microemulsion at 20–30% w/w of OXY was topically applied to cutaneous HSV-1 infected mouse five times daily. The formulations showed significant effective in treatment by delayed skin lesions development and protected the death comparing to the untreated control. The OXY contained microemulsion was more potent than 30% w/w OXY in Vaseline<sup>®</sup> and its potency also was equal with commercial product (5% w/w ACV cream).

Another interesting system is liposomes which can carry both hydrophilic and hydrophobic compounds. Nimthasanasiri *et al.* (2015) achieved the optimized liposome of OXY, extracted from heartwood of *A. lakoocha* Roxb, using Tween80<sup>®</sup> as stabilizer. The OXY-liposome had particle size around 49-50 nm with low size distribution in range of 0.179-0.296 (PDI) and also showed the stable particles with zeta potential (ZP) of -28.0 to -34.1 mV. Furthermore, the liposomes containing 20 mg of OXY had high entrapment efficiency (EE) about 83-89%. Besides a topical delivery, both lipid-based systems including microemulsion and liposome have been remarkably potential to deliver numerous active molecules in various routes including oral route.

Other than these formulations, an idea of oral delivery systems of OXY might be inspired from other topical formulations of OXY. For example, Lipipun *et al.* (2011) introduced efficient formulation of cream containing 10%-20% w/w of OXY to treat cutaneous HSV infection. The results from *in vivo* studies indicated that both 10% and 20% OXY cream applied three times daily ( $p < 0.01$ ) were significantly more effective than that of 30% OXY in Vaseline<sup>®</sup> and equal potency with 5% ACV cream applied two times daily ( $p > 0.05$ ). Regardless of the frequency, the potency of the OXY-based cream depended on applied dose. In this study, cream formulation was prepared using emulsion-based technique. Another example using this technique is o/w emulsion (lotion) contained 0.10% w/w *A. lakoocha* extract. The o/w emulsion containing OXY was significantly higher whitening efficacy than the lotion base after 2-3 weeks of daily application ( $p < 0.05$ ). This technique could produce pharmaceutical formulations for many applications including oral drug delivery such as nanoemulsion and nanoparticles. Comparing to cream, OXY-based ointment was significantly less efficacy against HSV



skin infection owing to high dose (30% w/w of OXY) and high frequency (five times daily) of topical application needed (Chuanasa *et al.*, 2008).

## **1.2.2 Lipid nanoparticle systems**

### **1.2.2.1 Introduction**

During the decades, lipid-based drug delivery systems (LBDDS) have received much attention in improving oral bioavailability of several drugs. The use of traditional colloidal systems e.g. emulsion, liposome, polymeric microparticles and nanoparticles, has some limitations such as cytotoxicity and slow degradation of the polymeric material, residual contamination of organic solvents and degraded products, physical instability and drug leakage during storage, a burst release of drugs, and limited or expensive large scale production (Diederichs and Müller, 1994; Schwarz *et al.*, 1994; Müller *et al.*, 1996). The lipid nanoparticles have been introduced to overcome these drawbacks of other colloidal carriers. Owing to their many advantages especially using of physiologically acceptance lipids, the lipid nanoparticles has become promising manner for therapeutic desires. The lipid nanoparticles comprised of sole solid lipids or mixture of solid lipid and liquid oil surrounded by a single surfactant and/or mixed surfactant and a co-surfactant. For oral delivery, the product named lipid nanopellets have been firstly produced by lipid recrystallization of solid microparticles after emulsion cooling process to RT (Speiser, 1990; Severino *et al.*, 2011a). The lipid nanoparticle systems such as solid lipid nanoparticles (SLN) and nanostructured lipid carriers (NLC) have enhanced oral bioavailability of different entrapped compounds of both types of hydrophobic and hydrophilic compounds (Almeida and Souto, 2007; Souto and Müller, 2010).

### **1.2.2.2 Solid lipid nanoparticles (SLN)**

Solid lipid nanoparticles (SLN) are one type of lipid nanoparticles which consist of a solid lipid matrix emulsified by surfactant and/or co-surfactant. The particles are solid at both room and body temperatures. A mean particle size of the SLN is about 50-1000 nm (Üner, 2006). Although, the SLN possess many advantages over other colloidal carriers as described below, however it has some limitations such as low

loading capacity of drugs and drug expulsion during storage (Muchow *et al.*, 2008). Long term instability of SLN is due to the perfect crystalline structure of the lipid matrix. A drug is usually accommodated between the fatty acid chains or in amorphous clusters in crystal imperfections. The dense perfection of lipid crystal of SLN would have little space to add the drugs. Moreover, rearrangement of lipid molecules from high to low energy state results to expulsion of drug during storage (Bunjes *et al.*, 2003).

**Advantages** (Müller *et al.*, 2002; Severino *et al.*, 2011a)

- 1) Biocompatibility and safe due to the use of physiologically acceptance compositions which generally recognized as safe (GRAS) status for oral delivery
- 2) Easy feasibility to sterilize and to scale up in industry
- 3) Many simple methods for SLN preparation which no organic solvent required leading to no residual contamination in the formulations
- 4) Protection of drug incorporated particles from chemical and enzyme degradation
- 5) Controlled drug release for several hours results to enhance oral bioavailability of the drugs (zurMühlen *et al.*, 1998; Müller *et al.*, 2000; Hu *et al.*, 2006)
- 6) Improvement of long-term stability of non-stable drugs compared to traditional lipid formulations (Freitas and Müller, 1998; 1999)
- 7) Drug targeting by surface modification of the particles which reduces first pass metabolism and elimination of drug from the body (Lockman *et al.*, 2003)
- 8) Enhanced membrane permeability and inhibited efflux pump mechanism leads to increase drug absorption

Many factors have influenced on types of lipid nanoparticles such as nature of drug and lipid, type and amount of surfactant, preparation method, and temperature. Principally, there are three different pattern of drug incorporation in the SLN (Müller *et al.*, 1995; Müller *et al.*, 2000; Mehnert and Mäder, 2001) as present in Figure 5. First, a homogeneous matrix model (model 1) presents as solid solutions by pattern of molecularly dispersed drug throughout in the particle matrix. The release of drug from this model arises via drug diffusion from the solid lipid combines with erosion of the matrix in the GI tract. Second, drug-enriched shell model (model 2) can be explained via either lipid precipitation or drug solubility during preparation. At higher temperature, drug can dissolve more in aqueous surfactant solution (outer phase) and some part of drug moves out lipid phase during homogenization process. During cooling, the lipid core solidified before moving back of drug into lipid matrix leading to

the precipitated drug enriched in the particle shell. Thus, a burst release has been found from this model. Third, drug-enriched core model (model 3) can be described via drug preferentially dissolved in melted lipid phase at high temperature and during cooling occurred supersaturation and then drug precipitated before solidification of lipid particles. This might produce more sustained release.

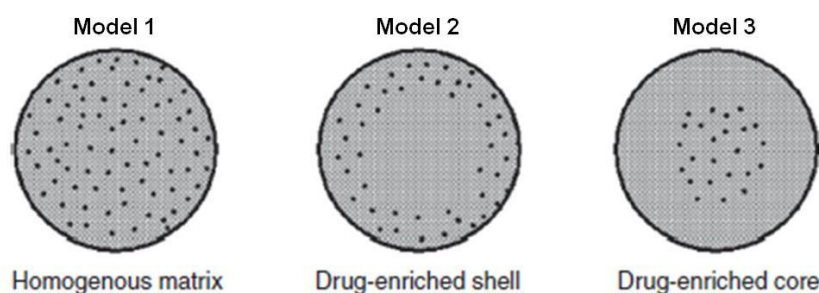


**Figure 5** Three different drug incorporation model of the SLN (Modified from Muchow *et al.*, 2008).

### 1.2.2.3 Nanostructured lipid carriers (NLC)

Nanostructured lipid carriers (NLC), second generation of lipid nanoparticles, have been produced to overcome the difficulties of SLN (Müller *et al.*, 2000). Approach of the NLC performs by imperfect special structure of lipid matrix to achieve more space of drug incorporation in order to improve drug loading and minimize drug leakage during storage. Based on this concept, some part of purified solid lipids is replaced with liquid lipid (oil). After solidification, the obtained nanoparticles are still solid at room and body temperatures and have a less-ordered crystalline structure of lipid matrix (Severino *et al.*, 2011b). Therefore, the difference of the two types is SLN produced from only solid lipid, while NLC was from mixing of solid lipid and oil (Muchow *et al.*, 2008). Generally, there are three types of the NLC (Figure 6) (Üner, 2006). First, imperfect type of NLC (type 1) is lipid matrix structure shows imperfectly by blending of different crystalline lipids with small amounts of chemically different oil leading to high drug loading in molecularly amorphous form. Next, amorphous type of NLC (type 2) occurs via obstruction of crystallization process of lipid matrix by incorporating special lipids like hydroxyoctacosanyl hydroxystearate, medium chain triglycerides (MCT) or isopropyl myristate. This NLC type is solid matrix in an

amorphous state, thus protect expulsion of drug (Radtke and Muller 2001). Last, multiple type of NLC (type 3) produces by distribution of multiple oil in fat in water (O/F/W). Generally, the solubility of the drug in the lipid phase decreases during the cooling process and the crystallization process during storage. Moreover, the solubility of some drugs in liquid oil is greater than in a solid lipid. Therefore, incorporating of liquid oil at higher quantity to the lipid phase produces oily nanocompartments forced by phase separation process. This NLC type could be load high drug amounts and also prevent drug expulsion by less ordered crystalline structure of NLC (Jenning *et al.*, 2000).

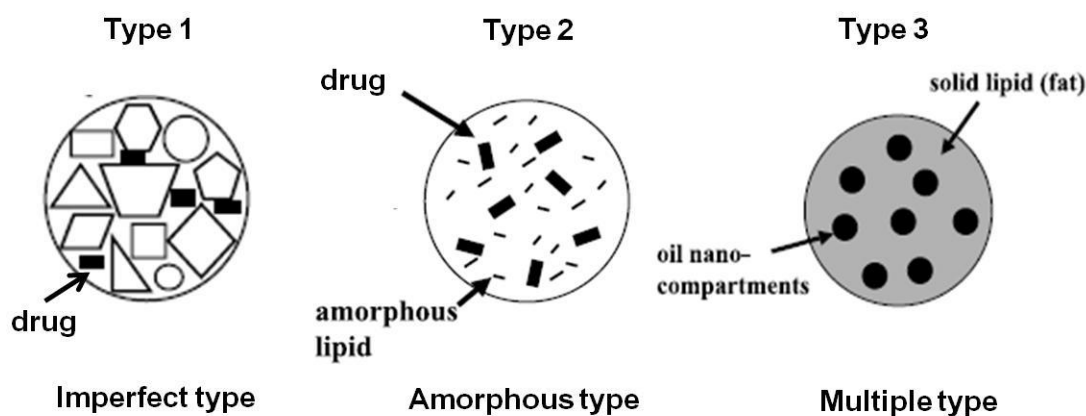


**Figure 6** Three different types of the NLC (Modified from Müller *et al.*, 2002).

#### 1.2.2.4 Compositions of lipid nanoparticles

The compositions are one of the key factors affecting properties of the lipid nanoparticles. First, the solid lipid, used as solid matrix of the nanoparticles, may influence on crystallization of the lipid particles upon cooling. This property affects to stability, release characteristics of the entrapped compound from the SLN and also loading capacity for the active compound. Moreover, the lipids possess absorption-promoting properties. Many types of lipid have been used such as triglycerides, partial glycerides, fatty acids, hard fats and waxes (Severino *et al.*, 2011a). However, pure homogenous lipids which generally used for SLN production result to low drug loading capacity, aggregation and instability of the lipid nanoparticles during cooling and storage process. So, heterogeneous lipids prefer for nanoparticle formation because generating less ordered structure (Mehnert and Mäder, 2001). As in the NLC production, a

combination of different lipid types or structures is used such as combination of solid lipid and oil. For example, the use of naturally occurring lipids composed of mono- di-, triglycerides lipid mixtures which contain fatty acids of varying chain lengths and degrees of unsaturation. The triglycerides are classified based on chain lengths as short (<5 carbons), medium (6-12 carbons), or long chain (>12 carbons). The increase of the length of the fatty acid chain and decrease of the degree of unsaturation affect to the melting point of the lipids (Hauss, 2007). Thus, understanding of the polymorphism, crystallinity and physicochemical structure of the lipid should be considered to produce good characters of lipid nanoparticles.

Another important composition for lipid nanoparticles manufacturing is surfactant alone or combination with co-surfactant. Both type and concentration of surfactants play a role in the stability of the lipid nanoparticles after preparation by repulsive interactions to prevent the agglomeration of the particles. Moreover, hydrophobic interaction between the surfactants and the lipid molecules prevents re-crystallization process of the lipid matrix during storage (Bunjes *et al.*, 2003). Also, the approximate quantity of surfactant influences the final particle size of the particles. Thus, the selection of proper surfactant is based on its properties such as charge, molecular weight, chemical structure, and hydrophilic-lipophilic balance (HLB). The HLB defines to the balance of hydrophilic and lipophilic groups that is benefits to choose the ideal surfactant at the suitable concentration. These are necessary to achieve good physicochemical properties of the systems (Weiss *et al.*, 2008). The solid lipid and surfactant/co-surfactant commonly employed in the lipid nanoparticles production for oral delivery have been summarized in Severino *et al.*, 2011a. The liquid lipids (oils) generally used in the preparation of the NLC for oral delivery is presented in Table 1.

**Table 1** Summary of liquid lipids (oils) used in the preparation of the NLC for oral delivery

Liquid lipids (oils)	Classification	References
Caprylic /Capric Triglyceride (Miglyol <sup>®</sup> 812, Labrafac <sup>®</sup> CC, Lexol <sup>®</sup> , Estasan 3575 <sup>®</sup> )	Medium chain triglyceride	Jores <i>et al.</i> , 2004; Lin <i>et al.</i> , 2007a; Zhuang <i>et al.</i> , 2010; Severino <i>et al.</i> , 2011b; Esposito <i>et al.</i> , 2012; Fang <i>et al.</i> , 2012; Neves <i>et al.</i> ,

Liquid lipids (oils)	Classification	References
		2013; Sangsen <i>et al.</i> , 2015
Lutein (20% lutein dispersed in corn oil)	Carotenoids (Long chain fatty acids)	Liu and Wu, 2010
Soybean oil	Long chain fatty acids	Zhang <i>et al.</i> , 2011
Oleic acid	Long chain fatty acids	Tiwari and Pathak, 2011
Olive oil	Mixed long chain fatty acids	How <i>et al.</i> , 2011
Squalene	Triterpene	Chen <i>et al.</i> , 2010

#### 1.2.2.5 Preparation methods of lipid nanoparticles

##### I) High pressure homogenization method

High pressure homogenization is a well-known method of lipid nanoparticles preparation for large scale industry. This technique can be divided into hot and cold homogenization techniques. Principle of both techniques is reducing the particle size by high pressure forces particle through small capillaries under extreme turbulence and shear force in order to obtain many tiny particles. For hot homogenization technique, the drug is solubilized in lipid phase which is melted at higher temperature of 5–10 °C over melting point. After that, the drug in melted lipid is dispersed in a hot aqueous surfactant phase at same temperature. The pre-emulsion obtains using high speed stirrer and then is homogenized by a high pressure homogenizer to produce o/w nanoemulsion. During cooling to RT, the lipid crystallization of the nanoemulsion leads to form the lipid nanoparticles. This technique is mostly suitable for lipophilic drugs. Meanwhile, cold homogenization technique is more suitable for labile drug and hydrophilic drugs since solid matrix reduces drug partitioning into aqueous phase and thermal exposure time of the drug (Müller *et al.*, 1995; Mehnert and Mäder, 2001). This method produces homogeneous particles in nanosized range, high yield of lipid particle production, reproducibility, no required organic solvents and possibility to scale-up production industry (Üner, 2006).

## **II) High shear homogenization and/or ultrasonication method**

High shear homogenization and ultrasonication are traditional production method of solid lipid nanodispersion. The simple and easy method requires instrument usually used in laboratory. Lipid phase and aqueous surfactant phase are separately heated at similar temperature and then the melted lipid is dispersed in the aqueous phase under stirrer. The dispersion continuously homogenized using high shear homogenizer or probe ultrasonicator. After that, the nanoemulsion is solidified to obtain lipid nanoparticles during cooling. Although this method has no organic solvent used, but physical instability during storage is observed. To improve stability of the system, combination of two production methods, reduction of lipid concentrations and increase of surfactant concentration were employed. (Speiser, 1990; Mehnert and Mäder, 2001; Mei *et al.*, 2003).

## **III) Microemulsion method**

This method produces the lipid nanoparticles followed by separate heating lipid phase and aqueous phase of surfactant/co-surfactant at the same temperature. Then, the aqueous surfactant solution is added into molten lipid under stirring and further obtains precipitated nanoparticles by dispersing the warm o/w microemulsion in large volume of cold water (about 1:50) under continuing stirrer (Gasco, 1997). To concentrate the particles, the ultrafiltration and lyophilization might be use. Solid lipids with low melting point about 50-70 °C are suitable for this technique. Unfortunately, difficult removing of plenty volume of water, high surfactant concentrations and some organic solvent used e.g. butanol are disadvantages of this method (Igartua *et al.*, 2002).

## **IV) Solvent emulsification evaporation or diffusion method**

This method provides the lipid nanoparticles by two different kinds of solvent including a water immiscible solvent e.g. toluene and chloroform and a water miscible solvent e.g. benzyl alcohol and ethyl formate. For the organic solvent, the lipid is solubilized in such solvent and then the lipid solution is emulsified in aqueous surfactant solution under stirring. Then, the solvent is evaporated at ambient condition or pressure reducing condition. The lipid nanoparticles are obtained by lipid precipitation upon solvent evaporation process (Sjöström and Bergenståhl, 1992; Shahgaldian *et al.*, 2003). The advantage of this method is no heating step in the preparation process.

Alternatively, use of the water miscible solvent in solvent emulsification-diffusion method is based on solvent diffusion in water upon precipitation of lipid nanoparticles. This method needs saturated organic solution in water to dissolve the lipid at high temperature. After that, this lipid solution is emulsified by adding aqueous surfactant solution under agitation to obtain o/w emulsion. When adds enough volume of water, which typical volume ratios of lipid solution to aqueous solution, are about 1:5-1:10 (Müller-Goyman and Schubert, 2003), the lipid nanoparticles precipitated by diffusion of organic solvent through the outer water phase. Then separating of the lipid nanoparticles is by centrifugation (Hu *et al.*, 2002; Quintanar-Guerrero *et al.*, 2005). However, the limitations of the method are toxicity from solvent residues in the formulations and the low particle concentration (< 15%) results in need more the concentration step (Trotta *et al.*, 2003).

#### **V) Water-in-oil-in-water double emulsion (w/o/w) method**

This method is developed from solvent emulsification evaporation to entrap the hydrophilic drug in the internal water phase of a w/o/w double emulsion. The technique operates by use of stabilizer to prevent drug partition into external phase during solvent evaporation process (Cortesi *et al.*, 2002). However, the obtained particles from this method are in large size which mostly micrometer range called lipospheres.

### **1.2.2.6 Characterization of lipid nanoparticles**

#### **I) Particle size and size distribution**

Particle size and size distribution are essential parameters of basic particle characterization. There are various factors affect both characters of the lipid nanoparticles for example lipid matrix, drug to lipid ratio, surfactant mixture and production processes. In addition, these parameters reflect stability of the nanoparticles. The photon correlation spectroscopy (PCS) is widely employed to measure the particle size. This method is indirect method which measures fluctuation of scattered light occurred from particle movement. The particle size in the range of nanometer to micrometer can be detected by this method (Sawant and Dodiya, 2008).



## **II) Particle charge**

Zeta potential (ZP) is used for indirect measurement of surface charge of the particles. Generally, the surface charge of the particles occurs from functional groups of the compositions or ion absorption at the surface of the particles. This value is measurement of hydrodynamically shear force around the particles or shear plane which could predict physical stability of colloidal formulations. In general, high ZP of the charged particles represents less particle aggregation due to electrical repulsion. The ZP values is greater than  $\pm 30$  mV indicating good physical stability while the value is higher than  $\pm 60$  mV indicating well stability of the formulation along its shelf-life. However, this rule is not included for the system containing steric or nonionic emulsifier, PEGylated molecules or large compounds (Freitas and Muller, 1998; Shahgaldian *et al.*, 2003).

## **III) Drug entrapment efficiency and loading capacity**

The entrapment efficiency (EE) represents the efficiency of the lipid matrix that could entrap the drug amount related to the initial incorporated drug. While, loading capacity is generally expressed percent of drug loading based on the lipid matrix. In order to assess the efficiency of drug entrapment, the lipid phase is separated from dispersed aqueous medium by different methods such as dialysis method (Gokce *et al.*, 2012), ultrafiltration (Neves *et al.*, 2013) and gel filtration (Jain *et al.*, 2005). Ultrafiltration and dialysis method use the membrane with different molecular weight cut-off and centrifugation to separate two phases. For ultrafiltration method, the sample is placed in the upper chamber and then moves into the recovery chamber through membrane filter by centrifugation. After analyzing drug concentration in the aqueous phase, the EE will obtain via indirect calculation. For dialysis method, the drug in aqueous phase needs the diffusion through the membrane to the outer solvent which might be the rate limiting step.

## **IV) Crystallization and polymorphism**

Crystallinity and polymorphic behavior of the lipid matrix, which are consequences from various factors e.g. nature structure of lipid itself, emulsifiers and the production method, affect to drug incorporation, release properties and stability of the lipid nanoparticles. The observation of the crystallization and polymorphism of the lipid nanoparticles after preparation and during storage is necessary. Differential

scanning calorimetry (DSC) and X-Ray diffractometry (XRD) are used to assess the states of the lipid. The DSC determines the difference of heat energy between sample and reference to provide state transformation of the sample in the tested temperature range. Meanwhile, the XRD shows the crystalline structure, side chain arrangement of the lipid and also the crystalline state of drug molecules in the lipid matrix. The co-determination by two techniques, DSC and XRD, is recommended to achieve the effective and precise polymorphic information (Müller *et al.*, 2000; Mehnert and Mäder, 2001).

#### **V) Morphological observation**

The morphology of the lipid nanoparticles can be determined by scanning electron microscopy (SEM), transmission electron microscopy (TEM) and atomic force microscopy (AFM). These techniques allow direct evaluating particle size, size distribution and drug incorporating positions in the lipid particles. The SEM provides electrons scanned from the surface, while TEM provides electrons transmitted through the sample. The sample preparation of SEM is easy by coating the dried sample with conductive layer. Meanwhile, TEM provides two-dimensional image and needs combination with other techniques such as staining, freeze fracturing and freeze substitution. The AFM is advanced scanning force microscopic technique which records atomic forces occurred between surface of sample and probing tip of AFM. The high resolution technique (up to 0.01 nm) gives a three-dimensional image of sample. Both contact and non-contact AFM could analyze non-conductive and hydrated samples (Sawant and Dodiya, 2008).

#### **VI) *In vitro* drug release**

Release mechanisms of drug molecules from the lipid nanoparticles take place by the drug diffusion out the lipid matrix and/or erosion or degradation of lipid matrix. Many factors have an effects to the release properties of drug e.g. production method, drug solubility in the lipid, drug and lipid interactions, surfactant used, lipid crystalline nature and also particle size (Müller *et al.*, 2000; Manjunath and Venkateswarlu, 2005; Souto *et al.*, 2006). For preliminary formulation studies, *in vitro* release is necessary to estimate the drug release phenomenon *in vivo* due to the biorelevant of the test. The data from the test is useful for forward process to clinical trials, and develop to the marketed products. Moreover, this test serves to determine

reproducibility of the method and consistency of the developed formulations as well as verify the product shelf-life. For determination of *in vitro* release of drug in oral delivery, the dialysis bag diffusion technique is widely used because this technique analyzes only free drug released from the particles. The dispersion of lipid nanoparticles is added in the dialysis bag and immersed in the release medium which normally is GI media. Upon the condition mimics the GI tract, the drug molecule will move the dialysis membrane through the release medium during time period. However, the bulk-equilibrium reverse dialysis technique is introduced to overcome some weakness of the conventional method particularly slow diffusion process. In the reverse dialysis method, the dispersion is directly placed in large volume of the release medium where provides perfect sink conditions. Therefore, this technique can truly reflect the release of drug in an environment *in vivo* (Levy and Benita, 1990; Washington, 1990).

According to oral lipid-formulation performance related to the lipid digestion processes in GI tract, evaluation of lipid digestibility of the formulations is thus mandatory to promote drug absorption and food effect associated study. *In vitro* dynamic lipolysis test has been emerged to study the effects of the lipid digestion on drug solubilization and release from the lipid-based formulations (Zangenberg *et al.*, 2001). The physiologically-relevant experiment is done in dissolution apparatus containing dissolution medium comprising of a mixture of bile salts, phospholipid and a dispersed dietary lipid under continuous agitation at 37 °C. The process starts from addition of pancreas lipase to the system. The lipolysis rate which depends on pH and free calcium concentration in the medium is controlled by a computer-controlled pump. The dissolution medium is sampling at the time point and a lipase inhibitor is added to stop the lipolysis. During lipolysis, a drug will dissolve in three phases of medium of (1) remains in the lipid (2) be solubilized in the aqueous phase in combination with lipolysis products (3) precipitates as the insoluble drug substance. After centrifugation of the samples, the drug partitioning in each phases is analyzed especially the aqueous layer has been extensively interesting to investigate absorption mechanisms of the drug along GI tract (Fatouros and Mullertz, 2007).

## **VII) *In vivo* absorption studies**

Owing to the incompletely information to understand fate of the lipid-based formulations form *in vitro* experiments, an animal studies of the oral

administration of the drug-formulation prior to clinical studies is importantly applied. However, factors such as animal species, drug dosing, and the number and types of collected sample fluids (Porter and Charman, 2007) should be considered since the developmental stage of the formulations. Rats, dogs and rabbits are utilized as the animal model for evaluating the oral lipid nanoparticle systems. Rats are generally the best choice for initial studies because of low cost and easy administration, while dogs are suitable for the final stages of studies. Although, difference in bile secretion of rat, human and others, in term of amount, rate and composition dilution have questioned to assess the lipid formulations in oral route (DeSesso and Jacobson, 2001). However, some investigators have recommended that the rat is comparable to the dog to use as a suitable model for estimating drug absorption in human from the lipid formulations (Chiou *et al.*, 2000). Since knowledge of lymphatic transport can be responsible for uptake of lipophilic drugs as well as absorption of the lipid from gut via bypass the hepatic first-pass metabolism and further to systemic circulation. And the system associated with chylomicrons which are driven by exogenously triglyceride. The development of formulations containing triglyceride and evaluation of lymphatic transport of the formulations are interesting investigated in animal model (Khoo *et al.*, 2001).

#### **1.2.2.7 Oral drug delivery by lipid nanoparticles**

Over last 20 years, many active drugs, both hydrophobic and hydrophilic compounds, have succeeded to improve bioavailability after oral administration by the lipid nanoparticle systems. The examples of oral delivery using the lipid nanoparticles are presented in Table 2 and Table 3 for poorly water-soluble compounds and hydrophilic compounds, respectively. Furthermore, the potential lipid nanoparticle formulations have been proceeding on the market for oral drug delivery as shown in Table 4. The cyclosporin A was the first drug accomplished formulated as SLN. The SLN formulation loading with cyclosporin A was designed to overcome high plasma concentration peak and reduced variation in plasma profile of traditional emulsion and microemulsion formulations of the drug (Müller *et al.*, 2006; 2008).

**Table 2** Examples of poorly water-soluble drugs and substances incorporated into lipid nanoparticles for oral delivery

Drug or substance	Lipid	Emulsifier/Co-emulsifier	System	Advantage	Reference
Clozapine	Trimyristin, Tripalmitin, Tristearin	Soy phosphatidylcholine, Poloxamer <sup>®</sup> 188	SLN	Increased bioavailability after intraduodenal administration and high distribution in brain and reticuloendothelial cell-containing organs	Manjunath and Venkateswarlu, 2005
Cyclosporine A	Imwitor <sup>®</sup> 900	Tagat <sup>®</sup> S, Sodium cholate	SLN	A low variation in bioavailability and controlled drug release compared to the first Sandimmun <sup>®</sup> formulation	Müller <i>et al.</i> , 2006; 2008
Vinpocetine	Glyceryl monostearate (GMS)	Polyoxyethylene hydrogenated castor oil, Tween <sup>®</sup> 80, Soya lecithin	SLN	Enhanced drug absorption by effect of surfactant amount	Luo <i>et al.</i> , 2006
	Compritol 888 ATO <sup>®</sup> , Monostearin, Miglyol 812N <sup>®</sup>	Solutol HS-15 <sup>®</sup> , Poloxamer <sup>®</sup> 188, Lecithin	NLC	Sustained drug release and improved relative oral bioavailability	Zhuang <i>et al.</i> , 2010
Cryptotanshinone	Compritol 888 ATO <sup>®</sup> , GMS, Stearic acid	Tween <sup>®</sup> 80, Soy lecithin	SLN	Changes in metabolism behavior and improved oral bioavailability	Hu <i>et al.</i> , 2010
Apomorphine	Tripalmitin, GMS	Hydrogenated soybean phosphatidylcholine, Poloxamer <sup>®</sup> 188, polyethylene glycol	SLN	Increased bioavailability and drug distribution at therapeutic site of action. A significantly exhibited the anti-parkinsonian activity in rats which 6-hydroxydopamine-induced lesions.	Tsai <i>et al.</i> , 2011

**Table 2** Examples of poorly water-soluble drugs and substances incorporated into lipid nanoparticles for oral delivery (continued)

Drug or substance	Lipid	Emulsifier/Co-emulsifier	System	Advantage	Reference
Lopinavir	Compritol 888 ATO <sup>®</sup>	Pluronic F127 <sup>®</sup>	SLN	Intestinal lymphatic targeting systems	Alex <i>et al.</i> , 2011
Risperidone	Compritol 888 ATO <sup>®</sup>	Tyloxapol <sup>®</sup> , Phospholipon 80H <sup>®</sup>	SLN	High entrapment efficacy, long-term stability, biocompatibility and dose-dependent drug transport across Caco-2 cells	Silva <i>et al.</i> , 2012
Curcumin	Compritol 888 ATO <sup>®</sup>	Tween <sup>®</sup> 80, Soy lecithin	SLN	High entrapment efficacy, good stability, prolonged release and enhanced drug level in blood	Kakkar <i>et al.</i> , 2010; 2011
	Purified phospholipids, Docosahexaenoic acid, Stearic acid	Soy lecithin	SLN	No adverse effects up to 720 mg/kg/day, good tolerability in both healthy and osteosarcoma patients	Gota <i>et al.</i> , 2010; Dadhaniya <i>et al.</i> , 2011
	GMS, Medium chain triglycerides (Lexol <sup>®</sup> )	Poloxamer <sup>®</sup> 188, Soy lecithin	NLC	A significantly improved oral bioavailability and ability to cross the blood-brain barrier	Fang <i>et al.</i> , 2012
Lutein	Monostearin, Stearic acid, Oleic acid	Tween <sup>®</sup> 20, PEG	NLC	Potential oral drug delivery system of the NLC modified with polyethylene glycol monostearate (PEG-SA)	Yuan <i>et al.</i> , 2007
	Precirol ATO5 <sup>®</sup> , Corn oil, Estasan 3575 <sup>®</sup>	Myverol 18-04K <sup>®</sup> , Poloxamer <sup>®</sup> 188	NLC	The ultrasonication duration and drug load impacting to the particle size	Liu and Wu, 2010

**Table 2** Examples of poorly water-soluble drugs and substances incorporated into lipid nanoparticles for oral delivery (continued)

Drug or substance	Lipid	Emulsifier/Co-emulsifier	System	Advantage	Reference
Etoposide	Monostearin, Soybean oil	Distearoyl phosphatidyl-ethanolamine, PEG-40, Soya lecithin	NLC	High cytotoxicity of DSPE-NLCs against human epithelial-like lung carcinoma cells and enhanced oral bioavailability	Zhang <i>et al.</i> , 2011
Bromocriptine	Tristearin, Miglyol <sup>®</sup>	Poloxamer <sup>®</sup> 188	NLC	Long-lasting therapeutic effects and extending drug half-life <i>in vivo</i>	Esposito <i>et al.</i> , 2012
Lovastatin	Precirol <sup>®</sup> , Squalene	Myverol <sup>®</sup> , soybean phosphatidylcholine, Poloxamer <sup>®</sup> 188	SLN and NLC	Enhanced oral bioavailability and good stability of the Myverol system in the gastric environment	Chen <i>et al.</i> , 2010
Simvastatin	GMS, Oleic acid	Poloxamer <sup>®</sup> 407	SLN and NLC	Superiority of NLC over SLN for improved oral bioavailability and drug targeting	Tiwari and Pathak, 2011
Resveratrol	Cetyl palmitate, Miglyol 812 <sup>®</sup>	Polysorbate 60	SLN and NLC	Good stability of the lipid nanoparticles after incubation in digestive fluids	Neves <i>et al.</i> , 2013

**Table 3** Examples of hydrophilic substances, proteins and peptides incorporated into lipid nanoparticles for oral delivery

Drug or substance	Lipid	Emulsifier/Co-emulsifier	System	Advantage	Reference
Lysozyme	Witepsol E 85 <sup>®</sup> , Softisan <sup>®</sup> 142, Monosteol <sup>®</sup> , Cetyl alcohol	Sodium cholate, Poloxamers <sup>®</sup> 182, Poloxamer <sup>®</sup> 188, Tween <sup>®</sup> 80, Superpolystate <sup>®</sup>	SLN	SLN as antigen carriers for vaccine delivery	Almeida <i>et al.</i> , 1997; Almeida and Souto, 2007
Insulin	Stearic acid	Wheat germ agglutinin (WGA), Poloxamer <sup>®</sup> 188, Soya lecithin	SLN	Promoting oral absorption compared to subcutaneous injection	Zhang <i>et al.</i> , 2006
	Cetyl palmitate	Poloxamer <sup>®</sup> 407	SLN	Prolonged hypoglycemic effect during 24 h	Sarmiento <i>et al.</i> , 2007
	Stearic acid	L-arginine, Soybean phospholipids, Poloxamer <sup>®</sup> 188	SLN	Modified release pattern and improved pharmacological availability	Zhang <i>et al.</i> , 2009
	Softisan <sup>®</sup> 100	Lutrol <sup>®</sup> F68, Soybean lecithin	SLN	No aggregation, low matrix crystallinity and lack toxicity	Fangueiro <i>et al.</i> , 2013
Insulin and Thymopentin	Stearic acid, Octadecyl alcohol, Cetyl palmitate, GMS, Glyceryl palmitostearate, Glyceryl tripalmitate, Glyceryl behenate	Solutol HS 15 <sup>®</sup> , Lecithin	SLN	Glyceryl palmitostearate is suitable lipid material of SLN for oral proteins delivery due to low burst release and high pharmacological availability.	Yang <i>et al.</i> , 2011



**Table 3** Examples of hydrophilic substances, proteins and peptides incorporated into lipid nanoparticles for oral delivery (continued)

Drug or substance	Lipid	Emulsifier/Co-emulsifier	System	Advantage	Reference
Gonadotropin release hormone	Monostearin	Polyvinyl alcohol	SLN	A novel preparation method for a prolonged release of hydrophilic peptide drugs	Hu <i>et al.</i> , 2004
Calcitonin	Tripalmitin	Poloxamer <sup>®</sup> 188	SLN	Potential carriers of the chitosan-coated lipid nanoparticles for peptide delivery	Garcia-Fuentes <i>et al.</i> , 2005
	Trimyristin	Poloxamer <sup>®</sup> 407	SLN	Lowering the basal blood calcium levels and sustaining hypocalcaemia over 8 h	Martins <i>et al.</i> , 2009
	Stearic acid, Tripalmitin, Trimyristin, Trilaurin	-	SLN	A significantly improved stability of drug-SLN and intensively increased the intracellular uptake of the drug by an active transport pathway	Chen <i>et al.</i> , 2013
BuspironeHCl	Cetyl alcohol	Tween <sup>®</sup> 20, Lecithin	SLN	High drug released (90%) during 4.5 h <i>in vitro</i> and significantly increased bioavailability	Varshosaz <i>et al.</i> , 2010
Zidovudine	Stearic acid, Tripalmitin, Tristearin, Trilaurin, Trimyristin	Tween <sup>®</sup> 80	SLN	Advantage of fatty acids over triglycerides in the SLN entrapment of hydrophilic drugs	Singh <i>et al.</i> , 2010
Bovine serum albumin	Softisan <sup>®</sup> 154	Phospholipon <sup>®</sup> 90G, Lecithin, Solutol <sup>®</sup> HS15	SLN	Albumin payload ranged from 2.5 to 15% in the SLN and low cytotoxicity in both haemolysis and neutral red test	Schubert and Müller-Goymann, 2005

**Table 4** Marketed products of lipid nanoparticles for oral drug delivery

<b>Marketed brand name</b>	<b>Drug and substance</b>	<b>System</b>	<b>Company</b>
SLN <sup>®</sup> suspension	Cyclosporin A	SLN	Pharmatec, Italy
Mucosolvan <sup>®</sup> retard capsules	Ambroxol hydrochloride	Lipid nanopellets	Boehringer-Ingelheim, Germany
Rifamsolin <sup>®</sup>	Rifampicin	SLN	AlphaRx, Canada
Longvida <sup>®</sup>	Curcumin	solid lipid particle	Verdure Sciences, USA

### 1.2.3 Self-microemulsifying drug delivery systems (SMEDDS)

#### 1.2.3.1 Introduction

Self-microemulsifying drug delivery systems (SMEDDS) are oily liquid formulation which often consisted of lipid liquid, surfactant or co-surfactant/co-solvent. The isotropic mixture of the system produces transparent o/w microemulsion upon dispersion in aqueous GI media with gentle agitation. The droplet sizes of thermodynamically stable microemulsion are less than 50 nm. The rationales like increased drug solubility, providing high dissolution rate, enhanced drug permeability, diminished hepatic metabolism, support to improve oral drug bioavailability of this liquid SMEDDS (Ingle *et al.*, 2013). Although, there are some disadvantages of the system including 1) drug precipitation on dilution in hydrophilic GI fluids; 2) drawbacks of soft gelatin capsules for encapsulation of marketed SMEDDS e.g. high cost, transmissible spongiform encephalopathy (TSE), consumer preference/religion with animal gelatin and migration of volatile co-solvents to the capsule shell; 3) problems of handling, storage and stability of liquid SMEDDS, so needs to formulating in solid dosage forms; 4) limited lymphatic absorption and targeting; 5) oxidation of the lipid used in SMEDDS which mostly contained unsaturated fatty acids and their derivatives (Dokania and Joshi, 2014).

### 1.2.3.2 Formulation compositions of SMEDDS

#### I) Oils

Oil is one of the important compositions in the SMEDDS due to its drug solubilizing property, self-emulsification facility and increased lymphatic transport of hydrophobic drugs leading to improved drug absorption. These properties are along with its triglyceride nature (Gursoy and Benita, 2004; Maurya *et al.*, 2010). Mostly, natural oils particularly medium- and long-chain triglycerides with different unsaturation degrees have been widely utilized in the SMEDDS formulations. Moreover, hydrogenated oils, which resistance to oxidative degradation, also have been used because their good drug solubility and emulsification abilities (Constantinides, 1995; Hauss, 2007). Another oil groups is semi-synthetic amphiphilic oils that prepared by chemically mixing medium chain saturated glyceride oils with one or more hydrophilic chemical molecules (Gibson, 2007). They are well compatible to soft and hard gelatin or HPMC capsules (Hauss, 2007). The examples of each group of oils are presented in Table 5.

#### II) Surfactants

Several surfactants usually use as compositions in the SMEDDS. Safety is an important factor to consider in selecting emulsifiers. The non-ionic surfactants are usually less toxic than ionic surfactants. The natural surfactants are safer than the synthetic ones, but their capacity of self-emulsification is limited (Gibson, 2007). Non-ionic surfactants with a relatively high HLB and hydrophilicity are one of the most widely suggestion to improve bioavailability in oral delivery of lipophilic drugs (Hauss, 2007). These properties perform rapid o/w microemulsion and good self-emulsifying system in GI media. The surfactant concentration is also important factor, so generally concentration used in the SMEDDS is in ranges of 30-90% w/w. The mixture of lipid and high surfactant amount leads to the formation of small droplet size of microemulsion. This occurred by more emulsifiers localized at interface of the oil and water consingning to stabilize the oil droplets (Gursoy and Benita, 2004; Gibson, 2007). However, high surfactant quantities occupy their dehydrating effects which may cause brittleness of hard and soft gelatin capsules. Furthermore, the surfactant contained SMEDDS showed enhancing of oral absorption in the Caco-2 cell culture model (Patel *et al.*, 2010).

### III) Co-surfatants/co-solvents

The SMEDDS preparation requires high quantities of surfactants. The fully-synthetic monomeric and polymeric glycolic excipients can be used as solvent in SMEDDS system because enabling to dissolve of large amounts of either drug in the lipid or hydrophilic surfactant. However, their water miscibility property results in drug precipitation upon dilution in the GI aqueous contents, thereby the concentration used should be considered. The commonly example for monomeric glycolic solvent is propylene glycol (PG). The PG can be used for soft gelatin capsule of hydrophobic drugs. Meanwhile, the polymeric glycol-based excipients is polyethylene glycols (PEGs) ranging from 200-600. However, PEGs are more chemically reactive and more irritating to the GI mucosa than natural oils. The PEGs contain peroxide impurities and secondary products from auto-oxidation which contribute to chemical instability of formulated drug. In addition, they are limited filling in hard gelatin capsules because their hygroscopicity compromise physical integrity of capsule (Gibson, 2007; Hauss, 2007). Organic solvents like alcohols can be used as solvent for SMEDDS, but their difficulties of evaporating into the shells of the soft or hard gelatin capsules resulting to drug precipitation (Gursoy and Benita, 2004). The examples of surfactant and co-surfactant or co-solvent used in SMEDDS formulations are presented in Table 5.

#### 1.2.3.3 Self-emulsification mechanisms

Self-emulsification arises when the entropy used in dispersion change is greater than the energy required to increase the surface area of the dispersion. Generally, free energy needs to create a new balance surface of the oil and water phases for an emulsion system. For SMEDDS, the free energy for microemulsion forming is very low, thus, the emulsification takes place spontaneously. Moreover, emulsification has been associated with easy penetration of SMEDDS into aqueous phase on gentle agitation. Emulsifying agents in the SMEDDS could facilitate this process and stabilize the system by forming an interface monolayer surrounded the microemulsion droplets, leading to reduction in the interfacial energy and coalescence of the droplets. Interacting to the interfacial phase of drug molecule may also influence on this microemulsion characteristics (Gursoy and Benita, 2004; Maurya *et al.*, 2010).

**Table 5** Examples of oils, surfactants, co-surfactants or co-solvents used in SMEDDS formulations

Oils	Surfactant	Co-surfactants/co-solvents
<b>Medium chain triglycerides</b>	<b>Sorbitan fatty acid esters</b>	<b>Monomeric glycolic</b>
Caprylic/Capric Triglyceride	Sorbitan monolaurate (Span <sup>®</sup> 20)	Propylene glycol (PG)
<b>Long chain triglycerides</b>	Sorbitan monostearate (Span <sup>®</sup> 60)	<b>Polymeric glycolic</b>
Castor oil	Sorbitan monooleate (Span <sup>®</sup> 80)	Polyethylene glycols (PEGs)
Coconut oil	<b>Polyoxyethylenesorbitan fatty acid esters</b>	<b>Others</b>
Corn oil	Polyoxyethylene 20 sorbitan monolaurate (Tween <sup>®</sup> 20)	Ethanol
Cottenseed oil	Polyoxyethylene 20 sorbitan monostearate (Tween <sup>®</sup> 60)	Diethyl glycol monoethyl ether (Transcutol P <sup>®</sup> )
Olive oil	Polyoxyethylene 20 sorbitan monooleate (Tween <sup>®</sup> 80)	
Palm oil	<b>Polyoxyethylene castor oil derivatives</b>	
Peanut oil	Polyoxyl-35-castor oil (Cremophor <sup>®</sup> EL)	
Peppermint oil	Polyoxyl-40-hydrogenated castor oil (Cremophor <sup>®</sup> RH 40)	
Rapeseed oil	<b>Propylene glycol based derivatives</b>	
Safflower oil	Propylene glycol caprylate	
Sesame oil	Propylene glycol monocaprylate	
Soybean oil	Propylene glycol laurate	
<b>Hydrogenated oils</b>	Propylene glycol monolaurate	
Hydrogenated castor oil	Propylene glycol caprylate/caprinate	
Hydrogenated palm Oil	<b>Polyethylene glycol based derivatives of vitamin E</b>	

**Table 5** Example of oils, surfactants, co-surfactants or co-solvents used in SMEDDS formulations (Continued)

Oils	Surfactant	Co-surfactants/co-solvents
<b>Semi-synthetic amphiphilic oils</b>	d-alpha-tocopheryl polyethylene glycol-1000 succinate (TPGS)	
Propylene glycol dicaprylate/dicaprate	<b>PEGylated glycerides</b>	
Propylene glycol monocaprylate	PEG-8 Caprylic/Capric Glycerides (Labrasol <sup>®</sup> )	
<b>Others</b>	PEG-6 Caprylic/Capric Glycerides (Softigen <sup>®</sup> 767)	
Ethyl oleate	Linoleoyl polyoxyl-6 glycerides/ Corn oil PEG-6 ester (Labrafil <sup>®</sup> M2125 CS)	
Oleic acid	Lauroyl macrogol-32 glycerides (Gelucire <sup>®</sup> 44/14)	
Ricinoleic acid	<b>Co-polymers of polyoxyethylene and polyoxypropylene</b>	
Medium chain mono- and di-glycerides	Poloxamer <sup>®</sup> 124, 188, 407	
	<b>Others</b>	
	Ethyl oleate	
	Isopropyl myristate	
	Polyglyceryl-3 Polyricinoleate (Imwitor <sup>®</sup> 600)	
	Glycerol Monocaprylate (Imwitor <sup>®</sup> 988)	
	Polyglyceryl-6 dioleate (Plurol Oleique <sup>®</sup> )	

#### 1.2.3.4 Characterization of SMEDDS formulations

##### I) Self-emulsification performance

The assessment of self-emulsification of SMEDDS formulation includes visual evaluation, emulsification time and robustness to dilution. The emulsification ability of the system in aqueous medium could clarify by the visual assessment. The SMEDDS formulation was usually introduced into water or aqueous medium under gently stirring using magnetic stirrer. The spontaneous and rapid formed transparent microemulsion was judged as 'good', meanwhile poor or no emulsion formation with coalescence appearance was judged as 'bad' (Shen and Zhong, 2006). Moreover, emulsification time of the SMEDDS which is one of important factor of self-emulsification performance should be evaluated. Generally, the SMEDDS should be rapidly and completely emulsified after dispersion in the aqueous medium. Thus, the emulsification time of the system is recorded (Singh *et al.*, 2009). The specific criteria to evaluate the self-microemulsification efficiency by visual grading system have been published (Singh *et al.*, 2009). Grade I represented a rapid forming microemulsion which is clear or slightly bluish in appearance (<1 min); Grade II represented rapid forming, slightly less clear emulsion which has a bluish white appearance (<2 min); Grade III represented bright white emulsion (similar to milk in appearance) (<3 min); Grade IV represented dull, grayish white emulsion with a slightly oily appearance that is slow to emulsify (>3 min); Grade V represented poor or minimal emulsification with large oil droplets present on the surface (>3 min). Furthermore, phase diagram is constructed to identify the self-microemulsifying region. According to the variation of gastric volume, robustness of the system to dilution should be determined by dispersion of SMEDDS in different volumes of aqueous medium and then assess the self-microemulsification using visual grading system.

##### II) Droplet size and size distribution

The droplet size and PDI of the microemulsion are important factors of the self-microemulsification characteristics. The droplet size affects the rate and amount of drug release, drug absorption as well as formulation stability. The PCS is powerful method for droplet size evaluation. Before measurement, the microemulsion is diluted with suitable aqueous dilution for appropriate measurement. The droplet size values

(<50 nm) indicate the microemulsion formation of SMEDDS. Microscopic technique is another method can employ to obtain accurate droplet size and size distribution (Gursoy and Benita, 2004).

### **III) Morphological observation**

The morphology of droplets obtained from the SMEDDS can be observed by TEM. Normally, the microemulsion droplets have spherical shape with smooth surface. Besides the shape, the technique can also measure the size and size distribution of the droplets.

### **IV) Total drug content**

The quantity of drug incorporated in the SMEDDS is one of properties should be considered especially for stability studies. This property depicts the drug encapsulation capacity of the formulation as well as the effects of formulation excipients on chemical stability of drug.

### **V) *In vitro* drug release**

The release of drug from oily formulations, which are often immiscible with aqueous medium, is crucial property to determine the potential of the SMEDDS. The biorelevant experimental method and dissolution media need to be apply for the assessing. Unlike of these, drug solubilization in the aqueous test media, surface area and droplet size of the dispersed droplets also reflect to *in vivo* performance. Upon *in vivo* phenomenon, drug released and absorbed from the oily formulations take place by direct transport of the oil droplets to the intestinal cells or lipid digestion and then micelle formation (Gursoy and Benita, 2004). Generally, the USP paddle method is utilized at the biorelevant condition for drug release study of the SMEDDS formulations comparing to unformulated drugs. An aliquot of samples are withdrawn and replaced immediately with equal volume of fresh medium to maintain sink condition. After that, the drug released amount is analyzed by suitable analytical methods such as UV-vis spectroscopy and HPLC. According to reflection of lipid digestion on the drug released *in vivo*, therefore the release medium containing lipolytic enzymes or *in vitro* lipolysis test is required in order to get the most biorelevant data.



### 1.2.3.5 Improved oral drug absorption by SMEDDS

Several advantages of the SMEDDS systems work to its improved oral bioavailability of many drugs. The main factors of SMEDDS for improved oral drug absorption are drug solubilization and small droplet size which reflecting the efficient drug release from the SMEDDS (Gursoy and Benita, 2004). The examples of the improved bioavailability of compounds in oral delivery by the SMEDDS have been found in published documents (Gursoy and Benita, 2004; Shukla *et al.*, 2012; Ingle *et al.*, 2013). Most investigations involving improvement of absorption profile of compounds are carried out in an *in vivo* study using mouse, rat, rabbit and dog as animal model (Kang *et al.*, 2004; Setthacheewakul *et al.*, 2010; Sermkaew *et al.*, 2013). Furthermore, some study is further conducted in clinical trials in human (Fischl *et al.*, 1997). Until now, the commercial products of drug formulated as liquid form of SMEDDS have been successful launched. The summary of the marketed products of the SMEDDS is revealed as in Table 6.

**Table 6** The commercial products of SMEDDS for oral delivery (Shukla *et al.*, 2012; Anand, 2015)

Compound or drug	Trade name	Company	Dosage form
Amprenavir	Agenerase	GSK	Soft gelatin capsule; 50 mg
Bexarotene	Targretin	Eisai	Soft gelatin capsule, 75 mg
Clofazimine	Lamprene	Norvartis	Soft gelatin capsule; 50 mg
Calcitriol	Rocaltrol	Roche	Soft gelatin capsule; 0.25 and 0.5 µg
Cyclosporin	Panimumbioral	Panacea Biotec	Capsule; 50 and 100 mg
Cyclosporin A	Gengraf	Abbott	Hard gelatin capsule; 25 and 100 mg
Cyclosporin A	Sandimmune	Norvartis	Soft gelatin capsule; 25, 50 and 100 mg
Cyclosporin A	Neoral	Norvartis	Soft gelatin capsule; 10, 25, 50 and 100 mg

Compound or drug	Trade name	Company	Dosage form
Doxercalciferol	Hetorol	Sandoz	Soft gelatin capsule; 0.5 µg
Dronabinol	Marinol	AbbVie Inc.	Soft gelatin capsule; 2.5 mg
Dutasteride	Avodat	GSK	Soft gelatin capsule; 0.5 µg
Efavirenz	Sustivas	Bristol-Meyers	Capsule; 50 and 200 mg Tablet; 600 mg
Isotretinoin	Accutane	Roche	Soft gelatin capsule; 10, 20, 40 mg
Progesterone	Prometrium	Schering Corporation	Soft gelatin capsule; 100 and 200 mg
Ritonavir	Norvir	Abott	Soft gelatin capsule; 50 and 100 mg
Saquinavir	Fortovase	Norvartis	Soft gelatin capsule; 200 mg
Valproic acid	Depakene	Abbott	Soft gelatin capsule; 250 mg

## 1.2.4 The permeation studies using Caco-2 cells model

### 1.2.4.5 Introduction

For oral route, all drugs are absorbed across the intestinal epithelium by various mechanisms through a mean of barriers including the mucus layer, the intestinal epithelial cells, the lamina propria and the capillaries endothelium. Among of these barriers, the epithelial monolayers are the most important barrier for drug permeation. Thus *in vitro* study using of the intestinal cells model should be estimate *in vivo* drug adsorption (Artursson and Karlsson, 1991). The Caco-2, human intestinal epithelial cell line, is derived from a human colorectal carcinoma obtained from a 72-year-old patient. It spontaneously differentiates become to monolayers of polarized enterocytes resemble intestinal epithelium under conventional cell culture conditions on porous membranes.

After reaching confluences, brush border membranes of the enterocytes present high level of several enzymes e.g. hydrolases and alkaline phosphatase and also develop junction complexes. Moreover, the various active transport contents e.g. sugars, amino acids, dipeptides and bile acids, are also expressed at the intestinal Caco-2 cell epithelium. In addition, the Caco-2 cell system exists the metabolism properties of both phase I metabolizing cytochrome P-450 (CYP) isozymes and phase II metabolizing enzymes (Gan and Thakker, 1997). The advantages of using the model could be conclude thereby 1) rapid and high throughput screening method for drug absorption studies; 2) benefits to determine including permeation, transport mechanisms as well as metabolism of either drug molecules or formulations at cellular levels; 3) providing data of intestinal toxicity of both drugs and formulations; 4) no differences of interspecies characteristics from human intestinal cells. However, there are significant limitations of the Caco-2 cells model for example 1) the characteristic of tight junctions of differentiated Caco-2 cells more resemble to colon than of the small intestine; 2) no presenting of the mucus layer on the Caco-2 cell monolayers due to devoid of the goblet cells; 3) no intestinal physiological abilities e.g. intestinal motility or transit time (Gan and Thakkerb, 1997). Though, the Caco-2 cells are still as an excellent *in vitro* model which widespread utilized to study intestinal absorption of either drug or formulations according to the good correlation of the Caco-2 monolayers to the human intestinal epithelium (Artursson and Karlsson, 1991). Furthermore, the FDA accepts the data from the *in vitro* Caco-2 cells assay (Press and Grandi, 2008) to classify the compounds in the Biopharmaceutical Classification System (BSC).

#### **1.2.4.6 Applications of the Caco-2 cells**

##### **I) Cytotoxicity test**

As the benefits described above, the Caco-2 cells model can be used for cytotoxicity test of active compounds or other component of formulations. Furthermore, the monolayers integrity can be confirmed via trans-epithelial electrical resistance (TEER) measurement. The MTT assay is widely used to evaluate the toxicity of the drugs (Freshney, 2005). For example, the effects of the surfactant used in

SMEDDS, e.g. Polysorbates and Labrasol<sup>®</sup>, on toxicity to the Caco-2 cells were studied by MTT assay (Ujihelyi *et al.*, 2012).

## II) *In vitro* drug permeability test and transport mechanisms

The Caco-2 cell monolayers were firstly used as a model of intestinal absorption in the late 1980s. Nowadays, the model becomes a standard tool for intestinal drug absorption studies and for transport mechanistic studies. The advantages of the permeability assay using Caco-2 cell monolayer are easy to handle, reliable and use small amounts of compounds. The transport contents and tight junctions are expressed after culturing 2-3 weeks to differentiate into enterocytes. In addition, P-gp and MRPs, which also are expressed at the cell membrane of Caco-2 cells, are responsible to an efflux pump systems of specific compounds from basolateral (BL) to apical (AP) side. The Caco-2 cells are cultured on semi-permeable polycarbonate support of inserts that place into a chamber to partition of AP and BL sides which represent the intestinal lumen and blood or mesenteric lymph sides, respectively. The permeability experiment is performed at 37 °C under mild shaking and appropriate transport media. The TEER is usually measured before and after the experiment to indicate the integrity and tightness of the cellular junctions of the monolayers which the TEER typically should be  $> 300 \Omega\text{cm}^2$ . Bidirectional transport experiments, the samples are added into either the AP or the BL side of each well of cell monolayers to study the influx or efflux transport across the intestinal cells. The sample in the receiving chamber is withdrawn at various time points and the sample is analyzed and expressed as the apparent permeability coefficient ( $P_{app}$ ). However, the  $P_{app}$  might be inter-assay variation, thus it is recommended to measure reference compounds along with each assay for examples, low (i.e. mannitol) and high permeability (i.e. propranolol) compounds (van Breemen and Li, 2005). For study of transport pathways, it might be estimated by the unequal  $P_{app}$  values in absorptive (AP-BL) and secretory (BL-AP) direction or decreasing of the  $P_{app}$  values with increasing concentrations of tested compound. In addition, the involvement of transporters or efflux systems of the compounds may assess by adding inhibitors of P-gp (i.e. verapamil) and MRPs (i.e. MK-571 and indomethacin). Changes of the  $P_{app}$  value in the conditions would confirm efflux mediated transport of the compound (Yee, 1997).

### III) Evaluation of drug metabolism

As known, CYP isozymes are substantial in the human small intestine especially CYP3A4 about <50% of all CYP isozymes. Although, underexpression of CYP isozymes of the Caco-2 cell monolayers comparing to the human small intestine or jejuna microsomes have been reported (van Breemen and Li, 2005). However, various types of other metabolising enzymes e.g. hydrolases, carboxylesterases, uridine diphosphoglucuronosyl-transferases, glutathione-S-transferases and cyatechol-O-methyl-transferase are expressed in the Caco-2 cells at the appropriate levels for intestinal drug metabolism studies. Particularly, significant expression level of the phase II metabolizing enzymes as sulfo-transferases and glucuronyl-transferases are useful for drug metabolism determination (Gan and Thakkerb, 1997). Because of most of pharmacologically active compounds is conjugated by these enzymes to reduce their activity or to eliminate from the body (Mei *et al.*, 2012; Hu *et al.*, 2014).

#### 1.2.5 Mechanisms of enhanced oral drug absorption by lipid-based drug delivery systems

##### 1.2.5.1 Lipid nanoparticles

Different mechanisms of lipid nanoparticle systems to enhance drug absorption can be described as follows (Muchow *et al.*, 2008):

##### 1) Improved drug solubilization and protection from degradation along GI tract

The lipid nanoparticles can increase the solubility of poor water-soluble compounds owing to its lipid nature and the facilities of the surfactants. The entrapped drug in the lipid matrix is protected from the degradation from enzyme and pH in GI tract resulting to exact reaching to absorption (Tiwari and Pathak, 2011).

##### 2) A bioadhesiveness of the lipid nanoparticles

Generally, the nanoparticles are high dispersibility and adhesive properties to gut wall which is increased contributing from surface area of the particles. The drugs are released precisely at intestinal absorptive site according to long residence contact time of adhesion. This adhesion process is very reproducible persuade to low variation of oral bioavailability.

### **3) An absorption enhancing effect of lipids and surfactant used**

The lipids usually used in the formulations are structurally similar to the fat in daily food. They can promote the oral absorption of drugs by stimulating bile secretion and thus enhance the direct uptake of intact particles by the gut wall and facilitate its draining into the lymphatic system (Tiwari and Pathak, 2011). The length of the fatty acid chains of lipid influences the absorption (Porter and Charman, 2001). Moreover, it has been investigated that oils i.e. oleic acid could be restrained metabolizing enzyme activity of CYP3A (Mountfield *et al.*, 2000).

Additionally, the presence of surfactant in the lipid formulations can promote mixed micelles formation resulting to increase lymphatic absorption. Moreover, some surfactants such as Poloxamer<sup>®</sup> (e.g. 188 and 407) and Tween80<sup>®</sup> have permeation enhancing effects. For example, deforming the cell membrane and opening the tight junction of the intestinal cells promote paracellular transport of lipid nanoparticles (Wu and Lee, 2009). Moreover, these surfactants inhibit efflux pump systems of P-gp and MRPs increase drug transport across the intestinal epithelium.

### **4) Small particle size**

Lipid nanoparticles are dispersed in the gut into ultrafine particle diameters of <200 nm which provide large surface area contributing very fast and efficient solubilization. The small nano-sizes promote the efficient direct uptake across intestinal cells and especially the lymphatic tissue.

### **5) Improved lymphatic absorption**

The colloidal nature of lipid nanoparticles presents dominantly the drug absorption by the lymphatic pathway. It has been documented that the lipid nanoparticles transport the drug through the specialized Peyer's patches (M cells) and the isolated follicles of the gut-associated lymphoid tissue of the intestinal lymphatic system to blood circulation (Bilia *et al.*, 2014). The lymphatic pathway avoids first-pass metabolism in liver leading to a longer retention time and increased the oral drug absorption *in vivo*. It has been reported that lipid containing C14-18 chains promoted lymphatic absorption (Porter and Charman, 2001).

### **6) Prolonged release**

A slow degradation of lipid matrix is required for this case. It can utilize the retardant lipid materials i.e. Compritol ATO 888<sup>®</sup> and/or stabilize the lipid particles

with a high MW stabilizer i.e. Poloxamer<sup>®</sup> to disturb anchoring of lipase complex (zurMühlen *et al.*, 1998). These properties of lipid nanoparticles serve prolonged half life in body of the drugs leading to reduce in dosing frequency. The facilitating of the Poloxamer<sup>®</sup> provides by its molecules contained both hydrophobic and hydrophilic groups, and also repulsion effect of a steric stabilization. The characteristics recommend their phagocytic resistance and prolong circulatory time of lipid nanoparticles (Tiwari and Pathak, 2011).

#### **7) Close association of lipid and active compound**

This property requires for the maximum effect of enhancing drug absorption. SLN can present the active compound between the side chains of fatty acid, while the compound is incorporated in imperfected crystalline lipid of NLC.

#### **1.2.5.2 SMEDDS**

The proposed absorption mechanisms of the liquid SMEDDS can be described as follows:

##### **1) Increase drug solubility and dissolution**

The SMEDDS, composed of oils and high amount of surfactants/co-surfactants, have ability to dissolve many drugs particularly lipophilic drugs. The drug incorporated in the microemulsion is maintained in soluble form in the gut lumen, thus preventing drug precipitation.

##### **2) Very small droplet size and high dispersibility**

Upon the partition into the GI fluid, the SMEDDS produces spontaneously small o/w microemulsions droplets. The droplets are highly dispersed in the medium. The small droplet sizes and disintegration affect to the extracellular release of the drug from the SMEDDS, thereby drug transport into the epithelium cells. Moreover, the large surface area of very fine droplets and high dispersibility refer to more adhesion and endocytotic internalization to the intestinal monolayers followed by intracellular release of the drug (Kogan *et al.*, 2008).

##### **3) An absorption promoting effect of lipid and surfactant used**

As known, lipids can promote the oral absorption of compounds like a “Trojan Horse” effect. This can be specifically explained via enzyme degradation of the lipids in the gut resulting to the formation of surface active mono- and diglycerides on

the surface of the lipid droplets. The process of detachment and micelles formation of these molecules prove the drug dissolved in the micelles. After that, the mixed micelles is formed subsequent by interaction of these micelles with surface-active bile salts to simultaneously drug absorb by direct passive uptake (Porter and Charman, 2001; Pouton, 2000; O'Driscoll, 2002).

Other than the advantages of liquid lipids, the surfactant is very important means of enhanced oral drug absorption by SMEDDS. Several benefits of surfactant impact on oral bioavailability improvement, for examples promoting mixed micelle formations imparting to increase lymphatic absorption (Pouton, 2000). Furthermore, the altering membrane fluidity, inhibiting efflux mediated systems and opening tight junction of the surfactant have been reported to support drug adsorption.

#### **4) Enhanced lymphatic transport**

The lymphatic transport has been recommended as a potential mechanism of improved bioavailability (Hauss *et al.*, 1998; Kommuru *et al.*, 2001). The SMEDDS offers rapid drug absorption allowing to high drug concentration in enterocytes and hence enhanced drug transport by concentration-partitioning gradients. Furthermore, the SMEDDS permeates through the lymphatic systems by promoting chylomicron triglyceride (O'Driscoll, 2002).



## OBJECTIVES

1. To develop and characterize OXY-loaded lipid nanoparticles including SLN and NLC.
2. To develop and characterize OXY-loaded SMEDDS.
3. To determine the permeability of the developed OXY-loaded lipid nanoparticles and OXY-loaded SMEDDS in Caco-2 cells.
4. To evaluate the *in vivo* oral absorption of the developed OXY-loaded lipid nanoparticles and OXY-loaded SMEDDS.
5. To evaluate the influence of surfactant on the physicochemical properties and oral absorption of OXY-loaded SMEDDS.

## RESULTS AND DISCUSSION

### 1. Development of OXY-loaded solid lipid nanoparticles (SLN) and nanostructured lipid carriers (NLC)

#### 1.1 Preparation and optimization of OXY-loaded SLN

In this study, the hot/high speed homogenization method using a high speed homogenizer (S 25N-8G, ULTRA-TURRAX<sup>®</sup>, IKA<sup>®</sup>, Germany) was used to produce lipid nanoparticles due to its simplicity and short preparation time. The good characteristics of SLN including small particle size (PS; <200nm), narrow sizedistribution (PDI~0.2-0.4), high entrapment efficiency (EE), high loading capacity (LC) and sustained release profile were optimized. Many factors influenced on these properties including preparation condition and formulated ingredients were also investigated. According to homogenization conditions, it was found that the particle size and size distribution decreased with increasing homogenization speed and time. Therefore, the speed rate of 24,000 rpm and the time of 15 min which produced homogeneous suspension (T6) were selected as the standard homogenization step for all tested formulations. Using the optimized conditions, the effects of formulation compositions on physicochemical properties of developed SLN were also determined. Regarding the proportions of solid lipid, the formulation containing a highest weight proportion of solid lipid (5% w/w; C2) provided the acceptance particle size and size distribution. Therefore, C2 which was expected to achieve a high drug loading was chosen for further development of the OXY-loaded SLN (OXY-SLN). For the types of the solid lipid, glyceryl monostearate (GMS) was compared to glyceryl behenate (C888). After incorporation of OXY, the C888-based SLN (F3) appeared to have better properties than GMS-based SLN (F8). The C888 was, thus, chosen as the solid lipid matrix in this study. This related to its amphiphilic characteristics with a high chemical stability that resulted in a good ability to encapsulate a lipophilic and/or hydrophilic drug (Kipp, 2004). In addition, a larger size and a greater PDI of the nanoparticles was obtained by increasing the incorporated OXY in the SLN formulations. This result was due to an insufficient amount of the lipid to encapsulate the drug. However, the F3 gave the high entrapment efficiency (> 80%) and also had the highest capacity for drug loading.

Therefore, the 0.3% w/w of OXY was the optimum OXY loaded in the SLN formulation. Another essential factor in the lipid nanoparticles is the surfactants. The soy lecithin, selected as a co-surfactant in this study, was an important composition for drug-loaded SLN without the drug readily separating from the formulations, irrespective of the lipid used (Luo *et al.*, 2006; Hu *et al.*, 2010). In our study, the soy lecithin (HLB of 5) was added to the system to adjust the HLB of other surfactants so as to enhance the ability to emulsify the lipid and stabilize the system. Seven different types of surfactant at the equal concentration were used to form the OXY-SLN. The formulations (S1, S2, and S5) containing Poloxamer<sup>®</sup> 188 (P188; HLB of 29) and/or Tween80<sup>®</sup> (HLB of 15) had a good appearance and did not flocculate. The mean particle sizes obtained from these formulations was <200 nm and they also had a narrow size distribution (PDI 0.22-0.27). On the basis of similar total drug content (TDC; about 100%), the EE of the S1, S2 and S5 formulations was satisfactorily high. The non-toxic and non-ionic P188 and Tween80<sup>®</sup> have been used as surfactants for the C888-based formulations due to their compatibility.

In order to develop a controlled release system, the conventional dialysis bag diffusion technique is widely used for measuring the release of drugs from colloidal solutions. The OXY suspension presented a cumulative release of OXY of 30% within 4 h in the SGF pH 1.2 and 80% within 48 h in the SIF pH 6.8, respectively. Meanwhile, the release curves of the three SLN formulations (S1, S2, S5) showed no initial burst release and slowed down considerably in both media. From the experimental data, the slowest release rate of S2 formulated using Tween80<sup>®</sup> was observed during the study times. The retarded release profile could be explained by the retardant property of C888 for a sustained release and the stronger solubilization of P188 compared to Tween80<sup>®</sup> (Sutananta *et al.*, 1995; Souto *et al.*, 2006; Wu and Lee, 2009; Hu *et al.*, 2010). Moreover, the S2 exhibited the highest %EE and %LC of  $90.55 \pm 0.28\%$  and  $5.54 \pm 0.02\%$  among the three SLN formulations. From all data, the S2 formulation comprising 5% w/w Compritol<sup>®</sup> 888 ATO (C888) with Tween80<sup>®</sup> (3.75%) combined with soy lecithin (1.875%) had an ability to entrap the 0.3% w/w OXY (Table 7). Based on these findings, the formulation S2 was judged to be the optimum SLN formulation, and will be utilized as the starting formulation for further NLC production.

**Table 7** Summary of homogenization conditions compositions and properties of the optimum S2 formulation

Formulation	Homogenization conditions		Compositions (% w/w)			Physicochemical properties						
	Speed (rpm)	Time (min)	Solid lipid (5%)	Surfactant (3.75%)	Co-surfactant (1.875%)	Appearance	PS (nm)	PDI	±	TDC (%)	EE (%)	LC(%)
							± SD	SD	± SD	± SD	± SD	
S2	24,000	15	C888	Tween80 <sup>®</sup>	Soy lecithin	Milky suspension	134.40 ± 0.57	0.25 ± 0.00		102.05 ± 1.97	90.55 ± 0.28	5.54 ± 0.02

## 1.2 Preparation and optimization of OXY-loaded NLC

The NLC were prepared by high speed homogenization method using a S 25N-18G high speed homogenizer. According to SLN production, the NLC were formulated by taking the SLN compositions as the starting formulation and differently lipid phase consisted of varied ratios of C888 and liquid lipid (Labrafac<sup>®</sup> CC; Lab CC) including 4:1 (NLC1), 3:2 (NLC2) and 2.5:2.5 (NLC3). The same concentration of OXY (0.3 %w/w) was added to each formulation OXY-loaded NLC (OXY-NLC). The result revealed that C888 and Lab CC of the three NLC formulations exhibited good miscibility in the nanoparticulate state.

Both blank formulation and SLN containing drug had a well milky appearance with low viscosity and non-flocculation (Figure 7). The small particle sizes (<110 nm) with a uniform size distribution and high ZP values (about -50 mV) were obtained. This indicated that the incorporated OXY (0.3 %w/w) did not change the physical properties of the SLN. In case of NLC, all the blank NLC and the OXY-NLC presented similarly a high ZP of above -30 mV. Compared with the OXY-SLN, the PS of OXY-NLC in all formulations was significantly smaller than that of the OXY-SLN ( $p < 0.05$ ) (Table 8). Therefore, addition of the Lab CC oil to the system did affect the particle sizes due to a decrease in the melting point of the solid lipid and a rapid distribution of the heat energy by oil in the emulsification process (Zhuang *et al.*, 2010).

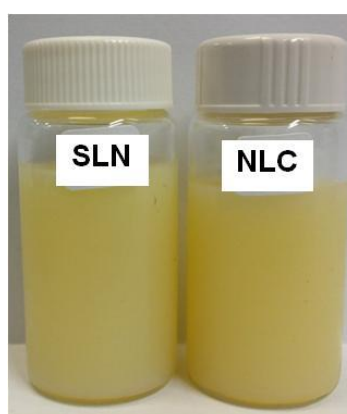


**Figure 7** The appearance of OXY-loaded lipid nanoparticles (SLN and NLC3)

All the developed SLN and NLC had 100% (w/w) of the incorporated OXY in the formulations indicating no drug loss occurred during the preparation process. After preparation (0 month), the %EE of the NLC including NLC1 and NLC3

was significantly higher than for the SLN ( $p < 0.05$ ) while, no significant difference of loading capacity of the SLN and NLC (~5% w/w, of solid lipid) ( $p > 0.05$ ). Thus, the NLC1 and NLC3 were selected to evaluate in the next step compared to the SLN. TEM observation revealed that both the NLC formulations had spherical uniform shape with smooth surfaces, and did not aggregate. The mean diameter of the SLN and NLC containing OXY from the TEM were in agreement with the results obtained by the PCS. Meanwhile, the morphology of SLN changed from spheres at 0 month (Figure 8A) to two-layered particles with irregular surfaces (Figure 8B) after storage for 3 months. These results indicated less stability of SLN than NLC (Üner, 2006).

**Table 8** Physicochemical characteristics and stability data at  $4 \pm 2^\circ\text{C}$  of the blank formulations, OXY-SLN and OXY-NLC

Code	PS (nm) $\pm$ SD	PDI $\pm$ SD	ZP (mV) $\pm$ SD	TDC (%)	EE (%)	LC (%)
0 month						
Blank SLN	97.7 $\pm$ 0.1	0.302 $\pm$ 0.003	-52.7 $\pm$ 1.2			
Blank NLC1	98.2 $\pm$ 0.5	0.302 $\pm$ 0.003	-49.8 $\pm$ 0.6			
Blank NLC2	97.9 $\pm$ 0.7	0.278 $\pm$ 0.011	-45.6 $\pm$ 0.1			
Blank NLC3	90.7 $\pm$ 0.4	0.278 $\pm$ 0.009	-41.7 $\pm$ 2.4			
SLN	107.5 $\pm$ 0.3	0.245 $\pm$ 0.004	-51.1 $\pm$ 1.0	100.7 $\pm$ 0.9	85.5 $\pm$ 0.8	5.2 $\pm$ 0.1
NLC1	99.3 $\pm$ 0.2	0.246 $\pm$ 0.005	-45.5 $\pm$ 0.6	101.3 $\pm$ 0.3	87.7 $\pm$ 0.4	5.3 $\pm$ 0.1
NLC2	99.8 $\pm$ 0.1	0.231 $\pm$ 0.006	-46.4 $\pm$ 0.4	102.1 $\pm$ 1.7	83.5 $\pm$ 1.1	5.1 $\pm$ 0.1
NLC3	96.0 $\pm$ 0.9	0.259 $\pm$ 0.006	-42.3 $\pm$ 0.9	101.1 $\pm$ 3.6	88.5 $\pm$ 0.1	5.4 $\pm$ 0.4
3 months						
SLN	111.0 $\pm$ 0.9	0.243 $\pm$ 0.012	-38.3 $\pm$ 1.1	102.9 $\pm$ 4.8	83.7 $\pm$ 0.1	5.2 $\pm$ 0.1
NLC1	101.8 $\pm$ 0.4	0.244 $\pm$ 0.001	-38.4 $\pm$ 1.3	99.7 $\pm$ 1.9	83.7 $\pm$ 0.5	5.0 $\pm$ 0.1
NLC3	97.6 $\pm$ 1.3	0.249 $\pm$ 0.008	-33.2 $\pm$ 2.2	101.7 $\pm$ 3.8	87.8 $\pm$ 0.3	5.2 $\pm$ 0.1
6 months						
SLN	122.4 $\pm$ 1.0	0.249 $\pm$ 0.010	-34.9 $\pm$ 1.0	97.7 $\pm$ 6.2	84.0 $\pm$ 0.5	5.1 $\pm$ 0.1
NLC1	101.9 $\pm$ 0.6	0.272 $\pm$ 0.003	-39.8 $\pm$ 0.3	96.0 $\pm$ 7.4	84.7 $\pm$ 0.5	5.1 $\pm$ 0.1

Code	PS (nm) $\pm$ SD	PDI $\pm$ SD	ZP (mV) $\pm$ SD	TDC (%)	EE (%)	LC (%)
NLC3	97.4 $\pm$ 0.8	0.251 $\pm$ 0.009	-41.5 $\pm$ 2.6	103.2 $\pm$ 1.1	87.7 $\pm$ 0.2	5.4 $\pm$ 0.1
9 months						
SLN	122.4 $\pm$ 1.3	0.259 $\pm$ 0.003	-30.0 $\pm$ 2.2	102.2 $\pm$ 1.3	83.2 $\pm$ 0.2	4.9 $\pm$ 0.1
NLC1	102.0 $\pm$ 1.3	0.256 $\pm$ 0.004	-37.4 $\pm$ 1.1	100.3 $\pm$ 2.7	84.3 $\pm$ 0.5	5.1 $\pm$ 0.0
NLC3	97.8 $\pm$ 0.5	0.278 $\pm$ 0.014	-39.5 $\pm$ 2.8	101.3 $\pm$ 1.0	84.7 $\pm$ 0.1	5.2 $\pm$ 0.1
12 months						
SLN	159.2 $\pm$ 0.6	0.259 $\pm$ 0.015	-27.7 $\pm$ 0.5	98.4 $\pm$ 2.1	78.0 $\pm$ 0.3	4.6 $\pm$ 0.0
NLC1	104.2 $\pm$ 0.4	0.229 $\pm$ 0.005	-37.0 $\pm$ 1.6	103.0 $\pm$ 3.7	83.0 $\pm$ 0.0	5.0 $\pm$ 0.0
NLC3	106.2 $\pm$ 0.5	0.295 $\pm$ 0.005	-41.0 $\pm$ 0.4	100.7 $\pm$ 0.5	84.5 $\pm$ 0.3	5.1 $\pm$ 0.0

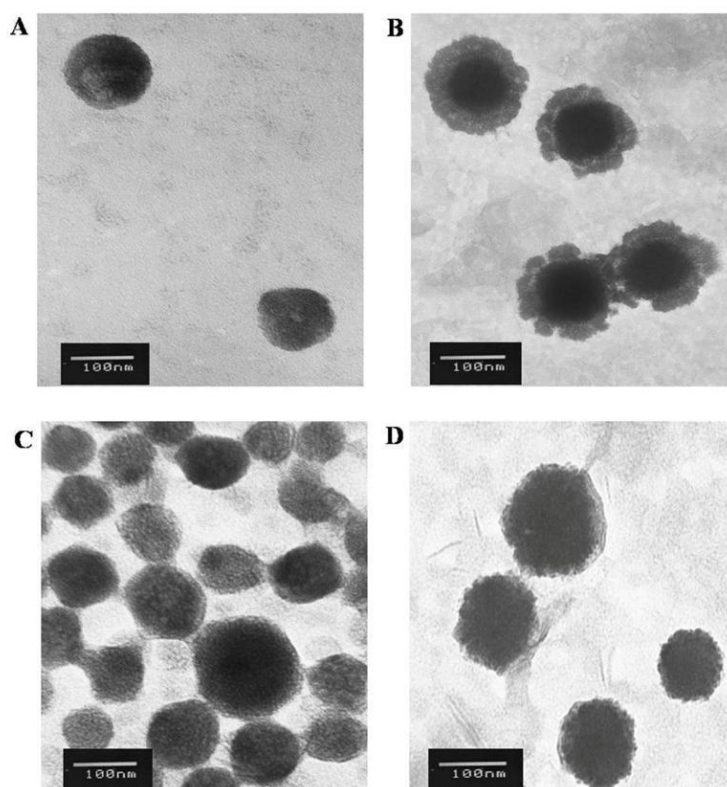


**Figure 8** TEM images at  $\times 100$  k of SLN (A) at 0 month; SLN (B), NLC1 (C), and NLC3 (D) after 3-months storage

The DSC thermogram of physical mixture reveals two melting peaks appeared at 109 °C and 71 °C representing the peaks of the OXY and C888. The loss of the endothermic peak of OXY in the developed SLN and NLC indicated that the OXY in the lipid phase was in an amorphous state and formed a solid solution within the matrix of nanoparticles (Figure 9). In addition, it was observed that the melting point of the C888 in the NLC3 had shifted to a lower temperature compared to the NLC1 and SLN, respectively. The results related to the oil present in the NLC systems which depressed the melting point of the lipid matrix in a concentration-dependent manner (Jenning *et al.*, 2000; Gokce *et al.*, 2012). This confirmed that NLC had a less ordered crystalline structure than SLN. The physical state of such systems was confirmed by the PXRD (Figure 10). The PXRD diagram of the physical mixture shows two characteristic peaks of C888 and a peak intensity of pure OXY. It indicated that the bulk matrix (C888) and OXY were crystalline. In contrast, there was no characteristic peak of crystalline OXY observed in the patterns of the three formulations indicating the molecular dispersion in an amorphous state of the incorporated OXY.

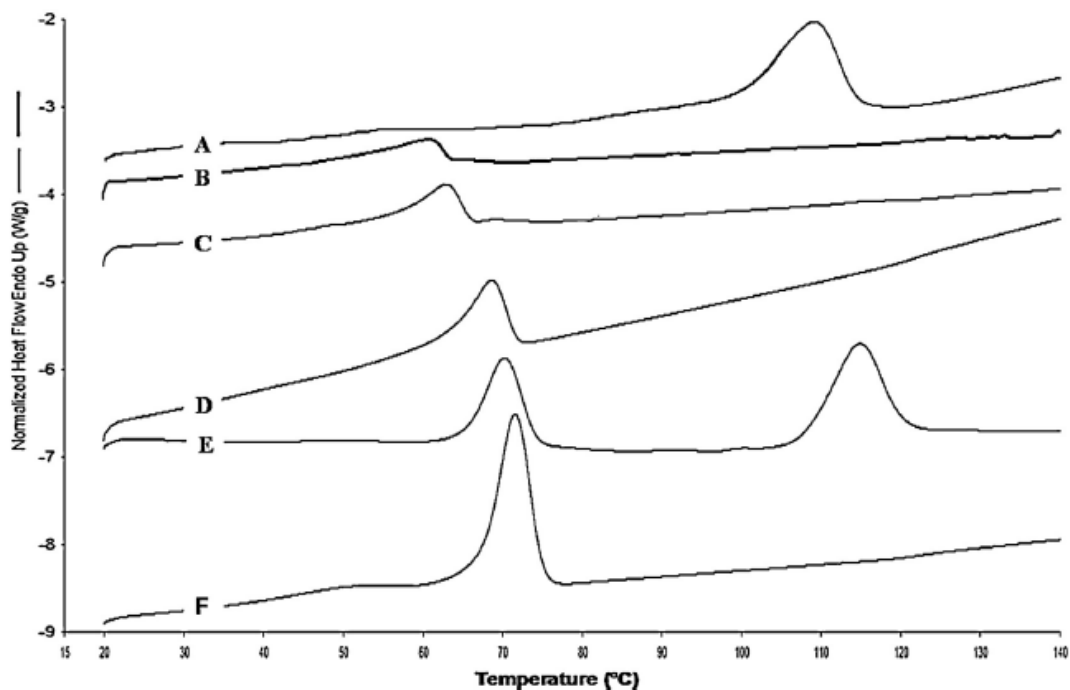


**Figure 9** DSC thermograms of OXY (A); freeze dried powders of NLC3 (B); NLC1 (C); SLN (D); physical mixtures of C888 and OXY (E); and C888 (F)



*In vitro* drug release study was carried out in SGF pH 1.2 and SIF pH 6.8. The OXY suspension tended to release a high amount of OXY in both medium. On the other hand, the release of OXY from the SLN and NLC formulations slowed down considerably in the SGF pH 1.2 and exhibited a sustained release up to 48 h in the SIF pH 6.8. Comparing each of the SLN and NLC formulations at pH 6.8, the slowest OXY release profile was observed in the NLC1 (Figure 11). The results indicated that the release rate of OXY might depend on the crystallinity of the lipid matrix. These results demonstrated that the OXY entrapped in SLN and NLC was protected from the strong acidic environment of stomach and therefore subsequently reached the small intestine. Moreover, the OXY release data from all developed SLN and NLC were best fitted to a Ritger-Peppas kinetic model as the  $r^2$  was close to 1. Based on the model,  $n$  values of the SLN and NLC were in the range of  $0.43 < n < 0.85$  indicating that the release from the lipid nanoparticles contributing to a combination of drug diffusion and erosion from the lipid matrix. Furthermore, the  $n$  values of the three formulations (SLN, NLC1 and NLC3) were close to 0.85 indicated that the erosion was the predominant release mechanism. So that the major amount of drug was enriched in the matrix and only small drug amount on the surface of the nanoparticles can diffuse into the medium.

There were no changes in the appearance and PDI for up to 12 months for the OXY-SLN and OXY-NLC under storage conditions ( $4 \pm 2^\circ\text{C}$ ). The increase of PS and the reduction of the ZP were remarkably observed during storage conditions for the SLN (Table 8). Meanwhile, the ZP of the NLC formulations remained in the high negative values (above 30 mV). Furthermore, the %EE and %LC of both NLC were significantly higher than those of the SLN after 12 months of storage ( $p < 0.05$ ). These results demonstrate the reduced stability of the SLN compared to the NLC which also agrees with the TEM analysis. Therefore, the NLC3 was selected for further *in vitro* permeability and *in vivo* absorption studies to ensure it was a potential carrier for the oral delivery of OXY.

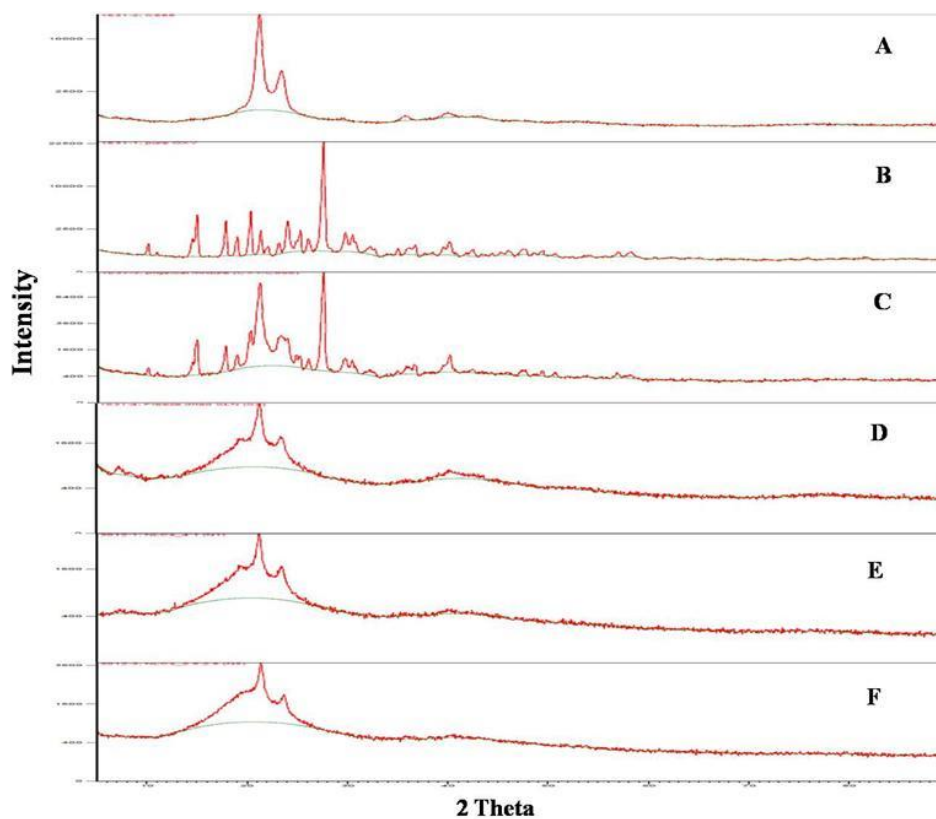


**Figure 10** Powder X-ray images of C888 (A); OXY (B); physical mixtures of C888 and OXY (C), and freeze dried powders of SLN (D); NLC1 (E) and NLC3 (F)

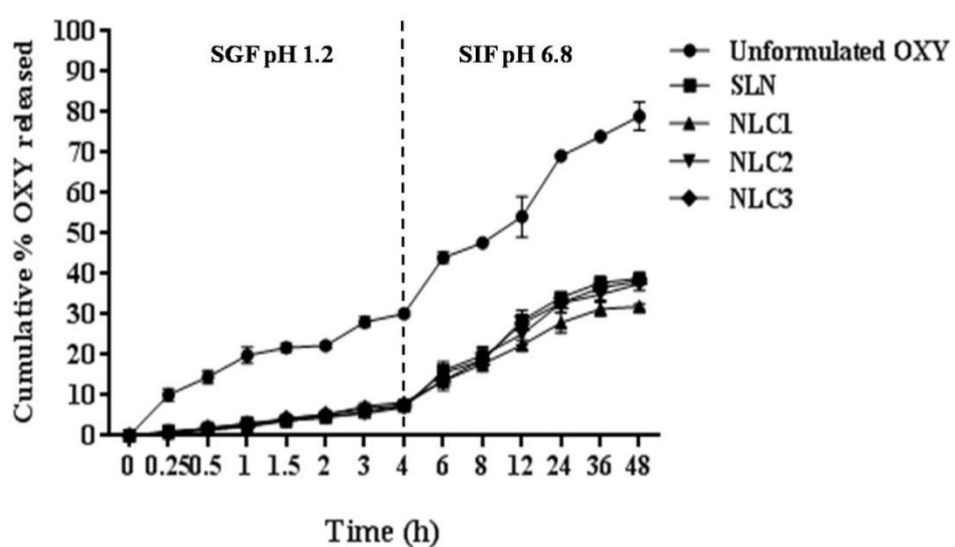


**Figure 11** *In vitro* OXY release profiles of SLN and NLC formulations with different lipid to oil ratios (NLC1, NLC2, NLC3) compared with the unformulated OXY in SGF (pH 1.2) and SIF (pH 6.8). Data represents the mean  $\pm$  SD (n = 3).

The MTT assay was used to determine an optimal OXY concentration for the permeability study. The highest non-toxic concentration of solubilized OXY was 400  $\mu\text{M}$ . Similar to the lipid nanoparticle systems, either blank formulations or formulations containing drug were compatible to the cells up to 400  $\mu\text{M}$  of OXY (Figure 12). At 400  $\mu\text{M}$  of OXY, the efflux ratio (ER) of the unformulated OXY was found 2.55 indicating a substrate for the efflux transporters of OXY. Moreover, the SLN and NLC were reduced 2.8 folds and 3.3 folds, respectively, in the secretory permeability of OXY, whereas only enhanced absorptive permeability of NLC compared to those of unformulated OXY (Figure 13). Thus, the lipid nanoparticles were significantly alleviated efflux transport of OXY with ER ( $\leq 1$ ) of 0.59 and 1.01 for NLC and SLN, respectively.

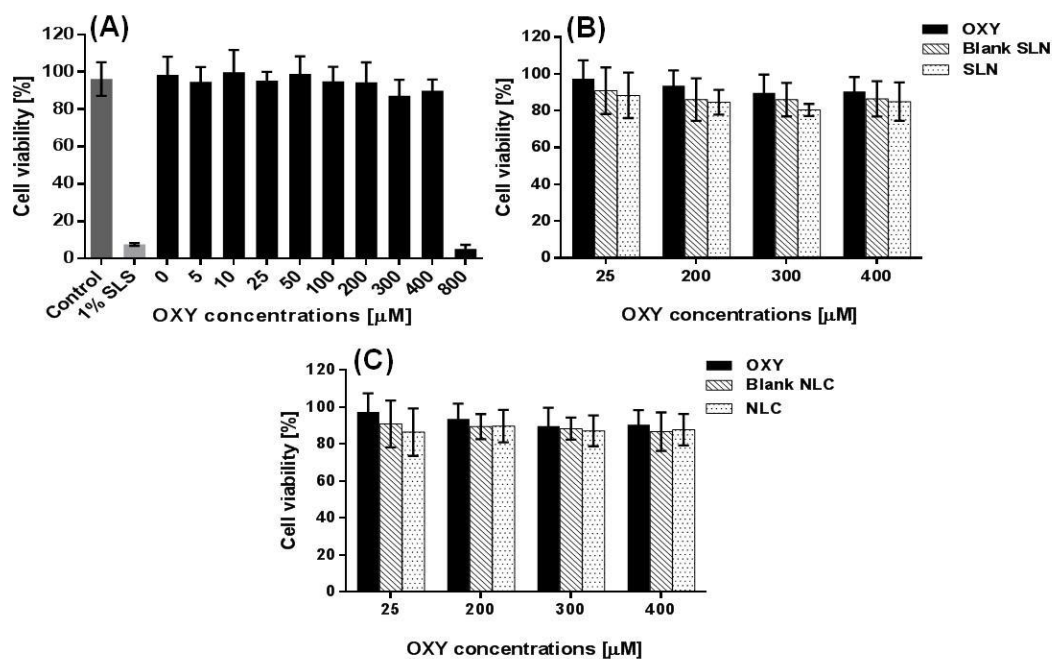


**Figure 12** The percentage of Caco-2 cell viability to different concentrations of OXY (A), OXY-loaded SLN (B) and OXY-loaded NLC (C) (n = 8), duplications.

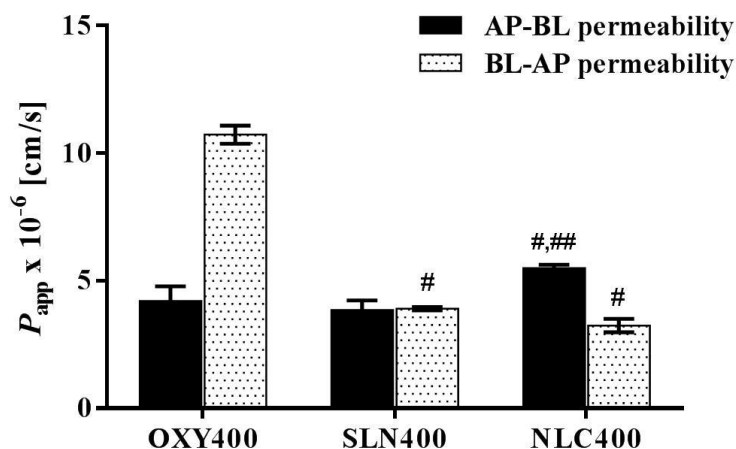


**Figure 13** Bidirectional transport across the Caco-2 monolayers of OXY and developed OXY-formulations. The data are presented as the apparent permeability coefficient ( $P_{app}$ ) in the absorptive (AP-BL) and the secretory directions (BL-AP). #  $p < 0.05$ , comparison with OXY400; ##  $p < 0.05$ , comparison with SLN400.

*In vivo* studies, the pharmacokinetic parameters in rats after oral administration of OXY in aqueous suspension or SLN and NLC at an equimolar dose are summarized in Figure 14 and Table 9. In comparison to the OXY suspension, the  $C_{max}$  of OXY administered as SLN was significantly decreased, while this from the NLC only slightly decreased. This data was consistent with the *in vitro* dissolution data. A greater  $AUC_{0-10h}$  ( $p < 0.05$ ) was obtained from the NLC (177.39%) and the SLN (124.91%), than from the unformulated OXY (100%) and indicated that there was a significantly improved systemic exposure to OXY. The *in vivo* results were in agreement with the *in vitro* permeability data. Possible mechanisms for improving the OXY bioavailability from NLC over SLN after oral administration have been speculated. Firstly, the significantly smaller particle sizes of the NLC ( $p < 0.05$ ) occupied a larger surface area than larger particles (i.e. SLN), a higher dispersibility and prolonged residence time to adhere at the absorptive site of the intestinal epithelium (How *et al.*, 2011). Secondly, the Lab CC oil used in the NLC had a greater solubilization capability for drugs (Pouton and Porter, 2008). Furthermore, the oil itself had permeation enhancing properties which improved oral drug absorption by many of ways, for example, mucoadhesive property of the vehicle and altering epithelial absorption (Lundin *et al.*, 1997). Furthermore, the medium chain triglyceride oil and lipid were structurally similar to the fat in daily food. They could

entrap the polar OXY and stimulate bile secretion, and thus enhance the uptake of intact particles by the gut wall and promote its draining into the lymphatic system. The absorption via the lymphatic system would also minimize rapid elimination of OXY. Finally, the sustained OXY release in the systemic circulation would achieve a longer availability of the drug in the body (Souto and Müller, 2010; Zhuang *et al.*, 2010; Tiwari and Pathak, 2011). Moreover, the surfactant used in the formulation might enhance intestinal permeability by several means i.e. inhibiting the efflux transporters of P-gp and MRPs family (Lo *et al.*, 2003; Shono *et al.*, 2004; How *et al.*, 2011). Furthermore, NLC entrapment could bypass the extensive first pass metabolism. Hence NLC is a promising carrier for improvements to the oral bioavailability of OXY. It was of interest that the multiple peaks of the plasma concentration of OXY observed in all the formulations tested would suggest enterohepatic recycling (EHC) of the absorbed OXY. Nevertheless, the time for the second mean peak (45 min) noted for each profile of formulation tested was the same (Figure 14). The consistency of the observation implied the altered absorption process of OXY, while disposition process could be minimally affected by the lipid nanoparticles.

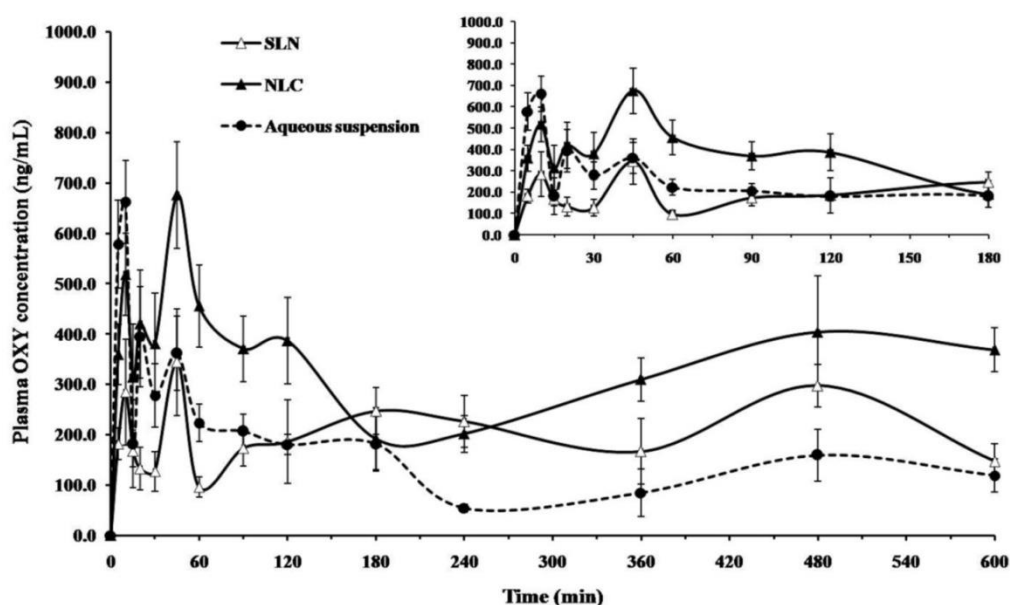


**Figure 14** Plasma concentrations of OXY vs. time profiles after oral administration of OXY-loaded SLN and NLC, compared with the unformulated OXY (180 mg/kg of OXY). Data represents the mean  $\pm$  SD ( $n = 7$ ).

**Table 9** Pharmacokinetics data of OXY after oral administration of OXY-loaded SLN and NLC, compared with the unformulated OXY (equivalent to 180 mg/kg of OXY). \*p < 0.05, comparison with aqueous suspension; # p < 0.05, comparison with SLN.

Parameters	OXY aqueous suspension	SLN	NLC
$C_{max}$ ( $\mu\text{g/mL}$ )	0.66 $\pm$ 0.08	0.28 $\pm$ 0.11 <sup>*</sup>	0.52 $\pm$ 0.08 <sup>*,#</sup>
$T_{max}$ (min)	10	10	10
AUC <sub>0-10h</sub> (ng h/mL)	1,897.34 $\pm$ 220.13	2,369.91 $\pm$ 268.84 <sup>*</sup>	3,365.78 $\pm$ 64.94 <sup>*,#</sup>
$F_{r, 0-10h}$ (%)	100	124.91	177.39

## 2. Development of OXY-loaded self-microemulsifying systems (SMEDDS)

The solubility of OXY in various vehicles was firstly determined to select the excipients for construction of ternary phase diagrams. In this study, all the selected excipients exhibited higher solubilization capacities for OXY than water (0.993  $\pm$  0.012 mg/mL) at RT. Capryol 90<sup>®</sup> was used as the oily phase with highest solubility for OXY (115.420  $\pm$  4.475 mg/mL) and Cremophor RH40<sup>®</sup> was selected as the main surfactant. Based on co-surfactant, the ternary phase diagrams of the Tween80<sup>®</sup>-(D2) and Labrasol<sup>®</sup>-(D3) based systems, provided large self-microemulsion region (Figure15). A fixed amount of OXY (40 mg/1g SMEDDS) was added into each system to find the most suitable surfactant concentration. The results demonstrated that only concentrations of Cremophor RH40<sup>®</sup> (40-45%) and co-surfactants (5-15%) in the formulations produced transparent microemulsions and no drug precipitation after 24 h. Therefore, two different concentration groups including a low (LS; 5% co-surfactant + 45% Cremophor RH40<sup>®</sup>) and high surfactant phase (HS; 15% co-surfactant + 40% Cremophor RH40<sup>®</sup>) of both types (D2 and D3) of SMEDDS were formulated. And the four formulations including low and high of Tween80<sup>®</sup> (LT and HT), and low and high of Labrasol<sup>®</sup> (LL and HL) of the OXY-SMEDDS were compared.

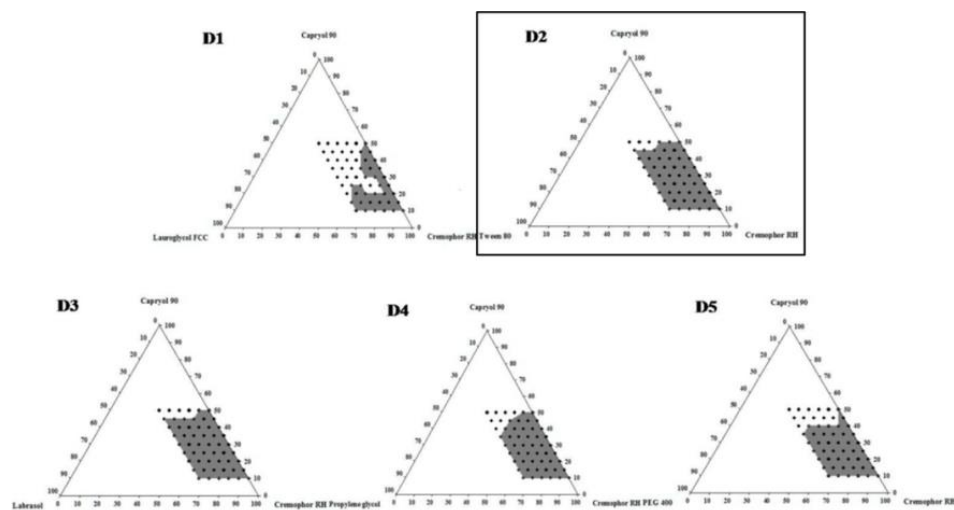


**Figure 15** Ternary phase diagram of Cremophor RH40<sup>®</sup>-based SMEDDS (system D) containing different co-surfactants including Lauroglycol FCC<sup>®</sup> (D1), Tween80<sup>®</sup> (D2), Labrasol<sup>®</sup> (D3), PG (D4) and PEG400 (D5). Gray areas represent the region of efficient self-microemulsification (Grade I), and the dots represent the compositions that were evaluated.

The four different formulations produced transparent microemulsion (visual grade I) after dilution with all of the dispersed media and the droplet size obtained was less than 50 nm (Figure 16). However, the Tween80<sup>®</sup>-based system (LT and HT) had a significantly smaller droplet size (~26 to 36 nm) than the Labrasol<sup>®</sup>-based system (LL and HL; ~34 to 45 nm) with all diluents used. In case of Tween80<sup>®</sup>-based system, the droplet sizes obtained from the HT formulation were significantly smaller ( $p < 0.05$ ) than from the LT formulation in all diluents. This finding indicated that the surfactant phase including the type and quantity did affect the microemulsion droplet size of the SMEDDS formulations. Meanwhile, there was no remarkable change in the total OXY content (~100% w/w) of the four SMEDDS formulations. The TEM micrographs (Figure 16) revealed that all microemulsions had a uniform spherical shape with no aggregation.

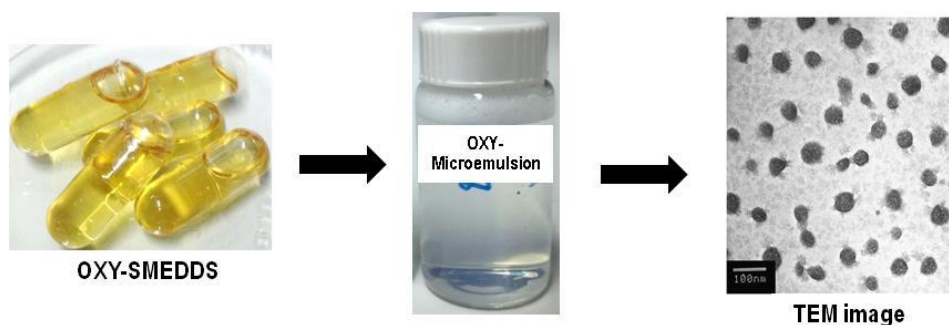


**Figure 16** Example of capsule filled with OXY-SMEDDS formulation which produced transparent microemulsion and its morphology observed by TEM

Using the capsule method, all formulations exhibited the rapid release of OXY with approximately 80% released within 10 min in the SGF pH 1.2 without pepsin at 37 °C (Figure 17). However, when using the dialysis bag method, the microemulsion containing OXY was trapped in the bag and allowed only free OXY (< 6% of the cumulative % released) to be released into the dissolution medium up to 2 h. These results implied that the major released content of OXY was in the microemulsion form.

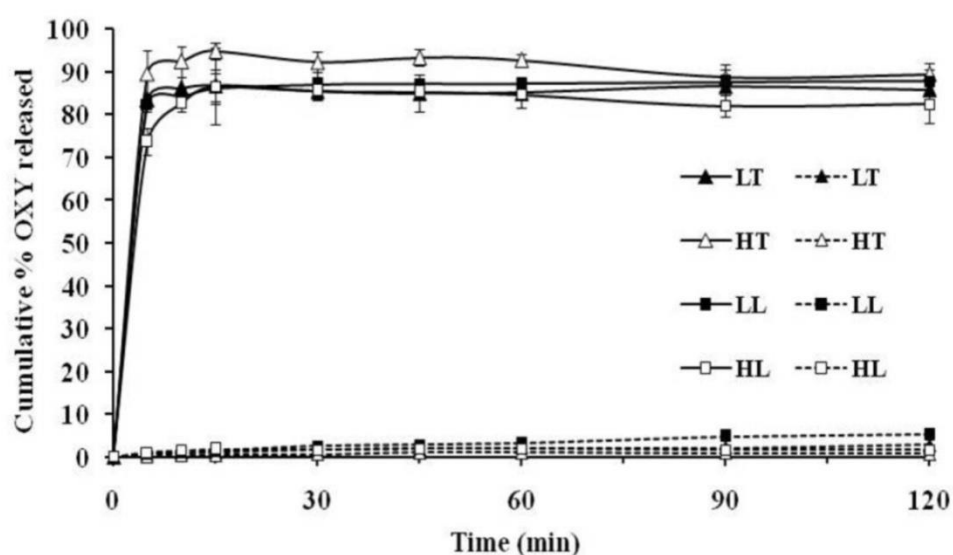


**Figure 17** The dissolution profiles of OXY from the capsule (dark lines) and the dialysis bag (dot line) filled with the SMEDDS formulations in simulated gastric fluid (SGF, pH 1.2) without pepsin. Data are represented by a mean  $\pm$  SD (n = 3).



After 24h-incubation with MTT, the formulations of both the Tween80<sup>®</sup> - (LT and HT) and Labrasol<sup>®</sup> - (LL and HL) based systems were compatible to Caco-2 intestinal cells up to the same OXY concentration of 100  $\mu\text{M}$ . However, the four SMEDDS were more toxic than the unformulated OXY according to no toxicity of pure OXY up to 400  $\mu\text{M}$  (Figure 18). Therefore, the OXY concentration in the SMEDDS should not be more than 100  $\mu\text{M}$ , to be considered as a nontoxic concentration for the transport study.

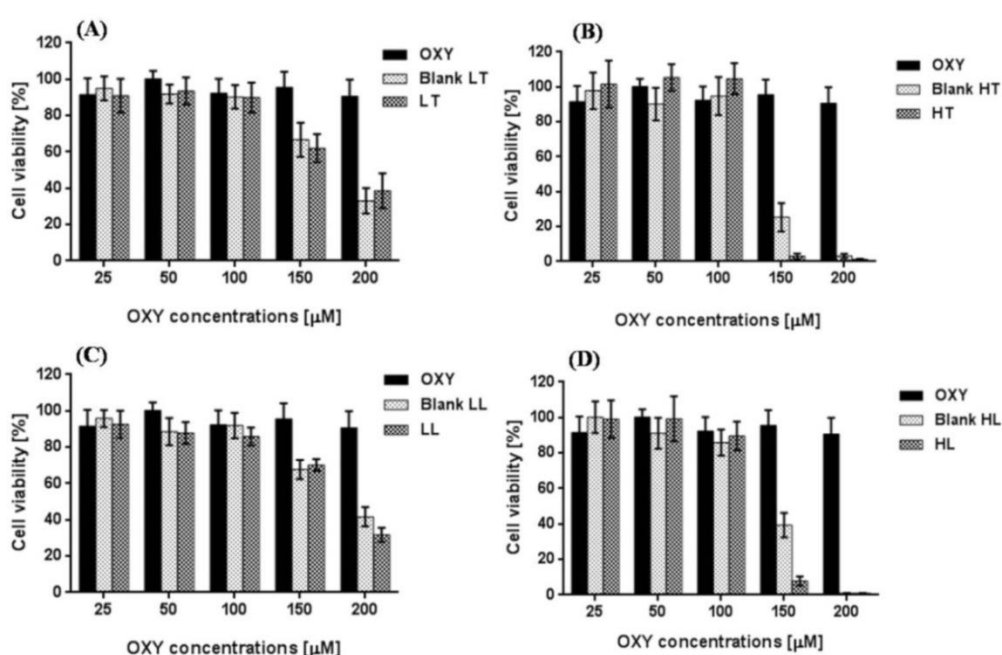


**Figure 18** The percentage of Caco-2 cell viability to different concentrations of OXY, blank SMEDDS and OXY-SMEDDS; A) LT, B) HT, C) LL, D) HL, (n = 8), duplications.

The ER of the solubilized OXY was found to be 5.02 at 100  $\mu\text{M}$  in the bidirectional studies. The significant increase of absorptive  $P_{app}$  (1.2-2.0 folds) and the significant decrease of secretory  $P_{app}$  of the OXY-SMEDDS formulations was consequence to a 5-fold reduction of the ER (0.94-1.14). This could imply that the SMEDDS formulated OXY enhanced the membrane permeability of OXY and inhibited the efflux pump. Moreover, the OXY-SMEDDS of the HS group (HT and HL) exhibited a better permeation across the Caco-2 monolayers (1.4-1.7 folds) than for the LS group (LT and LL) ( $p < 0.05$ ). However, a similar absorptive and secretory permeability was obtained from either the Tween80<sup>®</sup>-based or the Labrasol<sup>®</sup>-based systems, at the same

concentrations (Figure 19). This investigation indicated that the *in vitro* intestinal permeability of OXY was clearly improved by the developed SMEDDS.

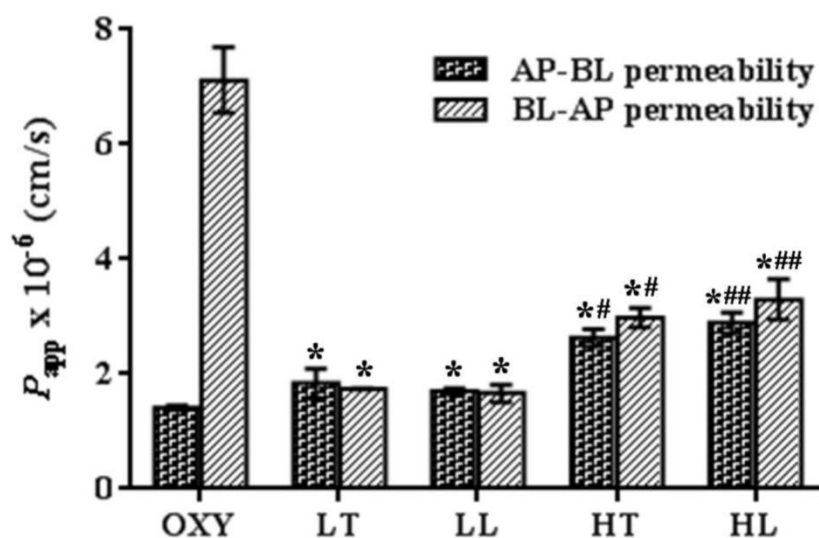


**Figure 19** Bidirectional transport across the Caco-2 monolayers of OXY and different OXY-SMEDDS. The data are presented as the apparent permeability coefficients ( $P_{app}$ ) in the absorptive (AP-BL) and the secretory directions (BL-AP).  $p < 0.05$ , comparison with OXY (\*); LT (#); LL (##) at the equivalent dose of OXY (100  $\mu$ M).

The pharmacokinetic parameters in rats receiving 180 mg/kg OXY either in aqueous suspensions or various SMEDDS formulations, are summarized in Figure 20 and Table 10. All the developed SMEDDS showed a significantly higher  $AUC_{0-10h}$  for OXY than for the unformulated OXY ( $p < 0.05$ ). However, only the Tween80<sup>®</sup>-based formulations (LT and HT) showed a significantly ( $p < 0.05$ ) higher  $C_{max}$  than the unformulated OXY ( $C_{max}$  0.66  $\pm$  0.08  $\mu$ g/mL). Furthermore, the  $T_{max}$  of OXY from the SMEDDS formulations was comparable to those from the unformulated OXY (10 min). For the Labrasol<sup>®</sup>-based system, the HL formulation ( $F_{r, 0-10h}$  218.32%) had a significantly higher  $AUC_{0-10h}$  ( $p < 0.05$ ) than the LL formulation ( $F_{r, 0-10h}$  137.98%) (Figure 20B and Table 10). Likewise, the HT formulation of Tween80<sup>®</sup>-based system was significantly greater ( $p < 0.05$ )  $C_{max}$  (2.5 folds) and  $AUC_{0-10h}$  (4.3 folds) of OXY than those of the LT formulation (Figure 20A and Table 10). The part of results correlated with the enhanced Caco-2 cell permeability data of these SMEDDS formulations. As in Table 10, at the same concentrations, Tween80<sup>®</sup>-based system (both LT and HT)

yielded a significantly greater  $C_{\max}$  (1.5-2.7 folds) ( $p < 0.05$ ) and  $AUC_{0-10h}$  (1.3-3.6 folds) for OXY than those of the Labrasol<sup>®</sup>-based system (LL and HL) (Figure 20C and 20D). On the contrary, there were no differences found between the *in vitro* permeability data of the OXY from such different systems in this study. Sometimes *in vitro* data could not predict *in vivo* data. This disparate phenomenon of absorption obtained from *in vitro* and *in vivo*, therefore, predicted that permeation of the intestine wall was not the determinant of the improved bioavailability of OXY offered by the SMEDDS systems. Among all SMEDDS formulations, the HT formulation that contained the highest amount of Tween80<sup>®</sup> yielded the greatest improved in the oral bioavailability of OXY ( $F_{r, 0-10h}$  786.32%). The superior enhancement of oral OXY absorption by the Tween80<sup>®</sup>-based system could be explained by the increased drug solubilization, effective stabilized and significantly reduced droplet size of microemulsion. Moreover, the high dispersibility and endocytotic internalization of the microemulsion were followed by intracellular release of the drug and increased transcellular pathway (Sha *et al.*, 2005; Lin *et al.*, 2007b; Kogan *et al.*, 2008). In addition, the restraining of the efflux transport and tight junction opening by Tween80<sup>®</sup> to move the intact microemulsion droplets through paracellular pathway were proposed (Zhang *et al.*, 2003; Rege *et al.*, 2002; Ujhelyi *et al.*, 2012). Then, it could bypass the first pass hepatic metabolism via increased lymphatic absorption by the Tween80<sup>®</sup> (Seeballuck *et al.*, 2004; Lind *et al.*, 2008). Furthermore, the rapid elimination of OXY might be minimized by inhibitory activity of the Tween80<sup>®</sup> that resulted in maintaining a longer resident time for the drug in the blood circulation (Ellis *et al.*, 1996). Surprisingly, the similarity of enterohepatic recycling (EHC) pattern of the SMEDDS containing the same co-surfactant was observed. The persistence of the EHC prolonged the exposure time of the OXY in the body (Gao *et al.*, 2014). These findings have indicated the advantages of the SMEDDS to enhance the bioavailability of the orally delivered OXY.

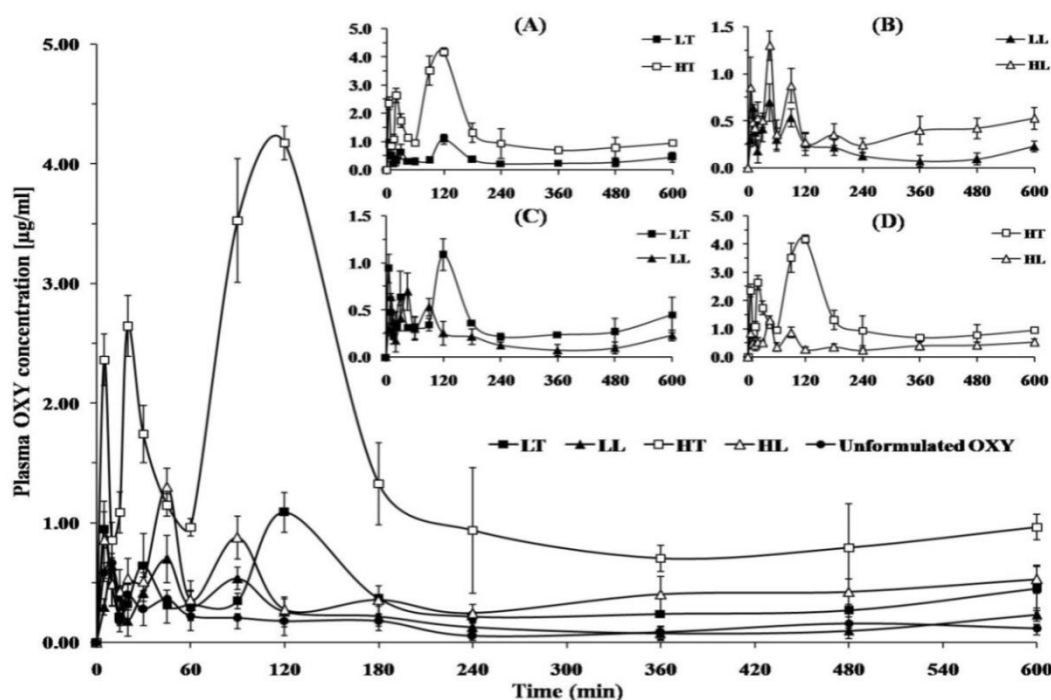


**Figure 20** Plasma concentrations vs. time profiles after the oral administration of OXY-SMEDDS and unformulated OXY (equivalent to 180 mg/kg of OXY). Comparison of different surfactant concentrations of SMEDDS; low LT and high HT (A), and low LL and high HL (B), for Tween80<sup>®</sup>-based (T) and Labrasol<sup>®</sup>-based (L) systems, respectively. Comparison of different surfactant types of SMEDDS; LT and LL (C), and HT and HL (D), for low (L) and high (H) concentrations, respectively. All values reported are mean values  $\pm$  SD (n = 7).

**Table 10** Pharmacokinetics data of OXY after the oral administration of different SMEDDS formulations and unformulated OXY (equivalent to 180 mg/kg of OXY). The values are presented as mean values  $\pm$  SD (n = 7).  $p < 0.05$ , in comparison with the unformulated OXY (\*); LT (\*\*); LL (\*\*\*) ; HL (#).

Parameters	$C_{max}$ ( $\mu\text{g/mL}$ )	$T_{max}$ (min)	$AUC_{0-10h}$ (ng h/mL)	$F_{r, 0-10h}$ (%)
Unformulated	0.66 $\pm$ 0.08	10	1,897.34 $\pm$ 220.13	100
OXY				
LT	0.94 $\pm$ 0.15 <sup>***</sup>	5	3,460.37 $\pm$ 188.39 <sup>***</sup>	182.38
LL	0.64 $\pm$ 0.04	10	2,617.86 $\pm$ 360.25 <sup>*</sup>	137.98
HT	2.36 $\pm$ 0.22 <sup>***,#</sup>	5	14,919.16 $\pm$ 522.00 <sup>***,#</sup>	786.32
HL	0.86 $\pm$ 0.32	5	4,142.33 $\pm$ 45.32 <sup>***</sup>	218.32

### 3. Comparison between lipid nanoparticles and self-microemulsifying system for oral delivery of OXY

In this study, the developed lipid formulations of OXY could be divided into two main groups based on the lipid phase of the formulations. First, lipid nanoparticle systems included SLN and NLC. The other was oily SMEDDS formulation. The lipid nanoparticles were prepared by mechanical techniques using the high shear homogenization, while the SMEDDS was simply produced by optimized concentrations of compositions (Figure 21). The liquid oil proportion in each formulation could be order as SMEDDS (45%) >NLC (2.5%) >SLN (0%). For surfactant phase, all formulations contain different Tween80<sup>®</sup> concentration of 10% (SMEDDS) > 3.75% (NLC = SLN). In addition, the drug loading of the SMEDDS (4% w/w) was much higher than that of the SLN and NLC (0.3 %w/w).

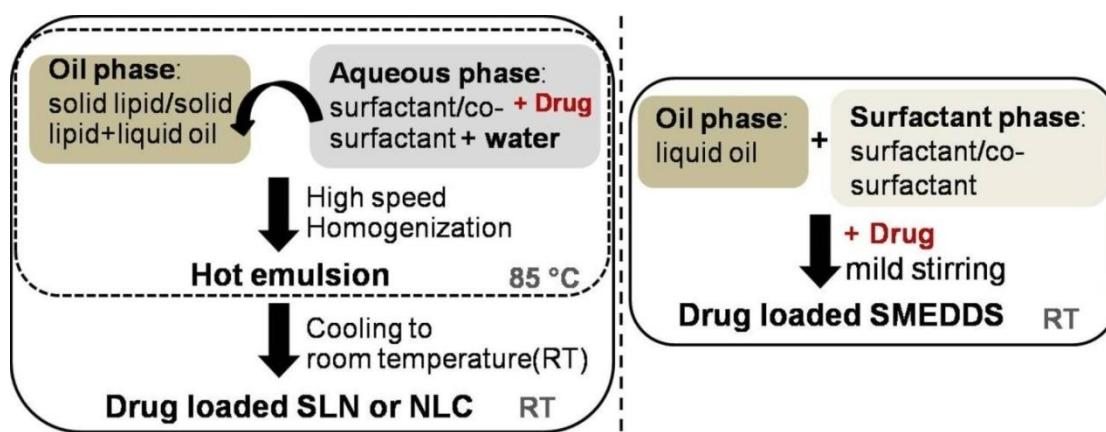


**Figure 21** Diagram of production process of lipid nanoparticles compared to preparation of SMEDDS

The dissimilarity on the selected storage temperatures for SMEDDS ( $30 \pm 2^\circ\text{C}$  and  $45 \pm 2^\circ\text{C}$ ) and lipid nanoparticles ( $4 \pm 2^\circ\text{C}$ ) could be explained by the difference of the composition in both systems. The temperature of refrigerator ( $4 \pm 2^\circ\text{C}$ ) was not suitable for SMEDDS system containing liquid oil (Capryol 90<sup>®</sup>) due to the oil would be wax at the low temperature. The conditions of room temperature (RT) or higher temperature were not proper for the lipid nanoparticles which comprised of the solid lipid and most of water. At RT, the contamination of the microorganism to the aqueous formulations was possible without adding preservative. Moreover, the high

temperature may cause the solid lipid to melt. The appearance of SMEDDS under accelerated conditions was changed to dark oily solution after storage of three months. Moreover, the mean PS of SLN was found to increase after three months of storage. Importantly, the total content of OXY in both lipid nanoparticles was almost 100% at various time points (0, 1, 3 months) whereas the OXY content in the SMEDDS was gradually decreased against the time (Figure 22). This result implied the instability of the oily SMEDDS according to the loss or degradation of drug. From the stability data, it might be concluded that the lipid nanoparticles are more stable than the oily formulations due to the efficiency of the solid lipid to protect the entrapped drug in the system.

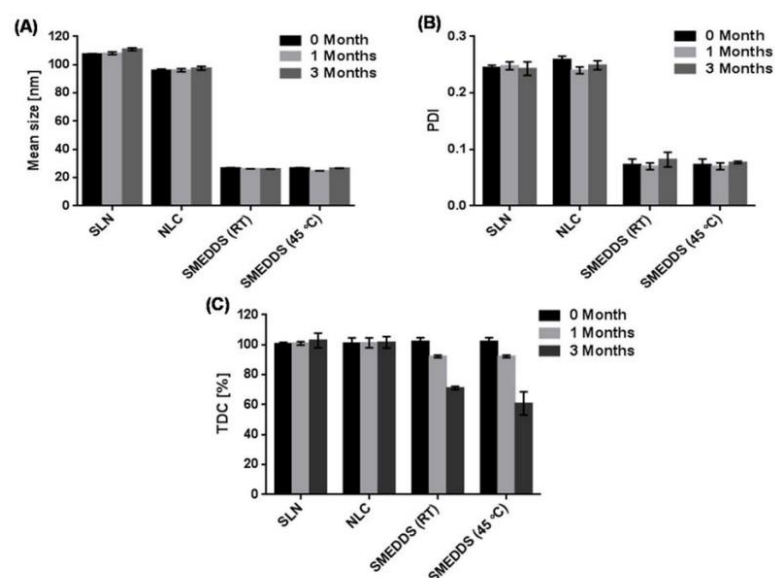


**Figure 22** Physical characteristics and stability data (0, 1, 3 months) of the OXY formulated as SLN, NLC and SMEDDS; (A) Mean size, (B) PDI and (C) %Total drug content (TDC). Data represents the mean  $\pm$  S.D. ( $n = 3$ ).

The cytotoxicity of SMEDDS (at 100  $\mu$ M) was 4-folds higher than that of lipid nanoparticles (at 400  $\mu$ M). The result might be related to the different compositions of the systems. As in previous report, the surfactants seem to be the major factor in cytotoxicity (Buyukozturk *et al.*, 2010; Ujhelyi *et al.*, 2012). In this study, the % surfactant phase (55 %w/w) of the SMEDDS was about 10 times greater than such of the lipid nanoparticles system (5.625 %w/w). Especially, the more % of Tween80<sup>®</sup> in SMEDDS

(10 %w/w) than the nanoparticles systems (3.75 %w/w) indicates the more toxic of the former system due to a concentration-dependent manner of cytotoxic properties of the surfactants (Ujhelyi *et al.*, 2012). In addition, the Capryol 90<sup>®</sup> oil of the SMEDDS which contained propylene glycol esters group implied the cytotoxicity on the Caco-2 cells at high concentration (Ujhelyi *et al.*, 2012; Thakkar and Desai, 2015). Meanwhile, the C888 solid lipid, long chain glyceride, and the Lab CC oil, medium chain triglyceride, commonly used in NLC was compatible to the intestinal cells because of the similarity of its structure to physiological lipids of the body.

As known, the low oral bioavailability of OXY was sequel from the low intestinal permeability which involved the efflux transport mechanism (Mei *et al.*, 2012; Sangsen *et al.*, 2016). From bidirection transport studies, only 1.5 and 3 times increase in *P<sub>app</sub>* of the secretory direction and the absorptive direction, respectively, consequence to the decrease in the ER of the drug from 5.02 to 2.55 when increasing the OXY concentration from 100  $\mu$ M to 400  $\mu$ M. This can be explained by the saturation of activity of the efflux transporters at Caco-2 cell monolayer. From the impact of the bioactive content, both formulations of the nanoparticles were compared to the SMEDDS system at the 100  $\mu$ M of OXY. At this level, the NLC, SLN and SMEDDS were significantly improved 3, 2.8, and 2.5 folds in *P<sub>app</sub>* (AP-BL) value of absorptive permeability, respectively, compared to unformulated OXY. Meanwhile, the *P<sub>app</sub>* value of secretory direction (BL-AP) of the NLC, SLN, and SMEDDS was found 1.3, 1.8, and 1.5 folds decrease, respectively, comparing to the unformulated OXY (Figure 23). Thus, the data indicated that no difference of the ER of the three formulations. Although the transport mechanisms of different lipid-based systems across the intestinal epithelium were diversified but the effectiveness of the mechanisms could be comparable. The lipid nanoparticles have been preferential uptake by specialized Peyer's patches (M cells) and the isolated follicles of the gut-associated lymphoid tissue located at the intestinal epithelium (Bilia *et al.*, 2014). Meanwhile, the microemulsion droplets of SMEDDS were mainly generated to be mixed micelles and then pass through chylomicron uptake mechanism by enterocytes. Finally, the compound formulated as solid lipid and oily formulations was further reached to systemic circulation (Bilia *et al.*, 2014; Porter *et al.*, 2008). Moreover, the inhibition activities on the efflux mediated transporter (s) and tight junction modulation of the surfactants in the lipid formulations promote thereby the oral absorption (Buyukozturk *et al.*, 2010; Thakkar and Desai, 2015; Ujhelyi *et al.*, 2012).

These have been the potential mechanisms of the lipid-based formulations implemented for the oral delivery.

Nevertheless, the data from the absorption study alone may not be able to predict explicitly oral drug bioavailability (Lasa-Saracíbar *et al.*, 2014; Mekjaruskul *et al.*, 2013). In particular of OXY, the three lipid formulations including SLN, NLC, and SMEDDS, were successfully improved *in vitro* absorption and oral bioavailability compared to the unformulated OXY. Although, the difference of the *in vitro* permeability of OXY from each formulation is not empirical as that observed their *in vivo* studies (Sangsen *et al.*, 2015; Sangsen *et al.*, 2016).

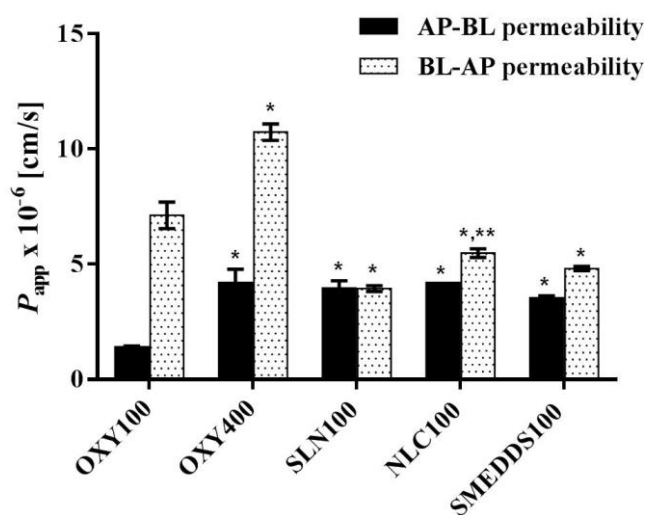


**Figure 23** Bidirectional transport across the Caco-2 monolayers of OXY and developed OXY-formulations. The data are presented as the apparent permeability coefficient ( $P_{app}$ ) in the absorptive (AP-BL) and the secretory directions (BL-AP). \* $p < 0.05$ , comparison with OXY100; \*\* $p < 0.05$ , comparison with SLN100.



## CONCLUDING REMARKS

OXY, is an active compound purified from Thai herbal plant “Ma-Haad”, offers many health benefits according to its potential pharmacological and biological activities. However, OXY has low oral bioavailability which limits its further use as a therapeutic agent or dietary supplement. In this study, the different lipid-based drug delivery systems (LBDDS) including lipid nanoparticles systems (SLN and NLC) and the SMEDDS have been developed for improved oral bioavailability of OXY. The OXY-loaded SLN were prepared by mechanical technique of the high speed homogenization. The OXY-loaded SLN formulation comprising Compritol<sup>®</sup> 888 ATO, Tween80<sup>®</sup> combined with soy lecithin had a good appearance, high entrapment efficiency and the most favorable physicochemical properties. The optimized SLN could retard OXY release in SGF pH 1.2 and SIF pH 6.8. The optimum amounts of miscible components of SLN with efficient preparation procedure were chosen to use as the starting conditions for NLC production. The NLC were formulated by replacing some quantity of Compritol<sup>®</sup> 888 ATO with liquid lipid (Labrafac<sup>®</sup> CC). Compared with OXY-loaded SLN, the OXY-loaded NLC showed a smaller and more uniform nanoparticle size, higher entrapment efficiency, and a satisfactory loading capacity. Moreover, the OXY-loaded NLC was more stable than the OXY-loaded SLN after a 12-months storage period. A sustained release of OXY without an initial burst effect was also achieved from the NLC. The lipid nanoparticles loaded with OXY were not toxic to the Caco-2 cells up to 400  $\mu$ M of OXY. Interestingly, the NLC was greater in decrease of the *P*<sub>app</sub> of the secretory permeability of OXY compared to that of SLN and unformulated OXY. Consequently, the NLC (ER, 0.59) was significantly reduced the efflux transport of OXY compared with SLN (ER, 1.01) and unformulated OXY (ER, 2.55). Furthermore, an enhanced oral bioavailability of OXY in rats was obtained using the NLC compared to both OXY-SLN and an OXY suspension.

The OXY-loaded SMEDDS were successfully developed by simple optimization of chemical compositions in the system. Although, the SMEDDS formulations presented a rapid OXY release (> 80% w/w) within 10 min in the SGF pH 1.2, the major released content of OXY was found to be in the microemulsion form. The co-surfactant types of SMEDDS influenced the droplet size according to the Tween80<sup>®</sup> -

based SMEDDS provided the smaller droplet sizes than Labrasol<sup>®</sup>-based SMEDDS. Moreover, the high concentration of surfactant used in the system also affectively reduced the microemulsion size in different media. All SMEDDS formulation was compatible to Caco-2 intestinal cells up to 100  $\mu$ M. For the transport study, the ER of the solubilized OXY was 5.02 at 100  $\mu$ M. The OXY-loaded SMEDDS enhanced the membrane permeability of OXY and inhibited the efflux pump mechanisms which were consequence to a 5-fold reduction of the efflux ratio (ER 0.94-1.14). Furthermore, the OXY-SMEDDS of the high surfactant group exhibited a better permeation across the Caco-2 monolayers (1.4-1.7 folds) than for the low surfactant group ( $p < 0.05$ ). All developed SMEDDS increased the pharmacokinetics of OXY while retaining the intact enterohepatic pattern of the OXY in Wistar rats. The greatest improvement of oral bioavailability of OXY *in vivo* ( $F_{r,0-10h}$  786.32%) was achieved from the SMEDDS containing high proportions of Tween80<sup>®</sup>.

Thus, there were the disparate physical properties of the two different systems (lipid nanoparticles and oily SMEDDS) include appearance, size, size distribution and entrapment efficiency. Also, the recommended storage conditions for two lipid systems were different. Moreover, the different compositions of the systems especially high concentrations of surfactant result to more toxicity of the SMEDDS than lipid nanoparticles when exposed to the Caco-2 cells. Even though, the oily SMEDDS were comparable with lipid nanoparticles to enhance *in vitro* oral absorption of OXY when comparing to unformulated OXY. The optimum OXY-SMEDDS exhibited the better improvement of *in vivo* oral bioavailability of OXY than the lipid nanoparticles and unformulated OXY.

This research noticeably indicates the benefits of SMEDDS in the enhancement of OXY oral absorption which may result from the increased permeability and inhibited efflux mediated mechanisms. Moreover, the SMEDDS presented the remarkable improvement of the oral bioavailability of OXY. This approach has raised the possibility of using this active compound in treating and preventing some importance diseases in future. However, for use as a commercial product, it is necessary to improve the storage stability of this system. In addition, SMEDDS could also be used as a potential carrier for oral delivery of other compounds which are substrates for efflux transporters.

## REFERENCES

- Alex MA, Chacko A, Jose S, Souto E. Lopinavir loaded solid lipid nanoparticles (SLN) for intestinal lymphatic targeting. *Eur J Pharm Sci.* 2011;42(1):11-8.
- Almeida AJ, Runge S, Müller RH. Peptide-loaded solid lipid nanoparticles (SLN): influence of production parameters. *Int J Pharm.* 1997;149(2):255-65.
- Almeida AJ, Souto E. Solid lipid nanoparticles as a drug delivery system for peptides and proteins. *Adv Drug Deliv Rev.* 2007;59(6):478-90.
- Anand S, Gupta R. Self-microemulsifying drug delivery system: a review. *WJPPS.* 2015;4(8):506-22.
- Andrabi SA, Spina MG, Lorenz P, Ebmeyer U, Wolf G, Horn TF. Oxyresveratrol (trans-2, 3', 4, 5'-tetrahydroxystilbene) is neuroprotective and inhibits the apoptotic cell death in transient cerebral ischemia. *Brain Res.* 2004;1017(1):98-107.
- Artursson P, Karlsson J. Correlation between oral drug absorption in humans and apparent drug permeability coefficients in human intestinal epithelial (Caco-2) cells. *Biochem Biophys Res Commun.* 1991;175(3):880-5.
- Ban JY, Jeon S-Y, Nguyen TTH, Bae K, Song K-S, Seonga YH. Neuroprotective effect of oxyresveratrol from *Smilacis chiniae* rhizome on amyloid beta protein (25-35)-induced neurotoxicity in cultured rat cortical neurons. *Biol Pharm Bull.* 2006;29(12):2419-24.
- Basset C, Rodrigues AM, Eparvier V, Silva MR, Lopes NP, Sabatier D, et al. Secondary metabolites from *Spirotropis longifolia* (DC) Baill and their antifungal activity against human pathogenic fungi. *Phytochemistry.* 2012;74:166-72.
- Bertram RM, Davies NM. Elucidating the pharmacodynamics and disposition of oxyresveratrol. the 2009 Summer Undergraduate Research Poster Symposium; Washington State University, Washington State, USA; 2009.
- Bertram RM, Takemoto JK, Remsberg CM, Vega-Villa KR, Sablani S, Davies NM. High-performance liquid chromatographic analysis: applications to nutraceutical content and urinary disposition of oxyresveratrol in rats. *Biomed Chrom.* 2010;24(5):516-21.

- Bilia AR, Isacchi B, Righeschi C, Guccione C, Bergonzi MC. Flavonoids loaded in nanocarriers: an opportunity to increase oral bioavailability and bioefficacy. *Food Nutr Sci*. 2014;5:1212-27.
- Breuer C, Wolf G, Andrabi SA, Lorenz P, Horn TF. Blood-brain barrier permeability to the neuroprotectant oxyresveratrol. *Neurosci Lett*. 2006;393(2):113-8.
- Bunjes H, Koch MH, Westesen K. Influence of emulsifiers on the crystallization of solid lipid nanoparticles. *J Pharm Sci*. 2003;92(7):1509-20.
- Buyukozturk F, Benneyan JC, Carrier RL. Impact of emulsion-based drug delivery systems on intestinal permeability and drug release kinetics. *J Control Release*. 2010;142(1):22-30.
- Chakraborty S, Shukla D, Mishra B, Singh S. Lipid-an emerging platform for oral delivery of drugs with poor bioavailability. *Eur J Pharm Biopharm*. 2009;73(1):1-15.
- Chao J, Yu M-S, Ho Y-S, Wang M, Chang RC-C. Dietary oxyresveratrol prevents parkinsonian mimetic 6-hydroxydopamine neurotoxicity. *Free Radic Biol Med*. 2008;45(7):1019-26.
- Charoenlarp P, Radomyos P, Harinasuta T. Treatment of taeniasis with Puag-Haad: a crude extract of *Artocarpus lakoocha* wood. *Southeast Asian J Trop Med Pub Hlth*. 1981;12:568-70.
- Charoenlarp P, Radomyos P, Bunnag D. The optimum dose of Puag-Haad in the treatment of Taeniasia. *J Med Assoc Thailand*. 1989;72:71-3.
- Charoenlarp P, Shaipanich C, Subhanka S, Lakkantinaporn P, Tanunkat A. Pharmacokinetics of the active constituent of Puag-haad in man. Symposium on Mahidol University Research and Development, ASEAN Institute Health Development; 1991 February 25-29; Salaya, Nakhon Pathom, Thailand: 1991.
- Charoenlarp P. The comparison study of the efficacy of pure "Puag-haad", praziquantel and niclosamide in treatment of *Taenia saginata*. The seminar report on the development of herbal medicine use in clinic; 1993 June 2-3; Faculty of Medicine Siriraj Hospital, Mahidol University. Bangkok: 1993.
- Chen C-C, Tsai T-H, Huang Z-R, Fang J-Y. Effects of lipophilic emulsifiers on the oral administration of lovastatin from nanostructured lipid carriers:

- physicochemical characterization and pharmacokinetics. *Eur J Pharm Biopharm.* 2010;74(3):474-82.
- Chen C, Fan T, Jin Y, Zhou Z, Yang Y, Zhu X, et al. Orally delivered salmon calcitonin-loaded solid lipid nanoparticles prepared by micelle-double emulsion method via the combined use of different solid lipids. *Nanomedicine.* 2013;8(7):1085-100.
- Chen Y-C, Tien Y-J, Chen C-H, Beltran FN, Amor EC, Wang R-J, et al. *Morus alba* and active compound oxyresveratrol exert anti-inflammatory activity via inhibition of leukocyte migration involving MEK/ERK signaling. *BMC Complement Altern Med.* 2013;13(1):45.
- Chiou WL, Jeong HY, Chung SM, Wu TC. Evaluation of using dog as an animal model to study the fraction of oral dose absorbed of 43 drugs in humans. *Pharm Res.* 2000;17(2):135-40.
- Chuanasa T, Phromjai J, Lipipun V, Likhitwitayawuid K, Suzuki M, Pramyothin P, et al. Anti-herpes simplex virus (HSV-1) activity of oxyresveratrol derived from Thai medicinal plant: mechanism of action and therapeutic efficacy on cutaneous HSV-1 infection in mice. *Antiviral Res.* 2008;80(1):62-70.
- Chung KO, Kim BY, Lee MH, Kim YR, Chung HY, Park JH, et al. *In-vitro* and *in-vivo* anti-inflammatory effect of oxyresveratrol from *Morus alba* L. *J Pharm Pharmacol.* 2003;55(12):1695-700.
- Constantinides PP. Lipid microemulsions for improving drug dissolution and oral absorption: physical and biopharmaceutical aspects. *Pharm Res.* 1995;12(11):1561-72.
- Cortesi R, Esposito E, Luca G, Nastruzzi C. Production of lipospheres as carriers for bioactive compounds. *Biomaterials.* 2002;23(11):2283-94.
- Dadhaniya P, Patel C, Muchhara J, Bhadja N, Mathuria N, Vachhani K, et al. Safety assessment of a solid lipid curcumin particle preparation: acute and subchronic toxicity studies. *Food Chem Toxicol.* 2011;49(8):1834-42.
- Dai J-R, Hallock YF, Cardellina JH, Boyd MR. HIV-Inhibitory and cytotoxic oligostilbenes from the leaves of *Hopea malibato* 1. *J Nat Prod.* 1998;61(3):351-3.
- Deng H, He X, Xu Y, Hu X. Oxyresveratrol from mulberry as a dihydrate. *Acta Cryst.* 2012;68:1318-9.

- DeSesso J, Jacobson C. Anatomical and physiological parameters affecting gastrointestinal absorption in humans and rats. *Food Chem Toxicol.* 2001;39(3):209-28.
- Diederichs J, Muller R. Liposomes in cosmetics and pharmaceutical products. *Pharm Ind.* 1994;56(3):267-75.
- Djapic N, Djarmati Z, Filip S, Jankov RM. A stilbene from the heartwood of *Maclura pomifera*: note. *J Serb Chem Soc.* 2003;68(3):235-7.
- Dokania S, Joshi AK. Self-microemulsifying drug delivery system (SMEDDS)-challenges and road ahead. *Drug Deliv.* 2014;1-16.
- Ellis AG, Crinis NA, Webster LK. Inhibition of etoposide elimination in the isolated perfused rat liver by Cremophor EL and Tween 80. *Cancer Chemother Pharmacol.* 1996;38(1):81-7.
- Esposito E, Mariani P, Ravani L, Contado C, Volta M, Bido S, et al. Nanoparticulate lipid dispersions for bromocriptine delivery: characterization and *in vivo* study. *Eur J Pharm Biopharm.* 2012;80(2):306-14.
- Fang M, Jin Y, Bao W, Gao H, Xu M, Wang D, et al. *In vitro* characterization and *in vivo* evaluation of nanostructured lipid curcumin carriers for intragastric administration. *Int J Nanomedicine.* 2012;7:5395.
- Fangueiro J, Gonzalez-Mira E, Martins-Lopes P, Egea M, Garcia M, Souto S, et al. A novel lipid nanocarrier for insulin delivery: production, characterization and toxicity testing. *Pharm Dev Technol.* 2013;18(3):545-9.
- Farnsworth NR, Bunyapraphatsara N. Thai medicinal plants: recommended for primary health care system. Bangkok: Medicinal Plant Information Center, Faculty of Pharmacy, Mahidol University; 1992.
- Fatourus DG, Müllertz A. Using *in vitro* dynamic lipolysis modeling as a tool for exploring IVIVC relationships for oral lipid-based formulations. In: Hauss DJ, editor. *Oral lipid-based formulations: enhancing the bioavailability of poorly water-soluble drugs.* New York: Informa healthcare; 2007. p. 257-72.
- Fischl MA, Richman DD, Flexner C, Para MF, Haubrich R, Karim A, et al. Phase I/II study of the toxicity, pharmacokinetics, and activity of the HIV protease inhibitor SC-52151. *J Acquir Immune Defic Syndr.* 1997;15(1):28-34.

- Freitas C, Müller RH. Effect of light and temperature on zeta potential and physical stability in solid lipid nanoparticle (SLN™) dispersions. *Int J Pharm.* 1998;168(2):221-9.
- Freitas C, Müller RH. Correlation between long-term stability of solid lipid nanoparticles (SLN™) and crystallinity of the lipid phase. *Eur J Pharm Biopharm.* 1999;47(2):125-32.
- Freshney RI. *Culture of animal cells: A manual of basic technique.* 5<sup>th</sup> ed. New Jersey: Wiley & Sons; 2005.
- Galindo I, Hernáez B, Berná J, Fenoll J, Cenis JL, Escribano JM, et al. Comparative inhibitory activity of the stilbenes resveratrol and oxyresveratrol on African swine fever virus replication. *Antiviral Res.* 2011;91(1):57-63.
- Gan L-SL, Thakker DR. Applications of the Caco-2 model in the design and development of orally active drugs: elucidation of biochemical and physical barriers posed by the intestinal epithelium. *Adv Drug Deliv Rev.* 1997;23(1-3):77-98.
- Gao Y, Shao J, Jiang Z, Chen J, Gu S, Yu S, Zheng K, Jia L. Drug enterohepatic circulation and disposition: constituents of systems pharmacokinetics. *Drug Discov Today.* 2014;19:326-40.
- Garcia-Fuentes M, Prego C, Torres D, Alonso MJ. A comparative study of the potential of solid triglyceride nanostructures coated with chitosan or poly(ethylene glycol) as carriers for oral calcitonin delivery. *Eur J Pharm Sci.* 2005;25(1):133-43.
- Gasco M. Solid lipid nanospheres from warm micro-emulsions: improvements in SLN production for more efficient drug delivery. *Pharm technol Eur.* 1997;9:52-8.
- Gautam P, Patel R. *Artocarpus Lakoocha* Roxb: an overview. *EJCAM.* 2014;1(1):10-4.
- Gibson L. Lipid-based excipients for oral drug delivery. In: Hauss DJ, editor. *Oral lipid-based formulations: enhancing the bioavailability of poorly water-soluble drugs.* New York: Informa healthcare; 2007. p. 33-62.
- Gokce EH, Korkmaz E, Dellera E, Sandri G, Bonferoni MC, Ozer O. Resveratrol-loaded solid lipid nanoparticles versus nanostructured lipid carriers: evaluation of antioxidant potential for dermal applications. *Int J Nanomedicine.* 2012;7:1841.

- Gota VS, Maru GB, Soni TG, Gandhi TR, Kochar N, Agarwal MG. Safety and pharmacokinetics of a solid lipid curcumin particle formulation in osteosarcoma patients and healthy volunteers. *J Agric Food Chem.* 2010;58(4):2095-9.
- Gursoy RN, Benita S. Self-emulsifying drug delivery systems (SEDDS) for improved oral delivery of lipophilic drugs. *Biomed Pharmacother.* 2004;58(3):173-82.
- Hauss DJ, Fogal SE, Ficorilli JV, Price CA, Roy T, Jayaraj AA, et al. Lipid-based delivery systems for improving the bioavailability and lymphatic transport of a poorly water-soluble LTB<sub>4</sub> inhibitor. *J Pharm Sci.* 1998;87(2):164-9.
- Hauss DJ. Oral lipid-based formulations. *Adv Drug Deliv Rev.* 2007;59(7):667-76.
- He H, Lu Y-H. Comparison of inhibitory activities and mechanisms of five mulberry plant bioactive components against  $\alpha$ -glucosidase. *J Agric Food Chem.* 2013;61(34):8110-9.
- How CW, Abdullah R, Abbasalipourkabar R. Physicochemical properties of nanostructured lipid carriers as colloidal carrier system stabilized with polysorbate 20 and polysorbate 80. *Afr J Biotechnol.* 2011;10(9):1684-9.
- Hu C, Chen Z, Yao R, Xu G. Inhibition of protein kinase C by stilbene derivatives from *Morus alba* L. *Nat Prod Res Dev.* 1995;8(2):13-6.
- Hu F, Yuan H, Zhang H, Fang M. Preparation of solid lipid nanoparticles with clobetasol propionate by a novel solvent diffusion method in aqueous system and physicochemical characterization. *Int J Pharm.* 2002;239(1):121-8.
- Hu FQ, Hong Y, Yuan H. Preparation and characterization of solid lipid nanoparticles containing peptide. *Int J Pharm.* 2004;273(1-2):29-35.
- Hu F-Q, Jiang S-P, Du Y-Z, Yuan H, Ye Y-Q, Zeng S. Preparation and characteristics of monostearin nanostructured lipid carriers. *Int J Pharm.* 2006;314(1):83-9.
- Hu L, Xing Q, Meng J, Shang C. Preparation and enhanced oral bioavailability of cryptotanshinone-loaded solid lipid nanoparticles. *AAPS PharmSciTech.* 2010;11(2):582-7.
- Hu N, Mei M, Ruan J, Wu W, Wang Y, Yan R. Regioselective glucuronidation of oxyresveratrol, a natural hydroxystilbene, by human liver and intestinal microsomes and recombinant UGTs. *Drug Metab Pharmacokinet.* 2014;29(3):229-36.



- Huang H, Guo D, Li P. Determination of stilbenoids in *Smilax china* L. by HPLC. *Chin J New Drugs*. 2008a;24:2122-24.
- Huang H, Zhang J, Chen G, Lu Z, Wang X, Sha N, et al. High performance liquid chromatographic method for the determination and pharmacokinetic studies of oxyresveratrol and resveratrol in rat plasma after oral administration of *Smilax china* extract. *Biomed Chrom*. 2008b;22(4):421-7.
- Huang H, Chen G, Lu Z, Zhang J, Guo DA. Distribution study of two constituents in rat after oral administration of *Smilax china* extract. *China J Chin Mater Med*. 2009a;34(19):2512-5.
- Huang H, Zhang J, Chen G, Lu Z, Sha N, Guo D. Simultaneous determination of oxyresveratrol and resveratrol in rat bile and urine by HPLC after oral administration of *Smilax china* extract. *Nat Prod Commun*. 2009b;4(6):825-30.
- Huang H, Chen G, Lu Z, Zhang J, Guo DA. Identification of seven metabolites of oxyresveratrol in rat urine and bile using liquid chromatography/tandem mass spectrometry. *Biomed Chrom*. 2010;24(4):426-32.
- Igartua M, Saulnier P, Heurtault B, Pech B, Proust JE, Pedraz JL, et al. Development and characterization of solid lipid nanoparticles loaded with magnetite. *Int J Pharm*. 2002;233(1-2):149-57.
- Ingle LM, Wankhade VP, Udasi TA, Tapar KK. New approaches for development and characterization of SMEDDS. *Int J Pharm Sci Res*. 2013;3(1):7-14.
- Jagtap U, Bapat V. Artocarpus: a review of its traditional uses, phytochemistry and pharmacology. *J Ethnopharmacol*. 2010;129(2):142-66.
- Jain S, Chourasia M, Masuriha R, Soni V, Jain A, Jain NK, et al. Solid lipid nanoparticles bearing flurbiprofen for transdermal delivery. *Drug Deliv*. 2005;12(4):207-15.
- Jenning V, Thünemann AF, Gohla SH. Characterisation of a novel solid lipid nanoparticle carrier system based on binary mixtures of liquid and solid lipids. *Int J Pharm*. 2000;199(2):167-77.
- Jin W, Na M, An R, Lee H, Bae K, Kang SS. Antioxidant compounds from twig of *Morus alba*. *Nat Prod Sci*. 2002;8:129-32.

- Jores K, Mehnert W, Drechsler M, Bunjes H, Johann C, Mäder K. Investigations on the structure of solid lipid nanoparticles (SLN) and oil-loaded solid lipid nanoparticles by photon correlation spectroscopy, field-flow fractionation and transmission electron microscopy. *J Control Release*. 2004;95(2):217-27.
- Joung DK, Choi SH, Kang OH, Kim SB, Mun SH, Seo YS, et al. Synergistic effects of oxyresveratrol in conjunction with antibiotics against methicillin-resistant *Staphylococcus aureus*. *Mol Med Rep*. 2015;12(1):663-7.
- Kakkar V, Singh S, Singla D, Sahwney S, Chauhan AS, Singh G, et al. Pharmacokinetic applicability of a validated liquid chromatography tandem mass spectroscopy method for orally administered curcumin loaded solid lipid nanoparticles to rats. *J Chromatogr B*. 2010;878(32):3427-31.
- Kakkar V, Singh S, Singla D, Kaur IP. Exploring solid lipid nanoparticles to enhance the oral bioavailability of curcumin. *Mol Nutr Food Res*. 2011;55(3):495-503.
- Kang BK, Lee JS, Chon SK, Jeong SY, Yuk SH, Khang G, et al. Development of self-microemulsifying drug delivery systems (SMEDDS) for oral bioavailability enhancement of simvastatin in beagle dogs. *Int J Pharm*. 2004;274(1):65-73.
- Khoo SM, Edwards GA, Porter CJ, Charman WN. A conscious dog model for assessing the absorption, enterocyte-based metabolism, and intestinal lymphatic transport of halofantrine. *J Pharm Sci*. 2001;90(10):1599-607.
- Kim S, Ko H, Park JE, Jung S, Lee SK, Chun Y-J. Design, synthesis, and discovery of novel trans-stilbene analogues as potent and selective human cytochrome P450 1B1 inhibitors. *J Med Chem*. 2002a;45(1):160-4.
- Kim YM, Yun J, Lee C-K, Lee H, Min KR, Kim Y. Oxyresveratrol and hydroxystilbene compound: inhibitory effect on tyrosinase and mechanism of action. *J Biol Chem*. 2002b;277:16340-4.
- Kim J-K, Kim M, Cho S-G, Kim M-K, Kim SW, Lim Y-H. Biotransformation of mulberroside A from *Morus alba* results in enhancement of tyrosinase inhibition. *J Ind Microbiol Biotechnol*. 2010;37(6):631-7.
- Kipp J. The role of solid nanoparticle technology in the parenteral delivery of poorly water-soluble drugs. *Int J Pharm*. 2004;284(1):109-22.

- Kochummen KM. Moraceae. In: Ministry of Primary Industries Malaysia: Forest Department, F, S, P, Ng, editors. Tree flora of Malaya: a manual for foresters vol. 3: London, Kuala Lumpur: Longman; 1978. p. 119-68.
- Kogan A, Kesselman E, Danino D, Aserin A, Garti N. Viability and permeability across Caco-2 cells of CBZ solubilized in fully dilutable microemulsions. *Colloids Surf B*. 2008;66(1):1-12.
- Kohli K, Chopra S, Dhar D, Arora S, Khar RK. Self-emulsifying drug delivery systems: an approach to enhance oral bioavailability. *Drug Discov Today*. 2010;15(21):958-65.
- Kommuru T, Gurley B, Khan M, Reddy I. Self-emulsifying drug delivery systems (SEDDS) of coenzyme Q 10: formulation development and bioavailability assessment. *Int J Pharm*. 2001;212(2):233-46.
- Lasa-Saracibar B, Guada M, Sebastián V, J Blanco-Prieto M. *In vitro* intestinal co-culture cell model to evaluate intestinal absorption of edelfosine lipid nanoparticles. *Curr Top Med Chem*. 2014;14(9):1124-32.
- Lee H, Kim D, Hong J, Lee J, Kim E. Oxyresveratrol suppresses lipopolysaccharide-induced inflammatory responses in murine macrophages. *Hum Exp Toxicol*. 2014;34(8):808-18.
- Levy M, Benita S. Drug release from submicronized o/w emulsion: a new in vitro kinetic evaluation model. *Int J Pharm*. 1990;66(1):29-37.
- Li H, Wu WKK, Zheng Z, Che CT, Li ZJ, Xu DD, et al. 3, 3', 4, 5, 5'-pentahydroxy-trans-stilbene, a resveratrol derivative, induces apoptosis in colorectal carcinoma cells via oxidative stress. *Eur J Pharmacol*. 2010;637(1):55-61.
- Likhitwitayawuid K, Sritularak B, Benchanak K, Lipipun V, Mathew J, Schinazi RF. Phenolics with antiviral activity from *Millettia erythrocalyx* and *Artocarpus lakoocha*. *Nat Prod Res*. 2005;19(2):177-82.
- Likhitwitayawuid K, Sornsute A, Sritularak B, Ploypradith P. Chemical transformations of oxyresveratrol (trans-2, 4, 3', 5'-tetrahydroxystilbene) into a potent tyrosinase inhibitor and a strong cytotoxic agent. *Bioorg Med Chem Lett*. 2006;16(21):5650-3.
- Likhitwitayawuid K. Stilbenes with tyrosinase inhibitory activity. *Curr Sci*. 2008;94(1):44.

- Likhitwitayawuid K, Ma-Haad: Benefits in medicine, cosmetic and agriculture. 1<sup>st</sup> ed. Bangkok: Chulalongkorn University Printing House; 2008.
- Lin X, Li X, Zheng L, Yu L, Zhang Q, Liu W. Preparation and characterization of monocaprates nanostructured lipid carriers. *Colloids Surf A*. 2007a;311(1):106-11.
- Lin Y, Shen Q, Katsumi H, Okada N, Fujita T, Jiang X, et al. Effects of Labrasol and other pharmaceutical excipients on the intestinal transport and absorption of rhodamine123, a p-glycoprotein substrate, in rats. *Biol Pharm Bull*. 2007b;30(7):1301-7.
- Lind ML, Jacobsen J, Holm R, Müllertz A. Intestinal lymphatic transport of halofantrine in rats assessed using a chylomicron flow blocking approach: the influence of polysorbate 60 and 80. *Eur J Pharm Sci*. 2008;35(3):211-8.
- Lipipun V, Sasivimolphan P, Yoshida Y, Daikoku T, Sritularak B, Ritthidej G, et al. Topical cream-based oxyresveratrol in the treatment of cutaneous HSV-1 infection in mice. *Antiviral Res*. 2011;91(2):154-60.
- Liu A-L, Yang F, Zhu M, Zhou D, Lin M, Lee S, et al. *In vitro* anti-influenza viral activities of stilbenoids from the lianas of *Gnetum pendulum*. *Planta Med*. 2010;76(16):1874-6.
- Liu C-H, Wu C-T. Optimization of nanostructured lipid carriers for lutein delivery. *Colloids Surf A*. 2010;353(2):149-56.
- Lo Y-I. Relationships between the hydrophilic-lipophilic balance values of pharmaceutical excipients and their multidrug resistance modulating effect in Caco-2 cells and rat intestines. *J Control Release*. 2003;90(1):37-48.
- Lockman PR, Koziara J, Roder KE, Paulson J, Abbruscato TJ, Mumper RJ, et al. *In vivo* and *in vitro* assessment of baseline blood-brain barrier parameters in the presence of novel nanoparticles. *Pharm Res*. 2003;20(5):705-13.
- Lorenz P, Roychowdhury S, Engelmann M, Wolf G, Horn TF. Oxyresveratrol and resveratrol are potent antioxidants and free radical scavengers: effect on nitrosative and oxidative stress derived from microglial cells. *Nitric Oxide*. 2003;9(2):64-76.
- Lundin PDP, Bojrup M, Ljusberg-Wahren H, Weström BR, Lundin S. Enhancing effects of monohexanoin and two other medium-chain glyceride vehicles on

- intestinal absorption of desmopressin (dDAVP). *J Pharmacol Exp Ther.* 1997;282(2):585-90.
- Luo Y, Chen D, Ren L, Zhao X, Qin J. Solid lipid nanoparticles for enhancing vinpocetine's oral bioavailability. *J Control Release.* 2006;114(1):53-9.
- Maneechai S, Likhitwitayawuid K, Sritularak B, Palanuvej C, Ruangrungsi N, Sirisa-Ard P. Quantitative analysis of oxyresveratrol content in *Artocarpus lakoocha* and 'Puag-Haad'. *Med Princ Pract.* 2009;18(3):223-7.
- Manjunath K, Venkateswarlu V. Pharmacokinetics, tissue distribution and bioavailability of clozapine solid lipid nanoparticles after intravenous and intraduodenal administration. *J Control Release.* 2005;107(2):215-28.
- Martins S, Silva A, Ferreira D, Souto E. Improving oral absorption of salmon calcitonin by trimyristin lipid nanoparticles. *J Biomed Nanotechnol.* 2009;5(1):76-83.
- Maurya D, Sultana Y, Kalam MA. Self-emulsifying drug delivery systems. In: Fanun M, editor. *Colloids in drug delivery (Surfactant science series)*. Florida: CRC Press; 2010. p. 299-310
- Mazimba O, Majinda RR, Motlhanka D. Antioxidant and antibacterial constituents from *Morus nigra*. *Afr J Pharm Pharmacol.* 2011;5(6):751-4.
- Mehnert W, Mäder K. Solid lipid nanoparticles: production, characterization and applications. *Adv Drug Deliv Rev.* 2001;47(2):165-96.
- Mei Z, Chen H, Weng T, Yang Y, Yang X. Solid lipid nanoparticle and microemulsion for topical delivery of triptolide. *Eur J Pharm Biopharm.* 2003;56(2):189-96.
- Mei M, Ruan J-Q, Wu W-J, Zhou R-N, Lei JP-C, Zhao H-Y, et al. *In vitro* pharmacokinetic characterization of mulberroside A, the main polyhydroxylated stilbene in mulberry (*Morus alba* L.), and its bacterial metabolite oxyresveratrol in traditional oral use. *J Agric Food Chem.* 2012;60(9):2299-308.
- Mekjaruskul C, Yang Y-T, Leed MGD, Sadgrove MP, Jay M, Sripanidkulchai B. Novel formulation strategies for enhancing oral delivery of methoxyflavones in *Kaempferia parviflora* by SMEDDS or complexation with 2-hydroxypropyl- $\beta$ -cyclodextrin. *Int J Pharm.* 2013;445(1-2):1-11.
- Mongolsuk S, Robertson A, Towers R. 2,4,3',5'-Tetrahydroxystilbene from *Artocarpus lakoocha*. *J Chem Soc.* 1957:2231-3.

- Mountfield RJ, Senepin S, Schleimer M, Walter I, Bittner B. Potential inhibitory effects of formulation ingredients on intestinal cytochrome P450. *Int J Pharm.* 2000;211(1):89-92.
- Mu H, Holm R, Müllertz A. Lipid-based formulations for oral administration of poorly water-soluble drugs. *Int J Pharm.* 2013;453(1):215-24.
- Muchow M, Maincent P, Müller RH. Lipid nanoparticles with a solid matrix (SLN<sup>®</sup>, NLC<sup>®</sup>, LDC<sup>®</sup>) for oral drug delivery. *Drug Dev Ind Pharm.* 2008;34(12):1394-405.
- Müller R, Mehnert W, Lucks J-S, Schwarz C, zurMühlen A, Meyhers H, et al. Solid lipid nanoparticles (SLN): an alternative colloidal carrier system for controlled drug delivery. *Eur J Pharm Biopharm.* 1995;41(1):62-9.
- Müller R, Maaßen S, Weyhers H, Specht F, Lucks J. Cytotoxicity of magnetite-loaded polylactide, polylactide/glycolide particles and solid lipid nanoparticles. *Int J Pharm.* 1996;138(1):85-94.
- Müller R, MaEder K, Gohla S. Solid lipid nanoparticles (SLN) for controlled drug delivery-a review of the state of the art. *Eur J Pharm Biopharm.* 2000;50(1):161-77.
- Müller R, Radtke M, Wissing S. Nanostructured lipid matrices for improved microencapsulation of drugs. *Int J Pharm.* 2002;242(1):121-8.
- Müller R, Runge S, Ravelli V, Mehnert W, Thünemann A, Souto E. Oral bioavailability of cyclosporine: solid lipid nanoparticles (SLN<sup>®</sup>) versus drug nanocrystals. *Int J Pharm.* 2006;317(1):82-9.
- Müller R, Runge S, Ravelli V, Thünemann A, Mehnert W, Souto E. Cyclosporine-loaded solid lipid nanoparticles (SLN<sup>®</sup>): drug-lipid physicochemical interactions and characterization of drug incorporation. *Eur J Pharm Biopharm.* 2008;68(3):535-44.
- Müller-Goymann C, Schubert M. Solvent injection as a new approach for manufacturing lipid nanoparticles-evaluation of the method and process parameters. *Eur J Pharm Biopharm.* 2003;55:125-31.
- Neves AR, Lúcio M, Martins S, Lima JLC, Reis S. Novel resveratrol nanodelivery systems based on lipid nanoparticles to enhance its oral bioavailability. *Int J Nanomedicine.* 2013;8:177-187.
- Ngamwat W, Permpipat U, Sithisomwong N, Chavalittumrong P, Chantarachaya C, Pecharaply D, Ousvaplanchai L, editors. Toxicity of Puag-haad extracts:

- the extracts from *Artocarpus lakoocha* Roxb. wood (Ma-haad). Abstracts of The first Princess Sciences Congress; 1987 December 10-13; Bangkok, Thailand. 1987.
- Nimthasanasiri K, Asasutjarit R, Tanguenyongwatana P, editors. Development of liposomes containing oxyresveratrol: comparative study of cholesterol and Tween 80 as vesicle stabilizer. Proceedings of the 34<sup>th</sup> National Graduate Research Conference; 2015 March 27; Khonkaen, Thailand. Khonkaen: Faculty of Medicine, Khonkaen University; 2015.
- O'Driscoll CM. Lipid-based formulations for intestinal lymphatic delivery. *Eur J Pharm Sci.* 2002;15(5):405-15.
- Oh H, Ko E-K, Jun J-Y, Oh M-H, Park S-U, Kang K-H, et al. Hepatoprotective and free radical scavenging activities of prenylflavonoids, coumarin, and stilbene from *Morus alba*. *Planta Med.* 2002;68(10):932-4.
- Patel MJ, Patel SS, Patel NM, Patel MM. A self-microemulsifying drug delivery system (SMEDDS). *Int J Pharm Sci Rev Res.* 2010;4:29-35
- Pheansri I. Evaluation of skin whitening effect of *Artocarpus lakoocha* extract, niacinamide, lactic acid, tranexamic acid and their combinations in guinea pigs and human volunteers [Master's thesis]. Bangkok: Chulalongkorn University; 2001.
- Porter C, Charman W. Transport and absorption of drugs via the lymphatic system. *Adv Drug Deliv Rev.* 2001;50(1-2):1-2.
- Porter CJ, Charman WN. Oral lipid-based formulations: using preclinical data to dictate formulation strategies for poorly water-soluble drugs. In: Hauss DJ, editor. Oral lipid-based formulations: enhancing the bioavailability of poorly water-soluble drugs. New York: Informa healthcare; 2007. p. 185-206.
- Porter CJ, Pouton CW, Cuine JF, Charman WN. Enhancing intestinal drug solubilisation using lipid-based delivery systems. *Adv Drug Deliv Rev.* 2008;60(6):673-91.
- Pouton CW. Lipid formulations for oral administration of drugs: non-emulsifying, self-emulsifying and 'self-microemulsifying' drug delivery systems. *Eur J Pharm Sci.* 2000;11:S93-S8.

- Pouton CW, Porter CJ. Formulation of lipid-based delivery systems for oral administration: materials, methods and strategies. *Adv Drug Deliv Rev.* 2008;60(6):625-37.
- Povichit N, Phrutivorapongkul A, Suttajit M, Chaiyasut C, Leelapornpisid P. Phenolic content and *in vitro* inhibitory effects on oxidation and protein glycation of some Thai medicinal plants. *Pak J Pharm Sci.* 2010a;23(4):403-8.
- Povichit N, Phrutivorapongkul A, Suttajit M, Leelapornpisid P. Antiglycation and antioxidant activities of oxyresveratrol extracted from the heartwood of *Artocarpus lakoocha* Roxb. *Maejo Int J Sci Technol.* 2010b;4(3):454-61.
- Press B, Di Grandi D. Permeability for intestinal absorption: Caco-2 assay and related issues. *Curr Drug Metab.* 2008;9(9):893-900.
- Prokop A, Davidson JM. Nanovehicular intracellular delivery systems. *J Pharm Sci.* 2008;97(9):3518-90.
- Qiu F, Komatsu K-i, Saito K-i, Kawasaki K, Yao X, Kano Y. Pharmacological properties of traditional medicines. XXII. Pharmacokinetic study of mulberroside A and its metabolites in rat. *Biol Pharm Bull.* 1996;19(11):1463-7.
- Quintanar-Guerrero D, Tamayo-Esquivel D, Ganem-Quintanar A, Allémann E, Doelker E. Adaptation and optimization of the emulsification-diffusion technique to prepare lipidic nanospheres. *Eur J Pharm Sci.* 2005;26(2):211-8.
- Radtke M, Müller RH. Nanostructured lipid drug carriers. *New Drugs.* 2001;2:48-52.
- Rege BD, Kao JPY, Polli JE. Effects of nonionic surfactants on membrane transporters in Caco-2 cell monolayers. *Eur J Pharm Sci.* 2002;16:237-46.
- Rodríguez-Bonilla P, López-Nicolás JM, García-Carmona F. Use of reversed phase high pressure liquid chromatography for the physicochemical and thermodynamic characterization of oxyresveratrol/ $\beta$ -cyclodextrin complexes. *J Chromatogr B.* 2010;878(19):1569-75.
- Sangsen Y, Wiwattanawongsa K, Likhitwitayawuid K, Sritularak B, Wiwattanapatapee R. Modification of oral absorption of oxyresveratrol using lipid based nanoparticles. *Colloids Surf B.* 2015;131:182-90.
- Sangsen Y, Wiwattanawongsa K, Likhitwitayawuid K, Sritularak B, Graidist P, Wiwattanapatapee R. Influence of surfactants in self-microemulsifying formulations on enhancing oral bioavailability of oxyresveratrol: studies in Caco-2 cells and *in vivo*. *Int J Pharm.* 2016;498(1-2):294-303.



- Saowakon N, Tansatit T, Wanichanon C, Chanakul W, Reutrakul V, Sobhon P. Fasciola gigantica: anthelmintic effect of the aqueous extract of *Artocarpus lakoocha*. *Exp Parasitol*. 2009;122(4):289-98.
- Sarmiento B, Martins S, Ferreira D, Souto EB. Oral insulin delivery by means of solid lipid nanoparticles. *Int J Nanomedicine*. 2007;2(4):743.
- Sasivimolphan P, Lipipun V, Likhitwitayawuid K, Takemoto M, Pramyothin P, Hattori M, et al. Inhibitory activity of oxyresveratrol on wild-type and drug-resistant varicella-zoster virus replication *in vitro*. *Antiviral Res*. 2009;84(1):95-7.
- Sasivimolphan P, Lipipun V, Ritthidej G, Chitphet K, Yoshida Y, Daikoku T, et al. Microemulsion-based oxyresveratrol for topical treatment of herpes simplex virus (HSV) infection: physicochemical properties and efficacy in cutaneous HSV-1 infection in mice. *AAPS PharmSciTech*. 2012;13(4):1266-75.
- Sawant KK, Dodiya SS. Recent advances and patents on solid lipid nanoparticles. *Recent Pat Drug Deliv Formul*. 2008;2(2):120-35.
- Schubert M, Müller-Goymann C. Characterisation of surface-modified solid lipid nanoparticles (SLN): influence of lecithin and nonionic emulsifier. *Eur J Pharm Biopharm*. 2005;61(1):77-86.
- Schwarz C, Mehnert W, Lucks J, Müller R. Solid lipid nanoparticles (SLN) for controlled drug delivery. I. Production, characterization and sterilization. *J Control Release*. 1994;30(1):83-96.
- Seeballuck F, Lawless E, Ashford MB, O'Driscoll CM. Stimulation of triglyceride-rich lipoprotein secretion by polysorbate 80: *in vitro* and *in vivo* correlation using Caco-2 cells and a cannulated rat intestinal lymphatic model. *Pharm Res*. 2004;21(12):2320-6.
- Seljak KB, Berginc K, Trontelj J, Zvonar A, Kristl A, Gašperlin M. A self-microemulsifying drug delivery system to overcome intestinal resveratrol toxicity and presystemic metabolism. *J Pharm Sci*. 2014;103(11):3491-500.
- Sermkaew N, Ketjinda W, Boonme P, Phadoongsombut N, Wiwattanapatapee R. Liquid and solid self-microemulsifying drug delivery systems for improving the oral bioavailability of andrographolide from a crude extract of *Andrographis paniculata*. *Eur J Pharm Sci*. 2013;50(3):459-66.

- Setthacheewakul S, Mahattanadul S, Phadoongsombut N, Pichayakorn W, Wiwattanapatapee R. Development and evaluation of self-microemulsifying liquid and pellet formulations of curcumin, and absorption studies in rats. *Eur J Pharm Biopharm.* 2010;76(3):475-85.
- Severino P, Andreani T, Macedo AS, Fangueiro JF, Santana MHA, Silva AM, et al. Current state-of-art and new trends on lipid nanoparticles (SLN and NLC) for oral drug delivery. *J Drug Deliv.* 2011a;2012:1-10.
- Severino P, Pinho SC, Souto EB, Santana MH. Crystallinity of Dynasan<sup>®</sup> 114 and Dynasan<sup>®</sup> 118 matrices for the production of stable Miglyol<sup>®</sup>-loaded nanoparticles. *J Therm Anal Calorim.* 2011b;108(1):101-8.
- Sha X, Yan G, Wu Y, Li J, Fang X. Effect of self-microemulsifying drug delivery systems containing Labrasol on tight junctions in Caco-2 cells. *Eur J Pharm Sci.* 2005;24(5):477-86.
- Shahgaldian P, Da Silva E, Coleman AW, Rather B, Zaworotko MJ. Para-acyl-calixarene based solid lipid nanoparticles (SLNs): a detailed study of preparation and stability parameters. *Int J Pharm.* 2003;253(1):23-38.
- Shen H, Zhong M. Preparation and evaluation of self-microemulsifying drug delivery systems (SMEDDS) containing atorvastatin. *J Pharm Pharmacol.* 2006;58(9):1183-91.
- Shono Y, Nishihara H, Matsuda Y, Furukawa S, Okada N, Fujita T, et al. Modulation of intestinal p-glycoprotein function by cremophor EL and other surfactants by an *in vitro* diffusion chamber method using the isolated rat intestinal membranes. *J Pharm Sci.* 2004;93(4):877-85.
- Shukla P, Prajapati S, Sharma Upendra K, Shivhare S, Akhtar A. A review on self-micro emulsifying drug delivery system: an approach to enhance the oral bioavailability of poorly water soluble drugs. *IRJP.* 2012;3(9):1-4.
- Silva A, Kumar A, Wild W, Ferreira D, Santos D, Forbes B. Long-term stability, biocompatibility and oral delivery potential of risperidone-loaded solid lipid nanoparticles. *Int J Pharm.* 2012;436(1):798-805.
- Singh AK, Chaurasiya A, Awasthi A, Mishra G, Asati D, Khar RK, et al. Oral bioavailability enhancement of exemestane from self-microemulsifying drug delivery system (SMEDDS). *AAPS PharmSciTech.* 2009;10(3):906-16.

- Singh S, Dobhal AK, Jain A, Pandit JK, Chakraborty S. Formulation and evaluation of solid lipid nanoparticles of a water soluble drug: zidovudine. *Chem Pharm Bul.* 2010;58(5):650-5.
- Sjöström B, Bergenståhl B. Preparation of submicron drug particles in lecithin-stabilized o/w emulsions I. Model studies of the precipitation of cholesteryl acetate. *Int J Pharm.* 1992;88(1):53-62.
- Souto E, Mehnert W, Müller R. Polymorphic behaviour of Compritol<sup>®</sup> 888 ATO as bulk lipid and as SLN and NLC. *J Microencapsul.* 2006;23(4):417-33.
- Souto EB, Müller RH. Lipid nanoparticles: effect on bioavailability and pharmacokinetic changes. In: Schäfer-Korting M, editor. *Drug delivery, Handbook of experimental pharmacology.* Heidelberg: Springer; 2010. p. 115-41.
- Speiser P, inventor; Rentschler Arzneimittel GmbH & Co., assignee. Lipid nanopelletsas drug carriers for oral administration. European patent EP 0167825 A2.1990 Jan 15.
- Sritularak B, De-Eknamkul W, Likhitwitayawuid K. Tyrosinase inhibitors from *Artocarpus lakoocha*. *Thai J Pharm Sci.* 1998;22:149-55.
- Sutananta W, Craig DQ, Newton JM. An evaluation of the mechanisms of drug release from glyceride bases. *J PharmPharmacol.* 1995;47(3):182-7.
- Takemoto JK, Bertram RM, Remsberg CM, Sablani SS, Davies NM. 13<sup>th</sup> Canadian Society for Pharmaceutical Sciences (CSPS), *J Pharm Pharm Sci.* 2010;13:1s.
- Tanunkat A. Absorption, metabolism and excretion of 2,4,3',5'-tetrahydroxystilbene in volunteers after oral administration of purified extract of Puag-haad [Master's Thesis]. Bangkok: Mahidol University; 1990.
- Tengamnuay P, Pengrungruangwong K, Likhitwitayawuid K, editors. Potent tyrosinase inhibitor from *Artocarpus lakoocha* heartwood extract. Proceedings of the IFSCC Conference; 22-24 Sep 2003; Seoul, Korea. Seoul: The Society of Cosmetic Scientists of Korea; 2003.
- Tengamnuay P, Pengrungruangwong K, Pheansri I, Likhitwitayawuid K. *Artocarpus lakoocha* heartwood extract as a novel cosmetic ingredient: evaluation of the *in vitro* anti-tyrosinase and *in vivo* skin whitening activities. *Int J Cosmet Sci.* 2006;28(4):269-76.

- Thakkar HP, Desai JL. Influence of excipients on drug absorption via modulation of intestinal transporters activity. *Asian J Pharmacol.* 2015;9(2):69-82.
- Thompson CJ, Docherty JJ, Boltz RC. Electrokinetic alteration of the surface of herpes simplex virus infected cells. *J Gen Virol.* 1978;39:449-61.
- Tian F, Wei H, Jia T, Tian H. An improved highly sensitive method to determine low oxycresveratrol concentrations in rat plasma and its pharmacokinetic application. *Biomed Chrom.* 2014;28(5):667-72.
- Tiwari R, Pathak K. Nanostructured lipid carrier versus solid lipid nanoparticles of simvastatin: comparative analysis of characteristics, pharmacokinetics and tissue uptake. *Int J Pharm.* 2011;415(1):232-43.
- Trotta M, Debernardi F, Caputo O. Preparation of solid lipid nanoparticles by a solvent emulsification-diffusion technique. *Int J Pharm.* 2003;257(1):153-60.
- Tsai MJ, Huang YB, Wu PC, Fu YS, Kao YR, Fang JY, et al. Oral apomorphine delivery from solid lipid nanoparticles with different monostearate emulsifiers: pharmacokinetic and behavioral evaluations. *J Pharm Sci.* 2011;100(2):547-57.
- Ujhelyi Z, Fenyvesi F, Váradi J, Fehér P, Kiss T, Veszelka S, et al. Evaluation of cytotoxicity of surfactants used in self-micro emulsifying drug delivery systems and their effects on paracellular transport in Caco-2 cell monolayer. *Eur J Pharm Sci.* 2012;47(3):564-73.
- Üner M. Preparation, characterization and physico-chemical properties of solid lipid nanoparticles (SLN) and nanostructured lipid carriers (NLC): their benefits as colloidal drug carrier systems. *Pharmazie.* 2006;61(5):375-86.
- van Breemen RB, Li Y. Caco-2 cell permeability assays to measure drug absorption. *Expert Opin Drug MetabToxicol.* 2005;1(2):175-85.
- Varshosaz J, Tabbakhian M, Mohammadi MY. Formulation and optimization of solid lipid nanoparticles of buspirone HCl for enhancement of its oral bioavailability. *J Liposome Res.* 2010;20(4):286-96.
- Venkateswarlu V, Manjunath K. Preparation, characterization and *in vitro* release kinetics of clozapine solid lipid nanoparticles. *J Control Release.* 2004;95(3):627-38.
- Wang W-X, Qian J-Y, Wang X-J, Jiang A-P, Jia A-Q. Anti-HIV-1 activities of extracts and phenolics from *Smilax china* L. *Pak J Pharm Sci.* 2014;27(1):147-51.

- Washington C. Drug release from microdisperse systems: a critical review. *Inter J Pharm.* 1990;58(1):1-12.
- Weber JT, Lamont M, Chibrikova L, Fekkes D, Vlug AS, Lorenz P, et al. Potential neuroprotective effects of oxyresveratrol against traumatic injury. *Eur J Pharmacol.* 2012;680(1):55-62.
- Weiss J, Decker EA, McClements DJ, Kristbergsson K, Helgason T, Awad T. Solid lipid nanoparticles as delivery systems for bioactive food components. *Food Biophys.* 2008;3(2):146-54.
- Wu G, Lee KYC. Effects of poloxamer 188 on phospholipid monolayer morphology: an atomic force microscopy study. *Langmuir.* 2009;25(4):2133-9.
- Wu L-S, Wang X-J, Wang H, Yang H-W, Jia A-Q, Ding Q. Cytotoxic polyphenols against breast tumor cell in *Smilax china* L. *J Ethnopharmacol.* 2010;130(3):460-4.
- Xiong Y, Guo DA, Huang HL. Chemical constituents from tubers of *Smilax china* L. *Modern Chinese Med.* 2008;10:20-22.
- Xu L, Liu C, Xiang W, Chen H, Qin X, Huang X. Advances in the study of oxyresveratrol. *Int J Pharmacol.* 2014;10(1):44-54.
- Yang R, Gao R, Li F, He H, Tang X. The influence of lipid characteristics on the formation, *in vitro* release, and *in vivo* absorption of protein-loaded SLN prepared by the double emulsion process. *Drug Dev Ind Pharm.* 2011;37(2):139-48.
- Yee S. *In vitro* permeability across Caco-2 cells (colonic) can predict *in vivo* (small intestinal) absorption in man-fact or myth. *Pharm Res.* 1997;14(6):763-6.
- Yoon SR, Yang SH, Suh JW, Shim SM. Fermentation of *Smilax china* root by *Aspergillus usami* and *Saccharomyces cerevisiae* promoted concentration of resveratrol and oxyresveratrol and the free-radical scavenging activity. *J Sci Food Agr.* 2014;94(9):1822-6.
- Yuan H, Wang L-L, Du Y-Z, You J, Hu F-Q, Zeng S. Preparation and characteristics of nanostructured lipid carriers for control-releasing progesterone by melt-emulsification. *Colloids Surf B.* 2007;60(2):174-9.
- Zangenberg NH, Müllertz A, Kristensen HG, Hovgaard L. A dynamic *in vitro* lipolysis model II: evaluation of the model. *Eur J Pharm Sci.* 2001;14(3):237-44.

- Zhang H, Yao M, Morrison RA, Chong S. Commonly used surfactant, Tween 80, improves absorption of p-glycoprotein substrate, digoxin, in rats. Arch Pharm Res. 2003;26(9):768-72.
- Zhang N, Ping Q, Huang G, Xu W, Cheng Y, Han X. Lectin-modified solid lipid nanoparticles as carriers for oral administration of insulin. Int J Pharm. 2006;327(1):153-9.
- Zhang T, Chen J, Zhang Y, Shen Q, Pan W. Characterization and evaluation of nanostructured lipid carrier as a vehicle for oral delivery of etoposide. Eur J Pharm Sci. 2011;43(3):174-9.
- Zhang Z, Lv H, Zhou J. Novel solid lipid nanoparticles as carriers for oral administration of insulin. Pharmazie. 2009;64(9):574-8.
- Zhao WJ, Guo YT, Tezuka Y, Kikuchi T. Chemical research on the stilbenes from *Veratrum nigrum* L. var. *ussuriense* Nakai. Chin J Med Chem. 1998;8:35-7
- Zhuang C-Y, Li N, Wang M, Zhang X-N, Pan W-S, Peng J-J, et al. Preparation and characterization of vinpocetine loaded nanostructured lipid carriers (NLC) for improved oral bioavailability. Int J Pharm. 2010;394(1):179-85.
- zurMühlen A, Schwarz C, Mehnert W. Solid lipid nanoparticles (SLN) for controlled drug delivery-drug release and release mechanism. Eur J Pharm Biopharm. 1998;45(2):149-55.

## APPENDICES

Appendix 1	Reprint of papers and manuscripts
Appendix 2	Vitae

**Reprint of papers and manuscripts**



## **PAPER 1**

Novel solid lipid nanoparticles for oral delivery of oxyresveratrol: Effect of the formulation parameters on the physicochemical properties and *in vitro* release

# Novel Solid Lipid Nanoparticles for Oral Delivery of Oxyresveratrol: Effect of the Formulation Parameters on the Physicochemical Properties and *in vitro* Release

Y. Sangsen, K. Likhitwitayawuid, B. Sritularak, K. Wiwattanawongsa, R. Wiwattanapatapee

**Abstract**—Novel solid lipid nanoparticles (SLNs) were developed to improve oral bioavailability of oxyresveratrol (OXY). The SLNs were prepared by a high speed homogenization technique, at an effective speed and time, using Compritol® 888 ATO (5% w/w) as the solid lipid. The appropriate weight proportions (0.3% w/w) of OXY affected the physicochemical properties of blank SLNs. The effects of surfactant types on the properties of the formulations such as particle size and entrapment efficacy were also investigated. Conclusively, Tween 80 combined with soy lecithin was the most appropriate surfactant to stabilize OXY-loaded SLNs. The mean particle size of the optimized formulation was  $134.40 \pm 0.57$  nm. *In vitro* drug release study, the selected S2 formulation showed a retarded release profile for OXY with no initial burst release compared to OXY suspension in the simulated gastrointestinal fluids. Therefore, these SLNs could provide a suitable system to develop for the oral OXY delivery.

**Keywords**—Solid lipid nanoparticles, Physicochemical properties, *in vitro* drug release, Oxyresveratrol.

## I. INTRODUCTION

**OXYRESVERATROL (OXY)** (*Trans*-2,4,3',5'-tetrahydroxystilbene), is a polyphenolic stilbene purified from the heartwood of a Thai traditional plant, *Artocarpus lakoocha* Roxburgh (Moraceae) [1]. It has been reported to exhibit tyrosinase inhibitory activity, acts as a potent antioxidant, is anti-inflammatory and has strong neuroprotective activity [2]-[5]. Recently, its antiviral activities have been established with activities against several types of herpes simplex virus (HSV-1 and HSV-2), various varicella zoster viruses (VZV), influenza virus as well as human immunodeficiency virus type 1 (HIV-1) [1], [6]-[9].

Y. Sangsen is with the Department of Pharmaceutical Technology, Faculty of Pharmaceutical Sciences, Prince of Songkla University, Songkhla 90112 Thailand (e-mail: s.yaowaporn@gmail.com).

K. Likhitwitayawuid and B. Sritularak are with the Department of Pharmacognosy and Pharmaceutical Botany, Faculty of Pharmaceutical Sciences, Chulalongkorn University, Bangkok 10330 Thailand (e-mails: Kittisak.L@chula.ac.th, Boonchoo.sr@chula.ac.th, respectively).

K. Wiwattanawongsa is with the Department of Clinical Pharmacy, Faculty of Pharmaceutical Sciences, Prince of Songkla University, Songkhla 90112 Thailand (e-mail: kamonthip.w@psu.ac.th).

R. Wiwattanapatapee is with the Department of Pharmaceutical Technology, Faculty of Pharmaceutical Sciences, Prince of Songkla University, Songkhla 90112 Thailand (phone: 667-428-8915; fax: 6674 428 148; e-mail: ruedeekorn.w@psu.ac.th).

These pharmacological activities have triggered efforts to transform OXY into therapeutic formulations. However, there are some limitations for the oral delivery of OXY such as poor absorption due to intermediate permeability and active efflux mediated mechanisms, extensive hepatic metabolism, and rapid elimination from the body results in a low oral bioavailability and limits the clinical use of OXY [10]-[12]. To overcome these difficulties, it will be necessary to design a formulation for OXY that will improve its oral bioavailability.

Lipid-based drug delivery systems, especially solid lipid nanoparticles (SLNs), have been a focus in the last few years for use as alternative colloidal drug carriers. SLNs are produced by replacing the liquid lipid (oil) component of an oil-in-water (O/W) emulsion with lipids that are solid at both room and body temperatures. The systems possess many advantages such as their physical stability, protection of labile drugs from chemical or enzyme degradation, controlled release, biodegradability, and biocompatibility all derived from physiologically accepted excipients that are generally recognized as safe (GRAS) status [13]-[15]. Moreover, many particle synthetic methods can be easily scaled up it to commercial products [16]. Until recently, SLNs have been investigated successfully as oral drug delivery systems for several drugs [17]-[22]. Nonetheless, there have been no reports from investigations using such systems as carriers for the oral delivery of OXY. Predominantly, the proposed mechanisms for the enhanced absorption of SLNs that have been documented involve direct uptake through the intestine, a decreased degradation in the gastrointestinal (GI) tract and reduced hepatic metabolism with a retarded clearance from the body because of its nano-size and the lipid used in the SLNs [23]. Apart from the effect on the stability of the formulations, surfactants also increase the intestinal permeability of SLNs containing a drug by paracellular transport and restraining efflux systems thus increasing transcellular pathways [23]-[25]. Therefore, the preparation processes and composition of such SLN formulations that affect their physicochemical properties as well as their release properties should be investigated to obtain effective SLNs for oral delivery of OXY.

The aim of this study was to evaluate the effects of the preparation conditions and formulated ingredients on their appearance, physicochemical characteristics, including

particle size, size distribution, total drug content, entrapment efficacy, drug loading capacity, and *in vitro* drug release properties of developed SLNs for consideration as potential carriers for the oral delivery of OXY.

## II. MATERIALS

OXY (>95% purity) was kindly obtained from the Department of Pharmacognosy and Pharmaceutical Botany, Faculty of Pharmaceutical Sciences, Chulalongkorn University (Bangkok, Thailand). Compritol® 888 ATO (glyceryl behenate; Com888) were from Gattefosse (Saint-Priest, France). Cremophor® EL (polyoxyethylene castor oil derivatives; Cre EL), and Poloxamer® 188 (polyoxyethylene esters of 12-hydroxystearic acid; P188) were from BASF (Ludwigshafen, Germany). Soy lecithin was from Rama Production Co., Ltd. (Bangkok, Thailand). Glycerol monostearate (GMS) and Propylene glycol (PG) were from PC Drug Center Co., Ltd. (Bangkok, Thailand). Tween80 (polyoxyethylene (20) sorbitan monooleate) was from S.Tong Chemicals Co., Ltd (Bangkok, Thailand). Acetonitrile and methanol (High Performance Liquid Chromatography; HPLC grade) were from RCI Labscan (Bangkok, Thailand). All other chemicals were of analytical grade.

## III. METHOD

### A. Formulations and Preparations of the OXY-Loaded SLNs

The SLNs containing with OXY were formulated by a high speed homogenization method. Briefly, the lipid phase: OXY and solid lipid - and the aqueous phase: surfactants combined with co-surfactant in deionized (DI) water were heated to 85°C, separately. Then, the hot aqueous phase was added to the lipid phase at 85°C under a magnetic stirrer at 600 rpm. An emulsion was obtained using a T 25 digital ULTRA-TURRAX® high speed homogenizer (IKA®, Germany) with a S25N-8G disperser. Subsequently the final dispersion was cooled to room temperature to solidify the nanoparticles. The formulations were stored in tightly sealed glass bottle until used. Before loading the drug into the SLN formulations, the homogenization speeds and times were varied to optimize the homogenization conditions (Table I). To select the most suitable components in the formulations, the degree (Table II) and types of solid lipid (Table IV), the amount of OXY (Table IV), and the types of surfactant (Table III) were investigated.

### B. Particle Size and Polydispersity Index Analysis

The mean particle size (PS) and polydispersity index (PDI) of the lipid nanoparticles formed with each of the formulations were measured by photon correlation spectroscopy (Zetasizer Nano ZS®, Malvern Instruments, UK) using the dynamic light scattering technique. The samples were diluted with DI water to produce the most suitable concentration to allow for accurate measurements. Aliquots of these lipid nanoparticles were loaded into cuvettes and their size was measured. Light scattering was monitored at a 173° angle at a temperature of 25°C. All measurements were

performed in triplicate and the data are presented as a mean ± standard deviations (S.D.).

TABLE I  
VARIATION OF HOMOGENIZATION CONDITIONS ON THE BLANK SLNS

Compositions	Formulations (% w/w)					
	T1	T2	T3	T4	T5	T6
<i>Lipid phase</i>						
Com888			1.2			
<i>Aqueous phase</i>						
Tween80			0.90			
Soy lecithin			0.45			
DI water			97.450			
Speed (rpm)	10,000	15,000	20,000	24,000	24,000	24,000
Time (min)	5	5	5	5	10	15

TABLE II  
DIFFERENT WEIGHT PROPORTIONS OF SOLID LIPID OF THE BLANK SLNS

Compositions	Formulations (% w/w)				
	C1	C2	C3	C4	C5
<i>Lipid phase</i>					
Com888	1.2	5	7.5	9	10
<i>Aqueous phase</i>					
P188:Tween80(1:1)	0.90	3.75	5.625	6.75	7.50
Soy lecithin	0.450	1.875	2.812	3.375	3.750
DI water	97.450	89.375	84.062	80.875	78.750

### C. Determination of the Total Drug Content

The total drug content (TDC) in the developed OXY-loaded SLNs was determined. Briefly, aliquots of 1mL of the OXY-loaded SLN dispersion were dissolved in methanol and the mixture was blended using a mixer (Vortex-gene 2, Becthai Bangkok Equipment & Chemical, Thailand) at a maximum speed for 15min in order to facilitate complete dissolution. Then, the obtained suspension was allowed to filter through a 0.45µm membrane filter and diluted appropriately with the HPLC mobile phase. The resulting solution was analyzed by the HPLC method. The percentage of TDC was calculated by using (1) where  $OXY_{cal}$  was the total content of OXY calculated from the experiment and the  $OXY_{ther}$  was the theoretical drug content.

$$TDC (\%) = \frac{OXY_{cal}}{OXY_{ther}} \times 100 \quad (1)$$

### D. Drug Entrapment Efficiency and Drug Loading Capacity

The encapsulation efficiency (EE) and loading capacity (LC) of each of the developed OXY-loaded SLNs were evaluated. The EE of the formulations was calculated by determining the amount of free drug that was not entrapped in the formulations. The drug loading content was the ratio of incorporated drug to lipid (w/w). One mL of the OXY-loaded SLN dispersion was placed in the dialysis bag (molecular weight cut off; MWCO 12–14 kDa). These bags were then placed in a centrifuge tube and the tube was filled with methanol and centrifuged at 13,500 rpm for 15min. The mixture of solvent containing the non-entrapped drug was

then analyzed by the HPLC method. The percentage of EE and LC was calculated by using (2) and (3), respectively, where  $OXY_{cal}$  was the total amount of OXY, the  $OXY_f$  was the amount of non entrapped OXY in the solvent, and the  $Tlipid$  was the total weight of lipid in the formulation.

$$EE(\%) = \frac{(OXY_{cal} - OXY_f)}{OXY_{cal}} \times 100 \quad (2)$$

$$LC(\%) = \frac{(OXY_{cal} - OXY_f)}{Tlipid} \times 100 \quad (3)$$

TABLE III  
DIFFERENT SURFACTANT TYPES OF THE OXY-LOADED SLNS

Compositions	Formulations (% w/w)						
	S1	S2	S3	S4	S5	S6	S7
OXY				0.3			
<i>Lipid phase</i>							
Com888				5			
<i>Aqueous phase</i>							
<i>Surfactants</i>							
P188	3.75						
Tween80		3.75					
Cre EL			3.75				
PG				3.75			
P188:Tween80(1:1)					3.75		
P188:Cre EL(1:1)						3.75	
P188:PG(1:1)							3.75
Soy lecithin				1.875			
DI water				89.075			

#### E. In Vitro Drug Release Study

The *in vitro* release study of OXY from the developed formulations was carried out by the dialysis bag diffusion technique [23]. Briefly, the OXY-loaded SLN dispersion equivalent to 10mg OXY was filled into the dialysis bag (MWCO 12–14 kDa). The bag was immersed in 200 mL of release medium in a chamber of the USP30 dissolution apparatus 2 (Hanson Research Corporation, USA), stirred at 100rpm and maintained at a temperature  $37 \pm 0.5^\circ\text{C}$ . The dissolution medium was either simulated gastric fluid (SGF, pH 1.2) without pepsin or simulated intestinal fluid (SIF, pH 6.8) without pancreatin, respectively. Five mL aliquots of were withdrawn at various time intervals and replaced with fresh dissolution medium. Samples were filtered using a 0.45

um filter and analyzed using the HPLC method. Three separate replicate studies were conducted for each of the formulations, and the data are presented as a mean  $\pm$  S.D. ( $n = 3$ ). The release profiles of the OXY from the SLNs were compared to an unformulated OXY.

#### F. Kinetic Analysis of In Vitro Drug Release Study

The Ritger–Peppas model has been widely used in many studies for analysis of the drug release kinetics in the matrix [26]. The Ritger–Peppas kinetic model is described by using (4) where  $Mt/M_\infty$  is the fraction of the drug released at time  $t$ ,  $K$  is the constant for incorporating the structural and geometrical characteristics of the dosage form, and  $n$  is the release exponent that indicates the drug release mechanism. For the Fickian diffusion from the spheres,  $n = 0.43$  while for the anomalous transport,  $n$  is between 0.43 and 0.85 and for a case II transport (zero-order release),  $n = 0.85$ .

$$\frac{Mt}{M_\infty} = Kt^n \quad (4)$$

#### G. High Performance Liquid Chromatography (HPLC) Analysis of OXY

The quantitative determination of OXY was performed using an Agilent HPLC system (HP 1100, Agilent, USA) with a C18 column (VertiSep™ pHendure 4.6 x 250mm, 5- $\mu\text{m}$ , Ligand Scientific, Bangkok, Thailand), and a UV detector set at the wavelength of 320nm. Chromatographic conditions: the eluent was an isocratic solvent system at ambient temperature with a flow rate and injection volume of 1.0mL/min and 20 $\mu\text{L}$ , respectively. The mobile phase consisted of acetonitrile and 0.5% v/v aqueous acetic acid in the ratio of 27:73 v/v. The retention time of OXY was about 7 min. The calibration curve for OXY was constructed by plotting the concentrations versus the corresponding mean peak areas that were calculated from three determinations. A good linearity was achieved with a correlation coefficient ( $r^2$ ) of 0.9994 over the concentration range of 0.2–10  $\mu\text{g/mL}$ . The intra-day precision was obtained by three repeated injections of each concentration of samples that showed the percent relative standard deviation (% RSD) of 0.14 to 0.86. The inter-day precision of the method gave a %RSD that ranged from 0.45 to 1.26. The recovery percentage of the method was between  $95.50 \pm 4.40$  and  $101.87 \pm 1.61$ .

TABLE IV  
DIFFERENT LIPID TYPES AND WEIGHT PROPORTIONS OF OXY ON THE SLNS

Compositions	Formulations (% w/w)							
	F1	F2	F3	F4	F5	F6	F7	F8
OXY	0.1	0.2	0.3	0.4	0.5	1	2	0.3
<i>Lipid phase</i>								
Com888	5	5	5	5	5	5	5	
GMS								5
<i>Aqueous phase</i>								
P188:Tween80(1:1)				3.75				
Soy lecithin				1.875				
DI water	89.275	89.175	89.075	88.975	88.875	88.375	87.375	89.075



### H. Statistical Analysis

All results were expressed as a mean  $\pm$  S.D. Statistical comparisons were performed by the Student's *T*-test or one-way ANOVA. Differences were considered significant at a *p*-value ( $P < 0.05$ ).

## IV. RESULTS AND DISCUSSION

### A. Effect of the Homogenization Conditions on the Physical Properties of the Blank SLNs

SLNs can be prepared by various methods including hot and cold homogenization, high speed homogenization, ultrasonication, solvent emulsification and evaporation, and microemulsion [16], [21], [22], [27]-[29]. For this study, the hot high speed homogenization method was used due to it being simple and quick. The homogenization conditions, in term of speeds and times were optimized to obtain particles that were nano-sized (<200nm) and had a narrow size distribution (PDI  $\sim$  0.2-0.4) so that the reduced particle size improved the surface area of the SLNs. One of the fundamental principles for the design of nanoparticles systems is the increase of the interfacial energy because of the high curvatures of small sized particles as this result in an increase of the solubility of a given substance [30]. Moreover, this small size allows for an efficient uptake in the intestine particularly in the lymphoid tissue thus bypassing the first pass metabolism and resulting in an improvement of drug absorption [23]. The effects of the homogenization speed and time on the physical properties of blank SLN formulation are summarized in Table V. The homogenizer speed was varied from 10,000 to 24,000 rpm (T1-T4) with a fixed time of 5 min. When the speed rates increased, the particle size was reduced and the size distribution narrowed. The T4 appeared as a milky suspension with < 200 nm particle size, thus 24,000 rpm was fixed as the optimum homogenization speed. The time was varied from 5 to 15 min (T4-T6). The increased time for mixing reduced the particle size of the homogeneous T6 suspension and produced the smallest size and narrowest distribution of particles. Therefore, the speed rate of 24,000 rpm and a time of 15min were selected as the standard homogenization step for all formulations.

TABLE V  
EFFECT OF THE HOMOGENIZATION CONDITIONS ON THE PHYSICAL PROPERTIES OF THE BLANK SLNS

Compositions	Formulations (% w/w)					
	T1	T2	T3	T4	T5	T6
Appearance	Milky cream	Viscous and milky suspension		Milky suspension		White suspension
Aggregation <sup>a</sup>	/	/	/	-	-	-
PS (nm)	-	563.20 $\pm$ 69.83	251.60 $\pm$ 1.57	174.20 $\pm$ 0.06	137.70 $\pm$ 0.17	130.20 $\pm$ 0.40
PDI	-	0.57 $\pm$	0.39 $\pm$	0.28 $\pm$	0.24 $\pm$	0.17 $\pm$
		0.07	0.01	0.01	0.01	0.01

<sup>a</sup> Visual observations on particle aggregation in the formulations: (/) denoting the observed aggregates of particles. Data represent a mean  $\pm$  S.D. (n = 3).

### B. Effect of the Weight Proportions of the Solid Lipid on the Physical Properties of the Blank SLNs

The amount of the lipid matrix also had an important effect on the particle size, size distribution, drug loading, and the stability of SLNs, and this should be taken into consideration during the screening and development of the formulations [14], [19]. The composition of the blank SLN formulations that had different weight proportions of solid lipid and the effect of them on the physical properties of such formulations are summarized in Tables II and VI, respectively. When the weight proportions of the solid lipid increased, the particle size and size distribution of SLNs increased, so it was difficult to obtain a small and uniform size distribution when the solid lipid in the formulations was increased because the Com888 had a high viscosity. A good appearance was obtained with the non flocculated C1 and C2 formulations. The particle sizes and size distribution of both these formulations were not significantly different ( $P > 0.05$ ) as they were each around 100-120nm in PS and 0.2-0.3 in PDI. Therefore, the formulation containing a high weight proportion of solid lipid (5% w/w; C2) that was expected to achieve a high drug loading was chosen for further development of the OXY-loaded SLNs.

### C. The Effect of the Weight Proportions of OXY on the Physicochemical Properties of the SLNs

To investigate the effects of the amount of the incorporated OXY on the selected C2 formulation, the OXY loaded into the formulations was varied from 0.1 to 2 % w/w as shown in Table IV (F1-F7). The effects of the loaded OXY on the physicochemical properties of the SLNs are summarized in Table VII. A larger size of the nanoparticles was obtained by increasing the amount of the OXY in the SLN formulations and the PDI detected were greater. Until the weight proportion of the OXY was higher than 0.5% w/w, a cream-like appearance was observed (F6 and F7). This result was thought to be due to an insufficient amount of the lipid to encapsulate the drug. The particle size and the PDI of the F1-F3 formulations were less than 200nm and 0.4, respectively, and followed the expected values. The OXY had high entrapment efficiency in all of the three formulations (> 80 %). However, the highest capacity for drug loading ( $4.85 \pm 0.01$  %w/w) was obtained in the F3 formulation. Moreover, the PS of the F3 was significantly larger than the blank SLNs (C2) ( $P < 0.05$ ), thus the presence of the OXY did significantly affect the PS of the blank SLNs. Therefore, the optimum OXY loaded for the SLN formulation was determined to be the F3 that contained 0.3% w/w of the OXY with good characteristics.

TABLE VI  
EFFECT OF THE WEIGHT PROPORTIONS OF SOLID LIPID ON THE PHYSICAL PROPERTIES OF THE BLANK SLNS

Physical properties	Formulations				
	C1	C2	C3	C4	C5
Appearance	White suspension		Viscous and milky suspension		Milky suspension
Aggregation <sup>a</sup>	-	-	/	/	/
PS (nm)	108.10 ± 0.74	110.10 ± 0.95	312.70 ± 4.13	377.10 ± 10.97	196.60 ± 0.89
PDI	0.27± 0.01	0.24± 0.01	0.44± 0.02	0.45± 0.03	0.28± 0.00

<sup>a</sup> Visual observations on particle aggregation in the formulations: (/) denoting observed aggregates of particles. Data represents a mean ± S.D. (n = 3).

#### D. Effect of the Lipid Types on the Physical Properties of the OXY Loaded-SLNs

Apart from the degree of the solid lipid, the type of lipid matrix had another important effect on the physicochemical properties and the drug release properties of the SLN formulations [14], [19]. Two types of solid lipid including glyceryl behenate (Com888) and glyceryl monostearate (GMS) were used as the lipid phase (5% w/w) and compared as shown in Table VII. After incorporation of OXY (0.3% w/w) into both types of the formulations, the Com888-based (F3) and GMS-based (F8) SLNs were observed to be a homogenous suspensions and yellowish cream, respectively. The Com888 was chosen as the solid lipid matrix in this study. This was associated with having an amphiphilic characteristic with a high chemical stability that resulted in a good ability to encapsulate a lipophilic and/or hydrophilic drug [30]. Reference [19] showed that SLNs prepared from such solid lipid displayed favorable physicochemical characteristics such as particle size, size distribution and morphology.

TABLE VII  
EFFECT OF LIPID TYPES AND THE WEIGHT PROPORTIONS OF OXY ON THE PHYSICO-CHEMICAL PROPERTIES OF THE SLNS

Properties	Formulations				
	F1	F2	F3	F4	F5
Appearance	Yellowish suspension			Viscous and yellowish suspension	
Aggregation <sup>a</sup>	-	-	-	/	/
PS (nm)	95.90 ± 0.04	126.60 ± 0.31	158.00 ± 0.76	389.30 ± 5.77	620.70 ± 15.62
PDI	0.27± 0.01	0.20± 0.02	0.23± 0.01	0.31± 0.04	0.49± 0.00
TDC (%)	108.82 ± 2.13	91.98 ± 6.38	93.79 ± 4.70	94.80 ± 9.18	96.38 ± 8.83
EE (%)	90.87± 0.08	83.54± 0.13	86.14± 0.17	86.01± 0.05	87.45± 0.10
DL (%)	1.98± 0.00	3.07± 0.00	4.85± 0.01	6.52± 0.00	8.43± 0.01

<sup>a</sup> Visual observations on particle aggregation in the formulations: (/) denoting the observed aggregates of particles. Data represents a mean ± S.D. (n = 3).

<sup>b</sup>F6-F8 appeared as a yellowish cream.

#### E. Effect of Surfactants Types on the Physicochemical Properties of the OXY Loaded-SLNs

The surfactants used in the SLNs as permeability enhancers also contributed to both the particle stability and an improved bioavailability of the SLNs. There have been many data reported that the soy lecithin, used as a co-surfactant in this study, was an important factor for drug-loaded SLNs without the drug readily separating from the formulations, irrespective of the lipid used [17], [19]. The lecithin was mainly distributed at the interface of the oil and the aqueous phase. In our study, the soy lecithin (hydrophilic-lipophilic balance; HLB of 5) was added to the system to adjust the HLB of other surfactants so as to enhance the ability to emulsify the lipid and stabilize the system. The OXY-loaded SLN formulations with seven different types of a single or a combination of surfactants and the effect of them on the physicochemical properties of the formulations are summarized in Table III and VIII, respectively. All the surfactants used in this experiment formed particles. However, the formulations containing Cre EL (S3 and S6) and PG (S4 and S7), that provided a high solubility for OXY (data was not shown), showed undesirable physical characteristics such as having a large particle size (> 200nm) and a non-uniform size distribution. Whereas, for the formulations (S1, S2, and S5) containing P188 (HLB of 29) and/or Tween80 (HLB of 15) they had a good appearance and did not flocculate. The mean particle sizes obtained from these formulations was less than 200 nm (144.20 ± 1.10, 134.40 ± 0.57, 158.00 ± 0.76 nm for S1, S2, S5, respectively) and they also had a narrow size distribution (PDI 0.22-0.27). As in previous studies, the non-toxic and non-ionic P188 and Tween 80 were selected as surfactants for the Com888-based formulations due to their compatibility. The SLNs that were prepared using sufficient P188 and/or Tween80 as surfactants had a small particle size, uniform size distribution, and also good stability [17], [19], [21]. An important issue with respect to the use of nanoparticles as drug carriers is their capacity for drug loading and their entrapment efficiency on the basis of similar total drug content (about 100% TDC). It is clear that the entrapment efficiency of the S1, S2, and S5 formulations was satisfactorily high compared to such values of the SLNs loaded with other drugs in the previous reports [21]-[23]. The average drug loading of the three OXY-loaded SLNs was about 4-5% w/w of the lipid phase.

TABLE VIII  
EFFECT OF SURFACTANT TYPES ON THE PHYSICO-CHEMICAL PROPERTIES OF THE OXY-LOADED SLNS

Physicochemical properties	Formulations						
	S1	S2	S3	S4	S5	S6	S7
Appearance	Yellowish suspension	Milky suspension	Milky suspension	Milky suspension	Yellowish suspension	Milky cream	Milky suspension
Aggregation <sup>a</sup>	-	-	/	/	-	/	/
PS (nm)	144.20 ± 1.10	134.40 ± 0.57	288.70 ± 3.86	297.50 ± 1.79	158.00 ± 0.76	630.50 ± 36.08	384.30 ± 25.68
PDI	0.27 ± 0.00	0.25 ± 0.00	0.25 ± 0.01	0.40 ± 0.01	0.23 ± 0.01	0.58 ± 0.09	0.51 ± 0.08
TDC (%)	92.00 ± 5.43	102.05 ± 1.97	85.59 ± 2.64	73.73 ± 6.48	93.79 ± 4.70	87.25 ± 7.81	68.51 ± 6.48
EE (%)	78.64 ± 0.46	90.55 ± 0.28	85.21 ± 0.69	82.76 ± 0.95	86.14 ± 0.17	89.77 ± 0.39	86.93 ± 1.10
DL (%)	4.34 ± 0.02	5.54 ± 0.02	4.38 ± 0.03	3.66 ± 0.04	4.85 ± 0.01	4.70 ± 0.02	3.57 ± 0.04

<sup>a</sup>Visual observations on particle aggregation in the formulations: (/) denoting observed aggregates of particles. Data represents a mean ± S.D. (n = 3)

#### F. In Vitro Drug Release Study

In order to develop a controlled release system, it is vital to understand the release pattern, the mechanism and the kinetics. In this study, the conventional dialysis bag diffusion technique that is widely used for measuring the release of drugs from colloidal solutions was used. The *in vitro* OXY release profiles of the S1, S2, S5, and OXY suspension in the SGF pH 1.2 and SIF pH 6.8 are shown in Figs. 1 and 2, respectively. The cumulative amount of the OXY released from each formulation was plotted as a function of time and it was evident that the OXY suspension showed a cumulative release of OXY of 30% within 4 h in the SGF pH 1.2 and 80% within 48 h in the SIF pH 6.8, respectively. Comparing the release curves of the three OXY-loaded SLN formulations in pH 1.2 and pH 6.8, we concluded that these formulations showed no initial burst release in either medium. On the other hand the release of OXY from the SLNs slowed down considerably and it varied from 4.94% to 9.69% after 4 h in the SGF pH 1.2 depending on the types of surfactant present. Likewise, a retarded release profile from the three SLN formulations was demonstrated compared with that of the OXY suspension in the SIF pH 6.8. From the experimental data, the release rate of S2 formulated using Tween80 was slower than for S5 (P188:Tween80) and S1 (P188) during the study times. The difference of the % cumulative release was significant at 48 h with S2 (24.24 ± 0.67 %), S5 (37.30 ± 1.39 %), and S1 (48.46 ± 7.64 %), respectively ( $P < 0.05$ ). In addition the Com888 used in this study had previously been utilized as a retardant material for a sustained release dosage form, and this may be due to the stronger solubilization of P188 compared to Tween 80 [19], [25], [31]-[32]. Moreover, there was more non-entrapped drug in the particles S1 than in S5 and S2 that exhibited %EE of 78.64 ± 0.46%, 86.14 ± 0.17%, and 90.55 ± 0.28%, respectively. From these results, we concluded that the surfactants (Tween80 and P188) made an important contribution to the differences between the release from the three SLN formulations and their diffusion from the OXY suspension. The results indicated that the OXY was entrapped in the SLNs and was protected from the strong acidic environment of the stomach and then the SLNs containing the OXY subsequently reached the small intestine. Possibly, the major content of OXY in the SLNs could be

uptake by the intestinal cells and enter the body circulation to perform a sustained release *in vivo*.

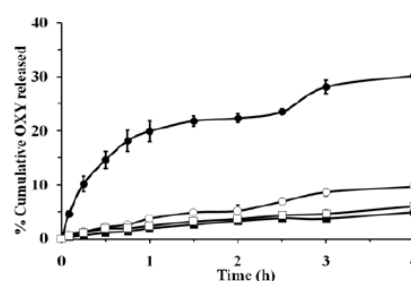


Fig. 1 The *in vitro* OXY release profiles from suspension (●), S1 (○), S2 (■), and S5 (□) in simulated gastric fluid (SGF, pH 1.2) without pepsin

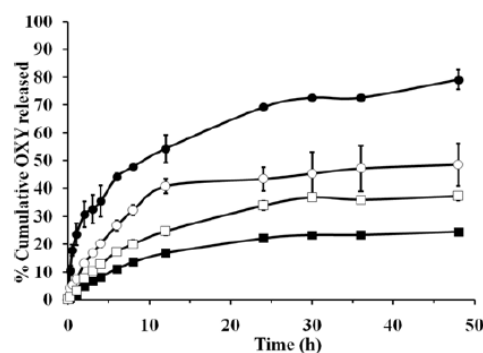


Fig. 2 The *in vitro* OXY release profiles from suspension (●), S1 (○), S2 (■), and S5 (□) in simulated intestinal fluid (SIF, pH 6.8) without pancreatin

#### G. Kinetic Analysis of *in vitro* Drug Release Study

To explain the release kinetics of OXY from the SLN formulations, the mean data for the fraction of OXY released in the SIF pH 6.8 was subjected to linear regression analysis using conventional mathematical models [33] and a Ritger-Peppas kinetics model [26]. The data for the drug release from



different types of surfactant (S1, S2, and S5) was mostly fitted to a Ritger–Peppas kinetics model and gave an  $R^2$  close to 1 for all the formulations as shown in Table IX. Based on the fitting result of the Ritger–Peppas model, the value of  $n$  was 0.5155, 0.7679, 0.6985 in the case of S1, S2, S5, respectively ( $0.43 < n < 0.85$ ), and this indicated that the mechanism of OXY release from the SLNs was by a mixing of the drug diffusion and the erosion of the lipid matrix. The  $n$  value was close to 0.85 in the case of the S2 formulation. This indicated that the effect of the erosion of the lipid matrix was predominant and the major amount of drug was enriched in the core of SLNs. The minor amount of drug in the shell can diffuse into the medium. In contrast, the release of the OXY from the S1 formulation appeared to be predominantly by a diffusion-controlled mechanism. OXY was mainly released by diffusion through the channels formed in the matrix into the medium.

TABLE IX  
LINEAR REGRESSION ANALYSES OF THE IN VITRO DRUG RELEASE DATA OF THE FORMULATIONS USING THE RITGER–PEPPAS KINETIC MODEL

Formulations	Ritger–Peppas model ( $Mt/M\infty = Kt^n$ )		
	K	n	$r^2$
S1	0.0889	0.5155	0.9587
S2	0.0204	0.7679	0.9423
S5	0.0376	0.6985	0.9585

#### V. CONCLUSION

In conclusion, the OXY-loaded SLN formulation (S2) comprising Compritol® 888 ATO with Tween80 combined with soy-lecithin had a good appearance, an ability to entrap the OXY drug, displayed the most favorable physicochemical properties, and had a retarded release of OXY in a SGF pH 1.2 and a SIF pH 6.8. Based on the data obtained in this work, the formulation S2 was judged to be the optimum formulation, and will be further for *in vitro* permeability, and *in vivo* absorption studies to ensure it was a potential carrier for the oral delivery of OXY.

TABLE X  
SUMMARY OF HOMOGENIZATION CONDITIONS COMPOSITIONS AND PROPERTIES OF THE OPTIMUM S2 FORMULATION

Formulation n	Homogenization conditions		Compositions (% w/w)			Physicochemical properties					
	Speed (rpm)	Time (min)	Solid lipid (5%)	Surfactant (3.75%)	Co-surfactant (1.875%)	Appearance	PS(nm)	PDI	TDC (%)	EE (%)	DL (%)
S2	24,000	15	Com888	Tween80	Soy lecithin	Milky suspension	134.40 ±0.57	0.25 ±0.00	102.05 ±1.97	90.55 ±0.28	5.54 ±0.02

#### ACKNOWLEDGMENT

Financial support was granted by the Thailand Research Fund (BRG 5580004) and the Faculty of Pharmaceutical Sciences, Prince of Songkla University, Thailand. We also wish to thank Dr. Brian Hodgson for assistance with the English.

#### REFERENCES

- [1] K. Likhitwitayawuid, *et al.*, "Phenolics with antiviral activity from *Millettiaery throcalyx* and *Artocarpus lakoocha*," *Nat. Prod. Res.*, vol. 19, no. 2, pp. 177–182, Feb. 2005.
- [2] K. O. Chung, *et al.*, "In-vitro and in-vivo anti-inflammatory effect of oxysresveratrol from *Morus alba* L.," *J. Pharm. Pharmacol.*, vol. 55, no. 12, pp. 1695–1700, Dec. 2003.
- [3] P. Lorenz, S. Roychowdhury, M. Engelmann, G. Wolf, and T. F. W. Horn, "Oxysresveratrol and resveratrol are potent antioxidants and free radical scavengers: effect on nitrosative and oxidative stress derived from microglial cells," *Nitric Oxide*, vol. 9, no. 2, pp. 64–76, Sep. 2003.
- [4] P. Tengamnuay, K. Pengrungruangwong, I. Pheansri, and K. Likhitwitayawuid, "Artocarpus lakoocha heartwood extract as a novel cosmetic ingredient: evaluation of the *in vitro* anti-tyrosinase and *in vivo* skin whitening activities," *Int. J. Cosmet. Sci.*, vol. 28, no. 4, pp. 269–276, Aug. 2006.
- [5] J. T. Weber, *et al.*, "Potential neuroprotective effects of oxysresveratrol against traumatic injury," *Eur. J. Pharmacol.*, vol. 680, no. 1, pp. 55–62, Apr. 2012.
- [6] P. Sasivimolphan, *et al.*, "Inhibitory activity of oxysresveratrol on wild-type and drug-resistant varicella-zoster virus replication *in vitro*," *Antivir. Res.*, vol. 84, no. 1, pp. 95–97, Oct. 2009.
- [7] A. L. Liu, *et al.*, "In vitro anti-influenza viral activities of stilbenoids from the lianas of *Gnetum pendulum*," *Planta. Med.*, vol. 76, no. 16, pp. 1874–1876, Nov. 2010.
- [8] V. Lipipun, *et al.*, "Topical cream-based oxysresveratrol in the treatment of cutaneous HSV-1 infection in mice," *Antivir. Res.*, vol. 91, no. 2, pp. 154–160, Aug. 2011.
- [9] W. Wang, J. Qian, X. Wang, and A. Jia, "Anti-HIV-1 activities of extracts and phenolics from *Smilax China* L.," School of Environmental and Biological Engineering, Nanjing University of Science and Technology, Nanjing, private communication, 2013.
- [10] H. Huang, *et al.*, "High performance liquid chromatographic method for the determination and pharmacokinetic studies of oxysresveratrol and resveratrol in rat plasma after oral administration of Smilax china extract," *Biomed. Chromatogr.*, vol. 22, no. 4, pp. 421–427, Dec. 2007.
- [11] H. Huang, *et al.*, "Identification of seven metabolites of oxysresveratrol in rat urine and bile using liquid chromatography/tandem mass spectrometry," *Biomed. Chromatogr.*, vol. 24, no. 4, pp. 426–432, Aug. 2010.
- [12] M. Mei, *et al.*, "In vitro pharmacokinetic characterization of Mulberroside A, the main polyhydroxylated stilbene in mulberry (*Morus alba* L.), and its bacterial metabolite oxysresveratrol in traditional oral use," *J. Agr. Food Chem.*, vol. 60, no. 9, pp. 2299–2308, Dec. 2012.
- [13] R. H. Müller, K. Mäder, and S. Gohla, "Solid lipid nanoparticles (SLN) for controlled drug delivery – a review of the state of the art," *Eur. J. Pharm. Biopharm.*, vol. 50, no. 1, pp. 161–177, July 2000.
- [14] S. Chakraborty, D. Shukla, and S. Singh, "Lipid – an emerging platform for oral delivery of drugs with poor bioavailability," *Eur. J. Pharm. Biopharm.*, vol. 73, no. 1, pp. 1–15, Sep. 2009.
- [15] E. B. Souto, and R. H. Müller, "Lipid nanoparticles: effect on bioavailability and pharmacokinetic changes," in *Drug Delivery*, 1st ed. vol. 197, M. Schäfer-Korting, Ed. New York: Springer-Verlag, 2010, pp. 115–141.
- [16] W. Mehnert, and K. Mäder, "Solid lipid nanoparticles: production, characterization and applications," *Adv. Drug Deliv. Rev.*, vol. 47, no. 2, pp. 165–196, Apr. 2001.
- [17] Y. Luo, D. Chen, L. Ren, X. Zhao, and J. Qin, "Solid lipid nanoparticles for enhancing vinpocetine's oral bioavailability," *J. Control. Release*, vol. 114, no. 1, pp. 53–59, May 2006.



- [18] A. J. Almeida, and E. Souto, "Solid lipid nanoparticles as a drug delivery system for peptides and proteins," *Adv. Drug Deliv. Rev.*, vol. 59, no. 6, pp. 478-490, July 2007.
- [19] L. Hu, Q. Xing, J. Meng, and C. Shang, "Preparation and enhanced oral bioavailability of cryptotanshinone loaded solid lipid nanoparticles," *AAPS Pharm. Sci. Tech.*, vol. 11, no. 2, pp. 582-587, June 2010.
- [20] V. Kakkar, S. Singh, D. Singla, and I. P. Kaur, "Exploring solid lipid nanoparticles to enhance the oral bioavailability of curcumin," *Mol. Nutr. Food Res.*, vol. 55, no. 3, pp. 495-503, Aug. 2010.
- [21] E. H. Gokce, *et al.*, "Resveratrol-loaded solid lipid nanoparticles versus nanostructured lipid carriers: evaluation of antioxidant potential for dermal applications," *Int. J. Nanomedicine*, vol. 7, pp. 1841-1850, Apr. 2012.
- [22] A. R. Neves, M. Lúcio, S. Martins, J. L. C. Lima, and S. Reis, "Novel resveratrol nanodelivery systems based on lipid nanoparticles to enhance its oral bioavailability," *Int. J. Nanomedicine*, vol. 8, pp. 177-187, Jan. 2013.
- [23] R. Tiwari, and K. Pathak, "Nanostructured lipid carrier versus solid lipid nanoparticles of simvastatin: comparative analysis of characteristics, pharmacokinetics and tissue uptake," *Int. J. Pharm.*, vol. 415, no. 1, pp. 232-243, Aug. 2011.
- [24] M. Gibaldi, and S. Feldman, "Mechanisms of surfactant effects on drug absorption," *J. Pharm. Sci.*, vol. 59, no. 5, pp. 579-89, May 1970.
- [25] G. Wu, and K. Y. C. Lee, "Effects of poloxamer 188 on phospholipid monolayer morphology: an atomic force microscopy study," *Langmuir*, vol. 25, no. 4, pp. 2133-2139, Jan. 2009.
- [26] P. L. Ritger, and N. A. Peppas, "A simple equation for description of solute release I. Fickian and non-fickian release from non-swellable devices in the form of slabs, spheres, cylinders or discs," *J. Control. Rel.*, vol. 5, no. 1, pp. 23-36, June 1987.
- [27] C. Y. Zhuang, *et al.*, "Preparation and characterization of vinpocetine loaded nanostructured lipid carriers (NLC) for improved oral bioavailability," *Int. J. Pharm.*, vol. 394, no. 1, pp. 179-185, July 2010.
- [28] M. Trotta, F. Debernardi, and O. Caputo, "Preparation of solid lipid nanoparticles by a solvent emulsification-diffusion technique," *Int. J. Pharm.*, vol. 257, no. 1, pp. 153-160, May 2003.
- [29] F. Q. Hu, *et al.*, "Preparation and characterization of stearic acid nanostructured lipid carriers by solvent diffusion method in an aqueous system," *Colloids Surf. B Biointerfaces*, vol. 45, no. 3, pp. 167-173, Nov. 2005.
- [30] J. E. Kipp, "The role of solid nanoparticle technology in the parenteral delivery of poorly water-soluble drugs," *Int. J. Pharm.*, vol. 284, no. 1-2, pp. 109-22, Oct. 2004.
- [31] E. Souto, W. Mehnert, R. Müller, "Polymorphic behaviour of Compritol® 888 ATO as bulk lipid and as SLN and NLC," *J. Microencapsul.*, vol. 23, no. 4, pp. 417-433, June 2006.
- [32] W. Sutananta, D. Q. M. Craig, and J. M. Newton, "An evaluation of the mechanisms of drug release from glyceride bases," *J. Pharm. Pharmacol.*, vol. 47, no. 3, pp. 182-187, March 1995.
- [33] P. Costa, and J. M. Sousa Lobo, "Modeling and comparison of dissolution profiles," *Eur. J. Pharm. Sci.*, vol. 13, no. 2, pp. 123-33, Dec. 2000.

**PAPER 2**

Modification of oral absorption of oxyresveratrol using lipid based nanoparticles



Contents lists available at ScienceDirect

## Colloids and Surfaces B: Biointerfaces

journal homepage: [www.elsevier.com/locate/colsurfb](http://www.elsevier.com/locate/colsurfb)

## Modification of oral absorption of oxyresveratrol using lipid based nanoparticles



Yaowaporn Sangsen<sup>a,b</sup>, Kamonthip Wiwattanawongsa<sup>b,c</sup>, Kittisak Likhitwitayawuid<sup>d</sup>, Boonchoo Sritularak<sup>d</sup>, Ruedeekorn Wiwattanapatee<sup>a,b,\*</sup>

<sup>a</sup> Department of Pharmaceutical Technology, Faculty of Pharmaceutical Sciences, Prince of Songkla University, Hat-Yai, Songkhla 90112, Thailand

<sup>b</sup> Phytomedicine and Pharmaceutical Biotechnology Excellence Research Center, Faculty of Pharmaceutical Sciences, Prince of Songkla University, Hat-Yai, Songkhla 90112, Thailand

<sup>c</sup> Department of Clinical Pharmacy, Faculty of Pharmaceutical Sciences, Prince of Songkla University, Hat-Yai, Songkhla 90112, Thailand

<sup>d</sup> Department of Pharmacognosy and Pharmaceutical Botany, Faculty of Pharmaceutical Sciences, Chulalongkorn University, Bangkok 10330, Thailand

### ARTICLE INFO

#### Article history:

Received 19 December 2014

Received in revised form 23 April 2015

Accepted 24 April 2015

Available online 4 May 2015

#### Keywords:

Solid lipid nanoparticles

Nanostructured lipid carriers

Oxyresveratrol

Oral absorption

### ABSTRACT

The aim of this study was to develop and assess nanostructured lipid carriers (NLC) compared to solid lipid nanoparticles (SLN) for improving the oral bioavailability of oxyresveratrol (OXY). The OXY formulated as SLN (OXY-SLN) and NLC (OXY-NLC) were prepared by a high shear homogenization technique. The optimized OXY-NLC (NLC3) produced smaller nanoparticle sizes ( $96 \pm 0.9$  nm) than that of the OXY-SLN ( $108 \pm 0.3$  nm) with a homogeneous size distribution and a high zeta potential. The spherical NLC had a significantly higher efficiency for OXY entrapment ( $89 \pm 0.1\%$ ) and a better stability than the SLN after storage for 12 months at  $4 \pm 2$  °C according to parameters such as smaller particles, greater zeta potential and a higher loading capacity ( $p < 0.05$ ). Differential scanning calorimetry (DSC) showed a less ordered crystalline structure of NLC than SLN. The accumulated drug in an amorphous state in the NLC was also confirmed by powder X-ray diffraction (PXRD). The *in vitro* release profiles of the OXY-NLC showed a more sustained release compared to the SLN and unformulated OXY. The *in vivo* pharmacokinetic profiles implied enterohepatic recycling of OXY in the Wistar rat. Meanwhile, the oral absorption pattern of OXY was modified by both types of lipid nanoparticles. The SLN and NLC increased the relative bioavailability of OXY to 125% and 177%, respectively, compared with unformulated OXY. These findings indicated that NLC could be used as a potential carrier to improve the oral bioavailability of OXY.

© 2015 Elsevier B.V. All rights reserved.

### 1. Introduction

Oxyresveratrol (OXY) is a polyphenolic stilbene that is abundant in the heartwood of the plant, *Artocarpus lakoocha* Roxburgh (Moraceae) and is used in Thai traditional medicine. It has been reported to exhibit potent antioxidant/anti-inflammatory activities [1,2], inhibits tyrosinase enzyme [3], and has strong neuroprotective activities [4]. OXY has also been shown to possess antiviral activities against several types of herpes simplex virus (HSV-1 and HSV-2) [5,6], various varicella zoster virus (VZV) [7] as well as influenza virus [8]. However, the oral absorption of OXY is limited

due to its high polarity that affects its intermediate permeability with involved efflux mediated mechanism [9,10]. Once into the blood stream it is cleared by extensive hepatic metabolism and its rapid elimination results in a short half-life time ( $\sim 0.96$  h) in the body leading to a low oral bioavailability and largely restricts its clinical use [6,11–13]. In an effort to overcome this drawback, we have investigated the development of different formulations that could modify the oral absorption of OXY and improve its bioavailability.

Lipid-based drug delivery systems have been used as oral carriers of poorly water soluble drugs and/or proteins because of their potential to enhance drug absorption and oral bioavailability in a number of ways [14–16]. Besides traditional lipid-based formulations, solid lipid nanoparticles (SLN), composed of solid lipids that are solid at body and room temperature, have proved to be efficient and attractive alternatives as colloidal drug carriers. The SLN has many advantages such as good biocompatibility and

\* Corresponding author at: Department of Pharmaceutical Technology, Faculty of Pharmaceutical Sciences, Prince of Songkla University, Hat-Yai, Songkhla 90112, Thailand. Tel.: +66 74 288915; fax: +66 74 428148.

E-mail address: [ruedeekorn.w@psu.ac.th](mailto:ruedeekorn.w@psu.ac.th) (R. Wiwattanapatee).

biodegradability when prepared with physiologically acceptable excipients, protection the drug from degradation in the GI tract, controlled drug release, and enhanced drug absorption by many of ways [17]. Either hydrophobic or hydrophilic drug could be entrapped by lipid matrix of the nanoparticles which structurally similar to the fat in daily food. The lipid nanoparticles increased the permeability of drug entrapped across lipid bilayers of the epithelium and facilitate draining the drug into lymphatic absorption leading to avoid the extensive hepatic metabolism [18]. Moreover, the lipid matrix reduced exposure of the entrapped drug to intestinal efflux system. Also, the presence of surfactant in the SLN promotes the oral absorption of the drug due to its inhibiting activity to the efflux transporters and deforming the cell membrane [19,20]. In the second generation of lipid nanoparticles, nanostructured lipid carriers (NLC) have been produced that can replace the solid lipids of SLN with liquid lipids (oil) to generate special structures within a lipid matrix that improves the potential limitations of SLN such as drug loading capacity, early drug expulsion and long term stability [21]. Both SLN and NLC have been investigated successfully as drug delivery systems that enhance oral bioavailability for several drugs [18,20,22,23]. Nonetheless, there have been no reports on investigations using such systems as carriers for the oral delivery of polar OXY.

The objectives of this study were to develop lipid nanoparticles as a potential delivery system of OXY. Firstly, both SLN and NLC containing OXY were formulated and evaluated in terms of their physicochemical properties and *in vitro* drug release properties. Then, the stability of a selected NLC was assessed and comparing to the SLN. Finally, the improved NLC was investigated further by *in vivo* pharmacokinetic studies to compare with the SLN formulations and the unformulated OXY.

## 2. Materials and methods

### 2.1. Materials

Oxyresveratrol (off-white powder, >99% purity) was from the Department of Pharmacognosy and Pharmaceutical Botany, Faculty of Pharmaceutical Sciences, Chulalongkorn University (Bangkok, Thailand). Resveratrol ( $\geq 99\%$  purity) was from Sigma-Aldrich (Saint Louis, MO, USA). Compritol 888 ATO<sup>®</sup> (glyceryl behenate; C888) and Labrafac<sup>®</sup> CC (caprylic/capric triglycerides; Lab CC) were from Gattefossé (Saint-Priest, France). Soy lecithin was from Rama Production Co., Ltd. (Bangkok, Thailand). Polysorbate 80 (polyoxyethylene (20) sorbitan monooleate; Tween80) was from S. Tong Chemicals Co., Ltd (Bangkok, Thailand). Acetonitrile and methanol (HPLC grade) were from RCI Labscan (Bangkok, Thailand). All other chemicals were of analytical grade.

### 2.2. Preparation of OXY-loaded SLN and NLC

The OXY-loaded SLN (OXY-SLN) were prepared by a high shear homogenization method [24]. Briefly, the solid lipid (C888) of lipid phase and the aqueous phase: OXY, Tween80 and soy lecithin in deionized (DI) water were heated to 85 °C, separately. Then, the hot aqueous phase was added to the oil phase at 85 °C under stirring. An emulsion was obtained by using a high speed homogenizer (ULTRA-TURRAX<sup>®</sup>, IKA<sup>®</sup>, Germany) at 24,000 rpm for 15 min. Subsequently the final dispersion was cooled to room temperature to solidify the nanoparticles. The OXY-loaded NLC (OXY-NLC) were prepared using the same method, by replacing the C888 with liquid oil (Lab CC) in different ratios as shown in Table 1. Blank SLN and NLC were prepared in the same way, without the drug.

### 2.3. Physicochemical characterizations

#### 2.3.1. Measurements of particle size, polydispersity index and zeta potential

The mean particle size (PS), the polydispersity index (PDI) and the zeta potential (ZP) of the developed SLN and NLC were measured at 25 °C using a zeta potential analyzer (Zetasizer Nano ZS<sup>®</sup>, Malvern Instruments, UK). Prior to the measurements, all samples were diluted with DI water. The PS and size distribution (PDI) were monitored by the dynamic light scattering (DLS) technique at an angle of 173 °C. For the ZP, this was determined by measurement of the electrophoretic mobility. All measurements were performed in triplicate.

#### 2.3.2. Determination of total OXY content, entrapment efficiency and loading capacity

The total content (TC), the entrapment efficiency (EE) and the drug loading capacity (LC) of the OXY in SLN and NLC were determined as previously described [24]. The EE was calculated from the difference between the total incorporated amount of OXY and the amount of free OXY that was not entrapped in the nanoparticles. The LC was the proportion of the incorporated drug/lipid. The resulting solution was analyzed by a HPLC method. The total OXY content (%) in the formulations, the EE (%) and LC (%) were calculated by the following equations where  $OXY_{exp}$  was the total content of OXY calculated from the experiment,  $OXY_{ther}$  was the theoretical OXY content,  $OXY_f$  was the amount of non-entrapped OXY,  $T_{lipid}$  was the total weight of the lipid phase in the formulation.

$$TC(\%) = \left( \frac{OXY_{exp}}{OXY_{ther}} \right) \times 100$$

$$EE(\%) = \left[ \frac{OXY_{exp} - OXY_f}{OXY_{exp}} \right] \times 100$$

$$LC(\%) = \left[ \frac{OXY_{exp} - OXY_f}{T_{lipid}} \right] \times 100$$

#### 2.3.3. Determination of morphology

The morphology of SLN and NLC formulations was observed by transmission electron microscopy (TEM; JEOL Ltd., Tokyo, Japan) at 160 kV. The samples were placed on Formvar<sup>®</sup> grids and stained with 2% (w/v) phosphotungstic acid for 10 min. Any excess fluid was then removed, and the grid surface was air dried at room temperature.

#### 2.3.4. Analysis by differential scanning calorimetry (DSC) and powder X-ray diffraction (PXRD)

DSC and PXRD were used to identify the crystal form of the lipid and OXY dispersed in the lipid matrix. DSC analysis was performed using a DSC8000 differential scanning calorimeter (Perkin Elmer Inc., MA, USA). Accurately weighed samples were placed in aluminum pans and sealed with a lid. Al<sub>2</sub>O<sub>3</sub> was used as the reference. In the scanning process, a heating rate of 5 °C/min was applied in the temperature range from 20 °C to 150 °C.

PXRD studies were performed using the Phillips X-ray diffractometer (X'Pert MPD, the Netherlands) and Cu-K $\alpha$  radiation. The samples were scanned over a  $2\theta$  range of 0°–90° at a scan rate of 0.05°/s. The freeze drying procedure was performed by freeze dryer (FTS systems, Tokyo, Japan) to practically determine of the OXY-SLN and OXY-NLC formulations.



**Table 1**  
Composition of the produced SLN and NLC formulations.

Formulations	Compositions (% w/w)					
	Lipid phase		Aqueous phase			
	C888	Lab CC	Tween80	Soy lecithin	OXY	DI water
Blank SLN	5	–	3.75	1.875	–	89.375
Blank NLC1	4	1	3.75	1.875	–	89.375
Blank NLC2	3	2	3.75	1.875	–	89.375
Blank NLC3	2.5	2.5	3.75	1.875	–	89.375
SLN	5	–	3.75	1.875	0.3	89.075
NLC1	4	1	3.75	1.875	0.3	89.075
NLC2	3	2	3.75	1.875	0.3	89.075
NLC3	2.5	2.5	3.75	1.875	0.3	89.075

#### 2.4. The *in vitro* release of OXY

The *in vitro* release studies of OXY were performed using the dialysis bag diffusion technique with some modifications [18]. Briefly, a suspension of OXY-SLN or OXY-NLC (equivalent to 10 mg OXY) was added into the dialysis bag (MWCO 12–14 kDa). The bag was immersed in 200 mL of release medium in a chamber of the USP30 dissolution apparatus 2 (Hanson Research Corporation, USA), stirred at 100 rpm and maintained at  $37 \pm 0.5$  °C. The dissolution medium was simulated gastric fluid (SGF, pH 1.2) and simulated intestinal fluid (SIF, pH 6.8), respectively. 5 mL aliquots were withdrawn at various time intervals and replaced with fresh medium to maintain the sink condition. The samples were filtered and analyzed using the HPLC method. The cumulative percentage of the released drug from each formulation was calculated. Each determination was performed in triplicate.

The release kinetics of the drug in the matrix has been widely analyzed using the Ritger–Peppas model [25]. The kinetic model was used according to the following equation where  $M_t/M_\infty$  was the fraction of drug released at time  $t$ ,  $K$  was the constant incorporating structural and geometrical characteristics of the dosage form, and  $n$  was the release exponent that indicated the drug release mechanism. For the Fickian diffusion from the spheres,  $n = 0.43$ , while for the anomalous transport,  $n$  was between 0.43 and 0.85, and for a case II transport (zero-order release),  $n = 0.85$ .

$$\frac{M_t}{M_\infty} = Kt^n$$

#### 2.5. Formulation stability studies

To assess the stability of the formulations, the glass bottles with light protection containing the samples were stored in a refrigerator at  $4 \pm 2$  °C. The samples were taken at 0, 3, 6, 9 and 12 months. The optimum OXY-SLN and OXY-NLC formulations were determined for their appearance, PS, PDI, ZP, TC, EE and LC at each time point.

#### 2.6. Quantification of OXY

The quantitative determination of OXY was performed using an Agilent HPLC system (HP 1100, Agilent, USA). Chromatographic separations were achieved using a VertiSep® pH endure C18 5- $\mu$ m (4.6 mm  $\times$  250 mm) column and a guard column (4.6 mm  $\times$  10 mm) (Ligand Scientific, Bangkok, Thailand), and a UV detector at the wavelength of 320 nm. The mobile phase comprised acetonitrile and 0.5% (v/v) acetic acid (27:73, v/v). This isocratic solvent system was set at ambient temperature, with a flow rate and injection volume of 1.0 mL/min and 50  $\mu$ L, respectively. The internal standard method was used for analysis of OXY in the plasma samples. The retention time of OXY and resveratrol (an internal standard), were

approximately 7 and 12 min, respectively. The calibration curve for OXY was constructed by plotting concentrations *versus* the average peak area ratio of OXY to the internal standard, and calculated from three determinations. A linear relationship was demonstrated with a correlation coefficient ( $r^2$ ) of 0.9994 over the concentration range of 0.2–10  $\mu$ g/mL of OXY. The intra-day and inter-day precisions were obtained by three daily injections per each concentration of these spiked plasma samples over a 3 day period. The intra-day repeatability gave relative standard deviations (%RSD) of 1.00–2.32%, whereas the %RSD of the inter-day precision ranged from 2.23% to 10.26%, respectively. The recovery percentage of the method ranged from  $88.96 \pm 2.20$  to  $100.02 \pm 2.34$ . The limit of detection (LOD) and the lower limit of determination (LLOQ) was 0.02 and 0.1  $\mu$ g/mL, respectively.

#### 2.7. *In vivo* absorption studies

Male Wistar-strain rats (250–300 g) were provided by the Animal House, Faculty of Science, Prince of Songkla University. The rats were kept in the animal room and maintained on standard diet and free access to distilled water before the experiment. All animals received human care in compliance with the Guiding Principles for the Care and Use of Research Animals promulgated (MOE 0521.11/063). The overnight fasted rats were divided into three groups with seven rats ( $n = 7$ ) per each group. A single dose equivalent to 180 mg/kg OXY of either OXY aqueous suspension, or OXY-SLN, or OXY-NLC was administered to each group by oral gavage. Blood samples (250  $\mu$ L) were collected *via* the tail-clip method [26] at 0, 5, 10, 15, 20, 30, 45, 60, 90, 120, 180, 240, 360, 480 and 600 min after dosing, into heparinized tubes. The blood samples were centrifuged at 13,000 rpm 20 °C for 10 min, and the plasma samples were separated. Acetonitrile was added to the plasma sample, mixed, and allowed to stand for 5 min to precipitate the protein. The samples were centrifuged at 13,000 rpm at 20 °C for 10 min. The supernatant was filtered and subjected to the validated HPLC. The plasma pharmacokinetic parameters including the maximum concentration ( $C_{max}$ ), time to reach maximum concentration ( $T_{max}$ ) were determined, and the area under the concentration–time curve from 0 to 10 h ( $AUC_{0-10h}$ ) was calculated using the linear trapezoidal method. The relative bioavailability in 10 h ( $F_{r,0-10h}$ ) at the same dose was calculated as:

$$F_{r,0-10h} = \frac{AUC_{(0-10h)oral,formulation}}{AUC_{(0-10h)oral,suspension}} \times 100$$

#### 2.8. Statistical analysis

All results were expressed as a mean value  $\pm$  SD. Statistical comparisons were performed by the one-way ANOVA. Differences were considered significant at  $p < 0.05$ .

### 3. Results and discussion

#### 3.1. Preparation of OXY-loaded SLN and NLC

SLN and NLC can be prepared by various methods [21,27]. In this study, the hot/high speed homogenization method was used because it was simple and quick on the laboratory scale. In previous research studies, the SLN or NLC prepared using sufficient Tween80 (hydrophilic–lipophilic balance; HLB of 15) as surfactant demonstrated suitable physical characteristics, good stability, a sustained drug release and also improve bioavailability [24,27,28]. Therefore, Tween80, a non-toxic and non-ionic surfactant, was selected for use in this study. Moreover, soy lecithin (HLB of 5) was chosen as a co-surfactant to enhance the ability to emulsify the lipid and to improve the stability of the system. The NLC formulations were prepared by taking the SLN compositions as the starting formulation. Amounts of 20% (NLC1), 40% (NLC2), and 50%, w/w, (NLC3) of lipid (C888) were replaced with oil (Lab CC) in formulations. The C888 and Lab CC of the three NLC formulations exhibited good miscibility in the nanoparticulate state. The effects of the lipid to oil ratios on the physicochemical properties of the formulations are summarized in Table 2.

#### 3.2. Physicochemical characterizations

##### 3.2.1. Measurements of particle size, polydispersity index and zeta potential

The SLN formulation containing Tween80 had a well milky appearance with low viscosity and non-flocculation. The PS of the OXY-SLN was less than 110 nm with a uniform size distribution (PDI of 0.2–0.4) the same as for the blank SLN. In addition, the ZP of OXY-SLN and the blank SLN were in a similar range of around –50 mV. This indicated that the incorporated OXY did not change the physical properties of the SLN.

In the case of the NLC formulations containing OXY, larger particle sizes were observed when compared to the blank NLC but the narrow PDI detected was similar. However, the PS of the OXY-NLC was still in the acceptable range (<200 nm) [18]. Compared with the SLN, the PS of NLC in all formulations was significantly smaller than those of the SLN ( $p < 0.05$ ). Therefore, addition of the Lab CC oil to the system did affect the particle sizes. This result can be explained by the emulsification process; oils are generally liquid and contain a high proportion of unsaturated fatty acid reduces the melting point of the solid lipid [29]. Moreover, the oils inside the NLC system may help to encourage homogeneity and allow for a rapid distribution of the heat energy during the heating step. This may result in a more efficient emulsification for the NLC system and the production of smaller size of the formed emulsion droplets, and may result in smaller nanoparticles after the cooling step. However, both of the SLN and NLC produced were submicron colloidal carriers that were suitable for gastrointestinal (GI) absorption and oral delivery [18,29,30].

Similar to the SLN, all the blank NLC and the OXY-NLC presented a high negative ZP of above –30 mV. Likewise, incorporation of the OXY did not change the ZP of the blank NLC ( $p > 0.05$ ). Therefore, the developed lipid nanoparticles in this work were considered to be physically stable due to the electrostatic repulsion conferred by the chemical nature of the lipid matrix, the polysorbate surfactant and the soy lecithin used, and also the adsorption of the negatively charged ions onto the surface of the lipid nanoparticles.

##### 3.2.2. Total content, entrapment efficiency and loading capacity

All the developed SLN and NLC had 100% (w/w) of the added OXY in the formulations and no drug loss occurred during the preparation process. After preparation (0 month), the %EE of the NLC including NLC1 and NLC3 was significantly higher than for the SLN

( $p < 0.05$ ). The LC of the SLN and NLC (~5%, w/w, of solid lipid) was not significantly different ( $p > 0.05$ ). Thus, the NLC1 and NLC3 were selected to evaluate in the next step compared to the SLN. Furthermore, the %EE of each SLN and NLC formulations (Table 2) were satisfactorily high, compared to such values presented in previous reports [22,23,31]. This indicated that they had suitable systems for entrapment of OXY.

##### 3.2.3. Determination of morphology

The morphology of the selected SLN, NLC1, and NLC3 after 3-months storage was determined by TEM as shown in Fig. 1. Both the NLC formulations had spherical uniform shapes with smooth surfaces, and did not aggregate. Meanwhile, the morphology of SLN changed from spheres at 0 month (Fig. 1A) to two-layered particles with irregular surfaces (Fig. 1B) after storage for 3 months. This result indicated that a high amount of the drug was localized on the surface of the particles and meant that there was less SLN stability [21]. From the TEM analysis, the mean diameter of the SLN and NLC containing the OXY was in the range of 80–100 nm that was in agreement with the results obtained by the DLS. The slightly different size of the particles observed using the different methods were based on different techniques [32].

##### 3.2.4. Analysis by differential scanning calorimetry (DSC) and powder X-ray diffraction (PXRD)

DSC analysis was one method used to investigate the polymorphic forms, crystallinity and the state of the drug and lipid nanoparticles by determining the variation of temperature and energy at a phase transition. The DSC curves of all samples are shown in Fig. 2. For the OXY (Fig. 2A) and C888 (Fig. 2F), the melting process took place with a maximum peak at 109 °C and 71 °C, respectively. These melting peaks all appeared and had almost the same value in the thermogram of their 1:1 of physical mixture. The loss of the endothermic peak of OXY in the developed SLN and NLC indicated that the OXY in the lipid phase was in an amorphous state and formed a solid solution within the matrix of nanoparticles. In addition it was observed that the melting point of the C888 in the NLC3 had shifted to a lower temperature compared to the NLC1 and SLN, respectively. The results confirmed previous studies that had reported that when oil was added to the system this depressed the melting point in a concentration-dependent manner [28,33]. This confirmed that NLC had a less ordered crystalline structure than SLN.

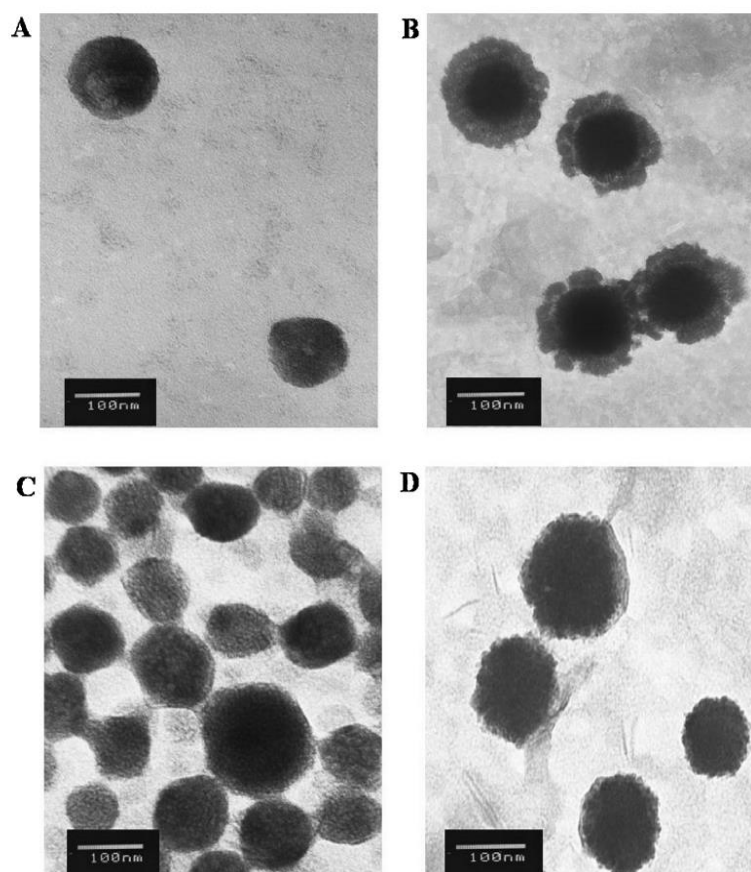
The physical state of the OXY incorporated into SLN and NLC was confirmed by the PXRD, and the patterns of all samples are shown in Fig. 3. The PXRD diagram of the physical mixture showed two characteristic wide peaks (20.5° and 23.5°) of C888 and a peak intensity of pure OXY. It indicated that the bulk matrix (C888) and OXY were crystalline. In contrast, there was no sharp characteristic peak for crystalline OXY observed in the patterns of the three formulations. Only, the predominant broad and small peaks at the 2 $\theta$  scattered angles of 21° and 24° appeared which could be attributed to the crystalline structure of C888. The results indicated that the OXY in both the SLN and NLC formulations was dispersed molecularly in an amorphous state.

##### 3.3. The *in vitro* release of OXY

In this study, the *in vitro* OXY release profiles of the formulations compared to the OXY suspension in SGF pH1.2 and SIF pH 6.8 at body temperature (37 °C) are shown in Fig. 4. The OXY suspension tended to release a high amount of OXY in both medium. On the other hand, the release of OXY from the SLN and NLC formulations slowed down considerably in the SGF pH1.2 and exhibited a sustained release up to 48 h in the SIF pH 6.8. This might be the result of the glyceryl behenate which has previously been utilized

**Table 2**Physicochemical characteristics and stability data at  $4 \pm 2^\circ\text{C}$  of the blank formulations, OXY-SLN and OXY-NLC. Data represents the mean  $\pm$  SD ( $n=3$ ).

Code	PS (nm)	PDI	ZP (mV)	TC (%)	EE (%)	LC (%)
0 month						
Blank SLN	98 $\pm$ 0.1	0.30 $\pm$ 0.00	-53 $\pm$ 1.2			
Blank NLC1	98 $\pm$ 0.5	0.30 $\pm$ 0.00	-50 $\pm$ 0.6			
Blank NLC2	98 $\pm$ 0.7	0.28 $\pm$ 0.01	-46 $\pm$ 0.1			
Blank NLC3	91 $\pm$ 0.4	0.28 $\pm$ 0.01	-42 $\pm$ 2.4			
SLN	108 $\pm$ 0.3	0.24 $\pm$ 0.00	-51 $\pm$ 1.0	101 $\pm$ 0.9	86 $\pm$ 0.8	5.2 $\pm$ 0.1
NLC1	99 $\pm$ 0.2	0.25 $\pm$ 0.01	-46 $\pm$ 0.6	101 $\pm$ 0.3	88 $\pm$ 0.4	5.3 $\pm$ 0.1
NLC2	100 $\pm$ 0.1	0.23 $\pm$ 0.01	-46 $\pm$ 0.4	102 $\pm$ 1.7	84 $\pm$ 1.1	5.1 $\pm$ 0.1
NLC3	96 $\pm$ 0.9	0.26 $\pm$ 0.01	-42 $\pm$ 0.9	101 $\pm$ 3.6	89 $\pm$ 0.1	5.4 $\pm$ 0.4
3 months						
SLN	111 $\pm$ 0.9	0.24 $\pm$ 0.01	-38 $\pm$ 1.1	103 $\pm$ 4.8	84 $\pm$ 0.1	5.2 $\pm$ 0.1
NLC1	102 $\pm$ 0.4	0.24 $\pm$ 0.00	-38 $\pm$ 1.3	100 $\pm$ 1.9	84 $\pm$ 0.5	5.0 $\pm$ 0.1
NLC3	98 $\pm$ 1.3	0.25 $\pm$ 0.01	-33 $\pm$ 2.2	102 $\pm$ 3.8	88 $\pm$ 0.3	5.2 $\pm$ 0.1
6 months						
SLN	122 $\pm$ 1.0	0.25 $\pm$ 0.01	-35 $\pm$ 1.0	98 $\pm$ 6.2	84 $\pm$ 0.5	5.1 $\pm$ 0.1
NLC1	102 $\pm$ 0.6	0.27 $\pm$ 0.00	-40 $\pm$ 0.3	96 $\pm$ 7.4	85 $\pm$ 0.5	5.1 $\pm$ 0.1
NLC3	97 $\pm$ 0.8	0.25 $\pm$ 0.01	-42 $\pm$ 2.6	103 $\pm$ 1.1	88 $\pm$ 0.2	5.4 $\pm$ 0.1
9 months						
SLN	122 $\pm$ 1.3	0.26 $\pm$ 0.00	-30 $\pm$ 2.2	102 $\pm$ 1.3	83 $\pm$ 0.2	4.9 $\pm$ 0.1
NLC1	102 $\pm$ 1.3	0.26 $\pm$ 0.00	-37 $\pm$ 1.1	100 $\pm$ 2.7	84 $\pm$ 0.5	5.1 $\pm$ 0.0
NLC3	98 $\pm$ 0.5	0.28 $\pm$ 0.01	-40 $\pm$ 2.8	101 $\pm$ 1.0	85 $\pm$ 0.1	5.2 $\pm$ 0.1
12 months						
SLN	159 $\pm$ 0.6	0.26 $\pm$ 0.02	-28 $\pm$ 0.5	98 $\pm$ 2.1	78 $\pm$ 0.3	4.6 $\pm$ 0.0
NLC1	104 $\pm$ 0.4	0.23 $\pm$ 0.01	-37 $\pm$ 1.6	103 $\pm$ 3.7	83 $\pm$ 0.0	5.0 $\pm$ 0.0
NLC3	106 $\pm$ 0.5	0.30 $\pm$ 0.01	-41 $\pm$ 0.4	101 $\pm$ 0.5	85 $\pm$ 0.3	5.1 $\pm$ 0.0

Fig. 1. TEM images at  $\times 100\text{K}$  of SLN (A) at 0 month; SLN (B), NLC1 (C), and NLC3 (D) after 3-months storage.



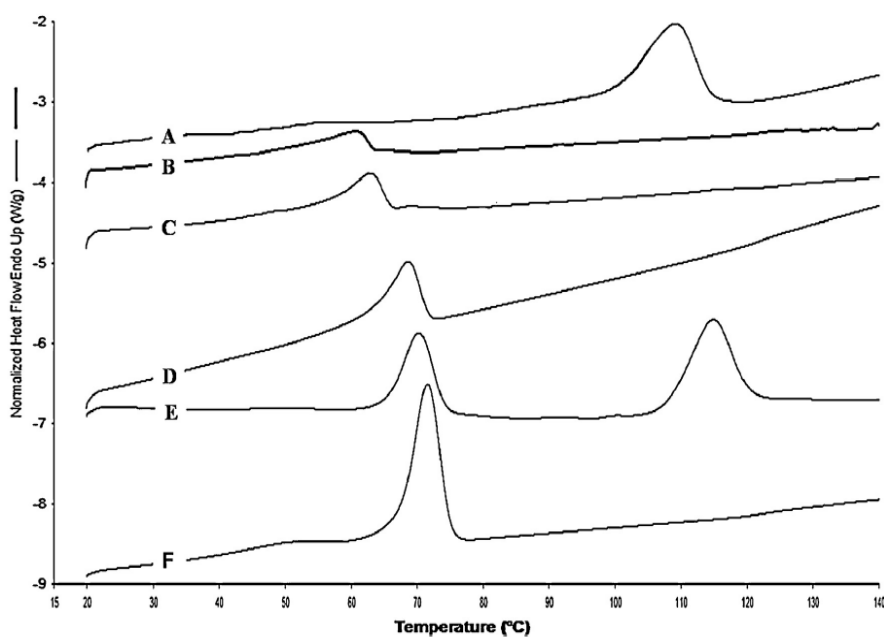


Fig. 2. DSC thermograms of OXY (A); freeze dried powders of NLC3 (B); NLC1 (C); SLN (D); physical mixtures of C888 and OXY (E); and C888 (F).

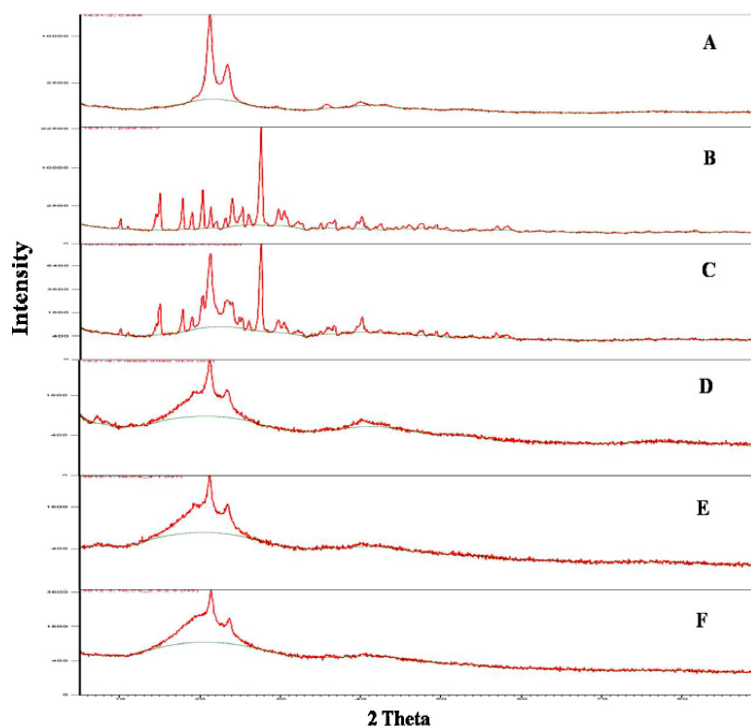


Fig. 3. Powder X-ray images of C888 (A); OXY (B); physical mixtures of C888 and OXY (C); and freeze dried powders of SLN (D); NLC1 (E) and NLC3 (F).

as a retardant material for a sustained-release dosage form [34–36]. In addition the developed SLN and NLC showed no burst of OXY release in the medium which presented that there was no free drug attached to the surface of the nanoparticles. Comparing each of the

SLN and NLC formulations at pH 6.8, the slowest OXY release profile was observed in the NLC1. The results indicated that the release rate of OXY might depend on the crystallinity of the lipid matrix. A less ordered lipid matrix was obtained in the presence of the



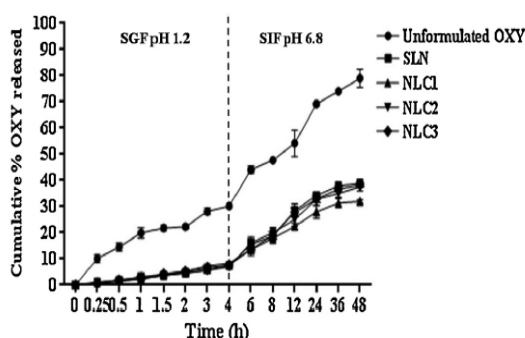


Fig. 4. *In vitro* OXY release profiles of SLN and NLC formulations with different lipid to oil ratios (NLC1, NLC2, NLC3) compared with the unformulated OXY in SGF (pH 1.2) and SIF (pH 6.8). Data represents the mean  $\pm$  SD ( $n=3$ ).

oil in the NLC which helped the drug to be accommodated in the matrix core of the NLC, and delayed its expulsion so promoted a more sustained release [21,23]. Nevertheless, a greater amount of Lab CC oil in the NLC formulations did not improve the sustained release of OXY (the NLC2 and NLC3). These results indicated that the OXY entrapped in SLN and NLC was protected from the strong acidic environment of the stomach and therefore subsequently reached the small intestinal. Furthermore, the more entrapped OXY in the NLC than SLN could be uptaken by the intestinal cells and enter the blood circulation to perform a more sustained *in vivo* release.

In order to develop a prolonged release system, it is vital to understand the release mechanism and kinetics. The OXY release data from all developed SLN and NLC were best fitted to a Ritger–Peppas kinetic model as the  $R^2$  was close to 1 (0.9655, 0.9466, 0.9783, 0.9659 for SLN, NLC1, NLC2, NLC3, respectively). Based on the results from the model, the values of  $n$  were 0.7298, 0.7956, 0.5486, 0.7388 for SLN, NLC1, NLC2, NLC3, respectively ( $0.43 < n < 0.85$ ). This indicated that the release of OXY from the SLN and NLC was due to a combination of drug diffusion and erosion from the lipid matrix. The  $n$  values of the three formulations (SLN, NLC1, and NLC3) were close to 0.85 indicated that the erosion was the predominant release mechanism and the major amount of drug was enriched in the matrix of the nanoparticles.

#### 3.4. Formulation stability studies

The stability data of the OXY-loaded formulations is summarized in Table 2. There were no changes in the appearance and PDI for up to 12 months for any of the OXY-SLN and OXY-NLC under storage conditions ( $4 \pm 2^\circ\text{C}$ ). Although, the PS of the three selected formulations increased during the storage time, this size still remained in the acceptable range ( $<200\text{ nm}$ ) [18]. The ZP is a key factor that can predict the stability of a colloidal dispersion. Reduction of the ZP was observed during storage conditions for all formulations especially in the SLN. Meanwhile, the ZP of the NLC formulations remained in the high negative values (above 30 mV) which could be considered to be stable dispersion due to the electric repulsion between the particles [17,27]. These results demonstrate the reduced stability of the SLN compared to the NLC which also agrees with the TEM analysis.

The total OXY content of all formulations did not change whereas the %EE and %LC of the SLN were evidently decreased under storage conditions. Furthermore, the %EE and %LC of both the NLC were significantly higher than those of the SLN after 12 months of storage ( $p < 0.05$ ). One explanation for this result was that the highly recrystallized lipid phase of the SLN dispersions resulted

Table 3

Pharmacokinetics data of OXY after oral administration of different formulations including SLN, NLC and an aqueous suspension of OXY (equivalent to 180 mg/kg of OXY). Data represents the mean  $\pm$  SD ( $n=7$ ).

Parameters	OXY aqueous suspension	SLN	NLC
$C_{\max}$ (ng/mL)	$662 \pm 82$	$284 \pm 105^*$	$518 \pm 81^{* \#}$
$T_{\max}$ (min)	10	10	10
$AUC_{0-10h}$ (ng h/mL)	$1897 \pm 220$	$2370 \pm 269^*$	$3366 \pm 65^{* \#}$
$F_{r,0-10h}$ (%)	100	125	177

\*  $p < 0.05$ , comparison with aqueous suspension.

#  $p < 0.05$ , comparison with SLN.

in the expulsion of the drug from the particles, whereas the less ordered crystalline structure of the NLC exhibited lattice defects in the lipid core that could offer spaces to accommodate the drug [21,23,33]. However, having the most appropriate amount of oil in the system was an important factor to ensure the crystalline structure of the NLC. Therefore, the NLC3 was selected for further *in vivo* absorption studies.

#### 3.5. *In vivo* absorption studies

The pharmacokinetic parameters in rats after oral administration of OXY in either the aqueous suspension or SLN or NLC at an equimolar dose are summarized in Table 3. Plasma concentrations *versus* time profiles are shown in Fig. 5. In comparison to the suspension, the  $C_{\max}$  of OXY administered as SLN was significantly decreased, while those from the NLC only slightly decreased. This data was consistent with the *in vitro* dissolution data. A greater  $AUC_{0-10h}$  ( $p < 0.05$ ) was obtained from the NLC (177%) and the SLN (125%), than from the unformulated OXY (100%) and indicated that there was a significantly improved systemic exposure to OXY.

The low oral bioavailability of OXY itself ( $F \sim 14\%$ ) could be attributed to a number of reasons [9,37]. In addition to its polar structure, the intestinal metabolism and extensive metabolic conjugation in the liver provided the main barriers to OXY absorption. Also, both the gut wall P-glycoprotein (P-gp) and the multidrug resistance-associated proteins (MRPs) have been reported to be involved in reducing the OXY absorption from the GI tract [10]. There is also a report that there is a rapid urinary and biliary excretion of OXY [11]. Possible mechanisms for improving the bioavailability of OXY from NLC after oral administration have been considered. Firstly, the significantly smaller particle sizes of the NLC ( $p < 0.05$ ) occupied a larger surface area than larger particles (e.g. SLN), a higher dispersibility, and prolonged residence time provided more amounts and longer time of drug to adhere at the absorptive site of the intestinal epithelium [38]. Secondly, the Lab CC oil used in the NLC had a greater solubilization capability for drugs [39]. Furthermore, the oil itself, which was the medium chain triglyceride oil, had a permeation enhancing property which improved oral drug absorption by many of ways, for example, mucoadhesive properties of the vehicle, altering epithelial absorption and promoting lymphatic uptake [40]. Apart from the effects of physical characteristics and the oil used in the NLC, the lipid used in the formulations was structurally similar to the fat in daily food. They could entrap the polar OXY in the particles and stimulate bile secretion, and thus enhance the uptake of intact particles by the gut wall and facilitate its draining into the lymphatic system. This is called an absorptive promotion effect of the NLC [18,20]. Moreover, the surfactant used in the formulation might enhance intestinal permeability by several means [19,38,41]. For example, Tween80 can alter the cell membrane integrity as well as inhibiting the efflux transporters such as P-gp, the MRPs family and other pump proteins that would lead to the improved transcellular permeability of the drug. Furthermore,

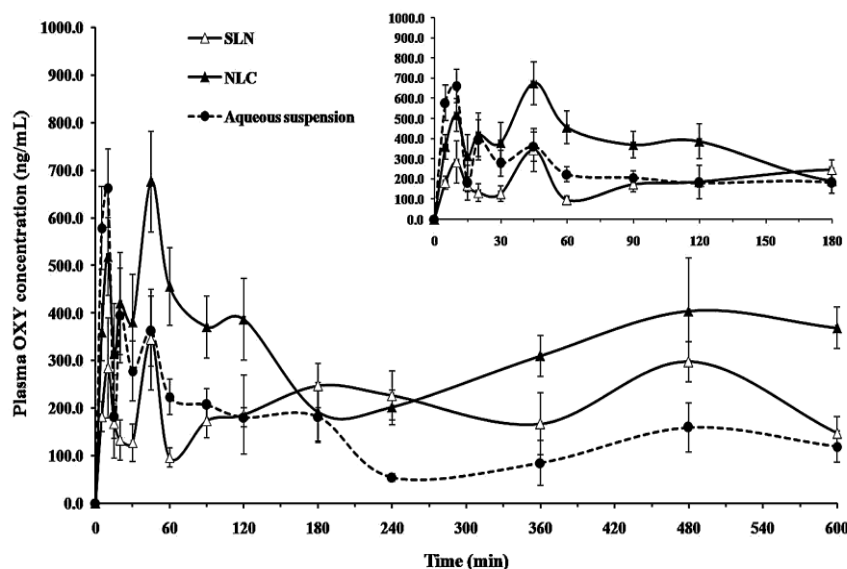


Fig. 5. Plasma concentrations of OXY vs. time profiles after oral administration of OXY formulated as SLN and NLC, compared with the unformulated OXY (180 mg/kg of OXY). Data represents the mean  $\pm$  SD ( $n = 7$ ).

NLC entrapment could bypass the liver thus the extensive first-pass metabolism could be avoided. The absorption *via* the lymphatic system would also minimize rapid elimination of OXY. Finally, the sustained OXY release in the systemic circulation would achieve a longer availability of the drug in the body [18,20,29]. Hence NLC is a promising carrier for improvements to the oral bioavailability of OXY.

It was of interest that the multiple peaks of the plasma concentration of OXY observed in all the formulation tested would suggest enterohepatic recycling (EHC) of the absorbed OXY. Although we have not determined the metabolites formed during the absorption study, it had been shown that a glucuronide conjugate was the predominant metabolite of OXY in urine and bile after oral OXY administration to rat [12]. In addition the EHC of resveratrol has been reported from secondary peak plasma concentrations between 4 and 8 h post-administration [42]. To confirm this phenomenon, studies involving the bile duct or duodenum cannulation should be further investigated. Nevertheless, the time for the second peak (45 min) noted for each profile of formulation tested was the same (Fig. 5). The consistency of the observation implied the altered absorption process, while disposition process could be minimally affected by either SLN or NLC.

#### 4. Conclusions

SLN and NLC containing OXY were formulated successfully by the hot/high speed homogenization technique using optimum amounts of miscible components that led to the enhancement of oral OXY absorption. The NLC formulations were much better than the SLN formulations because they had a smaller and more uniform nanoparticle size, higher entrapment efficiency, and a satisfactory loading capacity. Moreover, the OXY-NLC was more stable than the OXY-SLN after a 12-months storage period. A sustained release of OXY without an initial burst effect was achieved from the NLC. In *in vivo* absorption studies, an enhanced oral bioavailability of OXY was obtained using NLC compared to both OXY-SLN and an OXY suspension.

#### Acknowledgements

Financial support was granted by the Thailand Research Fund (BRG 5580004) and the Faculty of Pharmaceutical Sciences, Prince of Songkla University, Thailand. We also thank Dr. Brian Hodgson for assistance with the English.

#### References

- [1] K.O. Chung, B.Y. Kim, M.H. Lee, Y.R. Kim, H.Y. Chung, J.H. Park, J.O. Moon, J. Pharm. Pharmacol. 55 (2003) 1695.
- [2] P. Lorenz, S. Roychowdhury, M. Engelmann, G. Wolf, T.F.W. Horn, Nitric Oxide 9 (2003) 64.
- [3] P. Tengamnuay, K. Pengrungruangwong, I. Phansri, K. Likhitwitayawuid, Int. J. Cosmet. Sci. 28 (2006) 269.
- [4] J.T. Weber, M. Lamont, L. Chibrikova, D. Fekkes, A.S. Vluc, P. Lorenz, P. Kreutzmann, J.E. Slemmer, Eur. J. Pharmacol. 680 (2012) 55.
- [5] K. Likhitwitayawuid, B. Sritularak, K. Benchanak, V. Lipipun, J. Mathew, R.F. Schinazi, Nat. Prod. Res. 19 (2005) 177.
- [6] V. Lipipun, P. Sasivimolphan, Y. Yoshida, T. Daikoku, B. Sritularak, G. Ritthidej, K. Likhitwitayawuid, P. Pramyothin, M. Hattori, K. Shiraki, Antivir. Res. 91 (2011) 154.
- [7] P. Sasivimolphan, V. Lipipun, K. Likhitwitayawuid, M. Takemoto, P. Pramyothin, M. Hattori, K. Shiraki, Antivir. Res. 84 (2009) 95.
- [8] A.L. Liu, F. Yang, M. Zhu, D. Zhou, M. Lin, S.M.Y. Lee, Y.T. Wang, G.H. Du, Planta Med. 76 (2010) 1874.
- [9] F. Qiu, K. Komatsu, K. Saito, K. Kawasaki, X. Yao, Y. Kano, Biol. Pharm. Bull. 19 (1996) 1463.
- [10] M. Mei, J.Q. Ruan, W.J. Wu, R.N. Zhou, J.P.C. Lei, H.Y. Zhao, R. Yan, Y.T. Wang, J. Agric. Food Chem. 60 (2012) 2299.
- [11] P. Charoenlarp, C. Shaipanich, S. Subhanka, P. Lakkantaporn, A. Tanunkat, Pharmacokinetics of the active constituent of Puag-haad in man, in: Symposium on Mahidol University Research and Development, ASEAN Institute Health Development, 25–29 February, Salaya, Nakhon Pathom, 1991.
- [12] H. Huang, G. Chen, Z. Lu, J. Zhang, D.A. Guo, Biomed. Chromatogr. 24 (2010) 426.
- [13] A. Tanunkat, Absorption Metabolism and Excretion of 2, 3, 4, 5 Tetrahydroxy-stilbene in Volunteers after Oral Administration of Purified Extract of Puag-Haad, Mahidol University, Salaya, NakhonPathom, Thailand, 1990.
- [14] S. Chakraborty, D. Shukla, S. Singh, Eur. J. Pharm. Biopharm. 73 (2009) 1.
- [15] G. Fricker, T. Kromp, A. Wendel, A. Blume, J. Zirkel, H. Rebmann, C. Setzer, R.O. Quinkert, F. Martin, C. Müller-Goymann, Pharm. Res. 27 (2010) 1469.
- [16] P. Li, H.M. Nielsen, A. Müllertz, Expert Opin. Drug Deliv. 9 (2012) 1289.
- [17] R.H. Müller, K. Mäder, S. Gohla, Eur. J. Pharm. Biopharm. 50 (2000) 161.
- [18] R. Tiwari, K. Pathak, Int. J. Pharm. 415 (2011) 232.
- [19] Y. Shono, H. Nishihara, Y. Matsuda, S. Furukawa, N. Okada, T. Fujita, A. Yamamoto, J. Pharm. Sci. 93 (2004) 877.

- [20] E.B. Souto, R.H. Müller, in: M. Schäfer-Korting (Ed.), *Drug Delivery Handbook of Experimental Pharmacology*, vol. 197, Springer, Berlin, 2010 (Chapter 2).
- [21] M. Üner, *Pharmazie* 61 (2006) 375.
- [22] A.J. Almeida, E. Souto, *Adv. Drug Deliv. Rev.* 59 (2007) 478.
- [23] A.R. Neves, M. Lúcio, S. Martins, J.L. Lima, S. Reis, *Int. J. Nanomed.* 8 (2013) 177.
- [24] Y. Sangsen, K. Likhitwitayawuid, B. Sritularak, K. Wiwattanawongsa, R. Wiwat-anapatapee, *Int. J. Med. Sci. Eng.* 7 (2013) 103.
- [25] P.L. Ritger, N.A. Peppas, *J. Control. Release* 5 (1987) 23.
- [26] W.F. Clark, A. Parbtani, D.J. Philbrick, B.J. Holub, M.W. Huff, *J. Am. Soc. Nephrol.* 1 (1991) 1343.
- [27] W. Mehnert, K. Mäder, *Adv. Drug Deliv. Rev.* 47 (2001) 165.
- [28] E.H. Gokce, E. Korkmaz, E. Dellera, G. Sandri, M.C. Bonferoni, O. Ozer, *Int. J. Nanomed.* 7 (2012) 1841.
- [29] C.Y. Zhuang, N. Li, M. Wang, X.N. Zhang, W.S. Pan, J.J. Peng, Y.S. Pan, X. Tang, *Int. J. Pharm.* 394 (2010) 179.
- [30] E. Roger, F. Lagarce, E. Garcion, J.P. Benoit, *J. Control. Release* 140 (2009) 174.
- [31] C.C. Chen, T.H. Tsai, Z.R. Huang, J.Y. Fang, *Eur. J. Pharm. Biopharm.* 74 (2010) 474.
- [32] B. Akbari, M. Pirhadi Tavandashti, M. Zandrahimi, *IJMSE* 8 (2011) 48.
- [33] V. Jenning, A.F. Thünemann, S.H. Gohla, *Int. J. Pharm.* 199 (2000) 167.
- [34] W. Sutananta, D.Q.M. Craig, J.M. Newton, *J. Pharm. Pharmacol.* 47 (1995) 182.
- [35] E.B. Souto, W. Mehnert, R.H. Müller, *J. Microencapsul.* 23 (2006) 417.
- [36] L.D. Hu, Q. Xing, J. Meng, C. Shang, *AAPS PharmSciTech* 11 (2010) 582.
- [37] J.K. Takemoto, R.M. Bertram, C.M. Remsberg, S.S. Sablani, N.M. Davies, 13th Canadian Society for Pharmaceutical Sciences (CSPS), *J. Pharm. Pharm. Sci.* 13 (2010) 1s.
- [38] C.W. How, R. Abdullah, R. Abbasalipourkabar, *Afr. J. Biotechnol.* 10 (2013) 1684.
- [39] C.W. Pouton, C.J.H. Porter, *Adv. Drug Deliv. Rev.* 60 (2008) 625.
- [40] P.D.P. Lundin, M. Bojrup, H. Ljusberg-Wahren, B.R. Weström, S. Lundin, *J. Pharmacol. Exp. Ther.* 282 (1997) 595.
- [41] Y.L. Lo, *J. Control. Release* 90 (2003) 37.
- [42] J.F. Marier, P. Vachon, A. Gritsas, J. Zhang, J.P. Moreau, M.P. Ducharme, *J. Pharmacol. Exp. Ther.* 302 (2002) 369.

### **PAPER 3**

Influence of surfactants in self-microemulsifying formulations on enhancing oral bioavailability of oxyresveratrol: Studies in Caco-2 cells and *in vivo*



Contents lists available at ScienceDirect

International Journal of Pharmaceutics

journal homepage: [www.elsevier.com/locate/ijpharm](http://www.elsevier.com/locate/ijpharm)

## Influence of surfactants in self-microemulsifying formulations on enhancing oral bioavailability of oxyresveratrol: Studies in Caco-2 cells and *in vivo*



Yaowaporn Sangsen<sup>a,b</sup>, Kamonthip Wiwattanawongsa<sup>b,c</sup>, Kittisak Likhitwitayawuid<sup>d</sup>, Boonchoo Sritularak<sup>d</sup>, Potchanapond Graidist<sup>e,f</sup>, Ruedeekorn Wiwattanapatapee<sup>a,b,\*</sup>

<sup>a</sup> Department of Pharmaceutical Technology, Faculty of Pharmaceutical Sciences, Prince of Songkla University, Hat-Yai, Songkhla 90112, Thailand

<sup>b</sup> Phytomedicine and Pharmaceutical Biotechnology Excellence Research Center, Faculty of Pharmaceutical Sciences, Prince of Songkla University, Hat-Yai, Songkhla 90112, Thailand

<sup>c</sup> Department of Clinical Pharmacy, Faculty of Pharmaceutical Sciences, Prince of Songkla University, Hat-Yai, Songkhla 90112, Thailand

<sup>d</sup> Department of Pharmacognosy and Pharmaceutical Botany, Faculty of Pharmaceutical Sciences, Chulalongkorn University, Bangkok 10330, Thailand

<sup>e</sup> Department of Biomedical Sciences, Faculty of Medicine, Prince of Songkla University, Hat-Yai, Songkhla 90110, Thailand

<sup>f</sup> The Excellent Research Laboratory of Cancer Molecular Biology, Prince of Songkla University, Hat-Yai, Songkhla 90110, Thailand

### ARTICLE INFO

#### Article history:

Received 31 July 2015

Received in revised form 9 November 2015

Accepted 3 December 2015

Available online 8 December 2015

#### Keywords:

Self-microemulsifying drug delivery system  
SMEDDS  
Surfactants  
Caco-2 cells  
Oral absorption  
Oxyresveratrol

### ABSTRACT

Self-microemulsifying drug delivery systems (SMEDDS) containing two types (Tween80<sup>®</sup> and Labrasol<sup>®</sup>) and two levels (low; 5% and high; 15%) of co-surfactants were formulated to evaluate the impact of surfactant phase on physical properties and oral absorption of oxyresveratrol (OXY). All formulations showed a very rapid release in the simulated gastric fluid (SGF) pH 1.2. After dilution with different media, the microemulsion droplet sizes of the Tween80<sup>®</sup>-based (~26 to 36 nm) were smaller than that of the Labrasol<sup>®</sup>-based systems (~34 to 45 nm). Both systems with high levels of surfactant increased the Caco-2 cells permeability of OXY compared to those with low levels of surfactant (1.4–1.7 folds) and the unformulated OXY (1.9–2.0 folds). It was of interest, that there was a reduction (4.4–5.3 folds) in the efflux transport of OXY from both systems compared to the unformulated OXY. The results were in good agreement with the *in vivo* absorption studies of such OXY-formulations in rats. Significantly greater values of  $C_{max}$  and  $AUC_{0-10h}$  ( $p < 0.05$ ) were obtained from the high levels of Tween80<sup>®</sup>-based ( $F_{r,0-10h}$  786.32%) compared to those from the Labrasol<sup>®</sup>-based system ( $F_{r,0-10h}$  218.32%). These findings indicate the importance of formulation variables such as type and quantity of surfactant in the SMEDDS to enhance oral drug bioavailability.

© 2015 Elsevier B.V. All rights reserved.

### 1. Introduction

Oxyresveratrol (*trans*-2,4,3',5'-tetrahydroxystilbene; OXY) is a polyphenolic compound extracted from the heartwood of the Thai traditional herb, *Artocarpus lakoocha* Roxburgh (Moraceae). It has been reported to possess many pharmacological activities: it has anti-tyrosinase activity (Kim et al., 2002), is a strong antioxidant with anti-inflammatory activity (Chung et al., 2003), has a potent

neuroprotective activity (Breuer et al., 2006), has anti-herpetic activities effective against the herpes simplex virus (HSV-1 and HSV-2) (Lipipun et al., 2011; Sasivimolphan et al., 2012) and the varicella zoster virus (VZV) (Sasivimolphan et al., 2009), it is an anti-HIV agent (Likhitwitayawuid et al., 2005) and has anti-influenza virus activities (Liu et al., 2010). For oral delivery, the bioavailability of OXY is limited because of its restricted permeability and there is an active efflux pump transport by a P-glycoprotein (P-gp) and a family of multidrug resistance proteins (MRPs) (Mei et al., 2012). In addition, it undergoes a first pass hepatic metabolism and its rapid elimination causes a short residence time in the body (Charoenlarp et al., 1991; Huang et al., 2008, 2010).

Self-microemulsifying drug delivery systems (SMEDDS) are attractive lipid-based carriers that can improve oral bioavailability of several bioactive compounds (Gursoy and Benita, 2004; Kohli

\* Corresponding author at: Department of Pharmaceutical Technology, Faculty of Pharmaceutical Sciences, Prince of Songkla University, Hat Yai, Songkhla 90112, Thailand. Fax: +66 74 428148.

E-mail addresses: [s.yaowapom@gmail.com](mailto:s.yaowapom@gmail.com) (Y. Sangsen), [kamonthip.w@psu.ac.th](mailto:kamonthip.w@psu.ac.th) (K. Wiwattanawongsa), [kittisak.l@chula.ac.th](mailto:kittisak.l@chula.ac.th) (K. Likhitwitayawuid), [boonchoo.sr@chula.ac.th](mailto:boonchoo.sr@chula.ac.th) (B. Sritularak), [gpotchan@medicine.psu.ac.th](mailto:gpotchan@medicine.psu.ac.th) (P. Graidist), [ruedeekorn.w@psu.ac.th](mailto:ruedeekorn.w@psu.ac.th) (R. Wiwattanapatapee).



et al., 2010; Sermkaew et al., 2013a; Setthacheewakul et al., 2010). Isotropic mixtures of the systems composed of oils, surfactants, and co-surfactants or co-solvents that form transparent oil in water (o/w) microemulsions after dilution with an aqueous medium such as gastrointestinal (GI) fluid under the mild agitation of the gastric movements (Gursoy and Benita, 2004). These SMEDDS, are microemulsions with droplet sizes of less than 50 nm that provide many advantages *i.e.* they are easy to prepare and scale up to commercial products, are physically stable, have increased drug solubility, and can avoid damage by acid and enzymatic degradation in the GI tract (Kohli et al., 2010).

In addition, the surfactants/co-surfactants used in these SMEDDS have promoted their effective use. The benefits of the surfactants commonly used, *i.e.* polyoxyethylene castor oil derivatives (Cremophor<sup>®</sup>) and polyethylene glycol esters (Tween<sup>®</sup> and Labrasol<sup>®</sup>), have been investigated. In particular, the surfactants including Cremophor RH40<sup>®</sup>, Tween80<sup>®</sup> and Labrasol<sup>®</sup>, have good miscibility with many oil types and stabilized the microemulsion droplets (Gursoy and Benita, 2004; Sermkaew et al., 2013a; Setthacheewakul et al., 2010). Moreover, all these three surfactants have been reported to enhance drug permeability in many ways such as by increasing transcellular permeability and especially by inhibiting the efflux transport systems (Chiu et al., 2003; Lin et al., 2007; Seljak et al., 2014; Zhang et al., 2003). Also, Labrasol<sup>®</sup> enhanced the paracellular pathway by opening tight junctions (Sha et al., 2005; Ujhelyi et al., 2012). In addition, there are other benefits of Tween80<sup>®</sup> for example, it can bypass the pre-systemic metabolism in the liver, increase lymphatic absorption (Lind et al., 2008; Prokop and Davidson, 2008; Seeballuck et al., 2004), modify drug bio-distribution and reduce drug elimination all of which result in an improved bioavailability of the oral drug (Ellis et al., 1996). Because of these many advantages, SMEDDS is an interesting approach to promote the beneficial activities of OXY. Hence a study of the effect of the surfactant phase on drug absorption will be useful for the design of effective SMEDDS formulations for OXY.

The purposes of this work were to develop SMEDDS that would enhance the oral delivery of OXY by using different types and concentrations of surfactants/co-surfactants. The influence of the surfactants used on the physical properties and the *in vitro* release of the different formulations were evaluated. Then, the effect of the surfactant-based SMEDDS on the *in vitro* toxicity and drug permeability was compared using the Caco-2 cell models. Finally, the *in vivo* absorption studies on each of the formulations was investigated and compared with the unformulated OXY.

## 2. Materials and methods

### 2.1. Materials

OXY (off-white powder >99% purity) was obtained from the Department of Pharmacognosy, Faculty of Pharmaceutical Sciences, Chulalongkorn University (Bangkok, Thailand)

(Likhitwitayawuid et al., 2005; Sritularak et al., 1998). Capryol 90<sup>®</sup> and Labrasol<sup>®</sup> were from Gattefosse (Saint-Priest, France). Cremophor RH40<sup>®</sup> was from BASF (Ludwigshafen, Germany). Tween80<sup>®</sup> was from S.Tong Chemicals Co., Ltd (Bangkok, Thailand). Hard gelatin capsules (size 00) were from Capsugel (Bangkok, Thailand). Resveratrol (>99% purity) was from Sigma-Aldrich (Saint Louis, MO, USA). Acetonitrile and methanol (HPLC grade) were from RCI Labscan (Bangkok, Thailand). All other chemicals were of analytical grade. Human epithelial colorectal adenocarcinoma cell lines (Caco-2 cells; HTB-37) were from ATCC (Virginia, USA). Modified Eagle's Medium (MEM), Fetal Bovine Serum (FBS), Hanks' Balanced Salt Solution (HBSS), sodium pyruvate (100 mM), and Penicillin (100 IU/ml)-Streptomycin (100 mg/ml) (Pen-Strep) were from Gibco<sup>®</sup>, Invitrogen (NY, USA). 3-(4,5-dimethylthiazol-2-yl)-2,5-diphenyltetrazolium bromide (MTT) was from Molecular Probes, Invitrogen (OR, USA). Phosphate Buffered Saline (PBS, pH 7.4), 2-(*N*-morpholino) ethanesulfonic acid (MES) sodium salt, and 4-(2-hydroxyethyl) piperazine-1-ethanesulfonic acid (HEPES) were from Sigma (MO, USA). Dimethylsulfoxide (DMSO) was from Amresco (OH, USA). Transwell<sup>®</sup> 6-wells plate with polycarbonate filter inserts (pores: 3.0 μm, diameters: 24 mm, area: 4.67 cm<sup>2</sup>, Transwell Type 3414) were from Costar (Corning, NY, USA).

### 2.2. Development of the different surfactant-based SMEDDS of OXY

#### 2.2.1. Preparation of OXY-SMEDDS

To study the effects of the type and amount of surfactants in the SMEDDS on the oral bioavailability of OXY, four different SMEDDS formulations were developed. Capryol 90<sup>®</sup> and Cremophor RH40<sup>®</sup> were used as the oil phase and the main surfactant in all formulations. Two sets of SMEDDS containing different types of co-surfactant, Tween80<sup>®</sup> and Labrasol<sup>®</sup>, were compared. Each co-surfactant based system was divided into two groups that included a low amount of surfactant (LS) and a high amount of surfactant (HS) group. The formulations of the LS group, contained 50% of the surfactant phase (45% Cremophor RH40<sup>®</sup> and 5% co-surfactant) and 50% Capryol 90<sup>®</sup>, were coded as LT and LL for the SMEDDS containing Tween80<sup>®</sup> and Labrasol<sup>®</sup> respectively. For the HS group, the SMEDDS formulations contained 55% of the surfactant phase (40% Cremophor RH40<sup>®</sup> and 15% co-surfactant) and 45% Capryol 90<sup>®</sup> were coded as HT and HL for the SMEDDS containing Tween80<sup>®</sup> and Labrasol<sup>®</sup> respectively. The fixed OXY amounts (40 mg/1 g SMEDDS) were then added to each formulation. Then, the dispersions were stirred continuously until homogenous solutions were achieved. The formulations were then left for 48 h at room temperature. The 900 mg of the OXY-SMEDDS formulations were manually filled into hard gelatin capsules size 00. After filling, the two-piece capsules were sealed with a gelatin solution to protect the leakage of the oily liquid from the capsule shells during storage. The filled capsules were stored in tight containers and protected from light until used. The compositions of all of the developed OXY-SMEDDS are presented in Table 1.

**Table 1**  
Compositions of the different OXY-SMEDDS formulations.

Formulation code	Composition (% w/w)			OXY amount (mg/1 g SMEDDS)	
	Co-surfactant		Capryol 90 <sup>®</sup>		
	Type	Amount			
LT	Tween80 <sup>®</sup>	5	45	50	40
HT		15	40	45	40
LL	Labrasol <sup>®</sup>	5	45	50	40
HL		15	40	45	40

### 2.2.2. Effect of the surfactant phase on the physical properties and morphology of the developed OXY-SMEDDS

**2.2.2.1. Assessment of self-microemulsification performance.** The effect of the surfactant phase on the self-microemulsification performance of the SMEDDS containing drug was assessed according to the visual grading system as described previously (Singh et al., 2009). In this study, the formulations were subjected to various diluents, for example, DI water, simulated gastric fluid (SGF, pH 1.2), transport medium (TM) pH 6.5 and 7.4. Three replicates of each formulation were prepared.

**2.2.2.2. Microemulsion droplet size and size distribution.** The effect of the surfactant phase on the droplet size and polydispersity index (PDI) of the formulations was determined after dispersion in different media in the same way as for 2.2.2.1. After 24 h of dilution (at a ratio of 1:20), the OXY-microemulsions were measured by the dynamic light scattering (DLS) technique using Zetasizer Nano ZS<sup>®</sup> (Malvern Instruments, UK). Light scattering was monitored at a 173° angle at room temperature. All measurements were performed in triplicate.

**2.2.2.3. Total drug content.** The total drug content (TDC) in different formulations was determined as follows: each OXY-SMEDDS was diluted with DI water (20-fold dilution) at room temperature. An aliquot of 1 ml of the microemulsion was dissolved by methanol and mixed for 10 min in order to facilitate complete dissolution. Then, the obtained dispersion was analyzed for OXY by the HPLC method. The TDC could be calculated by the following Eq. (1). Where  $OXY_c$  is the TDC of the OXY calculated from the experiment and  $OXY_f$  is the theoretical drug content.

$$TDC(\%) = \left( \frac{OXY_c}{OXY_f} \right) \times 100 \quad (1)$$

**2.2.2.4. Morphology as determined by transmission electron microscopy (TEM).** The morphology of the different OXY-SMEDDS was observed by TEM (JEOL Ltd., Tokyo, Japan). The OXY-SMEDDS were diluted with DI water at a ratio of 1:20. The microemulsion was stained in 2% w/v phosphotungstic acid for 10 min. TEM micrographs of the OXY-microemulsions were photographed.

### 2.2.3. Effect of the surfactant phase of the SMEDDS on the in vitro release of OXY

The release properties of the four different SMEDDS containing OXY were carried out according to two different published methods (Kang et al., 2004; Sermkaew et al., 2013a). First, one capsule filled with 900 mg of the formulation (equivalent to 36 mg OXY) was subjected to release using dissolution by the USP 30 rotating paddle apparatus (Hanson Research Corporation, USA) (Sermkaew et al., 2013a) with 900 ml of SGF pH 1.2 without pepsin at 100 rpm and a temperature of  $37.0 \pm 0.5^\circ\text{C}$ . Five milliliters of aliquot were withdrawn and replaced with fresh medium at 5, 10, 15, 30, 45, 60, 90 and 120 min. For determination of the release profile of the free drug, the release studies were carried out by the dialysis bag diffusion technique (Kang et al., 2004). Unlike the first method mentioned above, the OXY-SMEDDS capsules were filled into the dialysis bag (molecular weight cut off; MWCO 12–14 kDa) to stop penetration of the drug contained in the microemulsion form and allow only the free drug to be dissolved in the medium. The samples were analyzed using the validated HPLC. Three separate replicate studies were conducted for each of the formulations.

### 2.3. Influence of the different surfactant based SMEDDS of OXY on permeability across Caco-2 cells

#### 2.3.1. Influence of the formulations on Caco-2 cell viability

The Caco-2 cells (passage number 25–29) were grown in MEM supplemented with 20% v/v FBS, 0.1 mM sodium pyruvate, and 1% v/v Pen-Strep. The cells were maintained at  $37^\circ\text{C}$  in an atmosphere at 5%  $\text{CO}_2$  and 90% RH.

Toxicity of the OXY, different blank formulations, and different OXY-SMEDDS was assessed by the MTT test (Freshney, 2005). The MTT assay is a quantitative and rapid colorimetric method based on the cleavage of a yellow tetrazolium salt (MTT) to insoluble purple formazan crystals by the mitochondrial dehydrogenase of viable cells. The OXY powder was solubilized in a DMSO/HBSS-HEPES mixture to obtain an OXY concentration of between 25 and 200  $\mu\text{M}$ . OXY-SMEDDS were diluted with HBSS-HEPES (TM pH 7.4) to obtain equal concentrations of OXY (25–200  $\mu\text{M}$ ). The blank formulations without drug which contained the same compositions of each OXY-SMEDDS were diluted at the same dilution factor of the drug-SMEDDS by the HBSS-HEPES. The Caco-2 cells were seeded in 96-well plates at a density of  $5 \times 10^4$  cells/well and incubated for 24 h. Then, 100  $\mu\text{l}$  of the OXY samples at different concentrations were added to each well. HBSS-HEPES and 1% sodium lauryl sulfate were used as negative control and positive controls, respectively. After 24 h treatment, the samples were removed and 0.5 mg/ml of MTT solution was added to each well and then incubated for another 4 h. After removing the MTT solution, DMSO was added to dissolve the formazan crystals formed by the living cells. The absorbance of the samples was measured with a microplate reader (DTX 880 Multimode Detector, Beckman Coulter Inc., Austria) at a wavelength of 570 nm. Duplicates were tested. The percentage of cell viability was calculated relative to the measured absorbance of the negative control that represented 100% cell viability.

#### 2.3.2. Caco-2 permeability studies

A Caco-2 cell permeability study, commonly used as an *in vitro* method to predict *in vivo* absorption of the compound, was performed to help to predict the ability to transport different SMEDDS formulations of OXY across the intestinal epithelium (Yee, 1997). The *in vitro* permeability studies of four OXY-SMEDDS (LT, LL, HT and HL) were carried out according to a previous report (Sermkaew et al., 2013b). The cells were seeded at a density of 60,000 cells/cm<sup>2</sup> of a Transwell<sup>®</sup> insert, and cultured until cells were completely differentiated (about 21–23 days). The culture medium was changed every alternate day in both the donor compartment and the receiver compartment. The stock OXY solution and different OXY-SMEDDS were diluted with either transport medium (TM) pH 6.5 or pH 7.4 for apical (AP) side loading and basolateral (BL) side loading, respectively, to obtain the non-toxic concentration of OXY of 100  $\mu\text{M}$ . Prior to the experiments, the culture medium was removed. Then, warmed TM ( $37^\circ\text{C}$ ) pH 6.5 and pH 7.4, was added. The transepithelial electrical resistance (TEER) value was measured using a Millicell<sup>®</sup>-ERS Voltmeter (Millipore Corp., Bedford, MA, USA) to evaluate the integrity of the cell monolayer. The monolayers with TEER > 300  $\Omega\text{cm}^2$  were used in the transport experiments.

For the absorptive transport (AP → BL) experiment, 1.5 ml of samples in TM pH 6.5 and 2.6 ml of blank TM pH 7.4 were added to the AP side (donor compartment) and the BL side (receiver compartment), respectively. For secretive transport (BL → AP) experiments, 2.6 ml of samples in TM pH 7.4 and 1.5 ml of blank TM pH 6.5 were added to the BL side (donor compartment) and the AP side (receiver compartment), respectively. Transport studies were performed on a shaking incubator maintained at  $37^\circ\text{C}$  with a



shaking rate of 100 rpm. Sample volumes of 400  $\mu\text{l}$  and 100  $\mu\text{l}$  were removed from the receiver compartment and donor compartment, respectively, in both the absorptive transport and secretive transport experiments at various times (5, 15, 30, 45, 60, 90, 120, 150 and 180 min). The withdrawn volumes from the receiver compartment in both experiments were replaced with the same volumes of the warmed fresh TM. At the end of experiments, the cells were washed with PBS pH 7.4. After that, the cells were scrapped from the polycarbonate filters to determine an accumulation of samples in the Caco-2 cells. Then, the cells were treated by sonication at 25 °C for 10 min. After centrifugation at 3,000  $\times$  g at 10 °C for 5 min, the supernatant was collected and stored at -20 °C until analyzed. The amounts of OXY were quantified by a validated HPLC method. The cumulative drug amount that permeated through the monolayer as measured in the receiver compartment was plotted against the sampling time to yield a linear slope. The apparent permeability coefficient ( $P_{app}$ ) and the efflux ratio (ER) were calculated using the following Eqs. (2) and (3), respectively.

$$P_{app} = \frac{(dQ/dt)}{(A C_0)} \quad (2)$$

where  $dQ/dt$  is the cumulative transport rate ( $\mu\text{g/s}$ ) defined as the slope obtained by linear regression of the cumulative transported amount ( $\mu\text{g}$ ) as a function of time ( $s$ ).  $A$  is the surface area of the filter (4.67  $\text{cm}^2$  in 6-wells insert).  $C_0$  is the initial concentration of OXY on the donor compartment ( $\mu\text{g/ml}$ ).

$$ER = \frac{P_{app}(BL - AP)}{P_{app}(AP - BL)} \quad (3)$$

where  $P_{app}$  (AP-BL) is the apparent permeability coefficient for the absorptive transport and  $P_{app}$  (BL-AP) is the apparent permeability coefficient for the secretory transport (Hubatsch et al., 2007).

### 2.3.3. Quantitative determination of OXY

The quantitative determination of OXY in the transport medium was by the HPLC method using resveratrol (RES) as an internal standard. The system consisted of an Agilent HPLC system (HP 1100, Agilent, USA) with a UV detector set at 320 nm. A reverse phase column: a Vertisep pH endure C18 4.6  $\times$  250 mm, 5  $\mu\text{m}$  column and guard column (Ligand Scientific, Bangkok, Thailand) were used. Chromatographic conditions: the isocratic solvent system consisted of acetonitrile and 0.5% v/v aqueous acetic acid (27:73 v/v) with a flow rate of 1.0 ml/min and an injection volume of 50  $\mu\text{l}$ . The OXY and RES exhibited a well-defined chromatographic peak with a retention time of about 7 and 12 min, respectively (data not shown). The calibration curve for OXY was constructed by plotting concentrations versus the ratios of the peak areas of OXY and RES from three determinations. A good linearity was achieved with a correlation coefficient ( $r^2$ ) of 0.9999 over the concentration range of 0.1–10  $\mu\text{g/ml}$ . The intra-day and inter-day precision studies were obtained by three daily injections for each concentration of the spiked medium samples over a 3 day period. The intra-day precision gave the percentage relative standard deviations (%RSD) of 0.97–2.90%, whereas the % RSD of inter-day precisions ranged from 7.67% to 12.55%, respectively. The recovery percentage of the method ranged from 90.18  $\pm$  2.38–102.46  $\pm$  3.99. The limit of detection (LOD) and the lower limit of quantification (LLOQ) was 0.01 and 0.1  $\mu\text{g/ml}$  respectively. The results of the validation of the *in vitro* HPLC method showed that the determination of OXY could be performed by this validated HPLC method with an acceptable accuracy and precision.

### 2.4. Pharmacokinetics of OXY following oral administration of the OXY-SMEDDS

Male Wistar-strain rats (250–300 g) were provided by the Animal House, Faculty of Science, Prince of Songkla University. All animals received human care and laboratory experiments were approved according to the guidelines of the Animal Care and Use Committee of Prince of Songkla University (MOE 0521.11/063). They were housed and maintained under standard rodent conditions (at 24 °C, 55% RH, 12 h light-dark cycle controls). The rats had unlimited access to water but were excluded from food for 12 h before the experiment. Thirty-five rats were divided into five groups. Each group was administered orally with the OXY aqueous suspension (control group) and different OXY-SMEDDS (LT, LL, HT and HL) at an equivalent OXY dose of 180 mg/kg body weight (Huang et al., 2008; Sangsen et al., 2015). Blood samples (250  $\mu\text{l}$ ) were collected via the rat tail clipping method (Clark et al., 1991) at various times (5, 10, 15, 20, 30, 45, 60, 90, 120, 180, 240, 360, 480, and 600 min) after oral dosing, into heparinized centrifuge tubes. The samples were centrifuged at 13,000 rpm 20 °C for 5 min and the plasma samples were selected for assay. The internal standard (RES) was spiked into the plasma. Then, an equal volume of acetonitrile (1:1 v/v) was added to the plasma sample, vortexed, sonicated and allowed to stand for 5 min to precipitate the protein. The samples were centrifuged at 13,000 rpm 20 °C for 5 min. The supernatant was filtered and injected to the validated HPLC analysis. Data from these samples ( $n=7$ ) were used to plot the profiles of the OXY absorption with time.

#### 2.4.1. HPLC analysis of plasma samples

For the determination of the quantity of OXY absorbed *in vivo*, the same HPLC system as that for the *in vitro* studies was used. The spiking technique was used for validation of the HPLC method. The calibration curve was plot between the OXY concentrations versus the peak area ratios of OXY and RES from three determinations. The OXY concentration range of 0.2–10  $\mu\text{g/ml}$  showed good linearity ( $r^2=0.9994$ ). The intraday repeatability obtained by three replicates per each concentration, gave a %RSD of 1.00–2.32%. The interday precision over a 3 day period gave a %RSD of 2.23–10.26%. The % recovery of the method ranged from 88.96  $\pm$  2.20 to 100.02  $\pm$  2.34. The LOD and LLOQ was 0.02 and 0.2  $\mu\text{g/ml}$ , respectively.

#### 2.4.2. Pharmacokinetic parameters

The main pharmacokinetic parameters of the unformulated OXY and OXY in different SMEDDS formulations were carried out using the Microsoft Excel 2007 Software (Microsoft Corporation, USA). The maximum concentration ( $C_{max}$ ) and time to reach maximum concentration ( $T_{max}$ ) were obtained directly from the plasma concentration-time curves. The area under the concentration-time curve ( $AUC_{0-10h}$ ) was determined using the trapezoidal rule. The relative bioavailability over 10 h ( $F_{r,0-10h}$ ) at the same dose of OXY formulated as SMEDDS compared to the OXY suspension, was calculated following Eq. (4):

$$F_{r,0-10h} = \frac{AUC_{(0-10h)oral, formulation}}{AUC_{(0-10h)oral, suspension}} \times 100 \quad (4)$$

### 2.5. Statistical analysis

Data were expressed as mean values  $\pm$  SD. Statistical comparisons were performed by one-way ANOVA using the SPSS version 22 software. Statistical probability ( $p$ ) values of less than 0.05 were considered to be significantly different. *In vitro* study and cell culture experiments were performed in triplicate, while *in vivo* studies were evaluated in seven replicates.



### 3. Results and discussion

#### 3.1. Development of different surfactant-based SMEDDS of OXY

##### 3.1.1. Preparation of OXY-SMEDDS

According to the high solubility of OXY in oil ( $115.420 \pm 4.475$  mg/ml), Capryol 90<sup>®</sup> was used as the oily phase of the SMEDDS. For the surfactant phase, Cremophor RH40<sup>®</sup> with high solubility for OXY ( $28.83 \pm 4.55$  mg/ml) was selected as the main surfactant. Although, the Cremophor RH40<sup>®</sup> showed good ability to emulsify Capryol 90<sup>®</sup>, the use of only this surfactant produced a gel structure that required a long time for emulsification. Thus, a co-surfactant was used in combination with this surfactant. Based on the good properties for an enhanced oral absorption of drugs, two different types of co-surfactant were used, Tween80<sup>®</sup> and Labrasol<sup>®</sup> with an OXY solubility of  $20.65 \pm 0.35$  mg/ml and  $18.05 \pm 1.68$  mg/ml, respectively. When considering the concentration of the surfactant phase, high oil content was required for a high drug loading capacity and this also lead to a lower proportion of the surfactant phase. However, a high proportion of the surfactant phase allowed for good characteristics of the formulations and also improved the drug bioavailability (Sermkaew et al., 2013a; Sethacheewakul et al., 2010). To find the most suitable surfactant concentration, each system was prepared using a fixed amount of the OXY (40 mg/1 g SMEDDS) and various surfactant phase concentrations. Unfortunately, the OXY-formulations in both systems (Tween80<sup>®</sup> based and Labrasol<sup>®</sup> based) that contained >55% w/w of surfactant phase did not produce a microemulsion. This might be because of the lower solubility of the OXY in the surfactant (Cremophor RH40<sup>®</sup>) and co-surfactants (Tween80<sup>®</sup> and Labrasol<sup>®</sup>) compared to that of the oil (Capryol 90<sup>®</sup>) used in these systems. Thus, the high proportion of the surfactant phase showed a low loading capacity that resulted in precipitation of the drug during the assessment of the efficacy of the self-microemulsification. Moreover, preliminary studies had shown that only concentrations of Cremophor RH40<sup>®</sup> (40–45%) and co-surfactants (5–15%) in the formulations produced transparent microemulsions and no drug precipitation after 24 h (data not shown). Therefore, two different concentration groups including a low (LS; 5% co-surfactant + 45% Cremophor RH40<sup>®</sup>) and high surfactant phase (HS; 15% co-surfactant + 40% Cremophor RH40<sup>®</sup>) of both types of SMEDDS were compared.

##### 3.1.2. Effect of the surfactant phase on the physical properties of the developed OXY-SMEDDS

The effect of the surfactant phase on the physical properties (self-microemulsification efficiency, droplet size, PDI and TDC) of the four different formulations (LT, LL, HT and HL) of the OXY-SMEDDS, dispersed in various media were investigated. The physical characteristics of the OXY-SMEDDS are presented in Table 2. The four formulations each produced transparent microemulsions (visual grade I) from the assessment of the self-microemulsification efficiency after dilution with all of the dispersed media. The OXY did not precipitate upon dilution or

after 24 h in all diluents (data not shown). This clearly indicated that these microemulsions kept the OXY solubilized. Hence the surfactants in the SMEDDS could emulsify and stabilize the drug-oil droplets in various dispersed media and was not dependent on the surfactant type or its concentration. For the distributions of size, the impact of the different surfactant phases on PDI of the SMEDDS in various media did not differ (PDI ~0.05 to 0.13). However, the Tween80<sup>®</sup>-based system (LT and HT) had a significantly smaller droplet size (~26 to 36 nm) than the Labrasol<sup>®</sup>-based system (LL and HL; ~34 to 45 nm) after dilution with all diluents. For the Tween80<sup>®</sup>-based system, the droplet sizes obtained from the HS formulation (HT) were significantly smaller ( $p < 0.05$ ) than from the LS formulation (LT) in all diluents. This finding indicated that the surfactant phase including the type and quantity did affect the microemulsion droplet size of the SMEDDS formulations. Furthermore, the various dispersing media also influenced the droplet size of the microemulsion. For all the formulations, the droplet size was increased when the SMEDDS were dispersed in SGF pH 1.2, TM pH 6.5, and TM pH 7.4 compared to their dispersal in DI water. Based on the DLS detection technique, the additional compositions such as the electrolyte in each medium might change the Brownian motion of the droplet and redirect fluctuations of the light signals to calculate their sizes (Tscharnuter, 2000). However, the droplet size obtained from all formulations remained less than 50 nm. Meanwhile, there was no remarkable change in the total OXY content (~100% w/w) of the four formulations of the surfactant-based SMEDDS.

For the effect of SMEDDS containing various surfactant phase on their morphology, TEM micrographs (Fig. 1) revealed that there were no differences observed on the morphology of the four formulations. All microemulsions had a uniform spherical shape with no aggregation. The OXY was mainly dispersed in the hydrophobic droplets that consisted of oil and surfactants. The electron micrographs showed that the major form of the OXY was as a microemulsion affect improving of the dissolution of OXY when compared to the unformulated OXY. From the photographs, the mean diameter of the four different formulations (<50 nm) was in agreement with the result obtained from the DLS measurements.

##### 3.1.3. Effect of the surfactant phase of the SMEDDS on the in vitro release of OXY

The *in vitro* release studies from the capsules filled with OXY-SMEDDS using the dissolution apparatus was used in order to identify the amount of OXY released in both the form of the free drug and as a microemulsion. The *in vitro* OXY release profiles from four formulations in the SGF pH 1.2 without pepsin at body temperature (37 °C) are shown in Fig. 2. All of the four formulations showed a rapid release of OXY and reached 80% w/w within 10 min so the different surfactant phase of the SMEDDS had no effect on the *in vitro* release of OXY. To evaluate the main release form of the OXY the release study of only the free drug was carried out by the dialysis bag method. The microemulsion containing drug was trapped in the bag and allowed only free OXY to be released into

Table 2

Effect of the surfactant phase on the droplet size, size distribution and the total drug content of the different OXY-SMEDDS. All values are presented as mean values  $\pm$  SD ( $n = 3$ ).  $p < 0.05$ , in comparison with the LT (\*) and HT (\*\*) in the same diluent.

Code	Droplet size (nm $\pm$ SD)				PDI $\pm$ SD				Total drug content (%)
	Water	SGF pH 1.2	TM pH 6.5	TM pH 7.4	Water	SGF pH 1.2	TM pH 6.5	TM pH 7.4	
LT	31.7 $\pm$ 0.6**	34.7 $\pm$ 0.1**	36.1 $\pm$ 0.1**	36.2 $\pm$ 0.1**	0.07 $\pm$ 0.01	0.06 $\pm$ 0.01	0.07 $\pm$ 0.01	0.06 $\pm$ 0.00	100.2 $\pm$ 1.0
HT	26.6 $\pm$ 0.1*	31.4 $\pm$ 0.2*	32.2 $\pm$ 0.1*	32.4 $\pm$ 0.2*	0.07 $\pm$ 0.00	0.08 $\pm$ 0.01	0.09 $\pm$ 0.01	0.08 $\pm$ 0.01	101.4 $\pm$ 1.2
LL	36.6 $\pm$ 0.4***	40.6 $\pm$ 0.2***	41.0 $\pm$ 0.1***	41.5 $\pm$ 0.0***	0.08 $\pm$ 0.02	0.07 $\pm$ 0.01	0.08 $\pm$ 0.00	0.09 $\pm$ 0.01	101.4 $\pm$ 1.7
HL	34.1 $\pm$ 0.2***	42.1 $\pm$ 0.2***	43.8 $\pm$ 0.4***	44.9 $\pm$ 0.2***	0.10 $\pm$ 0.01	0.10 $\pm$ 0.01	0.11 $\pm$ 0.01	0.13 $\pm$ 0.00	102.3 $\pm$ 0.5

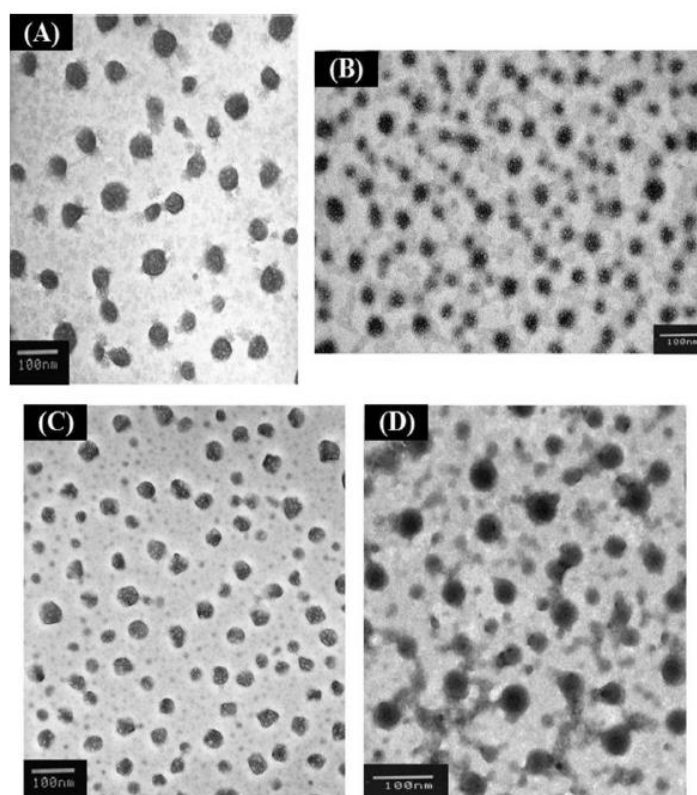


Fig. 1. TEM micrographs of the OXY-SMEDDS formulations; (A) LT, (B) HT, (C) LL, (D) HL ( $\times 50K$ ). Bar = 100 nm.

the dissolution medium. The release profiles showed that there was less than 6% of the cumulative % of OXY released from all formulations up to 2 h. These results implied that the major released content of OXY was in the microemulsion form. These forms entrapped the OXY and protected it from the strong environment of the stomach so it could subsequently reach its absorption site at the small intestine.

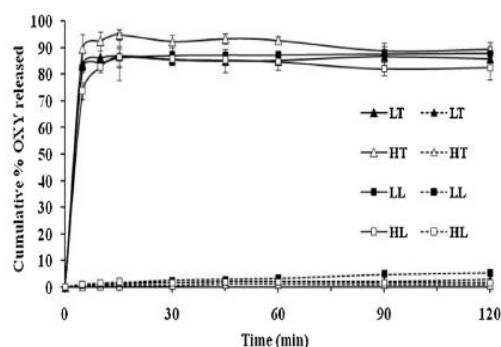


Fig. 2. The dissolution profiles of OXY from the capsule (dark lines) and the dialysis bag (dot line) filled with the SMEDDS formulations in simulated gastric fluid (SGF, pH 1.2) without pepsin. Data are represented by a mean  $\pm$  SD ( $n = 3$ ).

### 3.2. Influence of different surfactant-based SMEDDS on the permeability of OXY across the Caco-2 cells

#### 3.2.1. Influence on the viability of Caco-2 cells

To obtain an optimal OXY concentration for the permeability study, a cytotoxicity study using the MTT assay was used to evaluate the viability of the Caco-2 cells. From Fig. 3, almost 100% cell viability was obtained over the pure OXY concentrations from 25 to 200  $\mu$ M after incubation for 24 h. While the OXY-SMEDDS and blank formulations yielded greater than 80% viability but less than those from the unformulated OXY. The results demonstrated that some compositions of SMEDDS formulations were toxic to Caco-2 cells. In addition, the formulations of both the Tween80<sup>®</sup> and Labrasol<sup>®</sup>-based systems were compatible to Caco-2 intestinal cells up to the same OXY concentration of 100  $\mu$ M. Although, there was an increase of 5% of the surfactant proportion in both systems (50% and 55% of LS and HS groups, respectively), toxicity to the cells was not observed in the OXY concentration range of 25–100  $\mu$ M. Therefore, the OXY concentration in SMEDDS formulations should be not more than 100  $\mu$ M, to be considered as a nontoxic concentration for the transport study.

#### 3.2.2. Caco-2 permeability studies

The TEER values, measured before the transport experiments, were  $>300 \Omega\text{cm}^2$ , to indicate that the caco-2 cell monolayers were integral. From the bidirectional studies, the  $P_{app}$  and efflux ratio (ER) of the unformulated OXY and OXY formulated as SMEDDS are shown in Fig. 4 and Table 3. The ER of the OXY was more than 1 (ER 5.02), as a consequence of the higher  $P_{app}$  of OXY in the secretory



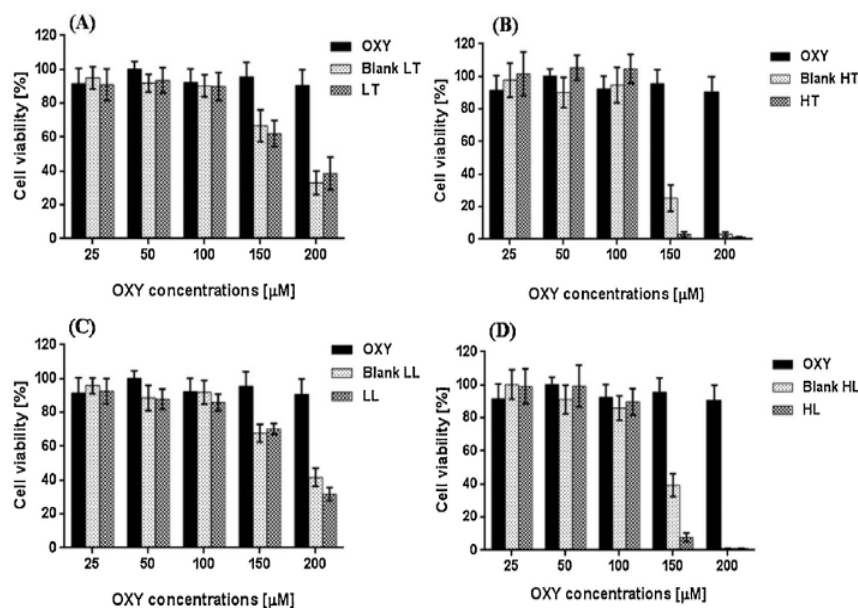


Fig. 3. The percentage of Caco-2 cell viability to different concentrations of OXY, blank SMEDDS and OXY-SMEDDS; (A) LT, (B) HT, (C) LL, (D) HL, (n=8), duplications.

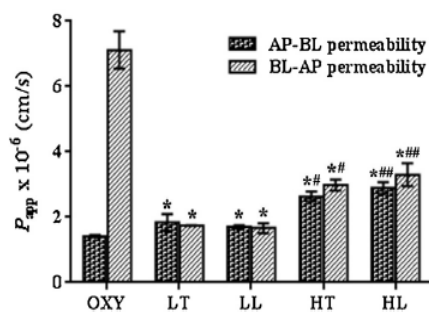


Fig. 4. Bidirectional transport across the Caco-2 monolayers of OXY and different OXY-SMEDDS. The data are presented as the apparent permeability coefficients ( $P_{app}$ ) in the absorptive (AP-BL) and the secretory directions (BL-AP).  $p < 0.05$ , comparison with OXY (\*); LT (#); LL (##) at the equivalent dose of OXY (100  $\mu\text{M}$ ).

direction ( $P_{app} 7.12 \pm 0.57 \times 10^{-6} \text{ cm/s}$ ) than the absorptive direction ( $P_{app} 1.42 \pm 0.04 \times 10^{-6} \text{ cm/s}$ ). This indicated that OXY might be a substrate for the efflux transporters. This result was in agreement with the previous reports that OXY could be classified as an intermediate permeability substance with  $P_{app}$  values below  $1 \times 10^{-5} \text{ cm/s}$  (Kogan et al., 2008) and involved the efflux transporters (P-gp and MRPs-mediated) (Mei et al., 2012). For the

absorptive transport (AP  $\rightarrow$  BL transport), the  $P_{app}$  values for the OXY-SMEDDS formulations were significantly greater than for the unformulated OXY (1.2–2.0 fold) ( $p < 0.05$ ). Meanwhile, the secretory  $P_{app}$  value of those formulations were significantly decreased compared to the unformulated OXY ( $p < 0.05$ ) and as a consequence this led to a 5-fold reduction of the efflux ratio (ER 0.94–1.14). This could imply that the SMEDDS formulated OXY enhanced the membrane permeability of OXY and inhibited the efflux pump. Moreover, the OXY entrapped in the SMEDDS in the HS group (HT and HL) exhibited a better permeation across the Caco-2 monolayers (1.4–1.7 folds) than for the LS group (LT and LL) ( $p < 0.05$ ). However, a similar absorptive and secretory permeability was obtained from either the Tween80<sup>®</sup>-based or the Labrasol<sup>®</sup>-based systems, at the same concentrations (Fig. 4). Various mechanisms for the enhanced *in vitro* drug permeability of the microemulsion that contained a high amount of surfactant (HT formulation) have been reported. For example, increased solubilizing capability of the drug, decreased degradation in the GI tract, stabilization of the small droplets, the high dispersibility of the nano-sized droplets that extended the contact time at the absorption side, endocytotic internalization of the microemulsion followed by intracellular release of the drug and increased transcellular pathway (Lin et al., 2007; Sha et al., 2005; Kogan et al., 2008). In addition, other mechanisms were also deduced, such as the reduction of the efflux by the surfactant used (Tween80<sup>®</sup>) in the SMEDDS, and tight junction opening to move

Table 3

The accumulation in the Caco-2 cells (%) and efflux ratio of OXY from different SMEDDS formulation compared to the unformulated OXY. The values are presented as mean values  $\pm$  SD (n=3).  $p < 0.05$ , in comparison with the unformulated OXY (\*).

Formulation	% OXY accumulation in cells		Efflux ratio; $P_{app}$ (BL-AP)/ $P_{app}$ (AP-BL)
	AP-BL	BL-AP	
OXY	0.69 $\pm$ 0.07	1.34 $\pm$ 0.11	5.02
LT	0.49 $\pm$ 0.06	0.50 $\pm$ 0.04	0.94*
LL	3.22 $\pm$ 0.65	0.42 $\pm$ 0.05	0.98*
HT	1.59 $\pm$ 0.58	1.12 $\pm$ 0.09	1.13*
HL	3.01 $\pm$ 0.16	1.88 $\pm$ 0.22	1.14*

the intact microemulsion droplets through paracellular pathway (Rege et al., 2002; Ujhelyi et al., 2012; Zhang et al., 2003). Rege and colleague reported inhibiting property of Tween80<sup>®</sup> on P-gp, located at BL side of the intestinal monolayer, such that increased absorptive and decreased secretory permeability of rhodamine 123 was observed. This inhibition related to the alteration of the membrane fluidity of lipid bilayers. Furthermore, it has been shown that polyethylene glycol including Tween80<sup>®</sup> and Labrasol<sup>®</sup> used in SMEDDS were able to significantly increase paracellular transport of Lucifer yellow (Ujhelyi et al., 2012). Nevertheless, more studies will be required to identify the absorption mechanism for the developed SMEDDS formulations.

In addition, all the developed SMEDDS showed that only trivial amounts of OXY were trapped in the Caco-2 cells (Table 3). This investigation indicated that the *in vitro* intestinal permeability of OXY was clearly improved by the developed SMEDDS. However, other pharmacokinetic parameters such as drug distribution, metabolism and elimination could not be eliminated by this experimental approach. Therefore, further *in vivo* absorption studies will be required in order to obtain this pharmacokinetic data to confirm the full potential of these developed formulations.

### 3.3. Influences of different surfactant-based SMEDDS on the *in vivo* absorption of OXY

The *in vivo* study was carried out to examine the effect of the surfactant on the absorption of OXY-SMEDDS after oral administration in rats. Plasma concentration-time profiles of the different OXY formulated compared to the unformulated OXY, are shown in Fig. 5. The pharmacokinetic parameters in rats receiving 180 mg/kg

OXY either in aqueous suspensions or various SMEDDS formulations, are summarized in Table 4. All the developed SMEDDS showed a significantly higher AUC<sub>0–10h</sub> for OXY than for the unformulated OXY ( $p < 0.05$ ), however, only the Tween80<sup>®</sup>-based formulations (LT and HT) showed a significantly ( $p < 0.05$ ) higher  $C_{max}$  than the unformulated OXY ( $C_{max}$   $0.66 \pm 0.08 \mu\text{g/ml}$ ). Furthermore, the  $T_{max}$  of the OXY from the SMEDDS formulations was comparable to those from the unformulated OXY (10 min). For the Labrasol<sup>®</sup>-based system, the HS formulation (HL;  $F_r$  218.32%) had a significantly higher AUC<sub>0–10h</sub> ( $p < 0.05$ ) than the LS formulation (LL;  $F_r$  137.98%), although there was no remarkable differences noticed in  $C_{max}$  between these two formulations (Fig. 5B and Table 4). Likewise, the increase in the surfactant phase of the Tween80<sup>®</sup>-based system significantly improved the oral absorption of OXY according to the significantly greater ( $p < 0.05$ )  $C_{max}$  (2.5 folds) and AUC<sub>0–10h</sub> (4.3 folds) of the HT formulations than those of the LT (Fig. 5A and Table 4). It was notable, that the increased proportions of Tween80<sup>®</sup> and Labrasol<sup>®</sup>, and the decreased Cremophor RH40<sup>®</sup> concentrations in the HS group, could be one way to enhance the oral absorption of OXY. The part of results correlated with the enhanced Caco-2 cell permeability data of these SMEDDS formulations. In Fig. 5C and D, the effect of types of co-surfactant used on the OXY absorption *in vivo* was noticed. As in Table 4, at the same concentrations, Tween 80<sup>®</sup>-based system (both LT and HT) yielded a significantly greater  $C_{max}$  (1.5–2.7 folds) ( $p < 0.05$ ) and AUC<sub>0–10h</sub> (1.3–3.6 folds) for OXY than those of the Labrasol<sup>®</sup>-based system (LL and HL). On the contrary, there were no differences found between the *in vitro* permeability data of the OXY from such different systems in this study. Sometimes *in vitro* data could not predict *in vivo* data, especially for those compounds

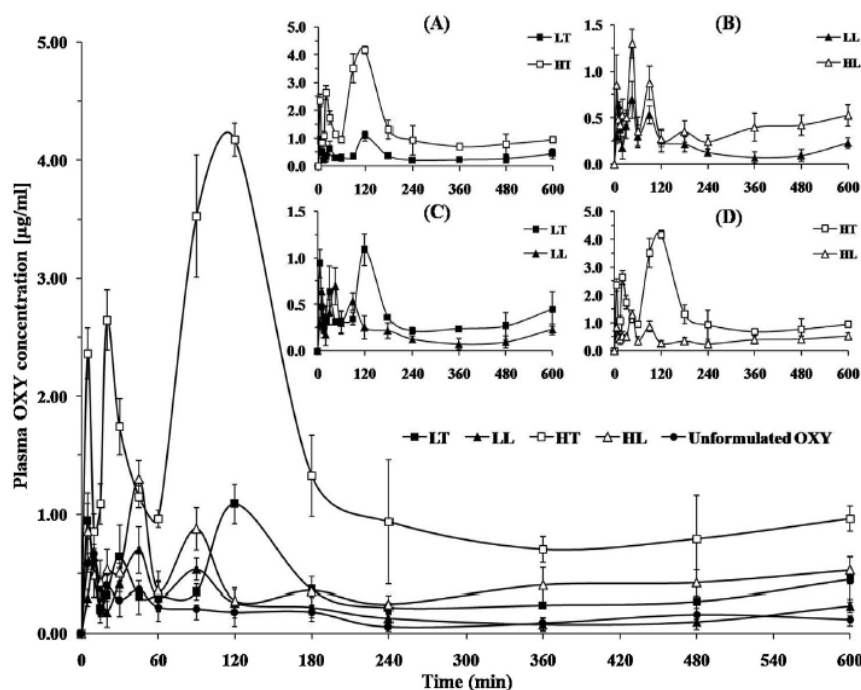


Fig. 5. Plasma concentrations vs. time profiles after the oral administration of OXY formulated as SMEDDS and unformulated OXY after dosing with OXY of 180 mg/kg. Comparison of different surfactant concentrations of SMEDDS; low LT and high HT (A), and low LL and high HL (B), for Tween80<sup>®</sup>-based (T) and Labrasol<sup>®</sup>-based (L) systems, respectively. Comparison of different surfactant types of SMEDDS; Labrasol<sup>®</sup>-based LT and LL (C), and Tween80<sup>®</sup>-based HT and HL (D), for low (L) and high (H) concentrations, respectively. All values reported are mean values  $\pm$ SD ( $n = 7$ ).

**Table 4**

Pharmacokinetics data of OXY after the oral administration of different SMEDDS formulations and an unformulated OXY (equivalent to 180 mg/kg of OXY). The values are presented as mean values  $\pm$  SD ( $n=7$ ),  $p < 0.05$ , in comparison with the unformulated OXY (\*); LT (\*\*); LL (\*\*\*) ; HL (#).

Parameters	$C_{max}$ ( $\mu\text{g/ml}$ )	$T_{max}$ (min)	$AUC_{0-10h}$ (ng h/ml)	$F_{0-10h}$ (%)
Unformulated OXY	$0.66 \pm 0.08$	10	$1,897.34 \pm 220.13$	100
LT	$0.94 \pm 0.15^{***}$	5	$3,460.37 \pm 188.39^{***}$	182.38
LL	$0.64 \pm 0.04$	10	$2,617.86 \pm 360.25^*$	137.98
HT	$2.36 \pm 0.22^{**,*\#}$	5	$14,919.16 \pm 522.00^{**,*\#}$	786.32
HL	$0.86 \pm 0.32$	5	$4,142.33 \pm 45.32^{***}$	218.32

with low bioavailability and complicated absorption mechanism involved. This disparate phenomenon obtained from the absorption experiment *in vitro* and *in vivo*, therefore, predicted that permeation of the intestine wall was not the determinant of the improved bioavailability of OXY offered by the SMEDDS systems. Significant oral bioavailability improvement of the OXY-SMEDDS might result from several reasons including the optimized physicochemical characteristics, the increase of the *in vitro* permeability and also pharmacokinetics. The superior enhancement of oral absorption by the Tween80<sup>®</sup>-based system could be explained by the effective stabilized and significantly reduced droplet size of microemulsion in all diluents as in Table 2. Then, it could bypass the first pass hepatic metabolism *via* the lymphatic pathway (Prokop and Davidson, 2008). This phenomenon was promoted by increased triglyceride secretion in the mesenteric lymph and the inhibitory activity on the efflux transport of the Tween80<sup>®</sup> that resulted in an increased lymphatic absorption of the drug (Lind et al., 2008; Seeballuck et al., 2004). Lind et al. (2008) suggested the Tween80<sup>®</sup> as a lymphotropic vehicle for lipid-based formulations. It could enhance halofantrine transport to the lymphatic system and the systemic blood circulation, compared to those of halofantrine in triglyceride *via* the chylomicron flow blocking rat model using cycloheximide. Furthermore, Tween80<sup>®</sup> inhibited the elimination of the drug from the rat liver which showed intermediate effects on the distribution volume and its total clearance and elimination half-life (Ellis et al., 1996). This could also explain the minimization of the rapid elimination of OXY that resulted in maintaining a longer resident time for the drug in the blood circulation. Thus, the SMEDDS formulation (HT) yielded the greatest improved in the oral bioavailability of OXY ( $F_r$  786.32%) among other formulations and unformulated OXY. The results of our work agreed well to other investigations in promoting oral absorption by utilization of the optimum quantity of the Tween80<sup>®</sup>. Zhao et al. (2010) successfully developed a self-nanoemulsifying drug delivery system (SNEDDS) containing Tween80<sup>®</sup> (40.5% w/w) for the oral delivery of Zedoary turmeric oil (ZTO). The developed formulation improved stability of the active compound, also enhanced 1.7-fold and 2.5-fold, respectively, the AUC and  $C_{max}$  of the bioactive marker after oral administration in rats ( $F_r$  173.5%), had been revealed. As a result of our study, the HT that contained the highest amount of surfactants especially Tween80<sup>®</sup> was the optimal SMEDDS formulation to enhance the oral bioavailability of OXY.

It was of interest, that the multiple peak patterns of the plasma profile that are represented by the enterohepatic recycling (EHC) of the absorbed OXY was also observed in all the OXY-SMEDDS profiles. Moreover, the similarity of the pattern of the SMEDDS containing the same co-surfactant was observed. The persistence of the EHC prolonged the exposure time of the OXY in the body (Gao et al., 2014). However, more studies such as bile duct or duodenum cannulation to confirm this phenomenon should be further investigated (Marier et al., 2002). These findings have indicated the advantages of the SMEDDS formulation to enhance the bioavailability of the orally delivered OXY. However, further

studies should be considered to identify the mechanism for this oral improvement by these different SMEDDS.

#### 4. Conclusions

OXY formulated as self-microemulsifying drug delivery systems (SMEDDS) were successfully developed. The high concentration of surfactant used in the system affectively reduced the microemulsion size in different media, enhanced *in vitro* OXY permeability and reduced efflux mechanisms. Moreover, the co-surfactant types (Tween80<sup>®</sup> and Labrasol<sup>®</sup>) of SMEDDS also influenced the droplet size and increased the pharmacokinetic properties of OXY, while retaining the intact EHC pattern of the OXY *in vivo*. According to the improved oral bioavailability of OXY, the use of SMEDDS is a potential approach for the oral delivery of OXY.

#### Acknowledgements

Financial support was granted by the Thailand Research Fund (BRG 5580004) and the Faculty of Pharmaceutical Sciences, Prince of Songkla University, Thailand. We also thank Dr. Brian Hodgson for assistance with the English.

#### References

- Breuer, C., Wolf, G., Andrabi, S.A., Lorenz, P., Hom, T.F.W., 2006. Blood-brain barrier permeability to the neuroprotectant oxyresveratrol. *Neurosci. Lett.* 393, 113–118.
- Charoenlarp, P., Shaijanich, C., Subhanka, S., Lakkantinaporn, P., Tanunkat, A., 1991. Pharmacokinetics of the active constituent of Puag-haad in man. Symposium on Mahidol University Research and Development, ASEAN Institute Health Development, Salaya, Nakhon Pathom, 25–29 February.
- Chiu, Y.Y., Higaki, K., Neudeck, B.L., Bameett, J.L., Welage, L.S., Amidon, G.L., 2003. Human jejunal permeability of cyclosporin A: influence of surfactants on P-glycoprotein efflux in Caco-2 cells. *Pharm. Res.* 20, 749–756.
- Chung, K.O., Kim, B.Y., Lee, M.H., Kim, Y.R., Chung, H.Y., Park, J.H., Moon, J.O., 2003. *In-vitro* and *in-vivo* anti-inflammatory effect of oxyresveratrol from *Morus alba* L. *J. Pharm. Pharmacol.* 55, 1695–1700.
- Clark, W.F., Parbtani, A., Philbrick, D.J., Holub, B.J., Huff, M.W., 1991. Chronic effects of omega-3 fatty acids (fish oil) in a rat 5/6 renal ablation model. *J. Am. Soc. Nephrol.* 1, 1343–1353.
- Ellis, A.C., Crinis, N.A., Webster, L.K., 1996. Inhibition of etoposide elimination in the isolated perfused rat liver by Cremophor EL and Tween 80. *Cancer Chemother. Pharmacol.* 38, 81–87.
- Freshney, R.I., 2005. *Culture of Animal Cells: A Manual of Basic Technique*, fifth ed. A John Wiley & Sons, Inc., New Jersey.
- Gao, Y., Shao, J., Jiang, Z., Chen, J., Gu, S., Yu, S., Zheng, K., Jia, L., 2014. Drug enterohepatic circulation and disposition: constituents of systems pharmacokinetics. *Drug Discov. Today* 19, 326–340.
- Gursoy, R.N., Benita, S., 2004. Self-emulsifying drug delivery systems (SEDDS) for improved oral bioavailability of lipophilic drugs. *Biomed. Pharmacother.* 58, 173–182.
- Huang, H., Chena, G., Lua, Z., Zhang, J., Guo, D.A., 2010. Identification of seven metabolites of oxyresveratrol in rat urine and bile using liquid chromatography/tandem mass spectrometry. *Biomed. Chromatogr.* 24, 426–432.
- Huang, H., Zhang, J., Chen, G., Lu, Z., Wang, X., Sha, N., Shao, B., Li, P., Guo, D., 2008. High performance liquid chromatographic method for the determination and pharmacokinetic studies of oxyresveratrol and resveratrol in rat plasma after oral administration of Smilax china extract. *Biomed. Chromatogr.* 22, 421–427.
- Hubatsch, I., Ragnarsson, E.G.E., Artursson, P., 2007. Determination of drug permeability and prediction of drug absorption in Caco-2 monolayers. *Nat. Protoc.* 2, 2111–2119.



- Kang, B.K., Lee, J.S., Chon, S.K., Jeong, S.Y., Yuk, S.H., Khang, G., Lee, H.B., Cho, S.H., 2004. Development of self-microemulsifying drug delivery systems (SMEDDS) for oral bioavailability enhancement of simvastatin in beagle dogs. *Int. J. Pharm.* 274, 65–73.
- Kim, Y.M., Yun, J., Lee, C.K., Lee, H., Min, K.R., Kim, Y., 2002. Oxyresveratrol and hydroxystilbene compounds. *J. Biol. Chem.* 277, 16340–16344.
- Kogan, A., Kesselman, E., Danino, D., Asenin, A., Garti, N., 2008. Viability and permeability across Caco-2 cells of CBZ solubilized in fully dilutable microemulsions. *Colloids Surf. B*, 66, 1–12.
- Kohli, K., Chopra, S., Dhar, D., Arora, S., Khar, R.K., 2010. Self-emulsifying drug delivery systems: an approach to enhance oral bioavailability. *Drug Discov. Today* 15, 958–965.
- Likhitwitayawuid, K., Sritularak, B., Benchanak, K., Lipipun, V., Mathew, J., Schinazi, R.F., 2005. Phenolics with antiviral activity from *Millettia erythrocalyx* and *Artocarpus lakoocha*. *Nat. Prod. Res.* 19, 177–182.
- Lin, Y., Shen, Q., Katsumi, H., Okada, N., Fujita, T., Jiang, X., Yamamoto, A., 2007. Effects of Labrasol and other pharmaceutical excipients on the intestinal transport and absorption of rhodamine123, a P-glycoprotein substrate, in rats. *Biol. Pharm. Bull.* 30, 1301–1307.
- Lind, M.L., Jacobsen, J., Holm, R., Müllertz, A., 2008. Intestinal lymphatic transport of halofantrine in rats assessed using a chylomicron flow blocking approach: the influence of polysorbate 60 and 80. *Eur. J. Pharm. Sci.* 35, 211–218.
- Lipipun, V., Sasivimolphan, P., Yoshida, Y., Daikoku, T., Sritularak, B., Ritthidej, G., Likhitwitayawuid, K., Pramyothin, P., Hattori, M., Shiraki, K., 2011. Topical cream-based oxyresveratrol in the treatment of cutaneous HSV-1 infection in mice. *Antivir. Res.* 91, 154–160.
- Liu, A.L., Yang, F., Zhu, M., Zhou, D., Lin, M., Lee, S.M., Wang, Y.T., Du, G.H., 2010. *In vitro* anti-influenza viral activities of stilbenoids from the Lianas of *Gnetum pendulum*. *Planta Med.* 76, 1874–1876.
- Marier, J.F., Vachon, P., Gritsas, A., Zhang, J., Moreau, J.P., Ducharme, M.P., 2002. Metabolism and disposition of resveratrol in rats: extent of absorption, glucuronidation, and enterohepatic recirculation evidenced by a linked-rat model. *J. Pharmacol. Exp. Ther.* 302, 369–373.
- Mei, M., Ruan, J.Q., Wu, W.J., Zhou, R.N., Lei, J.P.C., Zhao, H.Y., Yan, R., Wang, Y.T., 2012. *In vitro* pharmacokinetic characterization of Mulberroside A, the main polyhydroxylated stilbene in mulberry (*Morus alba* L.), and its bacterial metabolite oxyresveratrol in traditional oral use. *J. Agric. Food Chem.* 60, 2299–2308.
- Prokop, A., Davidson, J.M., 2008. Nanovehicular intracellular delivery systems. *J. Pharm. Sci.* 97, 3518–3590.
- Rege, B.D., Kao, J.P.Y., Polli, J.E., 2002. Effects of nonionic surfactants on membrane transporters in Caco-2 cell monolayers. *Eur. J. Pharm. Sci.* 16, 237–246.
- Sangsen, Y., Wiwattanawongsa, K., Likhitwitayawuid, K., Sritularak, B., Wiwattanapatapee, R., 2015. Modification of oral absorption of oxyresveratrol using lipid based nanoparticles. *Colloids Surf. B* 131, 182–190.
- Sasivimolphan, P., Lipipun, V., Likhitwitayawuid, K., Takemoto, M., Pramyothin, P., Hattori, M., Shiraki, K., 2009. Inhibitory activity of oxyresveratrol on wild-type and drug-resistant varicella-zoster virus replication *in vitro*. *Antivir. Res.* 84, 95–97.
- Sasivimolphan, P., Lipipun, V., Ritthidej, G., Chitphet, K., Yoshida, Y., Daikoku, T., Sritularak, B., Likhitwitayawuid, K., Pramyothin, P., Hattori, M., Shiraki, K., 2012. Microemulsion-based oxyresveratrol for topical treatment of herpes simplex virus (HSV) infection: physicochemical properties and efficacy in cutaneous HSV-1 infection in mice. *AAPS PharmSciTech* 13, 1266–1275.
- Seeballuck, F., Lawless, E., Ashford, M.B., O'Driscoll, C.M., 2004. Stimulation of triglyceride-rich lipoprotein secretion by polysorbate 80: *In vitro* and *in vivo* correlation using Caco-2 cells and a cannulated rat intestinal lymphatic model. *Pharm. Res.* 21, 2320–2326.
- Seljak, K.B., Berginc, K., Trontelj, J., Zvonar, A., Kristl, A., Gašperlin, M., 2014. A self-microemulsifying drug delivery system to overcome intestinal resveratrol toxicity and presystemic metabolism. *J. Pharm. Sci.* 103, 3491–3500.
- Sermkaew, N., Ketjinda, W., Boonme, P., Phadoongsombut, N., Wiwattanapatapee, R., 2013a. Liquid and solid self-microemulsifying drug delivery systems for improving the oral bioavailability of andrographolide from a crude extract of *Andrographis paniculata*. *Eur. J. Pharm. Sci.* 50, 459–466.
- Sermkaew, N., Wiwattanawongsa, K., Ketjinda, W., Wiwattanapatapee, R., 2013b. Development, characterization and permeability assessment based on Caco-2 monolayers of self-microemulsifying floating tablets of tetrahydrocurcumin. *AAPS PharmSciTech* 14, 321–331.
- Setthacheewakul, S., Mahattanadul, S., Phadoongsombut, N., Pichayakorn, W., Wiwattanapatapee, R., 2010. Development and evaluation of self-microemulsifying liquid and pellet formulations of curcumin, and absorption studies in rats. *Eur. J. Pharm. Biopharm.* 76, 475–485.
- Sha, X., Yan, G., Wu, Y., Li, J., Fang, X., 2005. Effect of self-microemulsifying drug delivery systems containing Labrasol on tight junctions in Caco-2 cells. *Eur. J. Pharm. Sci.* 24, 477–486.
- Singh, A.K., Chaurasiya, A., Awasthi, A., Mishra, G., Asati, D., Khar, R.K., Mukherjee, R., 2009. Oral bioavailability enhancement of exemestane from self-microemulsifying drug delivery system (SMEDDS). *AAPS PharmSciTech* 10, 906–916.
- Sritularak, B., De-Eknamkul, W., Likhitwitayawuid, K., 1998. Tyrosinase inhibitors from *Artocarpus lakoocha*. *Thai J. Pharm. Sci.* 22, 149–155.
- Tschamuter, W., 2000. Photon correlation spectroscopy in particle sizing. In: Meyers, R.A. (Ed.), *Encyclopedia of Analytical Chemistry*. A John Wiley & Sons, Inc., Chichester, pp. 5469–5485.
- Ujhelyi, Z., Fenyvesi, F., Váradi, J., Fehér, P., Kiss, T., Veszelka, S., Deli, M., Vecsernyés, M., Bácskay, I., 2012. Evaluation of cytotoxicity of surfactants used in self-micro emulsifying drug delivery systems and their effects on paracellular transport in Caco-2 cell monolayer. *Eur. J. Pharm. Sci.* 47, 564–573.
- Yee, S., 1997. *In vitro* permeability across Caco-2 cells (colonic) can predict *in vivo* (small intestinal) absorption in man—fact or myth. *Pharm. Res.* 14, 763–766.
- Zhang, H., Yao, M., Morrison, R.A., Chong, S., 2003. Commonly used surfactant, Tween 80, improves absorption of P-glycoprotein substrate, digoxin, in rats. *Arch. Pharm. Res.* 26, 768–772.
- Zhao, Y., Wang, C., Chow, A.H.L., Ren, K., Gong, T., Zhang, Z., Zheng, Y., 2010. Self-nanoemulsifying drug delivery system (SNEDDS) for oral delivery of Zedoary essential oil: formulation and bioavailability studies. *Int. J. Pharm.* 383, 170–177.

**PAPER 4**

Comparisons between a self-microemulsifying system and lipid nanoparticles  
of oxyresveratrol on the physicochemical properties and Caco-2 cells  
permeability

(Submitted for publication)

**Comparisons between a self-microemulsifying system and lipid nanoparticles of oxyresveratrol on the physicochemical properties and Caco-2 cells permeability**

Yaowaporn Sangsen<sup>1,2</sup>, Ruedeekorn Wiwattanapatapee<sup>\*1,2</sup>, Kamonthip Wiwattanawongsa<sup>2,3</sup>, Kittisak Likhitwitayawuid<sup>4</sup> and Boonchoo Sritularak<sup>4</sup>

<sup>1</sup>*Department of Pharmaceutical Technology, Faculty of Pharmaceutical Sciences, Prince of Songkla University, Hat-Yai, Songkhla 90112, Thailand;*

<sup>2</sup>*Phytomedicine and Pharmaceutical Biotechnology Excellence Research Center, Faculty of Pharmaceutical Sciences, Prince of Songkla University, Hat-Yai, Songkhla 90112, Thailand;*

<sup>3</sup>*Department of Clinical Pharmacy, Faculty of Pharmaceutical Sciences, Prince of Songkla University, Hat-Yai, Songkhla 90112, Thailand;*

<sup>4</sup>*Department of Pharmacognosy and Pharmaceutical Botany, Faculty of Pharmaceutical Sciences, Chulalongkorn University, Bangkok 10330, Thailand*

\* Corresponding author: Ruedeekorn Wiwattanapatapee

Department of Pharmaceutical Technology, Faculty of Pharmaceutical Sciences, Prince of Songkla University, Hat Yai, Songkhla 90112, Thailand

Fax: 66 074 428148 Phone: 66 89 732 8989

E-mail: ruedeekorn.w@psu.ac.th



**Abstract:** The lipid-based formulations that included an oily self-microemulsifying drug delivery system (SMEDDS), solid lipid nanoparticles (SLN) and nanostructured lipid carriers (NLC) were developed for the oral delivery of oxyresveratrol (OXY). Each system was successfully formulated using different optimized compositions and methods. The developed liquid formulations looked different the yellowish oily SMEDDS and the low viscous suspensions of SLN and NLC. The physical properties and stability of the different systems were compared. The non-aqueous SMEDDS had about a 13-folds higher drug loading than the lipid nanoparticles. The particle sizes ( $26.94 \pm 0.08$  nm) of OXY-SMEDDS were significantly smaller than that of the NLC and SLN ( $p < 0.05$ ). Also, a narrow size distribution of the SMEDDS (PDI,  $0.073 \pm 0.010$ ) was obtained compared to the lipid nanoparticles (PDI, 0.2-0.3). After three months, the SMEDDS seemed to be less stable than the SLN and NLC at normal storage conditions according to the decrease of the total content of OXY. By using the MTT assay, the OXY-SMEDDS showed a 4-fold greater toxicity on the Caco-2 cells than the SLN and NLC containing OXY. At the non-toxic concentration of 100  $\mu$ M of OXY, the SMEDDS system and the lipid nanoparticles had a 2.5-3 fold enhanced permeability and 1.3-1.8 folds reduced efflux transport compared to the unformulated OXY ( $p < 0.05$ ). The improvement of the *in vitro* oral absorption of the lipid-based formulations could lead to an excellent delivery systems for OXY by the oral route.

**Keywords:** Self-microemulsifying drug delivery system; Solid lipid nanoparticles; Nanostructured lipid carriers; Stability; Caco-2 cells; *In vitro* permeability; Oxyresveratrol; Oral drug delivery.

## 1. INTRODUCTION

Oxyresveratrol (OXY), a drug extracted from a Thai traditional plant, has many pharmacological properties. In particular, it is a potent antioxidant, shows anti-viral activities, and has a neuroprotective effect [1-8]. However its low oral bioavailability, due to its low intestinal permeability that involves an efflux pump mechanism, in addition to its extensive hepatic metabolism and rapid elimination, restricts its application as a drug candidate [9-12]. In recent times, lipid based drug delivery systems (LBDDS) have opened up new approaches to overcome these obstacles as drug carriers. Lipid-based formulations may include oil solutions or suspensions, liposomes, emulsions, self-micro or self-nanoemulsifying drug delivery systems (SMEDDS/SNEDDS), and lipid nanoparticles i.e. solid lipid nanoparticles (SLN) or nanostructured lipid carriers (NLC) [14-17]. These approaches have improved the oral bioavailability and when implemented by enhanced drug in lipid excipients, that avoids a rate limiting dissolution step in the GI tract, and also increased drug permeation across the intestinal epithelium in many ways [14,16,18,19]. However, the distinguishing features of different lipid formulations, including the composition used, particle size, rate of dissolution, rate of dispersion, precipitation of a drug and degradation of the formulations can have distinct effects on the absorption mechanisms [16,20]. For example, SMEDDS, a mixture of oils and surfactants, produces very small and uniform droplets with a fast dispersion and a rapid release rate for any solubilized drug. The oral absorption may be best facilitated by generating mixed micelles of an emulsified lipid exposed to bile salts so they can be assimilated by enterocytes. In addition, permeation enhancers such as surfactant may stimulate inhibition of efflux transporters [17,21]. Meanwhile, lipid nanoparticles, both SLN and NLC, have been designed to address the limitations of conventional lipid formulations using nanotechnologies to produce nanosized particles from the lipid excipients with acceptable regulatory and safety profiles. The lipid nanoparticles can protect the entrapped drug from being degraded in the GI tract and maintain a sustained drug release. Then, the intact nanoparticles can be absorbed directly through specialized absorptive cells into the bloodstream via the lymphatic pathway [12,15,22]. These successful lipid-based formulations after launch such as the currently marketed products: Sandimmune<sup>®</sup> and Neoral<sup>®</sup> (Cyclosporine A), Sustivas<sup>®</sup> (Efavirenz), Fortovases<sup>®</sup> (Saquinavir), Norvirs<sup>®</sup> (Ritonavir), Lamprenes<sup>®</sup> (Clofazamine) [14,17]. Our

previous findings have indicated that the bioavailability of OXY after oral administration could be better when developed as lipid nanoparticles [23]. The manifest advantages of LBDDS, has provided us with an incentive to develop other lipid formulations of OXY especially SMEDDS. Thus to promote the capabilities of the various forms of pharmaceutical dosages for important drug molecules, the behavior and absorption fate of OXY from such lipid-based formulations needs to be considered. Consequently, the major propose of this study was to develop and compare lipid-based systems including SMEDDS, SLN and NLC, with good physicochemical properties and stability in order to orally deliver OXY. In addition, the toxicity and the enhanced drug permeation properties of each developed formulations was tested using the Caco-2 cells absorption model and compared to the unformulated OXY.

## 2. MATERIALS AND METHODS

### 2.1. Materials

OXY powder (> 99% purity) was obtained from the Department of Pharmacognosy, Faculty of Pharmaceutical Sciences, Chulalongkorn University (Bangkok, Thailand). Resveratrol ( $\geq$  99% purity) was from Sigma-Aldrich (Saint Louis, MO, USA). Compritol 888 ATO<sup>®</sup> (Com888), Capryol 90<sup>®</sup> (C90), Labrasol<sup>®</sup>, Labrafac CC<sup>®</sup> (LCC), Lauroglycol FCC<sup>®</sup>, Lauroglycol 90<sup>®</sup>, Labrafil M2125 CS<sup>®</sup>, and Plurol oleique<sup>®</sup> were from Gattefossé (Saint-Priest, France). Cremophor RH40<sup>®</sup> (CRH40) and Cremophor EL<sup>®</sup> were from BASF (Ludwigshafen, Germany). Oleic acid, propylene glycol (PG), and polyethylene glycol (PEG) 400 were from PC Drug Center Co., Ltd. (Bangkok, Thailand). Ethyl oleate was from Sigma Aldrich (Buchs, Switzerland). Soybean oil and corn oil were from Thai Vegetable Oil Public Co., Ltd. (Bangkok, Thailand). Tween80<sup>®</sup> (Tw80) was from S.Tong Chemicals Co., Ltd (Bangkok, Thailand). Soy lecithin (Lec) was from Rama Production Co., Ltd. (Bangkok, Thailand). Hard gelatin capsules (size 00) were from Capsugel (Bangkok, Thailand). Acetonitrile and methanol (HPLC grade) were from RCI Labscan (Bangkok, Thailand). 3,(4,5-dimethylthiazol-2-yl)-2,5-diphenyltetrazolium bromide (MTT) and Hanks balanced salt solution (HBSS) was from Gibco<sup>®</sup> (OR, USA). Phosphate buffered saline (PBS, pH 7.4), 2-(N-Morpholino) ethanesulfonic acid (MES) sodium salt and 4-(2-hydroxyethyl)

piperazine-1-ethanesulfonic acid (HEPES) were from Sigma (MO, USA). All other chemicals were of analytical grade.

## **2.2. Preparation of liquid SMEDDS, SLN and NLC of OXY**

### **2.2.1. Development of the oily SMEDDS**

#### **2.2.1.1. Solubility studies and construction of ternary phase diagrams**

The solubility of OXY in various vehicles, including oils (Capryol 90<sup>®</sup>, Labrafac CC<sup>®</sup>, Labrafac PG<sup>®</sup>, ethyl oleate, oleic acid, soybean oil and corn oil); surfactants (Cremophor EL<sup>®</sup>, Lauroglycol 90<sup>®</sup>, Labrafil M2125 CS<sup>®</sup> and Cremophor RH40<sup>®</sup>); co-surfactants (Lauroglycol FCC<sup>®</sup>, Tween80<sup>®</sup>, Labrasol<sup>®</sup> and Plurololeique<sup>®</sup>); and co-solvents (PG and PEG 400) was determined. The shake flask method at room temperature was used and maintained until the OXY achieved an equilibrium solubilization (72 h) [24]. The selected vehicles in SMEDDS from solubility studies were used to construct ternary phase diagrams using SigmaPlot 11.2.0 software (Systat Software Inc., CA, USA). A series of mixtures of the oil with a single surfactant or a combination of surfactant and co-surfactant were prepared in different vials and mixed using a vortex mixer. The concentration range of each component was 10–50% oil, 25–90% surfactant and 0–25% co-surfactant. In Table 1, the SMEDDS system was named as systems A, B, C and D for: Cremophor EL<sup>®</sup>, Lauroglycol 90<sup>®</sup>, Labrafil M2125CS<sup>®</sup>, Cremophor RH40<sup>®</sup> based system, respectively. One gram of each mixture was dispersed in 20 mL of deionized (DI) water. The self-microemulsification performance of the SMEDDS was assessed visually according to the published visual grading system [25]. After identification of their self-microemulsifying regions, the SMEDDS systems were selected at their optimum component ratios for developing OXY-SMEDDS formulations.

#### **2.2.1.2. Preparation of oily SMEDDS of OXY**

According to the ternary phase diagram studies, the Cremophor RH40<sup>®</sup> - based system (system D) was chosen. Based on the co-surfactant/co-solvent used, these systems were coded as D1, D2, D3, D4 and D5 for Lauroglycol FCC<sup>®</sup>, Tween80<sup>®</sup>, Labrasol<sup>®</sup>, PG and PEG400, respectively (Table 1). However, only the D2 system was chosen for the incorporation of OXY. To find the optimal loading amount of OXY, varied OXY amounts were added to the optimum D2 formulations which comprised 45% C90,

45% CRH40 and 10% Tw80. Then, the mixtures were stirred continuously until a homogenous solution was achieved (Figure 1). The formulations were then left for 48 h at room temperature. The self-microemulsification performance of the OXY-SMEDDS was assessed by the visual grading system [25]. The 900 mg of the SMEDDS containing a fixed amount of OXY were manually filled into hard gelatin capsules size 00 and the capsule shells were sealed with gelatin solution. The filled capsules were stored in glass containers and protected from light until used.

### **2.2.2. Development of the lipid nanoparticles of OXY**

To compare with the oily formulations (SMEDDS), the lipid nanoparticles including SLN and NLC were utilized. The optimized formulations containing OXY were formulated following the published procedure [23]. The process was performed by a high speed homogenization method at 85 °C using a homogenization speed of 24,000 rpm for 15 min and then the nanoemulsion was cooled to obtain lipid nanoparticles at room temperature (Figure 1). Both formulations consisted of a lipid phase and an aqueous phase. The lipid phase contained only solid lipid for SLN while some parts of the lipid were replaced by liquid oil for the NLC. In a similar way the aqueous phase of both formulations consisted of OXY (0.3 %w/w), surfactant/co-surfactant and water. The formulation compositions of the developed systems of OXY are presented in Table 2.

### **2.3. Physical properties of the developed systems of OXY**

The physical properties of the developed formulations containing OXY (SMEDDS, SLN, NLC) were compared in terms of their mean size, size distribution (expressed as a polydispersity index or PDI), total drug content (TC) and efficiency of drug entrapment (DEE). The mean size and PDI were determined after a 20-fold dilution with DI water. The samples were measured using photon correlation spectroscopy (PCS) with a Zetasizer Nano ZS<sup>®</sup> (Malvern Instruments, UK). The TC of each formulation was investigated as in a previous report [26,27] by dissolving the sample in methanol. Meanwhile, the DEE of the lipid nanoparticles was evaluated according to the published method [23] using the indirect method to define the non-entrapped drug and then a back calculation to obtain the entrapped drug in the formulation. Finally, the resulting solution was diluted, filtered using 0.45 µM filters and analyzed for OXY by a

validated HPLC method [23]. Three replicated measurements of each system were performed in each study.

#### **2.4. Formulation stability**

The stability tests of the SMEDDS were evaluated according to the ICH guidelines [28] on the topic of Q1A (R2): stability testing of new drug substances and products. The hard gelatin capsules containing liquid OXY-SMEDDS were stored in air-tight glass containers and protected from light. The samples were maintained in a stability chamber (Patron AH-80, Taiwan) under intermediate conditions [ $30 \pm 2$  °C,  $65 \pm 5\%$  relative humidity (RH)], and a stability chamber (Memmert<sup>®</sup> HPP 260, USA) under accelerated conditions [ $45 \pm 2$  °C,  $75 \pm 5\%$  RH]. Meanwhile, the stability of the two lipid nanoparticles (SLN and NLC) was studied at  $4 \pm 2$  °C in a refrigerator. The samples were taken at 0, 1 and 3 months. Appearance, mean size, size distribution (PDI) and TC were determined at each time point for all the developed formulations. Moreover, the self-microemulsifying properties of OXY-SMEDDS were additionally evaluated.

#### **2.5. *In vitro* Caco-2 cells studies of the developed systems**

The Caco-2 cell line (HTB-37, ATCC, Virginia, USA), derived from a human colorectal adenocarcinoma, were grown in Modified Eagle's Medium (MEM, Gibco<sup>®</sup>, USA) supplemented with 20% (v/v) fetal bovine serum and 1% (v/v) of penicillin (100 IU/mL)-streptomycin (100 mg/mL) (Gibco<sup>®</sup>, USA). The cells were maintained at 37 °C in a fully humidified atmosphere with 5% CO<sub>2</sub> in air, and passaged every 2-3 days until, they reached an 80-100 % confluency of a cell monolayer. The cells were then released from the culture flasks using a 0.25% trypsin-EDTA solution (Gibco<sup>®</sup>, Canada). Viable cell numbers were then determined prior to use by live-cell staining using 0.4% trypan blue and by counting viable cells with a standard haemocytometer.

##### **2.5.1. Cytotoxicity test by MTT assay**

As damage of the intestinal epithelium sometimes affects the intestinal permeability of the samples hence cell viability was assessed by the standard MTT test [29] to optimize the non-toxic concentrations of the samples prior to the transport study. The stock solution of OXY in DMSO (Amresco<sup>®</sup>, USA) was prepared and then diluted with transport medium (HBSS-HEPES) pH 7.4 to obtain OXY concentrations that ranged from 0-800 µM. After evaluating the most suitable concentration range for the

OXY, the OXY-formulations including SLN, NLC, and SMEDDS, were evaluated by comparison with blank formulations and unformulated OXY. The samples were diluted with the HBSS-HEPES medium to obtain equivalent concentrations of OXY of 25-400  $\mu\text{M}$  for the lipid nanoparticles (SLN and NLC) and 25-200  $\mu\text{M}$  for the SMEDDS. Briefly, the Caco-2 cells were seeded in 96-well cell culture plates at a density of  $5 \times 10^4$  cells/well. After overnight incubation, the culture medium was removed, and the cells were washed with 100  $\mu\text{L}$  of PBS pH 7.4. 100  $\mu\text{L}$  of the samples were added to each well. 1 % sodium lauryl sulfate (SDS) and HBSS-HEPES medium were used as a negative control and positive control, respectively. After 24 h treatment, the samples were removed and the cells were washed with PBS pH 7.4. The cells were added with 50  $\mu\text{L}$  of 0.5 mg/ml MTT solution and then incubated for 4 h. After removing the MTT solution carefully, the formazan crystals formed by the viable cells were dissolved by adding DMSO. Duplicates were performed for each sample. The absorbance was measured at 570 nm by the microplate reader (DTX 880 Multimode Detector, Beckman Coulter Inc., Austria). The positive control (HBSS-HEPES medium) was presented as the 100% cell viability control. The percentage cell viability of the samples was calculated relative to the measured absorbance of the positive control. The  $\text{ABS}_{\text{sample}}$  and  $\text{ABS}_{\text{control}}$  represented the measured absorbance of the sample and the positive control, respectively.

$$\% \text{ Cell viability} = \frac{\text{ABS}_{\text{sample}}}{\text{ABS}_{\text{control}}} \times 100 \quad (1)$$

## **2.5.2. Caco-2 transport studies of OXY**

### **2.5.2.1. Preparation of the samples**

The samples (OXY solution in DMSO and each OXY-formulation) were diluted with transport medium pH 6.5 and pH 7.4 for apical (AP) side loading and basolateral (BL) side loading, respectively, to obtain the desired concentration of OXY. The transport medium was composed of HBSS containing 20 mM of MES or HEPES and adjusted to pH 6.5 (for apical compartment) and pH 7.4 (for basolateral compartment) by 1N HCl or 1N KOH.

### 2.5.2.2. Caco-2 transport study of the samples

The *in vitro* permeability studies were investigated as described in a previous report [27]. The Caco-2 cells (passage number 25-29) were used in this study. The cells were seeded on Transwell<sup>®</sup> 6-well plates (Costar<sup>®</sup>, USA) at a density of 60,000 cells per cm<sup>2</sup> of Transwell<sup>®</sup> insert (area: 4.67 cm<sup>2</sup>, Corning<sup>®</sup>, USA), and cultured until the cells had completely differentiated (about 21-23 days). The culture medium was changed every two days for both the donor compartment and the receiver compartment. Before the transport study, the transepithelial electrical resistance (TEER) value was measured using a Millicell<sup>®</sup>-ERS Voltmeter (Millipore Corp., Bedford, MA, USA) to evaluate the integrity of the cell monolayer. The Caco-2 cell monolayers with an average TEER values > 300  $\Omega\text{cm}^2$  indicated the cells were intact that were used in this study.

In the bidirectional experiment, the absorptive transport (AP-BL) experiment and the secretory transport (BL-AP) experiment, the effectiveness of the formulations to inhibit the active efflux transporter (s) of the monolayer were determined. For the absorptive transport experiment, 1.5 mL of samples in HBSS/MES medium pH 6.5 and 2.6 mL of HBSS/HEPES medium pH 7.4 were added to the apical side (donor compartment) and the basolateral side (receiver compartment), respectively. For the secretory transport (BL→AP) experiments, 2.6 mL of samples in HBSS/HEPES medium pH 7.4 and a 1.5 mL of blank HBSS/MES medium pH 6.5 were added to the basolateral side (donor compartment) and the apical side (receiver compartment), respectively. The transport studies were performed on a shaking incubator (HandyLAB<sup>®</sup> system, N-BIOTEK Co., Ltd, Korea) maintained at 37 ± 0.5 °C with a shaking rate of 100 rpm. At various times, sample volumes of 400  $\mu\text{L}$  and 100  $\mu\text{L}$  were removed from the receiver compartment and donor compartment, respectively, in the bidirectional experiments. Meanwhile, the volumes withdrawn from the receiver compartment in both experiments were immediately replaced with warmed fresh transport medium. To determine the accumulation of the drug in the Caco-2 cells, the cells were washed with PBS pH 7.4 and then scrapped from the insert filters at the end of experiments. After that, the cells were lysed and centrifuged to collect the supernatant. The amounts of OXY were quantified by the validated HPLC method. The amount of the cumulative drug that permeated through the Caco-2 monolayer as measured in the receiver



compartment was plotted against the sampling time to obtain a linear slope. Then, the apparent permeability coefficient ( $P_{app}$ ) and the efflux ratio (ER) [30] were calculated following Eqs. (2) and (3), respectively, and compared between each of the formulations. Where the  $dQ/dt$  was the cumulative transport rate ( $\mu\text{g/s}$ ) defined as the slope obtained by linear regression of the cumulative amount transported ( $\mu\text{g}$ ) as a function of time (s).  $A$  is the surface area of the filter ( $4.67\text{ cm}^2$  in the 6-wells insert).  $C_{int}$  is the initial concentration of OXY on the donor compartment ( $\mu\text{g/mL}$ ). Where  $P_{app}$  (AP-BL) is the apparent permeability coefficient for the absorptive transport and  $P_{app}$  (BL-AP) is the apparent permeability coefficient for the secretory transport.

$$P_{app} = \frac{(dQ/dt)}{AC_{int}} \quad (2)$$

$$ER = \frac{P_{app}(\text{BL-AP})}{P_{app}(\text{AP-BL})} \quad (3)$$

### 2.5.2.3. Oxyresveratrol analysis by HPLC

The high performance liquid chromatography (HPLC) system was used to determine the amount of OXY in the *in vitro* permeability studies as previously reported [27]. The HPLC system (HP 1100, Agilent, USA) with a UV detector at 320 nm was performed at ambient temperature. The reversed phase system consisted of a C18 column and guard column (VertiSep<sup>®</sup> pHendure, Ligand Scientific, Thailand) and the isocratic solvent system of acetonitrile and 0.5% v/v acetic acid (27:73 v/v) was used for elution. The system was set at a flow rate of 1.0 mL/min and an injection volume of 50  $\mu\text{L}$ . Resveratrol (RES) and transport medium was used as the internal standard and blank vehicle. The retention time of OXY and the internal standard was 7 and 12 min, respectively. For the standard curve, a good linearity ( $r^2 = 0.9999$ ) at the OXY concentrations of 0.1, 0.2, 0.5, 1, 2, 5, 10  $\mu\text{g/mL}$  was achieved from three determinations. The intra-day and inter-day precision studies were obtained by three daily injections of three OXY concentrations of spiked samples over a 3 day period. The percentage of the relative standard deviations (%RSD) for intra-day and inter-day precision were 0.97%-2.90% and 7.67%-12.55%, respectively. The accuracy of the method was expressed as the recovery percentage over the range of from  $90.18 \pm 2.38$

-  $102.46 \pm 3.99$ . The results showed that the HPLC method achieved an acceptable accuracy and precision that was valid for the determination of OXY in the *in vitro* cell culture studies.

## 2.6. Statistical analysis

All data was expressed as a mean  $\pm$  standard deviation (S.D.). The one-way ANOVA with a Tukey test was performed using Graphpad Prism<sup>®</sup> software (Graphpad software Inc.) to the statistical comparisons of the results. Statistical probability (p) values less than 0.05 were considered significantly different.

## 3. RESULTS AND DISCUSSION

### 3.1. Comparison of the preparation of liquid SMEDDS, SLN and NLC with OXY

In this study, the developed lipid formulations of OXY could be divided into two main groups based on the lipid phase of the formulations. First, the lipid nanoparticles system was defined as a solid lipid formulation that also included SLN and NLC. The difference of the oil phase of the SLN and NLC is the replacing of the solid lipid of SLN by liquid oil (LCC) in NLC. However, both nanoparticles were still solids that were suspended in the water phase of the surfactant at room and body temperature like a suspension. Another formulation was an oily formulation named SMEDDS. This system was self-spontaneously produced as a microemulsion when dispersed in the aqueous medium by mild agitation. The oil phase of this system was comprised of only liquid oil (C90). Therefore, the liquid oil proportion in each formulation could be arranged in the order of SMEDDS (45%) >NLC (2.5%) >SLN (0%). For consideration of the surfactant phase of the formulations, all formulations contain different Tween80<sup>®</sup> concentration: 10% (SMEDDS) > 3.75% (NLC = SLN) as shown in Table 2. Moreover, each system contained other suitable surfactants such as soy lecithin and Cremophor RH40<sup>®</sup> for the lipid nanoparticles system and the SMEDDS system, respectively. For drug loading in the formulations, the SMEDDS containing 4% w/w of OXY that was much more than for the SLN and NLC (0.3 %w/w).

### 3.1.1. Development of the oily SMEDDS of OXY

This self-microemulsifying system consisted of drug, oil and surfactant. When exposed to the small volume of an aqueous medium, the microemulsion of the drug was solubilized in the oily core and/or on the interface of the oil and surfactant and was produced spontaneously [16,17]. The drug solubility was affected by the hydrophobicity of the drugs, and the presence of oils, surfactants, and co-surfactants/co-solvents. In Figure 2, the solubility results revealed that OXY had a high solubility in PG ( $216.62 \pm 8.86$  mg/mL) and PEG 400 ( $116.37 \pm 1.66$  mg/mL), so these were chosen as the co-solvent. The high solubility in PG and PEG 400 was probably due to the structure of the OXY that has four hydroxyl (-OH) groups so it can form a hydrogen bond with the hydroxyl (-OH) groups of propylene glycol (diol) and the polyethylene oxide (PEO) groups of PEG 400. In a similar way, the surfactants were Lauroglycol 90<sup>®</sup> and Cremophor EL<sup>®</sup>, that were composed partly of PG and PEO groups, respectively, and they showed high solubilization capacities for OXY. Capryol 90<sup>®</sup> oil, composed partly of PG had the highest solubility for OXY ( $115.42 \pm 4.475$ mg/mL), so was selected for the oil phase. All of the selected excipients for the development of OXY-SMEDDS development exhibited a higher solubilization capacity for OXY than for the solubility of OXY in water ( $0.993 \pm 0.012$  mg/mL) at room temperature.

Thus, ternary phase diagrams of the selected excipients were constructed based on the solubility data. These could be divided into four groups based on the surfactants used including: system A, Cremophor EL<sup>®</sup>; system B, Lauroglycol 90<sup>®</sup>; system C, Labrafil M2125CS<sup>®</sup>; system D, Cremophor RH40<sup>®</sup>. However, the Lauroglycol 90<sup>®</sup> (system B) and Labrafil M2125CS<sup>®</sup> (system C) had poor ability to emulsify the selected C90 oil that appeared large oil droplets presented on the surface of the diluted emulsion. Moreover, the use of only either Cremophor EL<sup>®</sup> or Cremophor RH40<sup>®</sup> showed good ability to emulsify C90 oil but produced a gel structure that required a long time for emulsification. Thus, a co-surfactant/co-solvent was used in combination with such surfactants. Five different types of co-surfactant/co-solvent were used in this study (see Table 1). When considering the concentrations of the co-surfactant, a high PEG 400 proportion was incompatible with the hard gelatin capsules that were to be used to incorporate the liquid SMEDDS formulation [31]. So, the

concentrations of PEG 400 and the other four co-surfactants were maintained at only up to 25% w/w of the formulation. In addition, the components of system A showed less area of self-microemulsion regions in the ternary phase diagrams (Figure 3). For system D, the ternary phase diagrams of system D2, D3, D4 provided large self-microemulsion regions, and produced a microemulsion at a 50% oily phase (Figure 4). Thus, some weight ratios of the compositions from the D2, D3, and D4 systems were selected to manufacture the SMEDDS containing OXY.

The formulations that consisted of the 50% C90 oil and 50% surfactant phase (45% CRH40 and 5% co-surfactant) were coded as D2A, D3A, and D4A for the SMEDDS that contained the co-surfactant of Tween80<sup>®</sup>, Labrasol<sup>®</sup>, and PG, respectively. The solubility of OXY in D2A, D3A and D4A was  $61.47 \pm 2.00$ ,  $78.94 \pm 5.05$  and  $85.79 \pm 3.89$  mg/mL, respectively. Unfortunately, poorer physical properties of D3A and the instability of D4A after storage were observed. Thus, only D2A was used in further experiments. Nevertheless, the rapidly forming microemulsion (visual grade I) from the D2A after incorporation of OXY following its solubility was not obtained. To find the most suitable drug loading, varied amounts of OXY were added to the formulations. The good characteristics of the formulations were obtained when the maximum OXY loading was 40 mg/1 g of SMEDDS. A higher oil content was required for any higher drug loading capacity and also produced a lower proportion of the surfactant phase. However, a high proportion of the surfactant phase allowed for good characteristics of the formulations and also improved drug absorption [17,24,31,32]. Therefore, the SMEDDS containing 45% of the C90 oil and surfactant phase (45% CRH40 and 10% Tw80) were formulated to compare with the lipid nanoparticle systems (Table 2).

### **3.1.2. Development of the lipid nanoparticles of OXY**

In this study, the lipid nanoparticles of OXY were prepared by a mechanical technique using high shear homogenization. According to the benefits of the compositions used, the glyceryl behenate (Com888), polysorbate 80 (Tw80) and soy lecithin (Lec) was selected as the solid lipid, surfactant and co-surfactant, respectively, for SLN. In addition, the Caprylic/Capric triglyceride (LCC) was used as the liquid oil in the NLC. At 5% w/w of the lipid phase for both formulations, the optimized SLN was comprised of only solid lipid while the NLC consisted of 1:1 of the lipid (2.5%) and oil (2.5%). For the surfactant phase, the Tw80 (3.75%) combined with Lec (1.875%)

facilitated dissolving of the drug, emulsified between the lipid and aqueous, and stabilized the nanoparticles.

### ***3.2. Comparison of the physical properties of the developed systems of OXY***

The three developed systems for OXY were liquid form formulations as shown in Figure 5. The SLN and NLC appeared as a milky suspension of lipid particles suspended in a high amount of water (> 89 %w/w). In contrast, the SMEDDS appeared as a yellowish oily mixture of oil and surfactant/co-surfactant without water. The mean sizes of the three formulations containing OXY were in the nanosized range. However, the microemulsion droplet size of SMEDDS ( $26.94 \pm 0.08$  nm) was significantly smaller than the particle sizes of the NLC ( $96.01 \pm 0.89$  nm) and SLN ( $107.50 \pm 0.25$  nm), respectively. Moreover, the size distribution (PDI) of such a microemulsion ( $0.073 \pm 0.010$ ) was less than that of the SLN ( $0.245 \pm 0.004$ ) and NLC ( $0.259 \pm 0.006$ ) and indicated that the produced oil droplets of SMEDDS had more consistency than the lipid nanoparticles obtained by the developed method. The reasons for the difference might be from the formulation compositions especially the 10-fold higher surfactant/co-surfactant (55 %w/w) in the SMEDDS compared to the lipid nanoparticles (5.625 %w/w). The greater surfactant phase could be more effective for emulsifying the oil droplets in the aqueous phase during the preparation process and resulted in producing homogeneous small sizes of sample [17,24,27]. The above results showed that, the oil content also led to the production of smaller particle sizes for the NLC than the SLN. The LCC oil used in the NLC contained unsaturated fatty acid that reduced the melting point of the lipid phase and perhaps promoted a more rapid and homogenous distribution of the heat energy during the preparation heating process [33]. For the PDI, the greater number of preparation steps may lead to the more varied size distribution of the lipid nanoparticles. The heating and homogenization steps were raised to form different emulsion droplets and the gradual cooling down to room temperature may result in varied sizes of the lipid particles. However, these sizes and the PDI that produced the three developed formulations were in the acceptable range for intestinal absorption [17,22,34]. Furthermore, there was no difference in the total content of OXY in the three lipid formulations (~100 %w/w) indicating no drug loss occurred during the production process of both systems. Owing to there being no aqueous phase that would

allow the drug to diffuse out, the efficiency of drug entrapment of the SMEDDS was assumed to be 100% whereas the lower entrapment efficiency by the NLC ( $88.50 \pm 0.10$  %w/w) and SLN ( $85.50 \pm 0.80$  %w/w) was observed [23]. Because the formulations of lipid nanoparticles contained the plenty of water, some of drug could diffuse out to the aqueous phase particularly during the cooling down step. Nevertheless, the DEE of both lipid nanoparticles was appropriately high.

### 3.3. Comparisons of formulation stability

The stability of the three developed formulations was compared (Figure 6). The dissimilarity of the selected storage temperatures for the SMEDDS ( $30 \pm 2^\circ\text{C}$  and  $45 \pm 2^\circ\text{C}$ ) and lipid nanoparticles ( $4 \pm 2^\circ\text{C}$ ) could be explained by the differences of the composition of both systems. The temperature of refrigeration ( $4 \pm 2^\circ\text{C}$ ) was not suitable for the SMEDDS system as it consisted of liquid oil (C90). The temperature of refrigeration ( $4 \pm 2^\circ\text{C}$ ) was not suitable for the SMEDDS system as it consisted of liquid oil (C90). The oil would be a wax at this low temperature. The conditions of room temperature (RT) or higher temperature were not proper for the lipid nanoparticles that were comprised of solid lipid and more water. At RT, the contamination by microorganism in the aqueous formulations was possible if no preservative was added. Moreover, a too high temperature might be one reason of the solid lipid melted.

The only appearance of SMEDDS under the accelerated conditions was changed to a dark oily solution after storage for three months. However, the self-microemulsifying properties of OXY-SMEDDS after a 20-fold dilution with DI water showed a transparent microemulsion of OXY (visual grading I) during the storage period. For the mean size, only the mean particle size of the SLN significantly increased after three months of storage but this size still remained within the acceptable range ( $<200$  nm) [22]. Meanwhile, the PDI of all three formulations was not altered during storage and indicated that the particles were homogeneously dispersed in the vehicles and did not aggregated or flocculate. It was also important that the total content of OXY in both lipid nanoparticles was almost 100% at various time points (0, 1, 3 months) whereas the OXY content in the SMEDDS gradually decreased over time. This result implied that the oily SMEDDS were unstable according to the loss or degradation of the drug. From the stability data, it might be concluded that the lipid nanoparticles were

more stable than the oily formulations because of the efficiency of the solid lipid that protected the entrapped drug in the system.

### **3.4. Comparison of Caco-2 cells studies of the developed systems of OXY**

#### **3.4.1. Cytotoxicity test by MTT assay**

The toxicity of the developed lipid systems on the Caco-2 cells was compared as presented in Figure 7. Prior to the comparison, the non-toxic concentration of the solubilized OXY was assessed. The cells had > 80% viability in the OXY concentration range of 0-400  $\mu\text{M}$  (Figure 7A). Thus, the optimized concentration of OXY for comparisons of the formulation should not be greater than 400  $\mu\text{M}$ . In the lipid nanoparticle system (SLN and NLC), either the blank formulations or the formulations containing the drug were compatible to the cells up to 400  $\mu\text{M}$  of OXY. On the other hand, the result from the blank formulation and the OXY-SMEDDS revealed that the biocompatibility to the cells was only until 100  $\mu\text{M}$  of OXY. The 4-folds higher toxicity of SMEDDS compared to the lipid nanoparticles might result from the different compositions of the systems. Just as found in a previous report, the surfactants including their types and contents seemed to be the major factors in their cytotoxicity [21,35]. In this study, the % surfactant phase (55 %w/w) of the SMEDDS was about 10 times greater than for the lipid nanoparticles system (5.625 %w/w). Considering that Tween80<sup>®</sup> can be toxic, the specific mixture of Tween80<sup>®</sup> and other surfactant types might cause the difference [32,35]. In addition, the greater % of Tween80<sup>®</sup> in the SMEDDS (10 %w/w) than in the nanoparticles systems (3.75 %w/w) indicated that the more toxic nature of the former system was most likely due to the concentration of the cytotoxic properties of the surfactant [21]. The oil used in the SMEDDS is generally known to be safe for oral delivery. However, the Capryol 90<sup>®</sup> oil which contained propylene glycol esters group implied they could be cytotoxic on the Caco-2 cells at high concentrations [21,32]. Meanwhile, the Com888 solid lipid, long chain glyceride, and LCC oil, medium chain triglyceride, commonly used in NLC were compatible to the intestinal cells because its structure was similar to the physiological lipids of the body. Hence, the maximum non-toxic concentration of OXY for comparison to the lipid-based systems was 100  $\mu\text{M}$ .

### 3.4.2. Caco-2 cells transport studies of OXY

Figure 8 and Table 3 shows the results from the bidirectional studies of the unformulated OXY and OXY formulated as SLN, NLC and SMEDDS at different concentrations. The low oral bioavailability of OXY was due to its low intestinal permeability that was partly due to an efflux transporter mechanism [11,27]. In agreement with the published paper, the ER of the unformulated OXY was more than 1 at both 100  $\mu\text{M}$  and 400  $\mu\text{M}$ . In addition, there was only a 1.5 times and 3 times increase in  $P_{app}$  in the secretory direction and the absorptive direction, respectively, and as consequence there was a decrease in the ER of the drug from 5.02 to 2.55 when the OXY concentration was increased from 100  $\mu\text{M}$  to 400  $\mu\text{M}$ . This can be explained by the saturation of the activity of the efflux transporters at the Caco-2 cell monolayer. This finding indicated the importance of considering the amount of the drug before making comparisons among the different formulations. At 400  $\mu\text{M}$  of OXY, the SLN and NLC were reduced by 2.8 folds and 3.3 folds, respectively, for the secretory permeability of OXY, whereas it enhanced only the absorptive permeability of the NLC compared to those of the unformulated OXY. Thus, the lipid nanoparticle systems significantly alleviated efflux transport of OXY with an ER ( $\leq 1$ ) of 0.59 and 1.01 for the NLC and SLN, respectively. From the impact of the bioactive content, both formulations of the nanoparticles were compared to the SMEDDS system at the 100  $\mu\text{M}$  of OXY. At this level, the  $P_{app}$  (AP-BL) values of the NLC, SLN and SMEDDS were significantly improved by 3, 2.8, and 2.5 folds, respectively, compared to the unformulated OXY. In addition, the  $P_{app}$  (BL-AP) value in the secretory direction of the NLC, SLN, and SMEDDS decreased by a 1.3, 1.8, and 1.5 fold, respectively, compared to the unformulated OXY. The data concerned with the efflux ratio of the three formulations was not different. Although the mechanisms of transport across the intestinal epithelium by the different lipid-based systems were varied but the outcomes of the mechanisms might be comparable. The sustained drug release from the lipid nanoparticles could have special merit to protect the drug and transport the intact lipid nanoparticles via a transcellular pathway directly to the blood circulation [22,23]. They, however, did have a preferential uptake by the specialized Peyer's patches (M cells) and the isolated follicles of the gut-associated lymphoid tissue located in the intestinal epithelium [12]. However the produced microemulsion droplets of SMEDDS were mainly generated to form mixed



micelles when exposed to bile salts, cholesterol and phospholipids, and then pass through the chylomicron uptake mechanism used by the enterocytes. Finally, the compound formulated as the solid lipid and oily formulations was absorbed mainly into the lymphatic pathway before reaching the systemic circulation [12,20,23]. Moreover, the inhibitory activities on the efflux mediated transporter (s) and modulation of the tight junction by the surfactants in the lipid formulations resulted in promoting oral absorption [21,32,35]. These potential mechanisms for the lipid-based formulations facilitated oral delivery. The application of advanced techniques and sophisticated instruments such as immune cytochemical or fluorescence imaging by confocal microscopy [34], *in vitro* lipolysis coupled to synchrotron scattering techniques [20,36], should be considered to further clarify the absorption routes of the oral lipid formulations.

The reactions between the lipid bilayers of the Caco-2 cells and the lipid used in the formulations resulted in a greater entrapment of the OXY that was formulated as the lipid-based systems rather than by the OXY/DMSO solution (Table 3). Moreover, the % OXY accumulation in the cells (%) from the lipid nanoparticles system was significantly greater than that from the SMEDDS. This was possibly due to the nature of the formed nanoparticles that were more difficult to digest than the oily SMEDDS either inside or outside the cells, leading to the direct uptake of the drug entrapped in the particles and a greater accumulation in the cells [14,19,20].

Nevertheless, the permeability process is only one aspect of the main barriers to the use of oral delivery of the drug that included absorption, distribution, metabolism and elimination all of which can affect the bioavailability of the active compounds. The data from the absorption study alone may not be able to predict exactly the bioavailability of an orally delivered drug [37,38]. The compounds and/or formulations may have a major effect on other parts of the pharmacokinetics. However, all three lipid formulations including SLN, NLC, and SMEDDS, each successfully improved the *in vitro* absorption and oral bioavailability compared to the unformulated OXY. Although, the difference of the *in vitro* permeability of OXY from each formulation was not as empirical as that observed from the *in vivo* studies [23,27].

## **CONCLUSION**

The oily SMEDDS of OXY was developed by simple optimization of chemical compositions in the system. Meanwhile, the lipid nanoparticles (SLN and NLC)

containing OXY were prepared by mechanical technique of high speed homogenization. The disparate physical properties of the two different systems include appearance, size, size distribution and entrapment efficiency. Also, the recommended storage conditions for good stability of the two systems were different. Moreover, the different compositions of the systems especially high concentrations of surfactant result to more toxicity of the SMEDDS than lipid nanoparticles when exposed to the Caco-2 cells. The oily SMEDDS were comparable with lipid nanoparticles to enhance *in vitro* oral absorption of OXY according to increased permeability and reduced efflux transport across intestinal monolayers compared to unformulated OXY. This finding presented the effective of lipid formulations to minimize the OXY exposed to efflux mediated mechanism of the intestinal membrane. Therefore, the developed lipid-based formulations, SMEDDS, SLN and NLC, may be smart as oral drug delivery systems of OXY.

#### **CONFLICT OF INTEREST**

The authors declare that there are no conflicts of interest.

#### **ACKNOWLEDGEMENTS**

The financial support was granted by the Thailand Research Fund (BRG 5580004) and the Faculty of Pharmaceutical Sciences, Prince of Songkla University. The authors thank to Assist. Prof. Dr. Potchanapond Graidist for supporting on the cell culture experiments and allowing to work at the Excellent Research Laboratory of Cancer Molecular Biology at Department of Biomedical Sciences, Faculty of Medicine, Prince of Songkla University. We also thank Dr. Brian Hodgson for assistance with the English.

#### **REFERENCES**

- [1] Benet, L.Z. The role of BCS (biopharmaceutics classification system) and BDDCS (biopharmaceutics drug disposition classification system) in drug development. *J. Pharm. Sci.*, **2013**, *102*, 34–42.
- [2] Chung, K.O.; Kim, B.Y.; Lee, M.H.; Kim, Y.R.; Chung, H.Y.; Park, J.H.; Moon, J.O. *In vitro* and *in vivo* anti-inflammatory effect of oxyresveratrol from *Morus Alba* L. *J. Pharm. Pharmacol.*, **2003**, *55*, 1695-1700.
- [3] Aftab, N.; Likhitwitayawuid, K.; Viera, A. Comparative antioxidant activities and synergism of resveratrol and oxyresveratrol. *Nat. Prod. Res.*, **2010**, *24*, 1726–1733.

- [4] Tengamnuay, P.; Pengrungruangwong, K.; Pheansri, I.; Likhitwitayawuid, K. *Artocarpus lakoocha* heartwood extract as a novel cosmetic ingredient: evaluation of the *in vitro* anti-tyrosinase and *in vivo* skin whitening activities. *Int. J. Cosmetic Sci.*, **2006**, *28*, 269-276.
- [5] Weber, J.T.; Lamont, M.; Chibrikova, L.; Fekkes, D.; Vlug, A.S.; Lorenz, P.; Kreutzmann, P.; Slemmer, J.E. Potential neuroprotective effects of oxyresveratrol against traumatic injury. *Eur. J. Pharmacol.*, **2012**, *680*, 55-62.
- [6] Sasivimolphan, P.; Lipipun, V.; Likhitwitayawuid, K.; Takemoto, M.; Pramyothin, P.; Hattori, M.; Shiraki, K. Inhibitory activity of oxyresveratrol on wild-type and drug-resistant varicella-zoster virus replication *in vitro*. *Antiviral Res.*, **2009**, *84*, 95-97.
- [7] Sasivimolphan, P., Lipipun, V.; Ritthidej, G.; Chitphet, K.; Yoshida, Y.; Daikoku, T.; Sritularak, B.; Likhitwitayawuid, K.; Pramyothin, P.; Hattori, M.; Shiraki, K. Microemulsion-based oxyresveratrol for topical treatment of herpes simplex virus (HSV) infection: physicochemical properties and efficacy in cutaneous HSV-1 infection in mice. *AAPS PharmSciTech*, **2012**, *13*, 1266-1275.
- [8] Likhitwitayawuid, K.; Sritularak, B.; Benchanak, K.; Lipipun, V.; Mathew, J.; Schinazi, R.F. Phenolics with antiviral activity from *Millettia Erythrocalyx* and *Artocarpus Lakoocha*. *Nat. Prod. Res.*, **2005**, *19*, 177-182.
- [9] Chao, J.; Yu, M.S.; Ho, Y.S.; Wang, M.; Chang, R.C. Dietary oxyresveratrol prevents parkinsonian mimetic 6-hydroxydopamine neurotoxicity. *Free Radic. Biol. Med.*, **2008**, *45*, 1019–1026.
- [10] Qiu, F.; Komatsu, K.; Saito, K.; Kawasaki, K.; Yao, X.; Kano, Y. Pharmacological properties of traditional medicines. XXII. Pharmacokinetic study of mulberroside A and its metabolites in rat. *Biol. Pharm. Bull.*, **1996**, *9*, 1463-1467.
- [11] Mei, M.; Ruan, J.Q.; Wu, W.J.; Zhou, R.N.; Lei, J.P.C.; Zhao, H.Y.; Yan, R.; Wang, Y.T. *In vitro* pharmacokinetic characterization of mulberroside A, the main polyhydroxylated stilbene in mulberry (*Morus alba* L.), and its bacterial metabolite oxyresveratrol in traditional oral use. *J. Agric. Food Chem.*, **2012**, *60*, 2299-2308.
- [12] Huang, H.; Chen, G.; Lu, Z.; Zhang, J., Guo, D. Identification of seven metabolites of oxyresveratrol in rat urine and bile using liquid chromatography/tandem mass spectrometry. *Biomed. Chrom.*, **2010**, *24*, 426-432.

- [13] Huang, H.; Zhang, J.; Chen, G.; Lu, Z.; Wang, X.; Sha, N.; Shao, B.; Li, P.; Guo, D. High performance liquid chromatographic method for the determination and pharmacokinetic studies of oxyresveratrol and resveratrol in rat plasma after oral administration of *Smilax China* extract. *Biomed.Chrom.*, **2008**, *22*, 421-427.
- [14] Mu, H.; Holm, R.; Müllertz, A. Lipid-based formulations for oral administration of poorly water-soluble drugs. *Int. J. Pharm.*, **2013**, *453*, 215-224.
- [15] Yoon, G.; Park, J.W.; Yoon, I.S. Solid lipid nanoparticles (SLNs) and nanostructured lipid carriers (NLCs): recent advances in drug delivery. *J. Pharm. Investig.*, **2013**, *43*, 353-362.
- [16] Pouton, C.W.; Porter, C.J.H. Formulation of lipid-based delivery systems for oral administration: materials, methods and strategies. *Adv. Drug Deliv. Rev.*, **2008**, *60*, 625-637.
- [17] Gursoy, R.N.; Benita, S. Self-emulsifying drug delivery systems (SEDDS) for improved oral bioavailability of lipophilic drugs. *Biomed. Pharmacother.*, **2004**, *58*, 173–182.
- [18] Constantinides, P.P. Lipid microemulsions for improving drug dissolution and oral absorption: physical and biopharmaceutical aspects. *Pharm. Res.*, **1995**, *12*, 1561-1572.
- [19] Han, S.F.; Yao, T.T.; Zhang, X.X.; Gan, L.; Zhu, C.L.; Yua, H.Z.; Gan, Y. Lipid-based formulations to enhance oral bioavailability of the poorly water-soluble drug anetholtrithione: effects of lipid composition and formulation. *Int. J. Pharm.*, **2009**, *379*, 18–24.
- [20] Porter, C.J.H.; Pouton, C.W.; Cuine, J.F.; Charman, W.N. Enhancing intestinal drug solubilisation using lipid-based delivery systems. *Adv. Drug Deliv. Rev.*, **2008**, *60*, 673-691.
- [21] Ujhelyi, Z.; Fenyvesi, F.; Váradi, J.; Fehér, P.; Kiss, T.; Veszélka, S.; Deli, M.; Vecsernyés, M.; Bácskay, I. Evaluation of cytotoxicity of surfactants used in self-micro emulsifying drug delivery systems and their effects on paracellular transport in Caco-2 cell monolayer. *Eur. J. Pharm. Sci.*, **2012**, *47*, 564-573.
- [22] Tiwari, R.; Pathak, K. Nanostructured lipid carrier versus solid lipid nanoparticles of simvastatin: comparative analysis of characteristics, pharmacokinetics and tissue uptake. *Int. J. Pharm.*, **2011**, *415*, 232-243.

- [23] Sangsen, Y.; Wiwattanawongsa, K.; Likhitwitayawuid, K.; Sritularak, B.; Wiwattanapataptee, R. Modification of oral absorption of oxyresveratrol using lipid based nanoparticles. *Colloids Surf., B*, **2015**, *131*, 182-190.
- [24] Setthacheewakul, S.; Mahattanadul, S.; Phadoongsombut, N.; Pichayakorn, W.; Wiwattanapataptee, R. Development and evaluation of self-microemulsifying liquid and pellet formulations of curcumin, and absorption studies in rats. *Eur. J. Pharm. Biopharm.*, **2010**, *76*, 475-485.
- [25] Singh, A.K., Chaurasiya, A.; Awasthi, A.; Mishra, G.; Asati, D.; Khar, R.K.; Mukherjee, R. Oral bioavailability enhancement of exemestane from self-microemulsifying drug delivery system (SMEDDS). *AAPS PharmSciTech*, **2009**, *10*, 906-916.
- [26] Sangsen, Y.; Likhitwitayawuid, K.; Sritularak, B.; Wiwattanawongsa, K.; Wiwattanapataptee, R. Novel solid lipid nanoparticles for oral delivery of oxyresveratrol: effect of the formulation parameters on the physicochemical properties and *in vitro* release. *Int. J. Med. Sci. Eng.*, **2013**, *7*, 506-513.
- [27] Sangsen, Y.; Wiwattanawongsa, K.; Likhitwitayawuid, K.; Sritularak, B.; Graidist, P.; Wiwattanapataptee, R. Influence of surfactants in self-microemulsifying formulations on enhancing oral bioavailability of oxyresveratrol: studies in Caco-2 cells and *in vivo*. *Int. J. Pharm.*, **2016**, *498*, 294-303.
- [28] International Conference on Harmonization (ICH). Guidance for Industry Q1A (R2) Stability Testing of New Drug Substances and Products. Food and Drug Administration. <http://www.fda.gov/cber/gdlns/ichstab.pdf> (November 2003).
- [29] Freshney, R.I. *Culture of Animal Cells: A Manual of Basic Technique*, 5<sup>th</sup> ed.; Wiley & Sons: New Jersey, **2005**.
- [30] Hubatsch, I.; Ragnarsson, E.G.E.; Artursson, P. Determination of drug permeability and prediction of drug absorption in Caco-2 monolayers. *Nat. Protoc.*, **2007**, *2*, 2111-2119.
- [31] Sermkaew, N.; Ketjinda, W.; Boonme, P.; Phadoongsombut, N.; Wiwattanapataptee, R. Liquid and solid self-microemulsifying drug delivery systems for improving the oral bioavailability of andrographolide from a crude extract of *Andrographis Paniculata*. *Eur. J. Pharm. Sci.*, **2013**, *50*, 459-466.

- [32] Thakkar, H.P.; Desai, J.L. Influence of excipients on drug absorption via modulation of intestinal transporters activity. *Asian J. Pharmacol.*, **2015**, *9*, 69-82.
- [33] Gokce, E.H.; Korkmaz, E.; Dellera, E.; Sandri, G.; Bonferoni, M.C.; Ozer, O. Resveratrol-loaded solid lipid nanoparticles versus nanostructured lipid carriers: evaluation of antioxidant potential for dermal applications. *Int. J. Nanomed.*, **2012**, *7*, 1841-1850.
- [34] Roger, E.; Lagarce, F.; Garcion, E.; Benoit, J.P. Lipid nanocarriers improve paclitaxel transport throughout human intestinal epithelial cells by using vesicle-mediated transcytosis. *J. Control. Release*, **2009**, *140*, 174-181.
- [35] Buyukozturk, F.; Benneyan, J.C.; Carrier, R.L. Impact of emulsion-based drug delivery systems on intestinal permeability and drug release kinetics. *J. Control. Release*, **2010**, *142*, 22-30.
- [36] Phan, S.; Salentinig, S.; Prestidge, C. A.; Boyd, B.J. Self-assembled structures formed during lipid digestion: characterization and implications for oral lipid-based drug delivery systems. *Drug Deliv. Transl. Res.*, **2014**, *4*, 275-294.
- [37] Lasa-Saracibar, B.; Guada, M.; Sebastián, V.; Blanco-Prieto, M.J. *In vitro* intestinal co-culture cell model to evaluate intestinal absorption of edelfosine lipid nanoparticles. *Curr.Top. Med. Chem.*, **2014**, *14*, 1124-1132.
- [38] Mekjaruskul, C.; Yang, Y.T.; Leed, M.G.D.; Sadgrove, M. P.; Jay, M.; Sripanidkulchai, B. Novel formulation strategies for enhancing oral delivery of methoxy flavones in *Kaempferia Parviflora* by SMEDDS or complexation with 2-hydroxypropyl- $\beta$ -cyclodextrin. *Int. J. Pharm.*, **2013**, *445*, 1-11.

### List of tables

**Table 1** The components of different SMEDDS

Formulation Components (Formulation system code)		
Oil	Surfactants	Co-surfactants
Capryol 90 <sup>®</sup>	Cremophor EL <sup>®</sup> (A)	Lauroglycol FCC <sup>®</sup> (1)
	Lauroglycol 90 <sup>®</sup> (B)	Tween80 <sup>®</sup> (2)
	Labrafil M2125CS <sup>®</sup> (C)	Labrasol <sup>®</sup> (3)
	Cremophor RH40 <sup>®</sup> (D)	PG (4)
		PEG 400 (5)

**Table 2** Compositions of the developed lipid formulations of OXY

Formulation	Composition (% w/w)					% w/w of OXY
	Lipid phase		Surfactant phase			
	Solid lipid	Liquid oil	Surfactant	Co-surfactant	DI Water	
SLN	Com888 (5)	-	Tw80(3.75)	Lec(1.875)	89.075	0.3
NLC	Com888 (2.5)	LCC(2.5)	Tw80(3.75)	Lec(1.875)	89.075	0.3
SMEDDS	-	C90(45)	CRH40(45)	Tw80(10)	-	4

**Table 3** The accumulation of OXY in caco-2 cells (%) and the efflux ratio of the developed lipid formulations compared to the unformulated OXY

Formulation	OXY concentrations (µM)	% OXY accumulation in cells		Efflux ratio (ER)
		AP-BL	BL-AP	
OXY	100	0.69 ± 0.07	1.34 ± 0.11	5.02
	400	1.42 ± 0.26	0.62 ± 0.24	2.55
SLN	100	2.02 ± 0.30	1.40 ± 0.06	0.99
	400	2.41 ± 0.03	0.74 ± 0.16	1.01
NLC	100	2.80 ± 0.52	1.35 ± 0.06	1.30
	400	1.95 ± 0.08	0.47 ± 0.19	0.59

SMEDDS	100	0.78 ±0.18	0.47 ±0.04	1.36
--------	-----	------------	------------	------

Figure legends

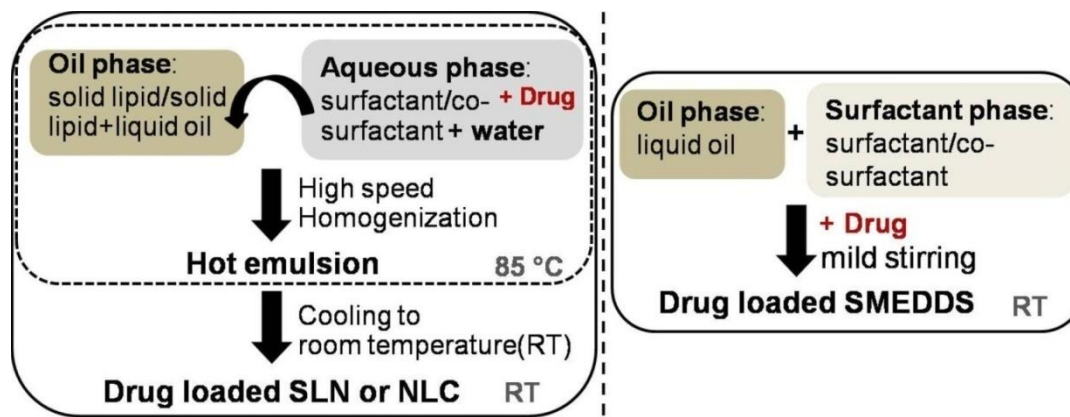


Figure 1 Diagram of the production process for lipid nanoparticles compared to the preparation of SMEDDS

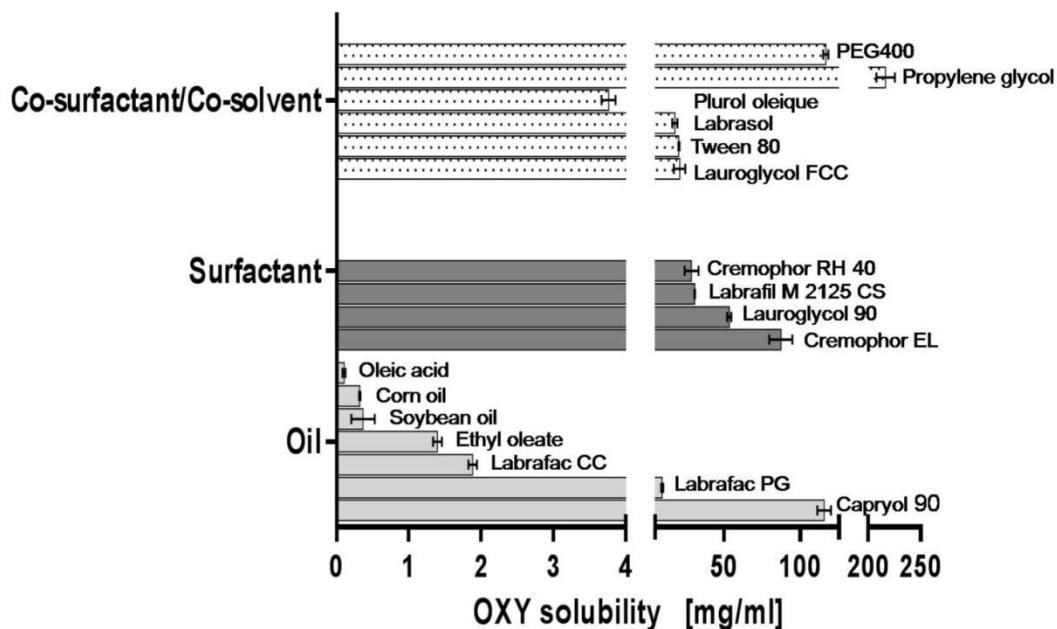
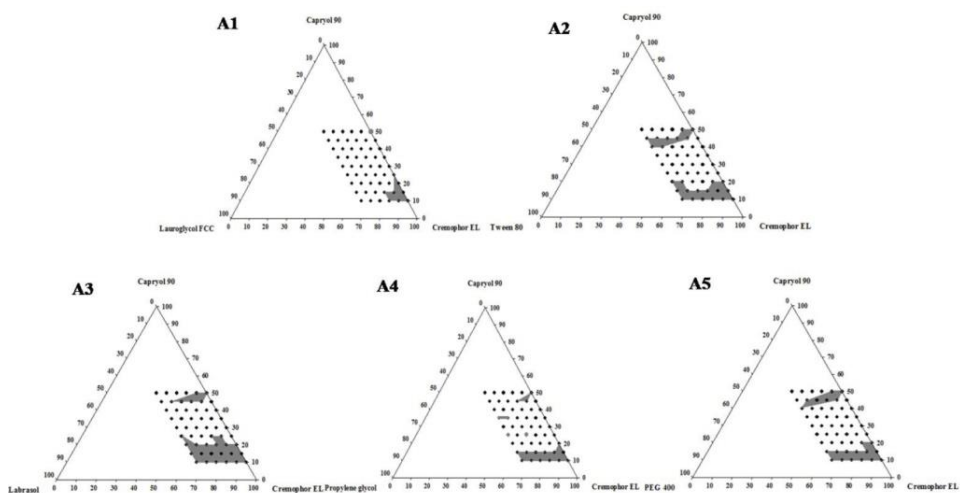
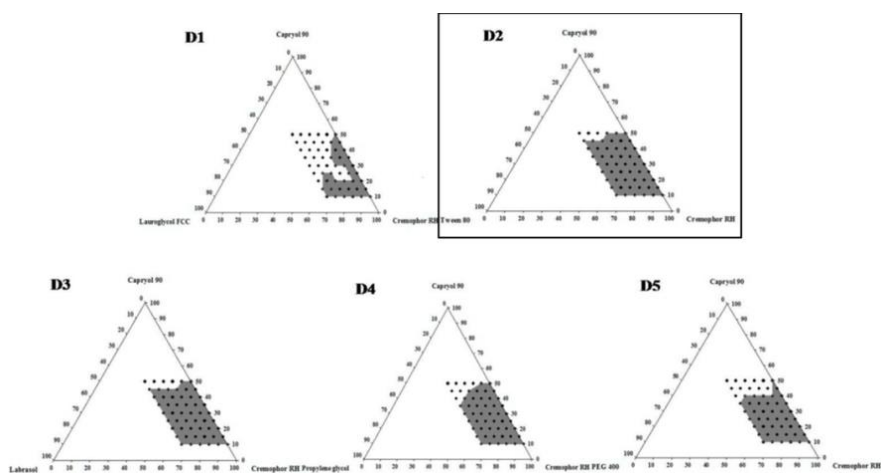


Figure 2 The solubility data of the OXY in various vehicles of SMEDDS systems. Data represents the mean ± S.D. (n = 3).





**Figure 3** Ternary phase diagram of Cremophor EL<sup>®</sup>-based SMEDDS (system A) containing different co-surfactants including Lauroglycol FCC<sup>®</sup> (A1), Tween80<sup>®</sup> (A2), Labrasol<sup>®</sup> (A3), PG (A4) and PEG400 (A5). Gray areas represent the region of efficient self-microemulsification (Grade I), and the dots represent the compositions that were evaluated.



**Figure 4** Ternary phase diagram of Cremophor RH40<sup>®</sup>-based SMEDDS (system D) containing different co-surfactants including Lauroglycol FCC<sup>®</sup> (D1), Tween80<sup>®</sup> (D2), Labrasol<sup>®</sup> (D3), PG (D4) and PEG400 (D5). Gray areas represent the region of efficient self-microemulsification (Grade I), and the dots represent the compositions that were evaluated.

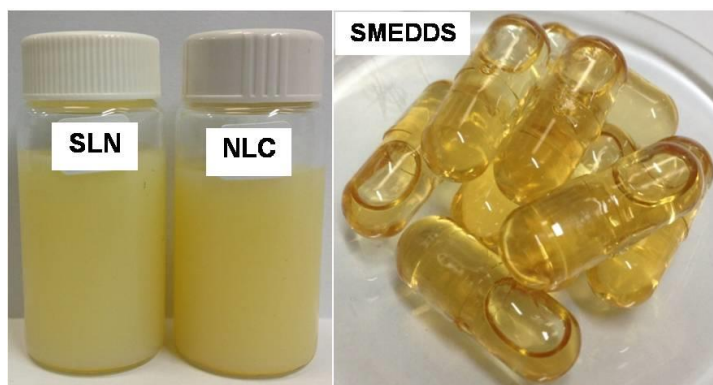


**Figure 5** Photographs of formulations of lipid nanoparticles (SLN and NLC) and SMEDDS containing OXY

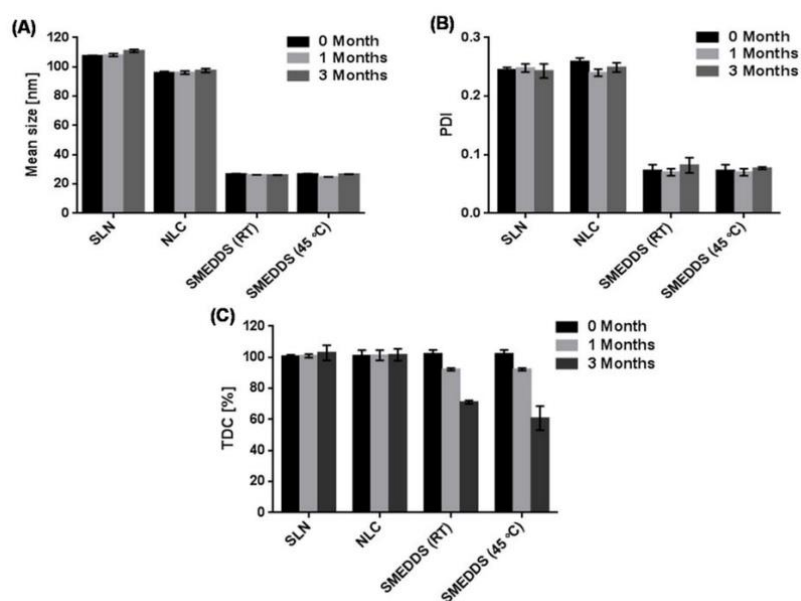


**Figure 6** Physical characteristics and stability data (0, 1, 3 months) of the OXY formulated as SLN, NLC and SMEDDS; (A) Mean size, (B) PDI and (C) %Total drug content (TC). Data represents the mean  $\pm$  S.D. (n = 3).

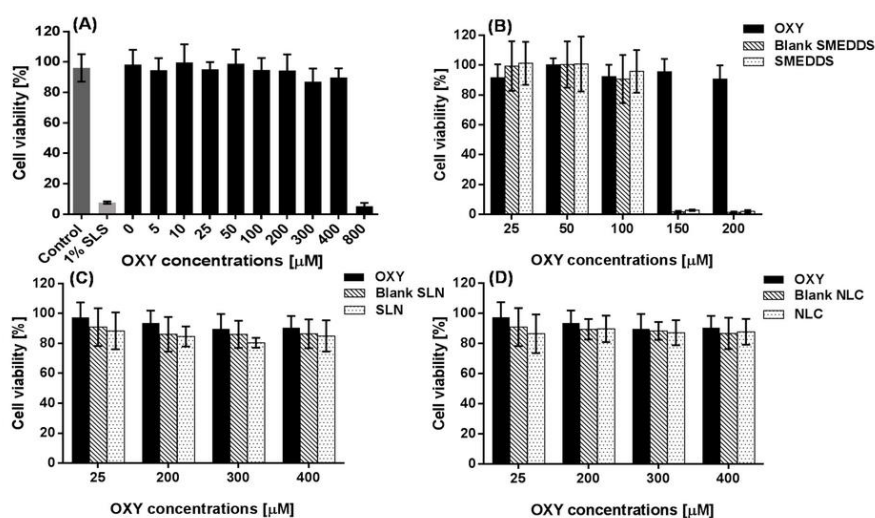


**Figure 7** The percentage of Caco-2 cell viability to different concentrations of OXY (A), blank formulations and OXY-formulations of SMEDDS (B), SLN (C), NLC (D) ( $n = 8$ ), duplications.

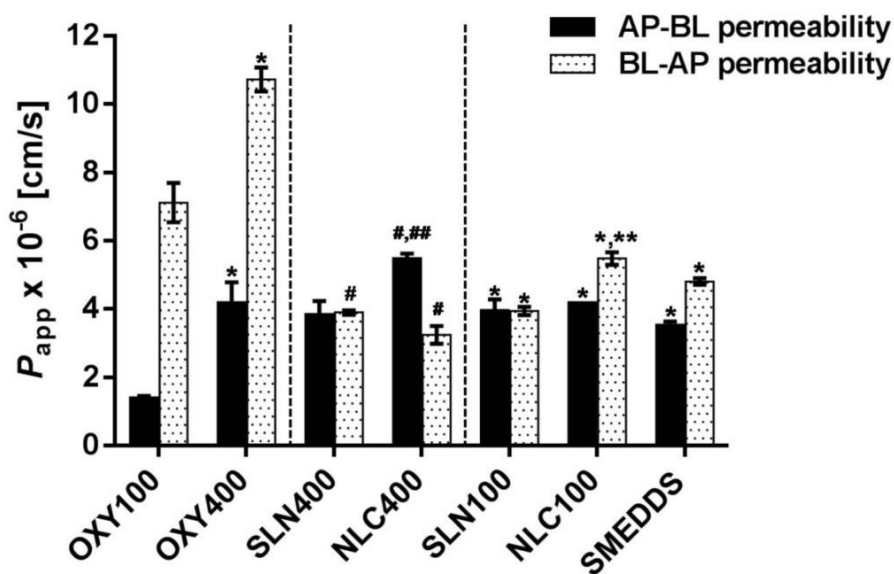


**Figure 8** Bidirectional transport across the Caco-2 monolayers of OXY and developed OXY-formulations. The data are presented as the apparent permeability coefficient ( $P_{app}$ ) in the absorptive (AP-BL) and the secretory directions (BL-AP).

\* $p < 0.05$ , comparison with OXY100;

\*\* $p < 0.05$ , comparison with SLN100;

#  $p < 0.05$ , comparison with OXY400;

##  $p < 0.05$ , comparison with SLN400.

## VITAE

**Name** Miss Yaowaporn Sangsen

**Student ID** 5210730004

### Educational Attainment

Degree	Name of Institution	Year of Graduation
Bachelor of Pharmacy (First Class Honours)	Prince of Songkla University	2009

### Scholarship Awards during Enrolment

#### Scholarships

1. **Research Assistantship**, Faculty of Pharmaceutical Sciences, Prince of Songkla University, Thailand.
2. **Research Assistantship**, Drug Delivery System Excellence Center, Prince of Songkla University, Thailand.
3. **Scholarship (Waive of Tuition fee)**, Faculty of Pharmaceutical Sciences, Prince of Songkla University, Thailand.
4. **The Thailand Research Fund** (Research Contract Number: BRG 5580004).

#### Award

1. **Winner of poster presentation**, The 3<sup>rd</sup> International Conference and Exhibition on Pharmaceutical, Nutraceutical and Cosmetical Technology (PharmaTech<sup>®</sup> 2014). Bangkok, Thailand, December 1-2, 2014.  
(Remark: This award is not related to Ph.D. thesis)

### List of Publications

1. **Sangsen, Y.**, Likhitwitayawuid, K., Sritularak, B., Wiwattanawongsa, K. and Wiwattanapatapee, R. 2013. Novel solid lipid nanoparticles for oral delivery of oxyresveratrol: Effect of the formulation parameters on the physicochemical properties and *in vitro* release. Int. J. Med. Sci. Eng. 7: 873-897.
2. **Sangsen, Y.**, Laochai, P., Chotsathidchai, P., Wiwattanapatapee, R. 2015. Effect of solid lipid and liquid oil ratios on properties of nanostructured lipid

carriers for oral curcumin delivery. *Adv. Mat. Res.* 1060: 62-65.

(Remark: This publication is not related to Ph.D. thesis)

3. **Sangsen, Y.**, Wiwattanawongsa, K., Likhitwitayawuid, K., Sritularak, B. and Wiwattanapataptee, R. 2015. Modification of oral absorption of oxyresveratrol using lipid based nanoparticles. *Colloids Surf., B.* 131: 182-190.
4. **Sangsen, Y.**, Wiwattanawongsa, K., Likhitwitayawuid, K., Sritularak, B., Graidist, P. and Wiwattanapataptee, R. 2016. Influence of surfactants in self-microemulsifying formulations on enhancing oral bioavailability of oxyresveratrol: Studies in Caco-2 cells and *in vivo*. *Int. J. Pharm.* 498(1-2): 294-303.
5. **Sangsen, Y.**, Wiwattanawongsa, K., Likhitwitayawuid, K., Sritularak, B. and Wiwattanapataptee, R. Comparison between oily system and lipid nanoparticles of oxyresveratrol on the physicochemical properties and Caco-2 cells oral absorption (Submitted for publication).

#### List of Abstracts and Proceedings

1. Oungbho, K., **Sangsen, Y.**, Tangtrakulwanich, B., Ovatlarnporn, C. 2009. Hydroxyapatite-plaster of paris-chitosan composite tablets for treatment of osteomyelitis. The 2<sup>nd</sup> TERMIS World congress 2009 in conjunction with 2009 Seoul Stem Cell Symposium, Seoul, South Korea, 31 August - 3 September, 2009 (abstract).  
(Remark: This abstract is not related to Ph.D. thesis)
2. **Sangsen, Y.**, Oungbho, K. 2010. Biocompatibility of collagen scaffolds from skin of a novel marine sources. International Bone-Tissue-Engineering Congress (Bone-tec 2010), Hannover, Germany, 7-10 October, 2010, 64 (abstract).  
(Remark: This abstract is not related to Ph.D. thesis)
3. Oungbho, K., **Sangsen, Y.** 2010. Biocompatibility of collagen scaffolds from cartilages of novel marine sources. International Bone-Tissue-Engineering Congress (Bone-tec 2010), Hannover, Germany, 7-10 October, 2010, 53 (abstract).  
(Remark: This abstract is not related to Ph.D. thesis)

4. **Sangsen, Y.**, Oungbho, K., Benjakul, S. 2011. Evaluation of collagen scaffolds from shark cartilages for tissue engineering application. U.S. Thai Pharmacy Consortium for the Development of Pharmacy Education in Thailand, Phuket, Thailand, 1-3 June, 2011, 107 (abstract).

(Remark: This abstract is not related to Ph.D. thesis)

5. **Sangsen, Y.**, Benjakul, S., Oungbho, K. 2011. Fabrication of novel shark collagen-pectin scaffolds for tissue engineering. The 4<sup>th</sup> Biomedical Engineering International Conference (BMEiCON-2011), Chiang Mai, Thailand, 29-31 January 2012, 273-278.

(Remark: This proceeding is not related to Ph.D. thesis)